



Geneeskundige **S**tichting **K**oningin **E**lisabeth
Fondation **M**édicale **R**eine **E**lisabeth
Königin-**E**lisabeth-**S**tiftung für **M**edizin
Queen **E**lisabeth **M**edical **F**oundation

Verlag – Rapport – Bericht – Report

2016

G.S.K.E. – F.M.R.E. – K.E.S.M. – Q.E.M.F.

www.fmre-gske.be
www.fmre-gske.eu
www.fmre-gske.com

Het jaar 2016, gekarakteriseerd door wetenschappelijke activiteiten van hoog niveau en het verder zetten van opmerkelijke neurowetenschappelijke projecten, eindigt in alle droefheid met het onverwacht overlijden van zijn Voorzitter, professor de Barys, op 14 december 2016.

De professor de Barys was gedurende 26 jaar, van 1990 tot 2016, Wetenschappelijk Directeur. In maart 2016 was hij voorzitter geworden van de Stichting en besteedde hij veel energie aan de werking ervan. In mei heeft hij nog de Academische zitting voorgezeten en in oktober begeleidde hij nog H.K.H Prinses Astrid tijdens haar bezoek aan de laboratoria Prof. A. Massie van de VUB te Brussel. De Stichting is veel verschuldigd aan Prof. de Barys. Zijn enorme toewijding tijdens die 26 jaar in het bestuur van de stichting zal gegrifd blijven in het geheugen en verdient onze bewondering en ons respect. Een bijzonder eerbetoen zal plaatsvinden tijdens wetenschappelijke bijeenkomst in mei 2017.

De wetenschappelijke bijeenkomst in mei 2016, onder het Erevoorzitterschap van Prinses Astrid, was de gelegenheid, om naar de uiteenzetting van de laureaten van de bijzonder briljante projecten die gerealiseerd zijn dank zij de steun van Stichting, te luisteren:

- Prijs Burggravin Valine de Spoelberch: aan Prof. Ann Massie en Prof. Smolders van de VUB voor hun project:
"System Xc- as a potential target for novel neuroprotective strategies: focus on parkinson's disease and its psychiatric comorbidities".
- Prijs Solvay : aan Prof. Claudia Bagni van de KU Leuven voor haar project:
"CYFIP1-pathies: shared pathways in intellectual disabilities and psychiatric disorders".
- Prijs Jaques et Janine Delruelle aan Prof. Jan Gettemans van de Ugent voor zijn project :
"Offsetting gelsolin degradation in a transgene mouse model by means of chaperone nanobodies".

Tijdens deze plechtigheid heeft mevrouw Marie Ressler, wetenschappelijk assistente van het Koninklijk Instituut voor het Kunstpatrimonium (KIK), een mooie voordracht gegeven over Architect Lacoste die het gebouw van de Geneeskundige Stichting heeft gerealiseerd in Art Deco stijl in 1930. Onuitgegeven fotomateriaal over het gebouw werd getoond met een uitzonderlijke deskundige uitleg.

Een muzikaal intermezzo werd verzorgd door Vladyslava Luchenko, Tanguy Parisot en Natana Hoffman, solisten van de Muziekkapel Koningin Elisabeth.

De plechtigheid werd afgesloten met een receptie waarop de onderzoekers konden kennis maken met de aanwezigen, de personaliteiten en de mecenasen.

Het jaar 2016 is het derde jaar van de driejaarlijkse onderzoekskredieten toegekend aan de in 2013 ingediende projecten en is ook het jaar waarin de nieuwe projecten voor de jaren 2017-2019 werden geevalueerd.

Meer dan 80 projecten van zeer goede kwaliteit, in het domein van de fundamentele Neurowetenschappen, moleculaire en cellulaire benadering, werden ingediend.

Het Wetenschappelijk Comité, samengesteld uit professoren van Belgische Universiteiten, is tweemaal samengekomen en heeft 16 projecten geselecteerd die gedurende drie jaar zullen gesteund worden.

De Raad van Bestuur heeft de besluiten geanalyseerd en de orientaties van zijn onderzoekssteun voor de komende drie jaar gedefinieerd.

Wij danken ook Prinses Astrid voor Haar niet aflatende steun aan de activiteiten van de Stichting en haar aanwezigheid tijdens de bezoeken aan de universitaire laboratoria en wetenschappelijke vergaderingen. Wij danken de Raad van Bestuur die zorgt voor een goed administratief beheer en die borg staat voor de duurzaamheid van de activiteiten van de Stichting.

Wij danken de lokale, academische en politieke autoriteiten die ons verwelkomen tijdens de bezoeken en we danken de leden van het Wetenschappelijk Comité die veel tijd hebben besteed aan de beoordeling van de ingediende projecten.

Wij bieden aan de familie van Professor de Barys onze grote erkentelijkheid aan voor al het werk dat de professor heeft verricht voor de stichting die hem zo dierbaar was.

Prof. dr. Jean-Marie Maloteaux,
wetenschappelijk directeur
Brussel, 30 december 2016

Cette année 2016, si elle se caractérisa par des activités scientifiques de haut niveau et la mise en route de projets remarquables en neurosciences, se termina dans la tristesse avec le décès brutal de son Président, le Professeur de Barys, le 14 décembre 2016.

Le Professeur de Barys fut le Directeur scientifique de la Fondation durant 26 ans, entre 1990 et 2016. En mars 2016 il était devenu Président de la Fondation et consacrait une grande énergie au fonctionnement de celle-ci. En mai 2016, il avait présidé la journée scientifique et un peu plus tard, en Octobre, il accompagnait SAR la Princesse Astrid lors de la visite des laboratoires du Professeur A. Massie de la VUB, à Bruxelles. La Fondation doit beaucoup au Professeur de Barys. L'immense dévouement dont il fit preuve au cours de ces 26 ans passés à la Direction de la Fondation restera gravé dans les mémoires et mérite notre admiration et notre respect. Un hommage particulier lui sera rendu lors de la réunion scientifique en mai 2017.

La journée scientifique du mois de mai 2016, placée sous la présidence d'honneur de la Princesse Astrid, fut l'occasion d'entendre les lauréats des prix récompensant des travaux particulièrement brillants réalisés grâce au soutien de la Fondation :

- Prix Vicomtesse Valine de Spoelberch : au Prof. Ann Massie et Prof. Smolders de la VUB :
"System Xc- as a potential target for novel neuroprotective strategies: focus on parkinson's disease and its psychiatric comorbidities".
- Prix Solvay : au Prof Claudia Bagni de la KU Leuven pour son projet:
"CYFIP1-pathies: shared pathways in intellectual disabilities and psychiatric disorders".
- Prix Jaques et Janine Delruelle au Prof. Jan Gettemans de l'Ugent pour son projet :
"Offsetting gelsolin degradation in a transgene mouse model by means of chaperone nanobodies".

Au cours de cette cérémonie, Mme Ressler, assistante scientifique de l'Institut Royal du Patrimoine Artistique (IRPA) réalisa une très belle présentation consacrée à l'architecte Lacoste qui réalisa le bâtiment de la Fondation médicale en 1930 dans le style art déco. Des documents photographiques inédits et des explications sur l'architecture remarquable du bâtiment furent présentés. Un intermède musical fut assuré par Vladyslava Luchenko, Tanguy Parisot et Natana Hoffman, solistes de la Chapelle Musicale Reine Elisabeth.

La réception qui clôtura la réunion a permis aux chercheurs de rencontrer les membres de l'assemblée, les mécènes et les personnalités présentes.

L'année 2016 fut la troisième année de la triennale de soutien des projets soumis en 2013 et fut l'année au cours de laquelle les nouveaux projets soumis pour les années 2017-2019 furent évalués. Plus de 80 projets de haut niveau scientifique furent déposés, dans le domaine des neurosciences fondamentales, approches moléculaires et cellulaires. Le Comité Scientifique, composé de Professeurs des Universités belges s'est réuni à deux reprises et a sélectionné 16 projets qui seront soutenus pendant trois ans. Le Conseil d'administration a analysé les conclusions du jury et a défini les orientations de son soutien à la recherche pour les trois ans à venir.

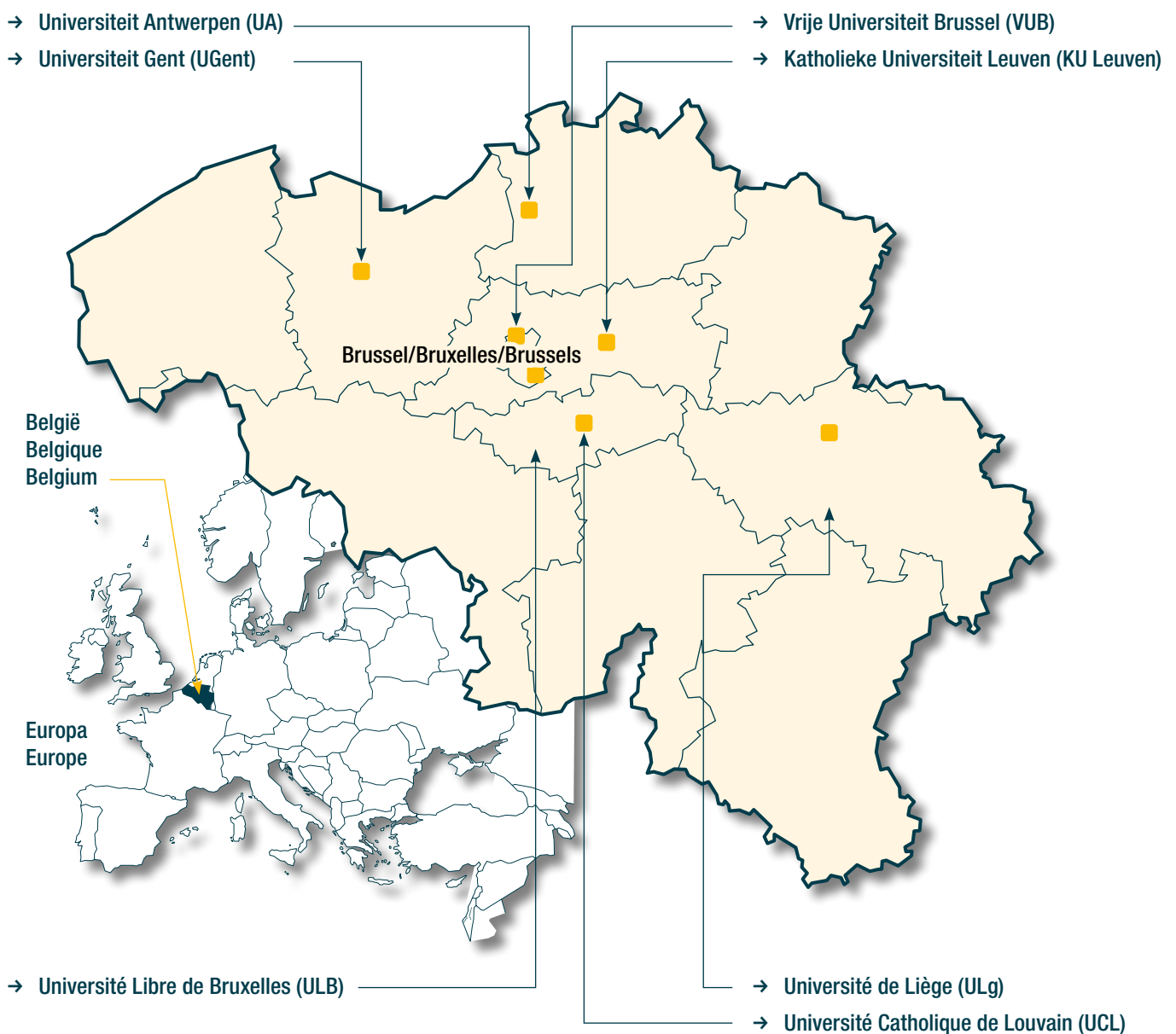
Nous adressons nos vifs remerciements à la Princesse Astrid pour son soutien constant aux activités de la Fondation et pour sa présence aux visites de laboratoires universitaires et aux réunions scientifiques. Nous remercions le Conseil d'administration qui veille à la bonne gestion administrative et qui assure la pérennité des activités de la Fondation. Nous remercions les autorités locales, académiques et politiques qui nous ont accueilli lors des visites et nous remercions les membres du Comité Scientifique qui ont consacré beaucoup de temps à l'évaluation des projets déposés. Nous adressons à la famille du Professeur de Barys l'assurance d'une grande reconnaissance pour tout le travail que celui-ci a accompli pour la Fondation qui lui était si chère.

Prof. dr. Jean-Marie Maloteaux,
directeur scientifique
Bruxelles, 30 décembre 2016

Universiteiten met onderzoeksprogramma's die gesteund worden door de G.S.K.E.

Universités ayant des programmes de recherche subventionnés par la F.M.R.E.

Universities having research programs supported by the Q.E.M.F.

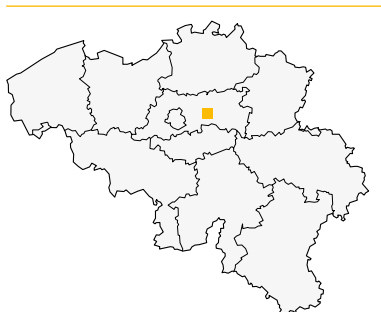


Onderzoeksprogramma's gefinancierd door de G.S.K.E. -
Programma 2014-2016

Programmes de recherche subventionnés par la F.M.R.E. -
Programme 2014-2016

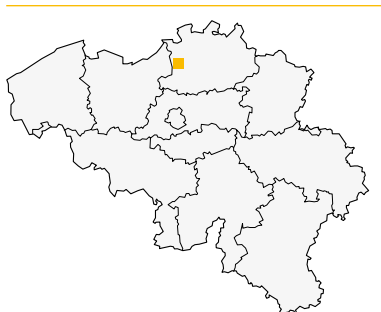
Q.E.M.F. funded research projects -
Program 2014-2016

KU Leuven



- **Prof. dr. Claudia Bagni**
CYFIP1-pathies: shared pathways in intellectual disabilities and psychiatric disorders.
- **Prof. dr. Wim Robberecht**
The ephrin axon repellent system in amyotrophic lateral sclerosis.

UA



- **Prof. dr. Marc Cruts, PhD & prof. Ilse Gijselinck**
Integrative-Omics studies of frontotemporal lobar degeneration and related diseases.
- **Prof. dr. Stefanie Dedeurwaerdere, PhD**
Translocator protein expression in temporal lobe epilepsy: picturing a Janus face?

UCL



- **Prof. dr. Etienne Olivier, PhD & dr. Alexandre Zénon**
Parkinson's disease revisited: a new vision of basal ganglia functions in the context of the Parkinson's disease.
- **Prof. dr. Jean-Noël Octave**
Alteration of cholesterol turnover in Alzheimer disease: molecular mechanisms and therapeutic applications.
- **Prof. Fadel Tissir, PhD**
Shaping the nervous system: role of the planar cell polarity genes.

UGent



- **Prof. dr. Jan Gettemans, PhD**
Offsetting gelsolin degradation in a transgene mouse model by means of chaperone nanobodies.
- **Prof. dr. Geert van Loo, PhD**
Endoplasmic reticulum stress in autoimmune central nervous system inflammation and demyelination.

ULB



- **Prof. dr. Serge N. Schiffmann**
Basal ganglia's functions and disorders: from specific genes and signalling pathways to neuronal sub-populations.
- **Prof. Pierre Vanderhaeghen, PhD & dr. Anja Hasche**
How to make cortical neurons: mechanisms, evolution and diseases.

ULg



- **Prof. dr. Pierre Maquet & dr. Christophe Phillips, ir**
Decoding spontaneous mnemonic brain activity during post-training wakefulness and sleep using high-density EEG and electro-corticography.
- **Dr. Laurent Nguyen & dr. Brigitte Malgrange**
Deciphering the role of protein acetylation in primary ciliogenesis.

VUB



- **Prof. dr. Ann Massie, PhD & prof. dr. Ilse Smolders**
System Xc- as a potential target for novel neuroprotective strategies: focus on parkinson's disease and its psychiatric comorbidities.

Final reports of the university research groups, supported by the Queen Elisabeth Medical Fondation in collaboration with the following professors and doctors (2016)

Prof. dr. Claudia Bagni	11
Prof. dr. Marc Cruts, PhD.	19
Prof. dr. Stefanie Dedeurwaerdere, PhD.	35
Julie Duque, Prof. dr. Etienne Olivier, PhD (†) & dr. Alexandre Zénon	47
Prof. dr. Jan Gettemans, PhD	59
Prof. dr. Pierre Maquet.	71
Prof. dr. Ann Massie, PhD & prof. dr. Ilse Smolders	77
Dr. Laurent Nguyen & dr. Brigitte Malgrange	99
Prof. dr. Jean-Noël Octave.	111
Prof. dr. Wim Robberecht	121
Prof. dr. Serge N. Schiffmann	141
Prof. Fadel Tissir, PhD	153
Prof. dr. Geert van Loo, PhD	169
Prof. Pierre Vanderhaeghen, PhD & dr. Anja Hasche	181



Geneeskundige Stichting Koningin Elisabeth
Fondation Médicale Reine Elisabeth
Königin-Elisabeth-Stiftung für Medizin
Queen Elisabeth Medical Foundation

Final report
of the research group of

Prof. dr. Claudia Bagni

Katholieke Universiteit Leuven (KU Leuven)

Principal investigator

Prof. dr. Claudia Bagni
Faculty of Medicine. Developmental and Molecular Genetics Section (VIB11)
Catholic University of Leuven, Belgium
T +32 16 33 09 44
F +32 16 33 09 39
claudia.bagni@med.kuleuven.be

Table of contents

1. Summary Research program
2. Achievements
3. Networking and collaborations
4. Relevance
5. Publications under the FMRE support
6. Team publications

CYFIP1-pathies: shared pathways in Intellectual Disabilities and Psychiatric Disorders”

1. Research program

The human synapse proteome is disrupted by gene mutations causing over 100 brain diseases. These synaptopathies cause major psychiatric, neurological and childhood developmental disorders. Altered synaptic connectivity and plasticity are evident in schizophrenia (SCZ), autism spectrum disorder (ASD), intellectual disability (ID), major depressive disorder (MDD), Alzheimer’s disease (AD) as well as epilepsy (EPY), all disorders characterized by spine dysmorphogenesis. One key molecule affecting synaptic structure and function is the Cytoplasmic FMRP Interacting Protein 1 (CYFIP1). At synapses CYFIP1 is involved in two distinct biological processes: with the protein causing the Fragile X Syndrome (FMRP), it modulates synaptic mRNA translation; as part of the WAVE regulatory complex, it is involved in actin cytoskeleton remodeling. We have recently shown, using a mouse model, that CYFIP1 shapes dendritic spines upon synaptic stimulation orchestrating these two molecular functions. Reduction of CYFIP1 leads to spine dysmorphogenesis and that the CYFIP1 interactome is enriched in proteins associated to SCZ, ASD, ID and EPY.

Deletions and duplications of the locus containing CYFIP1 have been identified in several neurological disorders. While those disorders are apparently heterogeneous, we believe that there are common defects in certain signaling pathways, and that CYFIP1 could be the “entry key” into a better understanding of these disorders. In this project we will undertake a “bed to bench and back” approach studying at cellular and molecular level patients with CYFIP1 mutations and patients with other synaptopathies affecting the CYFIP1 signaling pathways. Finally, we aim at setting the ground for appropriate pharmacological therapies for these heterogeneous groups of disabilities such as ASD, FXS, MDD, SCZ, AD.

2. Achievements

Achievement 1: Human sample collection. During the first year of this grant support we gathered brain specimens from publicly available biobanks as the Stanley Medical Research Institute and the Maryland Brain biobanks. Both provided us with protein extracts from different brain areas of patients with schizophrenia, bipolar disorder, FXS, ASD and unaffected controls. Furthermore, we have collected human skin primary cells (fibroblasts), lymphoblastoid cells and lymphocytes from patients with Autism Spectrum Disorders (ASDs) through our collaborators at UZ Leuven (Belgium) and at Tor Vergata Hospital (Italy). Preliminary data on human cingulate cortex showed that two CYFIP1 interactors are downregulated in patients with Schizophrenia (n=14) and Bipolar Disorder (n=13). Protein levels were analyzed blindly by Western blotting and normalized to Vinculin. *P-value<0.05. One-way ANOVA followed by post-hoc Bonferroni correction. This first data set showed that proteins that are part of the CYFIP1 interactome are down-regulated in human postmortem brains of patients with BD and SCZ, two typical examples of synaptopathies.

Achievement 2: Characterization of a patient with severe ASD and a double mutation in the CYFIP1 gene. 15q11.2 copy number variations have been found in patients featuring autism, schizophrenia, neurodevelopmental delay and intellectual disability (ID). Although the size of the region 15q11.2 is still under discussion, four genes are widely accepted to be involved: Non-imprinted in Prader-Willi/Angelman syndrome (*NIPA*) 1, *NIPA2*, Cytoplasmic FMRP interacting protein 1 (*CYFIP1*) and

Tubulin gamma complex associated protein 5 (*TUBGCP5*). Due to its crucial function during synaptic development and neuronal connectivity, CYFIP1 is thought to contribute to the clinical phenotype observed in patients with 15q11.2 variations. In a collaborative work with Prof. Koenrad De Vrient and Prof. Hilde Peeters we identified and characterized a patient with severe ASD with a BP1 and BP2 deletion on chromosome 15q as well a point mutation on the other allele. Sequence analysis revealed that the 15q11.2 del was inherited from the mother and the SNV from the father. Based on the crystal structure of WRC, molecular modeling of the alteration introduced by the CYFIP1 suggested a loss of electrostatic interaction between CYFIP1 and three key components of its interactome namely NCKAP1, WAVE, ABI2. We have recently identified an additional patient with 2 point mutations in CYFIP1 and severe ASD, the prediction is that both functional domains: binding to eIF4E and binding to the WRC are affected. We have generated fly models to study the molecular, cellular and behavioral effects of these two mutations.

Achievement 3. The CYFIP1 protein produced in patient's fibroblasts cannot be correctly assembled and interact with the macromolecular complex involved in actin polymerization.

At first we set up the conditions to immunoprecipitate CYFIP1 from primary skin cells (fibroblasts) of unaffected individuals (n=7) and from the patient with the point mutation in CYFIP1 described above collected and expanded the seven control fibroblasts and the patient fibroblasts. Upon transfection of YFP-CYFIP1 WT and YFP-CYFIP1 mut in HEK293T cells, we observed that the association of CYFIP1 with components of the WRC was reduced in cells transfected with mutated CYFIP1. CYFIP1 mut has a major impact on the direct interaction with ABI2 as well on the entire WRC suggesting that the SNV might compromise the stability and consequently the activity of the WRC affecting the downstream actin nucleating activity of the Arp2/3 complex. Increased protein synthesis and affected actin remodeling have been implicated in ASD. Because CYFIP1 links the two cellular processes at synapses (De Rubeis 2013), we investigated the dual contribution of 15q11.2 and CYFIP1 mut in these pathways in the patient's cells. Importantly, patient's fibroblasts showed an increase of newly synthesized proteins consistent with a role of CYFIP1 in negatively regulating protein translation (Napoli et al., 2008; De Rubeis et al., 2013). In addition, in collaboration with prof. Eric Klann, we have shown that in the mouse model to study the Fragile X Syndrome, the equilibrium between the CYFIP1/eIF4E and CYFIP1/Rac1 complexes is affected.

Achievement 4. Actin polymerization and cell movement is affected in patient's cell. Additionally, biochemical separation of filamentous (F) and globular (G) actin showed a reduced F/G actin ratio in patient's cells compared to control cells. Such a decrease is also supported by a reduction in phalloidin intensity. Patient's cells displayed as well a difference in the cell morphology, appearing more elongated (ratio major/minor axis). These deficits are CYFIP1 dependent because the reintroduction of YFP-CYFIP1 in patient's cells reverted these cellular phenotypes. These results unequivocally implicated CYFIP1 dysfunction in the observed cellular defects.

Achievement 5: In vivo characterization of the R826Q mutation in CYFIP1 using a Drosophila model. Because of the genetic heterogeneity between patients with ID, it has been a major challenge to comprehensively study genetic causes of ID. The fruit fly *Drosophila* has emerged as a very powerful organism for such endeavors. Using the genetic advantages of fly model, we generated flies expressing the R826Q mutation in the *CYFIP1* gene and characterized its function *in vivo*. The last year we performed the cloning of the R826Q mutation and we generated transgenic flies expressing the mutation under spatiotemporal conditions. We show that expression of the R826Q mutation in the *CYFIP1* gene recapitulates in *Drosophila* features of patients with ID and ASD.

Achievement 6: CYFIP1, eIF4E and FMR1 mRNA and protein levels are not altered in a group of patients with ASD. CYFIP1, eIF4E and FMR1 mRNA and protein levels were analyzed on a larger number (compared to the initial study during the first year) of from non-syndromic ASD aged 6-12 (n=15)

and control (n=13) by quantitative western blotting and real time qPCR respectively. Importantly, we observed the a specific signaling pathway regulating FMRP functions is affected in a specific group of patients with ASD. We are currently correlating this molecular signature to the clinical features of these patients with ASD (Rosina, Battan, Pacini et al., in preparation).

3. Networking and collaborations

The project results from the integration of complementary expertise, giving us the opportunity to create productive scientific collaborations in our Institute and with other institutions abroad. We are actively collaborating with clinicians and human geneticists at UZ Leuven (Prof. Koenrad De Vrient and Prof. Hilde Peeters) and at Tor Vergata Hospital (Prof. Paolo Curatolo). We have also initiated a new collaboration with Prof Pierre Billuart and Prof Thierry Bienvenu at Institut Cochin, INSERM Paris (France), with Prof. Eric Klann and Dr. Emanuela Santini New York University (USA) and with Prof. Frank Bradke and Dr. Sebastian Dupraz, Univeristy of Bonn (Germany). Finally, we have had a fruitful collaboration with the microscope imaging facility of the Center of Human Genetics, KU Leuven (Light Microscopy & Imaging Network, LiMoNe) to study actin remodeling.

4. Relevance

The work we have performed during the last 3 years with the support of the FMRE helped us to increase the current knowledge of CYFIP1 distribution and function/s in brain using a mouse and fly model and, importantly, human cells from 2 patients with mutation in the CYFIP1 gene. We are aiming at understanding how a single molecule, CYFIP1, affecting two key cellular processes as protein synthesis and actin remodeling if mutated or reduced causes ASD. Our data have so far identified impaired cellular processes that might explain the neuronal deficits in the two identified patients. We therefore think that CYFIP1 could be the entry key to a better understanding of ASD. We are extremely thankful to the *Fondation Médical Reine Elisabeth* for the support we received over the past years for our scientific activity at the K University of Leuven, Belgium.

5. Publications under the support of FMRE (2014-2016)

1. Achsel T, Bagni C. (2016). Cooperativity in RNA-protein interactions: the complex is more than the sum of its partners. *Curr Opin Neurobiol.* 2016 Aug;39:146-51.
2. Sabanov V, Braat S, D'Andrea L, Willemsen R, Zeidler S, Rooms L, Bagni C, Kooy RF, Balschun D. (2016). Impaired GABAergic inhibition in the hippocampus of Fmr1 knockout mice. *Neuropharmacology* Dec 21;116:71-81.
3. Panja D, Kenney JW, D'Andrea L, Zalfa F, Vedeler A, Wibrand K, Fukunaga R, Bagni C, Proud CG and Bramham CR (2014). "Sustained BDNF-TrkB signaling to MNK mediates two-stage translational control of LTP consolidation in the dentate gyrus in vivo" *Cell Reports*, 9:1430-45. doi: 10.1016/j.celrep.2014.10.016. Epub 2014 Nov 6.
4. Pasciuto E, Borrie SC, Kanellopoulos AK, Santos AR, Cappuyens E, D'Andrea L, Pacini L, Bagni C. (2015). Autism Spectrum Disorders: Translating human deficits into mouse behavior. *Neurobiol Learn Mem.* Jul 26. pii: S1074-7427(15)00134-3. doi: 10.1016/j.nlm.2015.07.013. [Epub ahead of print] Review. PubMed PMID:26220900.
5. Di Marino D, D'Annessa I, Tancredi H, Bagni C and Gallicchio E (2015). A Unique Binding Mode of the Eukaryotic Translation Initiation Factor 4E for Guiding the Design of Novel Peptide Inhibitors. *Protein Science.* 2015 Sep;24(9):1370-82. doi: 10.1002/pro.2708.
6. Di Marino D, Chillemi G, De Rubeis S, Tramontano A, Achsel T and Bagni C. (2015) MD and docking studies reveal that the functional switch of CYFIP1 is mediated by a butterfly-like Motion. *Journal of Chemical Theory and Computation*, 2015 April; 11,3401-3410; doi: 10.1021/ct500431h.
7. Santos AR, Kanellopoulos A and Bagni C (2014). Learning and Behavioral Deficits Associated with Absence of the Fragile X Mental Retardation Protein: what a fly and mouse models can teach us. *Learning and Memory*, 21: 543-555.
8. Di Marino D, Achsel T, Lacoux C, Falconi M, Bagni C. (2014). Molecular dynamics simulations show how the FMRP Ile304Asn mutation destabilizes the KH2 domain structure and affects its function. *J. Biomol. Struct. Dyn.* 32:337-50.

We have additional 5 publications under revision in which the FMRE is acknowledged.

6. Team key publications

(5 selected from 36 publications over the last five years)

1. Pasciuto E, Ahmed T, Wahle T, Gardoni F, D'Andrea L, Pacini L, Jacquemont S, Tassone F, Balschu D, Dotti CG, Vegh Z, D'Hooge R, Müller U, Di Luca M, De Strooper B and **Bagni C** (2015). Dysregulated ADAM10-mediated processing of APP during a critical time-window leads to synaptic deficits in fragile X syndrome. *Neuron*, 87: 382-398.
2. La Fata G, Gärtner A, Domínguez-Iturza N, Dresselaers T, Dawitz J, Poorthuis RB, Aversa M, Himmelreich U, Meredith RM, Achsel T, Dotti CG and **Bagni C** (2014). "The Fragile X Mental Retardation Protein regulates neuronal multipolar-bipolar transition and affects cortical circuitry in the developing cortex" *Nature Neurosci.*, doi: 10.1038/nn.3870. Epub ahead of print.
3. Pasciuto E and **Bagni C** (2014). "FMRP mRNA Targets and Associated Human Diseases" *Cell SnapShot*, 158 (6): 1446-1446.
4. Pasciuto E and **Bagni C** (2014). "FMRP Interacting Proteins" *Cell SnapShot* 159 (1):218-218.
5. De Rubeis S, Pasciuto W, Li Ka Wan, Fernández E, Di Marino D, Buzzi A, Ostroff L, Klann E, Zwartkruis F, Komiyama NH, Grant S, Choquet D, Poujol C, Achsel T, Posthuma D, Smit AB and **Bagni C** (2013). CYFIP1 coordinates mRNA translation and cytoskeleton remodeling to ensure proper dendritic spine formation. *Neuron*, 79: 1169-1182.



Geneeskundige Stichting Koningin Elisabeth
Fondation Médicale Reine Elisabeth
Königin-Elisabeth-Stiftung für Medizin
Queen Elisabeth Medical Foundation

Final report
of the research group of

Prof. dr. Marc Cruts, PhD

Universiteit Antwerpen (UA)

Principal investigator

Prof. dr. Marc Cruts, PhD

Co-investigators

Dr. Ilse Gijselinck, PhD

Neurodegenerative Brain Diseases Group
VIB Department of Molecular Genetics (former Department of Molecular Genetics)
Laboratory for Neurogenetics
Institute Born-Bunge
University of Antwerp Belgium

Table of contents

1. Scientific Report
 - Specific Aims
 - Aim 1: Unraveling Disease Mechanisms Associated with Known FTD Genes
 - C9orf72 repeat expansions
 - GRN missense mutations
 - Aim 2: Novel genes for FTD
 - TBK1
 - VPS13C
 - SORT1
 - TREM2
 - Aim 3: Onset age modifying genes for FTLD
 - A major onset age modifier locus on chromosome 12
 - TMEM106B
 - Genome-wide association study
 - References
2. Publications Acknowledging G.S.K.E. Funding
 - Articles in international journals
 - Articles in Books
 - Meeting abstracts in international journals
 - Abstracts in abstract books of international meetings
3. Activity Report
 - Honors, Prizes & Awards
 - Prizes
 - Travel Awards
 - Presentations
 - Invited lectures
 - Oral presentations
 - Poster presentations

Integrative -Omics Studies of Frontotemporal Lobar Degeneration and Related Diseases

1. Specific Aims

Frontotemporal dementia (FTD), semantic dementia (SD), and progressive nonfluent aphasia (PNFA) are disabling and irreversible clinical conditions that are characterized by progressive neuronal loss in the frontal and/or temporal cortices, collectively referred to as frontotemporal lobar degeneration (FTLD) (see Sieben et al. 2012 for review). Onset age of FTD ranges on average from 45 to 65 years and often affects people who are mid-career and raising a family. In this age group, FTD is the second most common type of neurodegenerative dementia after Alzheimer's disease (AD). Due to the aging population in Belgium and worldwide, the incidence of FTD will exponentially increase in the years to come; yet, no preventive or curative treatments are available today. To manage behavioral abnormalities associated with FTD, symptomatic treatments e.g. using psychopharmaca are frequently used (Boxer and Boeve 2007). To develop effective therapies aiming at delaying, halting or possibly preventing the disease, our understanding of the pathological mechanisms leading to the neurodegenerative processes in the patients' brains is essential.

In up to 50% of patients, familial aggregation has been observed suggesting highly penetrant genetic factors. At the start of this granting period, mutations in three genes *MAPT*, *GRN*, *C9orf72* were identified as a frequent cause of FTD (FTD Mutation Database, Cruts et al.), together explaining about 20 to 50% of familial FTD. In addition, rare mutations were reported in *VCP*, *TARDBP*, *FUS*, and *CHMP2B*. Until today, studies of these genes have provided limited insight in the associated pathomechanisms. To this end, and to improve differential diagnostic efficacy, the identification of additional disease genes causing or modifying the expression of the FTD symptoms is essential. Therefore, we aimed to further expand our understanding of the gene networks and biological processes that are affected in FTD. Further, onset age in FTD is typically highly variable, suggesting that genetic factors modify the onset age and severity of the clinical symptoms of the disease. We hypothesized that genes modifying onset age are excellent therapeutic targets to delay and/or prevent disease onset and progression. Therefore, we aimed to identify disease-modifying genes.

In this perspective, the specific objectives set out in this project were:

1. Unraveling the disease mechanisms associated with *C9orf72* repeat expansion
2. Identification of novel causal genes for FTLD
3. Identification of genes modifying onset age in FTLD

In addition to the preset objectives, objective 1 was extended with studies to unravel the disease mechanism associated with *GRN*, another major FTD gene that we had identified in 2006 (Cruts et al. 2006).

Progress in each of the objectives is detailed below. In summary, thanks to the support of the QEMF foundation, our research efforts have led to understanding of the disease mechanisms associated with the *GRN* and *C9orf72* genetic subtypes of FTD. Further, we have identified and characterized novel FTD genes *TBK1*, *VPS13C*, *SORT1* and *TREM2*. Further, we characterized an onset age modifier locus on chromosome 12. As a direct result of these achievements, improved early diagnosis can be offered to the patients and their families. Further, results obtained in this project have instigated ongoing cell biological studies of the functions and dysfunctions of pathways contributing to neurodegeneration in FTD.

2. Aim 1: Unraveling Disease Mechanisms Associated with Known FTD Genes

2.1. *C9orf72* repeat expansions

In 2012, we had identified a pathological repeat expansion in the proximal regulatory region of *C9orf72* as one of the most frequent causes of disease in the FTD/ALS spectrum (Gijselinck et al. 2012) (see QEMF 2011-2013 scientific report). Various disease mechanisms associated with pathological repeat expansions were proposed (Cruts et al. 2013). We now contributed to the investigation of the involvement of these disease mechanisms to FTD, focusing in particular on the loss-of-function and the pathological dipeptide repeat hypotheses.

Loss of function

We investigated the effect of repeat expansion size on onset age using Southern blot analysis in related and unrelated *C9orf72* expansion carriers. Repeat expansion sizes in blood ranged from 45 to over 2100 G₄C₂ units. We detected short expansions (45-78 units) in 6.5% of carriers and demonstrated segregation of a repeat of 50 units in an FTD family, indicating that expansions as short as 50 units may cause FTD. Also, we showed for the first time negative correlation between repeat expansion size and onset age ($P < 0.05$) (Figure 1) most likely explained by an association of methylation state of the 5' flanking CpG island and expansion size in blood ($P < 0.0001$) and brain ($P < 0.05$) (Figure 2). In several informative *C9orf72* parent-child transmissions, we identified earlier onset ages, larger expansion sizes and/or higher methylation states ($P = 0.0034$) of the 5' CpG island, reminiscent of genetic anticipation. Also, intermediate repeats of 7-24 units showed a slightly higher degree of methylation ($P < 0.0001$) and a decrease of *C9orf72* promoter activity ($P < 0.0001$) compared with normal short repeats of 2-6 units. Decrease of transcriptional activity was even more prominent in the presence of small deletions flanking the G₄C₂ repeat ($P < 0.0001$). Here we showed that increased methylation of CpG sequences in the *C9orf72* promoter may underlie the G₄C₂ repeat size-dependent loss of *C9orf72* function. These data provide insights into disease mechanisms and have important implications for diagnostic counseling and potential therapeutic approaches. The observations however do not exclude repeat size-dependent toxic gain-of-function mechanisms. (Gijselinck et al. 2016).

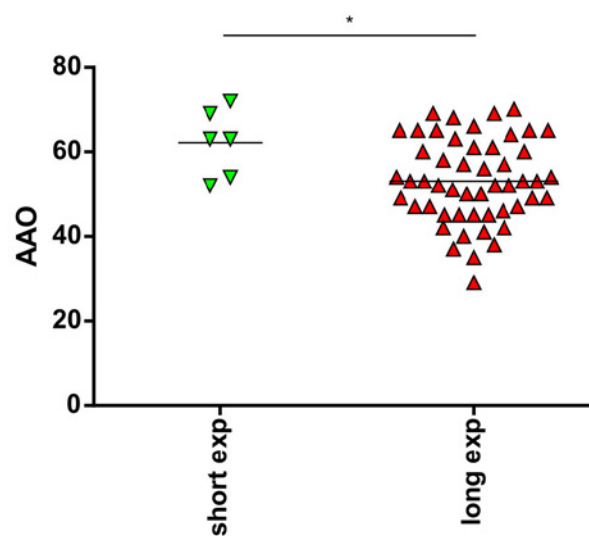


Figure 1. Association of G₄C₂ size with onset age of disease. Comparison of age at onset (AAO) between patients with a short expansion (<80 units) and patients with a long expansion (> 80 units) ($P < 0.05$) (Gijselinck et al. 2016).

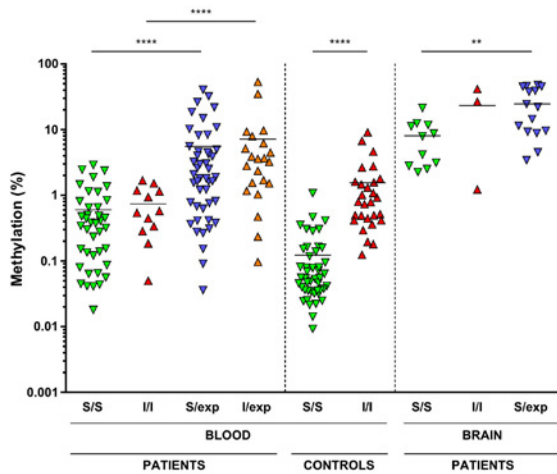


Figure 2. Association of G_4C_2 size with DNA methylation of the 5' flanking CpG island. *HhaI* MSRE-qPCR results of the 5' flanking CpG island are presented for expansion carriers (S/exp and I/exp) versus patients without expansion with short/short (S/S) and intermediate/intermediate (I/I) genotype stratified for normal short (S) or intermediate (I) repeat length of the normal alleles, and for controls with S/S and I/I genotype (Gijssels et al. 2016).

Dipeptide repeat pathology

Unconventional translation of G_4C_2 repeats produces dipeptide repeat proteins (DPRs) that may cause neurodegeneration. In a collaborative study with professor L Van Den Bosch, KU Leuven, we performed a modifier screen in *Drosophila* and discovered a critical role for importins and exportins, Ran-GTP cycle regulators, nuclear pore components, and arginine methylases in mediating DPR toxicity. Our findings provided evidence for an important role for nucleocytoplasmic transport in the pathogenic mechanism of *C9orf72* repeat expansion pathology in FTD and ALS (Boeynaems et al. 2016).

C9orf72 repeat and Parkinson disease

In another study, we investigated the role of $(G_4C_2)_n$ expansions in the etiology of Parkinson disease (PD) in the worldwide multicenter Genetic Epidemiology of Parkinson's Disease (GEO-PD) cohort.

C9orf72 (G_4C_2)_n repeat sizes were assessed in a GEO-PD cohort of 7,494 patients diagnosed with PD and 5,886 neurologically healthy control individuals ascertained in Europe, Asia, North America, and Australia. A pathogenic $(G_4C_2)_{n>60}$ expansion was detected in only 4 patients with PD (4/7,232; 0.055%), all with a positive family history of neurodegenerative dementia, amyotrophic lateral sclerosis, or atypical parkinsonism, while no carriers were detected with typical sporadic or familial PD. Meta-analysis revealed a small increase in risk of PD with an increasing number of G_4C_2 repeat units; however, we could not detect a robust association between the *C9orf72* (G_4C_2)_n repeat and PD, and the population attributable risk was low. Together, these findings indicate that expansions in *C9orf72* do not have a major role in the pathogenesis of PD. Testing for *C9orf72* repeat expansions should only be considered in patients with PD who have overt symptoms of frontotemporal lobar degeneration/amyotrophic lateral sclerosis or apparent family history of neurodegenerative dementia or motor neuron disease (Theuns et al. 2014).

2.2. GRN missense mutations

Progranulin (GRN) is a multifunctional secreted growth factor involved in various important cellular functions and loss-of-function mutations are a major cause of FTLD with TDP-43 positive pathology. The majority of FTLD-related *GRN* mutations are nonsense mutations resulting in reduced *GRN* expression through a haploinsufficiency mechanism. However, non-synonymous missense mutations, scattered over all *GRN* exons, have also been described as risk factors to develop other neurodegenerative brain diseases. While some missense variants alter the secretion efficiency of GRN or the conversion of the GRN precursor protein into individual granulin peptides, the pathogenic nature of most GRN variants remains to be determined. We identified a double missense mutation in *GRN* leading to amino acid changes p.D33E and p.G35R in a patient from Turkish origin. Genetic analyses of the transmission pattern in five offspring suggested a transmission of the mutation in cis. Biochemical and cell biological analysis of the double mutation and two additional, earlier described, patient-specific *GRN* missense mutations (p.C105R and p.V514M) revealed a reduced transport of the GRN p.D33E/G35R and p.C105R proteins through the secretory pathway leading to lowered levels of secreted GRN. Furthermore, we showed that loss of a conserved cysteine residue affects proper protein folding, resulting in reduced secretion and altered proteolytic processing by neutrophil elastase and proteinase 3. Our data thus indicated that GRN mutations may affect GRN homeostasis at multiple levels (Kleinberger et al. 2016).

3. Aim 2: Novel genes for FTD

3.1. **TBK1**

Mutations in the TANK-binding kinase 1 gene (*TBK1*) were identified in the FTD-ALS spectrum of diseases. We assessed the genetic contribution of *TBK1* in Belgian FTD and ALS patient cohorts with a significant part of genetically unresolved patients. We sequenced *TBK1* in a hospital-based cohort of 482 unrelated patients with FTD and FTD-ALS and 147 patients with ALS and an extended Belgian FTD-ALS family DR158. We followed up mutation carriers by segregation studies, transcript and protein expression analysis, and immunohistochemistry. We identified 11 patients carrying a loss-of-function (LOF) mutation resulting in an overall mutation frequency of 1.7% (11/629), 1.1% in patients with FTD (5/460), 3.4% in patients with ALS (5/147), and 4.5% in patients with FTD-ALS (1/22). We found 1 LOF mutation, p.Glu643del, in 6 unrelated patients segregating with disease in family DR158. Of 2 mutation carriers, brain and spinal cord was characterized by TDP-43-positive pathology. The LOF mutations including the p.Glu643del mutation led to loss of transcript or protein in blood and brain. *TBK1* LOF mutations are the third most frequent cause of clinical FTD in the Belgian clinically based patient cohort, after *C9orf72* and *GRN*, and the second most common cause of clinical ALS after *C9orf72*. These findings reinforce that FTD and ALS belong to the same disease continuum (Gijssels et al. 2015).

3.2. **VPS13C**

In about 60% of the familial FTD patients, the genetic cause remains unknown. We performed whole genome sequencing (WGS) on an affected sib pair suffering from early onset FTD. Analysis of WGS variants in an extended Belgian FTD patient and control cohort revealed the presence of the p.Ala444Pro missense mutation in the vacuolar protein sorting 13 homolog C gene (*VPS13C*) in five unrelated FTD patients while it was absent in control individuals. Screening of the 86 coding exons of *VPS13C* in the FTD population resulted in the identification of 21 additional mutations that were absent in controls. Immunofluorescence staining and immunoblotting analysis on lymphoblast cell lines of patients carrying *VPS13C* missense mutations demonstrated a decreased expression of endogenous *VPS13C* protein (**Figure 3**) in patients compared to controls, suggesting a loss-of-function mechanism. In addition, modelling of missense mutations in the yeast ortholog Vps13p revealed a possible effect on mitochondrial function (Philtjens et al., In Preparation).

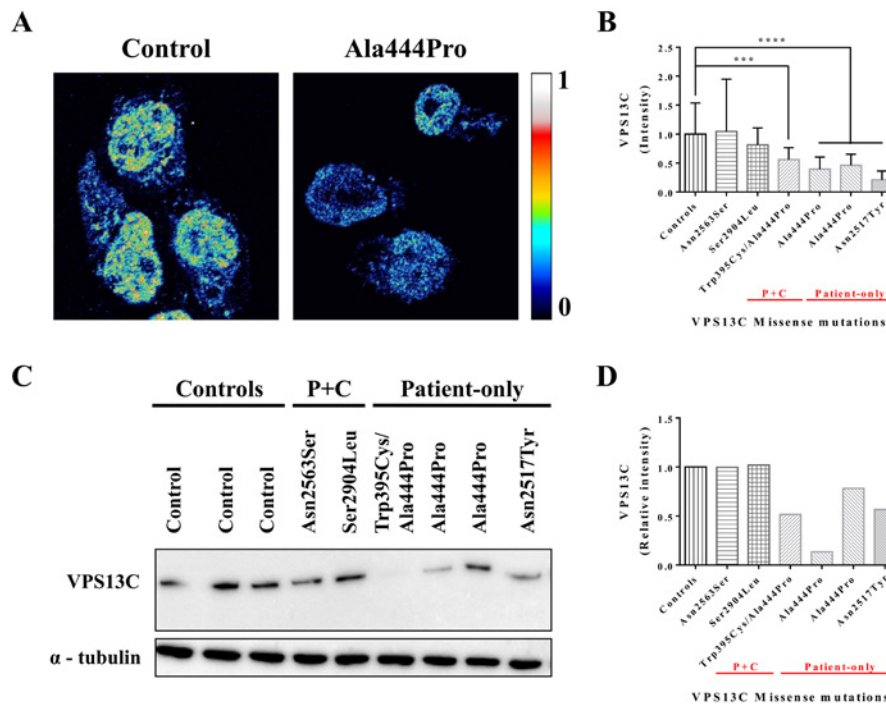


Figure 3: Decreased endogenous protein expression of VPS13C in mutation carriers compared to healthy controls. **(A)** Epstein Barr Virus transformed lymphoblast cells of a mutation-free control and patient DR481 carrying the *VPS13C* p.Ala444Pro missense mutation, immunostained for endogenous VPS13C. **(B)** Double-blind quantification of the corrected total cell fluorescence per cell averaged over two independent experiments per individual, both including 10 randomly selected cells per slide. Vertical lines indicate standard deviation. Controls: mutation-free control (n = 4); 'P + C': group patients carrying a mutation that was also observed in at least one control. 'Patient-only': group of mutations observed in patients only. **(C)** Western blot analysis of mutation-free controls (n = 3), patients carrying a *VPS13C* mutation that was present in both patients and controls (p.Asn2563Ser and p.Ser2904Leu) and patients-specific mutations (p.Trp395Cys/p.Ala444Pro, p.Ala444Pro, p.Asn2517Tyr and p.Thr1218Ala). **(D)** Quantification of VPS13C expression, normalized for the expression of α -tubulin. *** 0.0001 < P < 0.001; ****P < 0.0001.

3.3. SORT1

Sortilin 1 (*SORT1*) is the neuronal receptor of granulin. We aimed to ascertain the genetic role of *SORT1* in FTD by sequencing the complete coding region in a Belgian cohort of 537 FTD patients and 1,076 age-matched control persons. We identified three missense mutations in seven patients corresponding to a mutation frequency of 7/537 = 1.3%. All missense mutations occurred at highly conserved amino acids and were absent in the control group. Rare variant association analysis between patients and controls showed a significant increase in rare genetic variants with a minor allele frequency $\leq 1\%$ in FTD patients (p = 0.034). Furthermore, our analysis suggested that the variants clustered in the β -propeller domain (p = 0.011) mediating granulin binding. Together these data provided evidence that rare variants in the β propeller domain of *SORT1* that might increase risk for FTD in the Belgian cohort (Philtjens et al., Under Revision with Neurology Genetics).

3.4. TREM2

Homozygous mutations in exon 2 of *TREM2*, a gene involved in Nasu-Hakola disease, can cause frontotemporal dementia (FTD). Moreover, a rare *TREM2* exon 2 variant (p.R47H) was reported to increase the risk of Alzheimer's disease (AD) with an odds ratio as strong as that for *APOE* ϵ 4. We systematically screened the *TREM2* coding region within a Belgian study on neurodegenerative brain diseases comprising 1216 AD patients, 357 FTD patients, and 1094 controls. We observed an enrichment of rare variants across *TREM2* in both AD and FTD patients compared to controls, most notably in the extracellular IgV-set domain (relative risk = 3.84 [95% confidence interval = 1.29-11.44]; p = 0.009 for AD; relative risk = 6.19 [95% confidence interval = 1.86-20.61]; p = 0.0007 for FTD). None of the rare variants individually reached significant association, but the frequency of p.R47H was increased approximately 3-fold in both AD and FTD patients compared to controls, in line with previous reports. Meta-analysis including 11 previously screened AD cohorts confirmed the association of p.R47H

with AD ($p = 2.93 \times 10^{-17}$). Our data corroborate and extend previous findings to include an increased frequency of rare heterozygous *TREM2* variations in AD and FTD, and show that *TREM2* variants may play a role in neurodegenerative diseases in general (Cuyvers et al. 2014).

4. Aim 3: Onset age modifying genes for FTLD

4.1. A major onset age modifier locus on chromosome 12

In FTLD a wide distribution of onset age, ranging from 20 to 91 years, suggests a significant contribution of factors modifying the disease onset. In a Flanders-Belgian FTLD founder pedigree segregating a *GRN* null mutation and exhibiting a wide onset age range between 45 and 84 years, we excluded an effect on onset age of functional candidate modifiers such as the unaffected copy of *GRN* and variations in *TMEM106B*. In the family we identified a QTL for onset age with strong evidence of linkage on chromosome 12 (Bayes' factor > 10) (Shugart 2014). This locus of 7 Mb contains 119 genes and explains up to 91% of the genetic variance in onset age. A set of 122 candidate modifier variations was selected from whole genome sequencing data of 23 mutation carriers. All variations associated with onset age with a p -value < 0.01 ($n=19$) are located in intronic or intergenic regions throughout the priority region of the QTL. To identify the functional variation, *in silico* clues are being sought, as well as biological evidence in brain transcriptome and serum proteome data of the family and in targeted expression analyses of candidate modifier genes, by comparing expression levels between patients with early and late onset of disease. Candidate modifier variations and genes will be studied in extended patient cohorts. The identification of genetic modifiers may shed further light on the disease mechanisms of FTLD and may provide stepping stones for the development of therapies that can halt or delay, or even prevent the disease. (Wauters et al. 2014).

4.2. TMEM106B

Genetic variants at *TMEM106B* influence risk for the most common neuropathological subtype of FTLD, characterized by inclusions of TAR DNA-binding protein of 43 kDa (FTLD-TDP). Previous reports have shown that *TMEM106B* is a genetic modifier of FTLD-TDP caused by progranulin (*GRN*) mutations, with the major (risk) allele of rs1990622 associating with earlier age at onset of disease (Van Deerlin et al., 2010). Now, we reported that the rs1990622 genotype affects age at death in a single-site discovery cohort of FTLD patients with *C9orf72* repeat expansions ($n = 14$), with the major allele correlated with later age at death ($p = 0.024$). We replicated this modifier effect in a 30-site international neuropathological cohort of FTLD-TDP patients with *C9orf72* expansions ($n = 75$), again finding that the major allele associates with later age at death ($p = 0.016$), as well as later age at onset ($p = 0.019$). In contrast, the *TMEM106B* genotype does not affect age at onset or death in 241 FTLD-TDP cases negative for *GRN* mutations or *C9orf72* expansions. Thus, *TMEM106B* is a genetic modifier of FTLD with *C9orf72* expansions. Intriguingly, the genotype that confers increased risk for developing FTLD-TDP (major, or T, allele of rs1990622) is associated with later age at onset and death in *C9orf72* expansion carriers, providing an example of sign epistasis in human neurodegenerative disease (Gallagher et al. 2014).

4.3. Genome-wide association study

In a large international study, we sought to identify novel genetic risk loci associated with the FTD. We did a two-stage genome-wide association study on clinical FTD, analyzing samples from 3526 patients with FTD and 9402 healthy controls. To reduce genetic heterogeneity, all participants were of European ancestry. In the discovery phase (samples from 2154 patients with FTD and 4308 controls), we did separate association analyses for each FTD subtype (behavioral variant FTD, semantic dementia, progressive non-fluent aphasia, and FTD overlapping with motor neuron disease i.e. FTD-MND), followed by a meta-analysis of the entire dataset. We carried forward replication of the novel suggestive loci in an independent sample series comprising 1372 patients and 5094 controls, and then did joint phase and

brain expression and methylation quantitative trait loci (QTL) analyses for the associated ($p < 5 \times 10^{-8}$) single-nucleotide polymorphisms. We identified novel associations exceeding the genome-wide significance threshold of $p < 5 \times 10^{-8}$. Combined (joint) analyses of discovery and replication phases showed genome-wide significant association at 6p21.3, HLA locus (immune system), for rs9268877 ($p = 1.05 \times 10^{-8}$; odds ratio=1.204 [95% CI 1.11-1.30]), rs9268856 ($p = 5.51 \times 10^{-9}$; 0.809 [0.76-0.86]) and rs1980493 ($p = 1.57 \times 10^{-8}$, 0.775 [0.69-0.86]) in the entire cohort. We also identified a potential novel locus at 11q14, encompassing *RAB38/CTSC*, the transcripts of which are related to lysosomal biology, for the behavioral FTD subtype for which joint analyses showed suggestive association for rs302668 ($p = 2.44 \times 10^{-7}$; 0.814 [0.71-0.92]). Analysis of expression and methylation QTL data suggested that these loci might affect expression and methylation in cis. These findings suggest that immune system processes (link to 6p21.3) and possibly lysosomal and autophagy pathways (link to 11q14) are potentially involved in FTD. Our findings need to be replicated to better define the association of the newly identified loci with disease and to shed light on the pathomechanisms contributing to FTD (Ferrari et al. 2014). These novel loci may provide insight into genes and or pathways harboring genetic variability modifying onset age in FTLD.

5. References

- Boeynaems S, Bogaert E, Michiels E, Gijssels I, Sieben A, Jovicic A, De Baets G, Scheveneels W, Steyaert J, Cuijt I and others. 2016. Drosophila screen connects nuclear transport genes to DPR pathology in c9ALS/FTD. *Sci Rep* 6:20877.
- Boxer AL, Boeve BF. 2007. Frontotemporal dementia treatment: current symptomatic therapies and implications of recent genetic, biochemical, and neuroimaging studies. *Alzheimer Dis. Assoc. Disord.* 21(4):S79-S87.
- Cruts M, Gijssels I, van der Zee J, Engelborghs S, Wils H, Pirici D, Rademakers R, Vandenberghe R, Dermaut B, Martin JJ and others. 2006. Null mutations in progranulin cause ubiquitin-positive frontotemporal dementia linked to chromosome 17q21. *Nature* 442(7105):920-924.
- Cruts M, Gijssels I, Van Langenhove T, van der Zee J, Van Broeckhoven CL. 2013. Current insights into the C9orf72 repeat expansion diseases of the FTL/ALS spectrum. *Trends Neurosci.* 36(8):450-459.
- Cruts M, Theuns J, Van Broeckhoven C. 2012. Locus-specific mutation databases for neurodegenerative brain diseases. *Hum. Mutat.* 33(9):1340-1344.
- Cuyvers E, Bettens K, Philtjens S, Van Langenhove T, Gijssels I, van der Zee J, Engelborghs S, Vandenbulcke M, Van Dongen J, Geerts N and others. 2014. Investigating the role of rare heterozygous TREM2 variants in Alzheimer's disease and frontotemporal dementia. *Neurobiol Aging* 35(3):726 e11-9.
- Ferrari R, Hernandez DG, Nalls MA, Rohrer JD, Ramasamy A, Kwok JB, Dobson-Stone C, Brooks WS, Schofield PR, Halliday GM and others. 2014. Frontotemporal dementia and its subtypes: a genome-wide association study. *Lancet Neurol.* 13(7):686-699.
- Gallagher MD, Suh E, Grossman M, Elman L, McCluskey L, van Swieten JC, Al-Sarraj S, Neumann M, Gelpi E, Ghetti B and others. 2014. TMEM106B is a genetic modifier of frontotemporal lobar degeneration with C9orf72 hexanucleotide repeat expansions. *Acta Neuropathol.*
- Gijssels I, Van Langenhove T, van der Zee J, Slegers K, Philtjens S, Kleinberger G, Janssens J, Bettens K, Van Cauwenberghe C, Pereson S and others. 2012. A C9orf72 promoter repeat expansion in a Flanders-Belgian cohort with disorders of the frontotemporal lobar degeneration-amyotrophic lateral sclerosis spectrum: a gene identification study. *Lancet Neurol.* 11(1):54-65.
- Gijssels I, Van Mossevelde S, van der Zee J, Sieben A, Engelborghs S, De Bleecker J, Ivanoiu A, Deryck O, Edbauer D, Zhang M and others. 2016. The C9orf72 repeat size correlates with onset age of disease, DNA methylation and transcriptional downregulation of the promoter. *Mol Psychiatry* 21(8):1112-24.
- Gijssels I, Van Mossevelde S, van der Zee J, Sieben A, Philtjens S, Heeman B, Engelborghs S, Vandenbulcke M, De Baets G, Baumer V and others. 2015. Loss of TBK1 is a frequent cause of frontotemporal dementia in a Belgian cohort. *Neurology* 85(24):2116-25.
- Kleinberger G, Capell A, Brouwers N, Fellerer K, Slegers K, Cruts M, Van Broeckhoven C, Haass C. 2016. Reduced secretion and altered proteolytic processing caused by missense mutations in progranulin. *Neurobiol Aging* 39:220 e17-26.
- Shugart J. 2014. International Conference on Frontotemporal Dementias 2014: Stream of Genetics Pushes FTD Research Forward.
- Sieben A, Van Langenhove T, Engelborghs S, Martin JJ, Boon P, Cras P, De Deyn PP, Santens P, Van Broeckhoven C, Cruts M. 2012. The genetics and neuropathology of frontotemporal lobar degeneration. *Acta Neuropathol.* 124(3):353-372.
- Theuns J, Verstraeten A, Slegers K, Wauters E, Gijssels I, Smolders S, Crosiers D, Corsmit E, Elinck E, Sharma M and others. 2014. Global investigation and meta-analysis of the C9orf72 (G4C2)_n repeat in Parkinson disease. *Neurology* 83(21):1906-1913.
- Wauters E, Gijssels I, Van Langenhove T, Engelborghs S, Vandenbulcke M, Mattheijssens M, Peeters K, Martin JJ, Cras P, Santens P and others. 2014. An integrative approach to identify onset age modifier genes in a large founder *GRN* FTL/ALS family. *Am J Neurodegener Dis* 3(Suppl 1):271-271.

6. Publications Acknowledging G.S.K.E. Funding

6.1. Articles in international journals

- Ferrari,R., Hernandez,D.G., Nalls,M.A., Rohrer,J.D., Ramasamy,A., Kwok,J.B.J., Dobson-Stone,Carol, Brooks,W.S., Schofield,P.R., Halliday,G., Hodges,J., Piguat,O., Bartley,L., Thompson,E., Haan,E., Hernández,I., Ruiz,A., Boada,M., Borroni,B., Padovani,A., Cruchaga,C., Cairns,N.J., Benussi,L., Binetti,G., Ghidoni,R., Forloni,G., Galimberti,D., Fenoglio,C., Serpente,M., Scarpini,E., Clarimon,J., Lleo,A., Blesa,R., Landqvist,W., Nilsson,K., Nilsson,C., Mackenzie,I.R., Hsiung,G-Y, R., Mann,D., Grafman,J., Morris,C.M., Attems,J., Griffiths,T.D., McKeith,I.G., Thomas,A.J., Pietrini,P., Huey,E.D., Wassermann,E.M., Baborie,A., Jaros,E., Tierney,M.C., Pastor,P., Razquin,C., Ortega-Cubera,S., Alonso,E., Pernecky,R., Diehl-Schmid,J., Alexopoulos,P., Kurz,A., Rainero,I., Rubino,I., Pinessi,L., Rogaeva,E., St. George-Hyslop,P., Rossi,G., Tagliavani,F., Giaccone,G., Rowe,J.B., Schlachetzki,J.C., Uphill,J., Collinge,J., Mead,S., Danek,A., Van Deerlin,V.M., Grossman,M., Trojanowski,J.Q., van der Zee,J., Deschamps,W., Van Langenhove,T., **Cruts,M.**, Van Broeckhoven,C., Cappa,S.F., Le Ber,I., Hannequin,D., Golfer,V., Vercelletto,M., Brice,A., Nacmias,B., Sorbi,S., Bagnoli,S., Piaceri,I., Nielsen,J.E., Hjermand,L.E., Riemenschneider,M., Mayhaus,M., Ibach,B., Gasparoni,G., Pichler,I., Gu,W., Rossor,M.N., Fox,N., Warren,J.D., Spillanti,M., Morris,H.R., Rizzu,P., Heutink,P., Snowden,J.S., Rollinson,S., Richardson,A., Gerhard,A., Bruni,A.C., Maletta,R., Frangipane,F., Cupidi,C., Bernardi,L., Anfossi,M., Gallo,M., Conidi,M.E., Smirne,N., Rademakers,R., Baker,M., Dickson,D., Graff-Radford,N.R., Petersen,R.C., Knopman,D., Josephs,K.A., Boeve,B.F., Parisi,J.E., Seeley,W.W., Miller,B.L., Karydas,A.M., Rosen,H., Van Swieten,J., Dopfer,E.G., Seelaar,H., Pijnenburg,Y.A., Scheltens,P., Logroscino,G., Capozzo,R., Novelli,V., Puca,A.A., Franceschi,M., Postiglione,A., Milan,G., Sorrentino,P., Kristiansen,M., Chiang,H.-H., Graff,C., Pasquier,F., Rollin,A., Deramecourt,V., Lebert,F., Kapogiannis,D., Ferrucci,L., Pickering-Brown,S.M., Singleton,A., Hardy,J., Momeni,P.: Frontotemporal dementia and its subtypes: a genome wide association study, *Lancet Neurology* 13: 686-699 (2014) (PMID: 24943344) (I.F.: 21.823)
- Gallagher,M.D., Suh,E., Grossman,M., Elman,L., McCluskey,L., Van Swieten,J.C., al-Sarraj,S., Neumann,M., Gelpi,E., Ghetti,B., Rohrer,J.D., Halliday,G., Van Broeckhoven,C., Seilhean,D., Shaw,P.J., Frosch,M.P., Alafuzoff,I., Antonell,A., Bogdanovic,N., Brooks,W., Cairns,N.J., Cooper-Knock,J., Cotman,C.W., Cras,P., **Cruts,M.**, De Deyn,P.P., DeCarli,C., Dobson-Stone,Carol, Engelborghs,S., Fox,N., Galasko,D., Gearing,M., **Gijssels,I.**, Grafman,J., Hartikainen,P., Hatanpaa,K.J., Highley,J.R., Hodges,J., Hulette,C., Ince,P.G., Jin,L.W., Kirby,J., Kofler,J., Kwok,J.B.J., Levey,A.I., Liebermann,A., Llado,A., Martin,J.-J., Masliah,E., McDermott,C.J., McKee,A., McLean,C., Mead,S., Miller,C.A.: TMEM106B is a genetic modifier of frontotemporal lobar degeneration with C9orf72 hexanucleotide repeat expansions. *Acta Neuropathologica* 127: 407-18 (2014) (PMID: 24442578) (I.F.: 9.777)
- van der Zee,J., Van Langenhove,T., Kovacs,G.G., Dillen,L., Deschamps,W., Engelborghs,S., Matej,R., Vandenbulcke,M., Sieben,A., Dermaut,B., Smets,K., Van Damme,P., Merlin,C., Laureys,A., Van den Broeck,M., Mattheijssens,M., Peeters,K., Benussi,L., Binetti,G., Ghidoni,R., Borroni,B., Padovani,A., Archetti,S., Pastor,P., Razquin,C., Ortega-Cubera,S., Hernández,I., Boada,M., Ruiz,A., De Mendonca,A., Miltenberger-Miltenyi,G., Simões do Couto,F., Sorbi,S., Nacmias,B., Bagnoli,S., Graff,C., Chiang,H.-H., Thonberg,H., Pernecky,R., Diehl-Schmid,J., Alexopoulos,P., Frisoni,G., Bonvicini,C., Synofzik,M., Maetzler,W., Müller vom Hagen,J., Schöls,L., Haack,T.B., Strom,T.M., Prokisch,H., Dols-Icardo,O., Clarimon,J., Lleo,A., Santana,I., Rosario Almeida,M., Santiago,B., Heneka,M., Jessen,F., Ramirez,A., Sanchez-Valle,R., Llado,A., Gelpi,E., Sarafov,S., Tournev,I., Jordanova,A., Parobkova,E., Fabrizi,G.-M., Testi,S., Salmon,E., Ströbel,T., Santens,P., Robberecht,W., De Jonghe,P., Martin,J.-J., Cras,P., Vandenberghe,R., De Deyn,P.P., **Cruts,M.**, Sleegers,K., Van Broeckhoven,C., BELNEU consortium,, EU EOD consortium,: Rare mutations in SQSTM1 modify susceptibility for frontotemporal lobar degeneration. *Acta Neuropathologica* 128: 397-410 (2014) (PMID: 24899140) (I.F.: 9.777)
- Theuns,J., Verstraeten,A., Sleegers,K., Wauters,E., **Gijssels,I.**, Smolders,S., Crosiers,D., Corsmit,E., Elinck,E., Sharma,M., Krüger,R., Lesage,S., Brice,A., Chung,S.J., Kim,M.-J., Kim,Y.J., Ross,O.A., Wszolek,Z., Rogaeva,E., Xi,Z., Lang,A.E., Klein,C., Weissbach,A., Mellick,G., Silburn,P.A., Hadjigeorgiou,G., Dardiotis,E., Hattori,N., Ogaki,K., Tan,E., Zhao,Y., Aasly,J., Valente,E.M., Petrucci,S., Annesi,G., Quattrone,A., Ferrarese,C., Brighina,L., Deutschländer,A., Puschmann,A., Nilsson,C., Garraux,G., LeDoux,M.S., Pfeiffer,R.F., Boczarska-Jedynak,M., Opala,G., Maraganore,D.M., Engelborghs,S., De Deyn,P.P., Cras,P., **Cruts,M.**, Van Broeckhoven,C., on behalf of the GEO-PD Consortium,: Global investigation and meta-analysis of the C9orf72 (G4C2)_n repeat in Parkinson disease. *Neurology* 83: 1906-1913 (2014) (PMID: 25326098) (I.F.: 8.303)
- Cuyvers,E., Bettens,K., Philtjens,S., Van Langenhove,T., **Gijssels,I.**, van der Zee,J., Engelborghs,S., Vandenbulcke,M., Van Dongen,J., Geerts,N., Maes,G., Mattheijssens,M., Peeters,K., Cras,P., Vandenberghe,R., De Deyn,P., Van Broeckhoven,C., **Cruts,M.**, Sleegers,K., BELNEU consortium,: Investigating the role of rare heterozygous TREM2 variants in Alzheimer disease and frontotemporal dementia. *Neurobiology of Aging* 35: 726.e11-e19 (2014) (PMID: 24119542) (I.F.: 4.853)
- **Gijssels,I.**, Van Mossevelde,S., van der Zee,J., Sieben,A., Engelborghs,S., De Bleeker,J., Ivanou,I., Deryck,O., Edbauer,D., Zhang,M., Heeman,B., Bäumer,V., Van den Broeck,M., Mattheijssens,M., Peeters,K., Rogaeva,E., De Jonghe,P., Cras,P., Martin,J.-J., De Deyn,P.P., Van Broeckhoven,C., **Cruts,M.**, BELNEU consortium: The C9orf72 repeat size correlates with onset age of disease, DNA methylation and transcriptional downregulation of the promoter. *Molecular Psychiatry* 21: 1112-1124 (2016) (PMID: 26481318) (I.F.: 14.496)

- **Gijselinck,I.**, Van Mossevelde,S., van der Zee,J., Sieben,A., Philtjens,S., Heeman,B., Engelborghs,S., Vandenbulcke,M., De Baets,G., Bäumer,V., Cuijt,I., Van Den Broeck,M., Mattheijssens,M., Peeters,K., Rousseau,F., Vandenberghe,R., De Jonghe,P., Cras,P., De Deyn,P.P., Martin,J.-J., **Cruts,M.**, Van Broeckhoven,C., Belgian Neurology (BELNEU) consortium: Loss of TBK1 is a frequent cause of frontotemporal dementia in a Belgian cohort. *Neurology* 85: 2116-2125 (2015) (PMID: 26581300) (I.F.: 8.166)
- Kleinberger,G., Capell,A., Brouwers,N., Fellerer,K., Slegers,K., **Cruts,M.**, Van Broeckhoven,C., Haass,C.: Reduced secretion and altered proteolytic processing caused by missense mutations in progranulin. *Neurobiology of Aging* 39: 220.e17-26 (2016) (PMID: 26811050) (I.F.: 5.153)
- Boeynaems,S., Bogaert,E., Michiels,E., **Gijselinck,I.**, Sieben,A., Jovicic,A., De Baets,G., Scheveneels,W., Steyaert,J.G., Cuijt,I., Verstrepen,K.J., Callaerts,P., Rousseau,F., Schymkowitz,J., **Cruts,M.**, Van Broeckhoven,C., Van Damme,P., Gitler,A.D., Robberecht,W., Van Den Bosch,L.: Drosophila screen connects nuclear transport genes to DPR pathology in c9ALS/FTD. *Scientific Reports* 6: 20877 (2016) (PMID: 26869068) (I.F.: 5.228)
- Philtjens S., Van Mossevelde,S., Wauters,E., van der Zee,J., Van Langenhove,T., Vandenbulcke,M., Vandenberghe,R., Ivanoiu,A., Sieben,A., Willems,C., Van den Broeck,M., Peeters,M., Mattheijssens,M., Cras,P., De Deyn,P.P., Engelborghs,S., **Cruts,M.**, Van Broeckhoven,C.: SORT1 genetic variability and risk for frontotemporal dementia in a Belgina cohort. *Neurology Genetics* (Under Review)
- Philtjens,S., Van Mossevelde,S., Sieben,A., van der Zee,J., Wauters,E., **Gijselinck,I.**, Engelborghs,S., Versijpt,J., Van Langenhove,T., Cuijt,I., Geerts,N., Versteven.M., Mattheijssens,M., Peeters,K., Van den Broeck,M., Cras,P., De Deyn,P.P., Martin,J.J., **Cruts,M.**, Van Broeckhoven,C.: VPS13C mutations are associated with decreased expression of endogenous protein in frontotemporal dementia (In Preparation)

6.2. Articles in Books

- **Cruts,M.**, Engelborghs,S., van der Zee,J., Van Broeckhoven,C.: C9orf72-related amyotrophic lateral sclerosis and frontotemporal dementia, In: *GeneReviews®* [Internet] Edited by Edited by Roberta A Pagon, Editor-in-chief, Margaret P Adam, Holly H Ardinger, Thomas D Bird, Cynthia R Dolan, Chin-To Fong, Richard JH Smith, and Karen Stephens. (Seattle (WA): University of Washington, Seattle; 1993-2015: GeneReviews (2015). Internet publication <http://www.ncbi.nlm.nih.gov/books/NBK268647>
- **Cruts,M.**, Van Broeckhoven,C.: Genetics of frontotemporal dementia and related disorders, In: *Hodges' Frontotemporal Dementia* second edition Edited by Bradford C. Dickerson (Cambridge University Press) 185-196 (2016)

6.3. Meeting abstracts in international journals

- Philtjens,S., **Gijselinck,I.**, Van Langenhove,T., van der Zee,T., Engelborghs,S., Vandenbulcke,M., Vandenberghe,R., Santens,P., De Deyn,P.P., Van Broeckhoven,C., **Cruts,M.**, BELNEU consortium: Next generation sequencing identifies mutations in VPS13C associated with decreased expression of endogenous protein in Frontotemporal lobar degeneration. *Am J Neurodegener Dis* 3 Suppl 1: 13 (2014)
- Wauters,E., **Gijselinck,I.**, Van Langenhove,T., Engelborghs,S., Vandenbulcke,M., Mattheijssens,M., Peeters,K., Martin,J.-J., Cras,P., Santens,P., Vandenberghe,R., De Deyn,P.P., van der Zee,J., Slegers,K., Van Broeckhoven,C., **Cruts,M.**: An integrative approach to identify onset age modifier genes in a large founder GRN FTLN family. *Am J Neurodegener Dis* 3 Suppl 1: 271 (2014)
- **Gijselinck,I.**, Heeman,B., Van Langenhove,T., Philtjens,S., Wauters,E., van der Zee,J., Theuns,J., Engelborghs,S., Sieben,A., De Jonghe,P., Vandenberghe,R., Santens,P., De Bleeker,J., Robberecht,W., Cras,P., De Deyn,P.P., Van Broeckhoven,C., **Cruts,M.**, BELNEU consortium: C9orf72 G4C2 repeat size associates with genetic anticipation, hypermethylation and transcriptional down-regulation in FTLN and ALS. *Am J Neurodegener Dis* 3 Suppl 1: 275 (2014)
- **Cruts,M.**, **Gijselinck,I.**, Philtjens,S., van der Zee,J., Maes,G., Engelborghs,S., Vandenbulcke,M., Vandenberghe,R., Santens,P., De Deyn,P.P., Van Broeckhoven,C., BELNEU consortium: Genome-wide screen in FTLN/ALS patient cohorts for pathological G4C2 repeat expansions other than C9orf72. *Am J Neurodegener Dis* 3 Suppl 1: 280 (2014)
- **Cruts,M.**, Philtjens,S., **Gijselinck,I.**, Van Mossevelde,S., van der Zee,J., Van Langenhove,T., Engelborghs,S., Vandenbulcke,M., Vandenberghe,R., Santens,P., De Deyn,P., Van Broeckhoven,C.: VPS13C mutations associate with frontotemporal lobar degeneration and decreased protein expression. *Tremor and Other Hyperkinetic Movements: Proceedings of the Third Joint Symposium on Neuroacanthocytosis and Neurodegeneration with Brain Iron Accumulation: From Benchside to Bedside*: 13 (2014)
- **Gijselinck,I.**, Van Mossevelde,S., Sieben,A., Heeman,B., Engelborghs,S., Vandenbulcke,M., Cuijt,I., Van den Broeck,M., Peeters,K., Mattheijssens,M., Vandenberghe,R., De Jonghe,P., Cras,P., De Deyn,P.P., Martin,J.-J., **Cruts,M.**, Van Broeckhoven,C.: Loss-of-Function mutations in TBK1 are frequently associated with frontotemporal lobar degeneration in a Belgian patient cohort. *Alzheimer's and Dementia* 11: P333 (2015)
- Philtjens,S., Wauters,E., Van Mossevelde,S., van der Zee,J., Van Langenhove,T., Engelborghs,S., Vandenbulcke,M., Versteven,M., Peeters,K., Mattheijssens,M., Van den Broeck,M., Cras,P., Vandenberghe,R., De Deyn,P.P., **Cruts,M.**, Van

- Broeckhoven,C.: Unraveling the genetic role of SORT1 in the Belgian frontotemporal dementia population. *Journal of Neurochemistry Supp 1*: P175: 310-311 (2016)
- **Cruts,M., Gijssels,I.,** Van Mossevelde,S., van der Zee,J., Sieben,A., Engelborghs,S., De Bleecker,J., Ivanoiu,A., Deryck,O., Heeman,B., Bäumer,V., Van den Broeck,M., Mattheijssens,M., Peeters,K., De Jonghe,P., Cras,P., Martin,J-J., De Deyn,P.P., Van Broeckhoven,C.: Molecular mechanism of genetic anticipation in C9orf72 repeat expansion families. *Journal of Neurochemistry Supp 1*: P179: 312 (2016)
 - Wauters,E., Van Mossevelde,S., Slegers,K., **Gijssels,I.,** Philtjens,S., Sieben,A., Van Langenhove,T., Engelborghs,S., Vandenbulcke,M., Mattheijssens,M., Peeters,K., Cuijt,I., Martin,J-J., Cras,P., Santens,P., Vandenberghe,R., De Deyn,P.P., van der Zee,J., **Cruts,M.,** Van Broeckhoven,C.: The Belgian GRN founder family anno 2016: a textbook example of phenotypic heterogeneity. *Journal of Neurochemistry Supp 1*: P453: 418-419 (2016)

6.4. Abstracts in abstract books of international meetings

- Philtjens,S., **Gijssels,I.,** Van Langenhove,T., van der Zee,T., Engelborghs,S., Vandenbulcke,M., Vandenberghe,R., Santens,P., De Deyn,P.P., Van Broeckhoven,C., **Cruts,M.:** Whole genome sequencing identifies vps13c as a candidate gene for frontotemporal lobar degeneration. *Human Genome Meeting, Geneva Switzerland: OR014 (April 27-30, 2014)*
- **Gijssels,I.,** Van Langenhove,T., Philtjens,S., van der Zee,J., Engelborghs,S., Sieben,A., De Jonghe,P., Vandenberghe,R., Santens,P., De Bleecker,J., Robberecht,W., Cras,P., De Deyn,P.P., Van Broeckhoven,C., **Cruts,M.:** C9orf72 G4C2 repeat expansion size associates with genetic anticipation in FTLD and ALS. *Human Genome Meeting, Geneva Switzerland: OR014 (April 27-30, 2014)*
- Van Broeckhoven,C., **Gijssels,I.,** Van Mossevelde,S., van der Zee,J., Sieben,A., Heeman,B., Engelborghs,S., Vandenbulcke,M., Vandenberghe,R., De Jonghe,P., Cras,P., De Deyn,P.P., Martin,J-J., **Cruts,M.,** BELNEU consortium, EU EOD consortium: Loss-of-function mutations in TBK1 are a frequent cause of frontotemporal dementia and amyotrophic lateral sclerosis in Belgian and European cohorts. *American Society of Human Genetics 2015, Baltimore, MD, USA, October 6-10 : 105 (Oral) (2015)*
- **Cruts,M., Gijssels,I.,** Van Mossevelde,S., van der Zee,J., Sieben,A., Engelborghs,S., De Bleecker,J., Ivanoiu,A., Deryck,O., Edbauer,D., Zhang,M., Heeman,B., Rogaeva,E., De Jonghe,P., Cras,P., Martin,J-J., De Deyn,P.P., Van Broeckhoven,C., BELNEU consortium: The C9orf72 repeat expansion modulates onset age of FTD-ALS through increased DNA methylation and transcriptional downregulation *American Society of Human Genetics 2015, Baltimore, MD, USA, October 6-10 : 106 (Oral) (2015)*
- Wauters,E., **Gijssels,I.,** Van Mossevelde,S., Sieben,A., Van Langenhove,T., Mattheijssens,M., Peeters,K., Martin,J-J., van der Zee,J., Slegers,K., Van Broeckhoven,C., **Cruts,M.:** An integrative approach to identify onset age modifier genes in an extended Belgian GRN founder family *EMBO/EMBL Symposium: Mechanisms of neurodegeneration, Heidelberg, Germany, June 14-17 : 253 (Poster) (2015)*
- Philtjens,S., **Gijssels,I.,** Van Mossevelde,S., Sieben,A., Martin,J-J., van der Zee,J., Van Broeckhoven,C., **Cruts,M.:** Novel missense mutations in the vacuolar protein sorting 13 homolog C gene are associated with decreased endogenous protein expression in frontotemporal lobar degeneration. *EMBO/EMBL Symposium: Mechanisms of neurodegeneration, Heidelberg, Germany, June 14-17 : 192 (Poster) (2015)*
- **Gijssels,I.,** Van Mossevelde,S., Sieben,A., Heeman,B., Engelborghs,S., Vandenbulcke,M., Cuijt,I., Van den Broeck,M., Peeters,K., Mattheijssens,M., Vandenberghe,R., De Jonghe,P., Cras,P., De Deyn,P.P., Martin,J-J., **Cruts,M.,** Van Broeckhoven,C.: Loss-of-Function mutations in TBK1 are frequently associated with frontotemporal lobar degeneration in a Belgian patient cohort. *Alzheimer's Association International Conference 2015 (AAIC 2015), Washington, USA, July 18-23 : DT-02-01 (Oral) (2015)*

7. Activity Report

7.1. Honors, Prizes & Awards

Prizes

- Gijssels I.: Dr. Karel-Lodewijk Verleysen Award for medical research at Flemish universities to recognize groundbreaking medical research in the field of neurodegenerative brain diseases, Brussels Belgium, December 3, 2016

Travel Awards

- Gijssels I.: Funding of the FWO for participating in a conference abroad: 9th International Conference on Frontotemporal dementias, Vancouver, Canada, October 23-25, 2014
- Wauters E.: Student bursary, complimentary conference registration and accommodation, supported by the International Society for Frontotemporal Dementias to attend the 9th International Conference on Frontotemporal Dementias, Vancouver, Canada, October 23-25, 2014

7.2. Presentations

Invited lectures

International

- Cruts M.: *VPS13C* mutations associate with frontotemporal lobar degeneration and decreased protein expression. The Third Joint Symposium on Neuroacanthocytosis and Neurodegeneration With Brain Iron Accumulation. Stresa, Italy, October 30 – November 1 2014

Oral presentations

International

- Philtjens, S.: Whole genome sequencing identifies *vps13c* as a candidate gene for frontotemporal lobar degeneration. Human Genome Meeting 2014. Geneva, Switzerland, April 27-30 2014
- Philtjens S.: Next generation sequencing identifies mutations in *VPS13C* associated with decreased expression of endogenous protein in Frontotemporal lobar degeneration. 9th International Conference on Frontotemporal Dementias. Vancouver, Canada, October 23 – 25 2014
- Van Broeckhoven, C.: American Society of Human Genetics Annual Meeting 2015, Baltimore, USA, October 6-10, 2015. Loss-of-function mutations in *TBK1* are a frequent cause of frontotemporal dementia and amyotrophic lateral sclerosis in Belgian and European cohorts.
- Cruts, M.: American Society of Human Genetics Annual Meeting 2015, Baltimore, USA, October 6-10, 2015. The *C9orf72* repeat expansion modulates onset age of FTD-ALS through increased DNA methylation and transcriptional downregulation.
- Van Broeckhoven, C.: Alzheimer's Association International Conference 2015, Washington, USA, July 18-23, 2015. Loss-of-Function mutations in *TBK1* are frequently associated with frontotemporal lobar degeneration in a Belgian patient cohort.
- Philtjens, S.: EMBO | EMBL Symposium Mechanisms of Neurodegeneration, Heidelberg, Germany, June 14-17, 2015. Novel missense mutations in the vacuolar protein sorting 13 homolog C gene are associated with decreased endogenous protein expression in frontotemporal lobar degeneration.

National

Wauters E.: Identification of onset age modifier genes in frontotemporal lobar degeneration: an integrative family-based strategy. VIB Seminar 2014. Blankenberge, Belgium, April 28-30, 2014

Poster presentations

International

- Gijssels I.: *C9orf72* G4C2 repeat expansion size associates with genetic anticipation in FTLD and ALS. Human Genome Meeting 2014. Geneva, Switzerland, April 27-30 2014
- Wauters, E.: An integrative approach to identify onset age modifier genes in a large founder GRN FTLD family. 9th International Conference on Frontotemporal Dementias. Vancouver, Canada, October 23 – 25 2014
- Gijssels I.: *C9orf72* G4C2 repeat size associates with genetic anticipation, hyper-methylation and transcriptional down-regulation in FTLD and ALS. 9th International Conference on Frontotemporal Dementias. Vancouver, Canada, October 23 – 25 2014
- Cruts, M.: Genome-wide screen in FTLD/ALS patient cohorts for pathological G4C2 repeat expansions other than *C9orf72*. 9th International Conference on Frontotemporal Dementias. Vancouver, Canada, October 23 – 25 2014

- Wauters,E.: An integrative approach to identify onset age modifier genes in an extended Belgian GRN founder family. EMBO | EMBL Symposium Mechanisms of Neurodegeneration. Heidelberg, Germany, June 14-17 2015
- Philtjens, S: Novel missense mutations in the vacuolar protein sorting 13 homolog C gene are associated with decreased endogenous protein expression in frontotemporal lobar degeneration. EMBO | EMBL Symposium Mechanisms of Neurodegeneration, Heidelberg, Germany, June 14-17 2015.
- Cruts,M.: Molecular mechanism of genetic anticipation in C9orf72 repeat expansion families. 2016 International Conference of FTD (ICFTD2016), Munich, Germany, August 31 - September 2 2016
- Philtjens,S: Unraveling the genetic role of SORT1 in the Belgian frontotemporal dementia population. 2016 International Conference of FTD (ICFTD2016), Munich, Germany, August 31 - September 2 2016
- Wauters,E.: The Belgian GRN founder family anno 2016: a textbook example of phenotype heterogeneity. 2016 International Conference of FTD (ICFTD2016), Munich, Germany, August 31 - September 2 2016

National

- Wauters E.: An integrative approach to identify onset age modifier genes in a large founder GRN FTLD family. Annual Scientific IAP Meeting. Antwerp, Belgium, October 3, 2014



Geneeskundige Stichting Koningin Elisabeth
Fondation Médicale Reine Elisabeth
Königin-Elisabeth-Stiftung für Medizin
Queen Elisabeth Medical Foundation

Final report
of the research group of

Prof. dr. Stefanie Dedeurwaerdere, PhD

Universiteit Antwerpen (UA)

Principal investigator

Prof. dr. Stefanie Dedeurwaerdere, PhD
Head Experimental Laboratory of Translational Neuroscience and Otolaryngology

PhD Students

Halima Amhaoul, Daniele Bertoglio

Postdoc

Idrish Ali

Laboratory Assistant

Annemie Van Eetveldt

Department of Translational Neurosciences
Campus Drie Eiken
Universiteitsplein 1
2610 Wilrijk
T +32 3 265 26 38
Stefanie.Dedeurwaerdere@uantwerp.be

Table of contents

1. Scientific report of the progress made in 2016
 - Specific Aims
 - (A1&A2) Brain inflammation in a chronic epilepsy model: characterising the spatiotemporal evolution of the translocator protein using post-mortem and in vivo techniques
 - (A3) The effect of TSPO on brain inflammation and steroid synthesis
 - (A4) Non-invasive PET imaging of brain inflammation at disease onset predicts spontaneous recurrent seizures and reflects comorbidities 6
 - (A4) To unravel the role of TSPO in the development of chronic epilepsy
2. Budget
4. Scientific Activities
 - Publications acknowledging G.S.K.E support
 - Presentations at national and international scientific meetings
 - Invited lectures
 - Oral presentations
 - Poster presentations

Translocator protein expression in temporal lobe epilepsy: picturing a Janus face?

1. Scientific report of the progress made in 2015

Epilepsy is a chronic neurological condition characterized by recurrent seizures that affects about 65 millions of people worldwide. Epilepsy has a severe effect not only on the individual, but also on society since the estimated total cost of epilepsy in Europe in 2004 was over €15.5 billion. Temporal lobe epilepsy (TLE) is the most common and severe form of focal acquired epilepsy in humans and it is associated with psychiatric comorbidities such as anxiety and depression. Current drugs available are purely symptomatic, have many side effects, and in addition up to 40% of epilepsy patients still remain resistant to anti-epileptic drugs. Epileptogenesis is a dynamic disease process starting before the first symptoms/seizures occur. However, the neurobiological processes that result in acquired epilepsy still remain unclear, impeding the development of more potent, targeted and disease-modifying treatments.

1.1. Specific Aims

To fully exploit the potential of the translocator protein (TSPO) as an anti-inflammatory target or a biomarker for epilepsy on the long term, the objective of this proposal is to tease out the complexities of TSPO upregulation in a model of TLE.

The specific aims to meet this objective are:

- (A1) to describe the spatial and temporal profile of TSPO expression during epileptogenesis starting from the initiating insult until established epilepsy;
- (A2) to evaluate TSPO expression in multiple brain cell types during disease ontogenesis;
- (A3) to study the effect of TSPO on brain inflammation and steroid synthesis;
- (A4) to unravel the role of TSPO in the development of chronic epilepsy.

The experiments performed during 2014-2016 regarding the four aims resulted in several poster and oral presentations and publications of research papers in highly reputed journals such as *Brain*, *Behavior*, and *Immunity* (Impact Factor 2015= 5.874), *Neurobiology of Disease* (Impact Factor 2014= 5.078) and *Neuropharmacology* (Impact Factor 2015= 4.936). We have made significant progress regarding other remaining aims, resulting in research papers that are under revision for publication or in preparation.

1.2. (A1&2) Brain inflammation in a chronic epilepsy model: Evolving pattern of the translocator protein during epileptogenesis. (Amhaoul et al., *Neurobiol Dis* 2015)

A hallmark in the neuropathology of TLE is brain inflammation, which has been suggested as both a biomarker and new mechanism for treatments. TSPO, due to its high upregulation under neuroinflammatory conditions and the availability of selective Positron Emission Tomography (PET) tracers, is a candidate target. An important step to exploit this target is a thorough characterisation of the spatiotemporal profile of TSPO during epileptogenesis. In this regard, we have performed a detailed study that was published in *Neurobiology of Disease* in 2015. A detailed scientific insight regarding this study has been provided in our previous report (report 2015).

Under this aim, one of our research question was also to describe the cell type location of TSPO, more specifically to identify whether TSPO is also present on alternatively (M2) activated glial cell types. A regulatory role of TSPO expression on neuroinflammation in microglial cell lines has also been reported, revealing that an increased expression of TSPO is associated with enhanced M2 signalling (Bae et al. 2014). Moreover, a recent study reported an increase in the TSPO and CD206 (marker of M2) colocalised

cells in a mouse model of neuroinflammation induced by intracerebral hemorrhage as compared to the sham animals. At the same time, there was also increased colocalisation of TSPO with CD16/32 positive cells (a marker of M1) in this model (Bonsack et al., 2016, J. Neuroinflammation). Findings from these studies suggest that TSPO can be colocalised with both M1 and M2 polarised cells and may have a regulatory effect on neuroinflammation depending on the pathological environment.

With an aim to confirm these reports in our model of temporal lobe epilepsy, we performed multiple staining at brain sections from different time points. However, we did not observe any markers of M2 activation in glial cells. To address this issue, we decided to test this hypothesis in a mouse model of epilepsy, which were also implanted with interleukine-13 (IL-13) over-expressing cell grafts. IL-13 is an anti-inflammatory cytokine and a strong inducer of M2a microglia/macrophage activation. Accordingly, the site of cell grafts which gets infiltrated with microglia/macrophage due to immune response to these cells, are reported to express markers of M2 activation. While performing the evaluation of TSPO signals in this mouse model using autoradiographic technique, 2w after the intrahippocampal kainic acid injections, we observed a strong expression of TSPO on the area of cell graft (Figure 1A). We confirmed with double immunofluorescence imaging that the graft cells were indeed M2 positive, as suggested by expression of Ym1 (figure 1B) and also expressed TSPO (Figure 1C& D) (to be submitted). Thus our data is in line with previous findings that TSPO is co-expressed on not only M1 activated cells but are also present on M2 activated cells. More studies are needed to identify whether it has a regulatory role in epileptogenic environment.

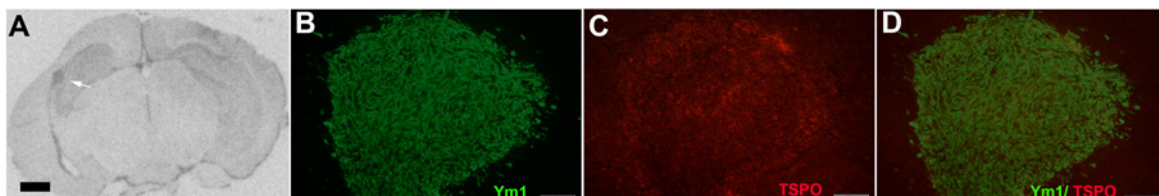


Figure 1: Translocator protein (TSPO) expression on M2 polarised microglia/macrophages. (A) A representative autoradiographic image is shown that displays strong expression of TSPO at the location of graft in the hippocampus. High magnification immunofluorescence images show expression of (B) Ym1 (green), a marker of M2 polarisation and (B) TSPO (red) on the graft site. A merged image is shown in (D). Scale bar for image A is 1 mm and for images B-D is 100 µm.

1.3. (A3) the effect of TSPO on brain inflammation and steroid synthesis

To provide insights in the role of TSPO in brain inflammation in a model of MTLE, we have performed experiments in a TSPO knockout strain of mice with c57bl/6 background. The project is described in more details in next section since it also provided details on effects of TSPO on epileptogenesis.

To investigate the link between TSPO and steroid synthesis, we analysed several brain samples for the presence of neurosteroid pregnenolone sulphate with mass spectrophotometric techniques together with our collaborator Prof. Giuseppe Biagini (Unimore, Italy) using Mass spectrophotometric analysis. Brains from Wistar rats were collected one week after the induction of KASE. One hemisphere of the brain was fresh frozen and retained for evaluating TSPO expression using autoradiographic analysis, whereas the other hemisphere was sent to Université de Paris Sud, for quantification of pregnenolone sulphate. We have obtained interesting data from our pilot study (n=5 rats) that showed direct correlation of the protein concentration of pregnenolone sulphate in the whole brain (minus cerebellum) to the expression of TSPO in the amygdala and piriform cortex (Figure 2). It is important to note that amygdala and piriform cortex are the two regions where there is highest expression of TSPO at one week time point after SE. More studies are needed including pharmacological intervention studies in both control and epileptic animals to confirm whether increasing or decreasing TSPO levels directly affect neurosteroid levels.

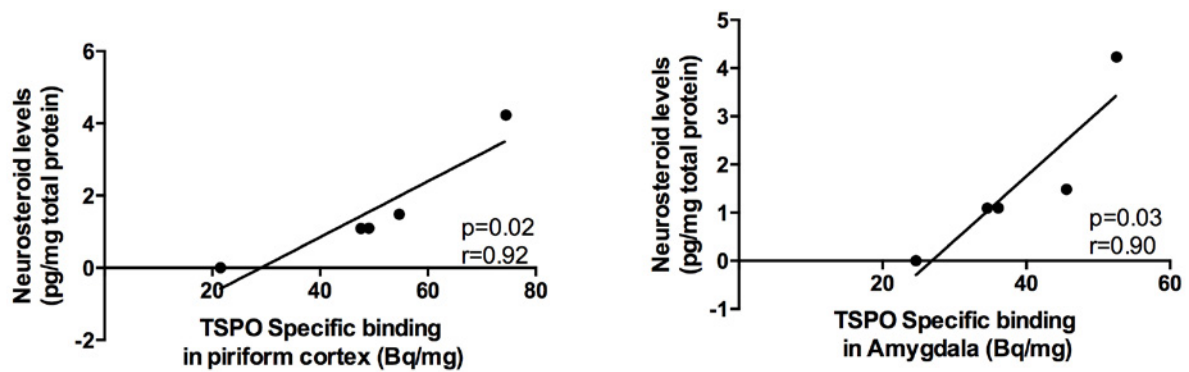


Figure 2: Graphs showing significant correlation between the levels of Pregnenolone sulphate and TSPO expression levels in the piriform cortex and amygdala.

1.4. (A4) Non-invasive PET imaging of brain inflammation at disease onset predicts spontaneous recurrent seizures and reflects comorbidities (Bertoglio et al., Article in press)

Post-traumatic epilepsy often occurs following a latent period of months to years as a consequence of a brain insult. Although this latent period clearly represents a therapeutic window, we have not been able to stratify patients at risk for post-traumatic epilepsy. Brain inflammation has been recognized as an important factor in the pathology of various types of epilepsy. The aim of the study was to determine network alterations associated with the process of epileptogenesis by means of TSPO PET scans, a biomarker of neuroinflammation, in the KASE model. We characterized the evolution profile of TSPO at 2 and 4 weeks post *status epilepticus* during epileptogenesis. Animals were recorded by video-EEG monitoring during the experiment. The recording started the day of the induction of *status epilepticus* for the entire period of the study (3 months) in order to obtain an exhaustive profile of the seizures for each animal. In addition, behavioural tests indicative of sensorimotor-related and depression-like comorbidities were performed.

We found that TSPO was highly up regulated 2 weeks post-SE in limbic structures (up to 2.1-fold increase compared to controls in temporal lobe, $P < 0.001$), whereas 4 weeks post-SE, upregulation decreased (up to 1.6-fold increase compared to controls in temporal lobe, $P < 0.01$) and was only apparent in a subset of these regions. Regional PET imaging did not correlate with spontaneous recurrent seizures (SRS) frequency (range 0.0 – 0.83 SRS/day), however, by applying a multivariate data-driven modelling approach based on TSPO PET imaging at 2 weeks post-SE, we accurately predicted the frequency of SRS ($R = 0.92$; $R^2 = 0.86$; $P < 0.0001$) at the onset of epilepsy (Figure 3).

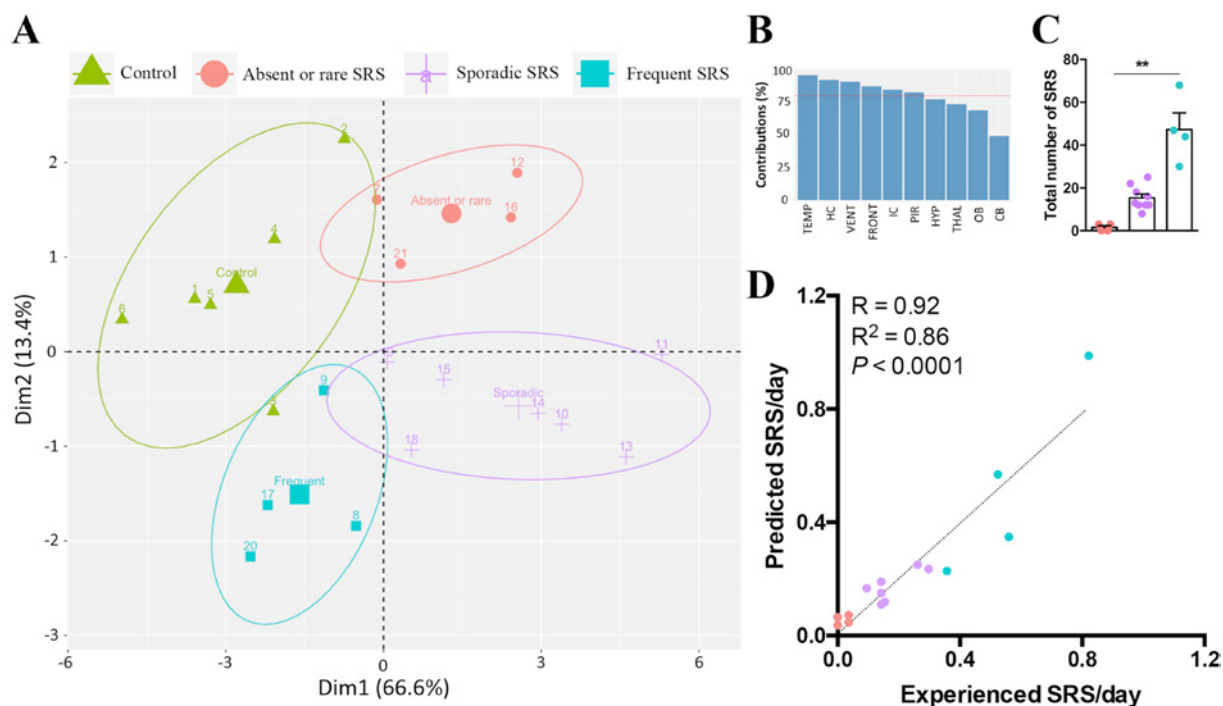


Figure 3. [18F]-PBR111 PET 2 weeks post-SE predicts SRS outcome. (A) Principal component analysis (PCA) of [18F]-PBR111 2 weeks post-SE ($n = 21$). PCA represents PET data in a two-dimensional space accounting for 80% of the total variability of the dataset. (B) Contribution of each VOI to explaining PCA variability. VOIs above the red line had a major influence; the temporal lobe and hippocampus were found to be the most relevant regions in explaining the variability in the dataset. (C) Differences in SRS experienced by the three subcategories of KASE animals determined based on PCA. Absent or rare SRS ($n = 4$), sporadic SRS ($n = 7$) and frequent SRS ($n = 4$). A Kruskal-Wallis test with a post-hoc Dunn's multiple comparison test. $**P < 0.01$. (D) Partial least squares regression generated a model that can predict SRS frequency for each subject ($n = 15$). The graph reports the number of experienced SRS/day (measured) versus the number of predicted SRS/day (estimated) for the model. Spearman's rank correlation. Each symbol represents one animal (A, C and D) SRS = spontaneous recurrent seizures; OB = olfactory bulb, FRONT = frontal cortex, IC = insular cortex, PIR = anterior piriform cortex, THA = thalamus, HYP = hypothalamus, HC = hippocampus, TEMP = extrahippocampal temporal lobe, CB = cerebellum

In addition, TSPO PET imaging at onset of epilepsy showed a clear relationship with behavioural tests performed during chronic epilepsy to determine depression-like and sensorimotor-related comorbidities (Figure 4). Whiskers nuisance task (WNT) has been performed 9 and 11 weeks post-SE. This test reflects damages and circuitry alteration of the somatosensory cortex, taking into account anxiety and aggressiveness of the animals. KASE rats showed significant higher scores than controls ($P < 0.01$ and $P < 0.05$, respectively), moreover the results positively correlated with TSPO levels during epileptogenesis (Figure 4A and 4B) in several brain regions (hippocampus, temporal lobe, insular cortex, endopiriform cortex, ventricles, and hypothalamus). Depression-like behaviour has been tested 12 weeks post-SE by means of sugar preference test (SPT) and forced swim test (FST). Sugar preference during the chronic phase was significantly lower in KASE rats ($P < 0.01$), and it negatively correlated with TSPO levels during epileptogenesis (Figure 4C) in several brain regions (hippocampus, temporal lobe, insular cortex, ventricles). Finally, KASE rats spent significantly longer time immobile during the FST ($P < 0.05$) as indication of behavioural-despair, and the immobility time positively correlated with TSPO levels during epileptogenesis (Figure 4D).

In conclusion, these results not only demonstrate TSPO PET imaging to be a valid prognostic biomarker to ascertain SRS frequency, but also to determine the severity of depression-like and somatosensory comorbidities. Because we scanned the animal at the start of the disease onset, our findings have a high clinical relevance.

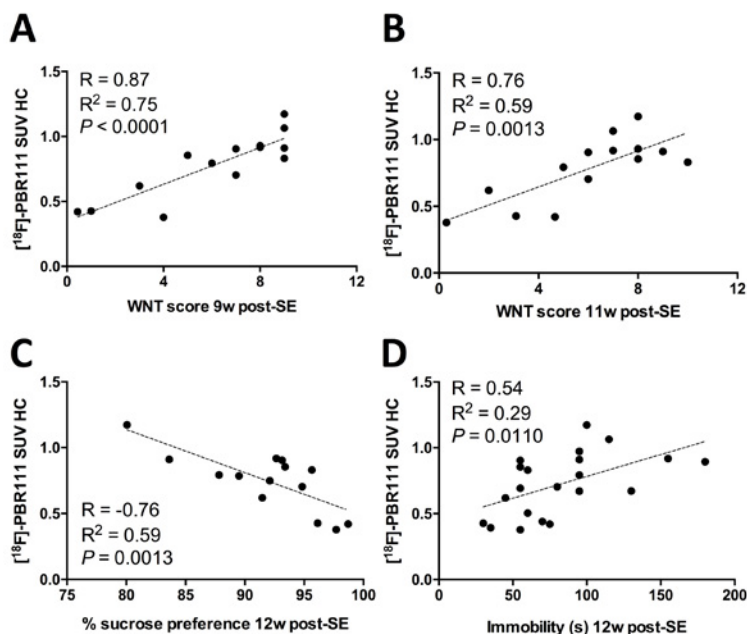


Figure 4. Relationship between TSPO during epileptogenesis and comorbidities during the chronic phase. A positive and significant relationship can be established between TSPO expression in hippocampus 2 weeks post-SE and WNT scores 9 and 11 weeks post-SE (A-B). A negative and significant relationship can be established between TSPO expression in hippocampus 2 weeks post-SE and SPT 12 weeks post-SE (C) as well as with the temporal lobe (D). Pearson correlation test. ** $P < 0.01$, *** $P < 0.001$, **** $P < 0.0001$. HC = hippocampus, SE = status epilepticus, SUV = standardized uptake value.

1.5. (A4) To unravel the role of TSPO in the development of chronic epilepsy. (Amhaoul et al., Neuropharmacology 2016 & Bertoglio et al. manuscript under preparation)

To identify the role of TSPO in brain inflammation and epileptogenesis, we collaborated with Prof. Marie-Claude Grégoire and Prof. Richard Banati from ANSTO (Australia) to use a recently generated TSPO KO mouse line. This study allows us to discern the effect of TSPO on brain inflammation (A3) and to evaluate the role of TSPO during disease ontogenesis of epilepsy (A4).

The aim of the study was to determine the effect of TSPO knockout on disease ontogenesis, seizure outcome, and brain inflammation in a rodent model of acquired epilepsy. The induction of SE was performed by intrahippocampal injection of KA to develop temporal lobe epilepsy. After the induction of SE, TSPO KO and WT were monitored during the disease ontogenesis by video-EEG recording to assess the latency to the first SRS and progression for a total of 3.5 weeks (24/7). Animals were vEEG monitored again for 10 days (24/7) when the disease was established (8-10 weeks post-SE) to evaluate SRS during chronic epilepsy.

We found that both KASE wt ($n = 17$) and KASE TSPO KO ($n = 14$) mice experienced a comparable SE following intra-hippocampal injection of KA (Figure 5). No difference was noticed ($P > 0.05$ for all variables) in duration of SE (KASE wt = 13.7 ± 2.1 h; KASE TSPO KO = 13.1 ± 2.1 h, Figure 5A), number of seizure events (KASE wt = 9.1 ± 1.7 ; KASE TSPO KO = 7.3 ± 1.8 , Figure 5B), and severity of SE (KASE wt = 4 ± 0.2 score; KASE TSPO KO = 3.3 ± 0.2 score, Figure 5C).



Figure 5. SE characterization in KASE wt and KASE TSPO KO mice. The two epileptic groups did not differ in duration of SE (A), number of seizures during SE (B), and severity of SE (C). Mann-Whitney U test. KASE wt ($n = 17$), KASE TSPO KO ($n = 14$). SE = status epilepticus, TSPO = translocator protein.

Six KASE wt and 3 KASE TSPO KO died following a severe SRS during the monitoring period. SRS were detected in all the KASE mice from both groups. The latency to the first SRS was 9.9 ± 1.8 days post-SE and 8.6 ± 1.2 days post-SE for KASE wt and KASE TSPO KO, respectively (Figure 6A). Also the average duration of SRS did not differ between the 2 epileptic groups (KASE wt = 44.6 ± 1.8 sec; KASE TSPO KO = 43 ± 2.2 sec, Figure 6B).

Furthermore, the SRS frequency at the different stages of the disease (early and chronic phases) did not significantly differ between the investigated groups ($P > 0.05$): SRS frequency during early phase was 1 ± 0.23 SRS/day for KASE wt and 0.8 ± 0.21 for KASE TSPO KO (Figure 6C). During the chronic phase, SRS frequency was 2.8 ± 1.2 SRS/day for KASE wt and 4.2 ± 1.8 SRS/day for KASE TSPO KO (Figure 6D).

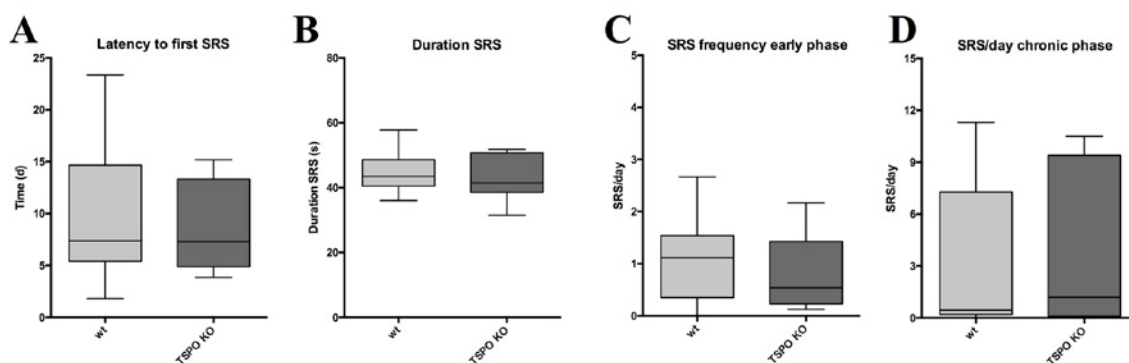


Figure 6. SRS evaluation in KASE wt and KASE TSPO KO mice. The two epileptic groups did not differ in latency to the first SRS (A), duration of SRS (B), SRS frequency during early phase (C), and SRS frequency during chronic phase (D). Mann-Whitney U test. KASE wt ($n = 9-17$), KASE TSPO KO ($n = 8-14$). SRS = spontaneous recurrent seizures, TSPO = translocator protein.

To ascertain that the genotype of the KO animals was correct, we repeated the genotyping at the end of the experiment (Figure 7). The knockout of TSPO was performed as previously described by our collaborator (Banati et al., 2014). As expected, the genotyping confirmed that all wt animals were $Tspo^{+/+}$ (683 bp), while TSPO KO mice were $Tspo^{-/-}$ (333 bp). Based on these results, it appears that the knockout of TSPO does not affect any of the investigated variables related to seizure development and occurrence.

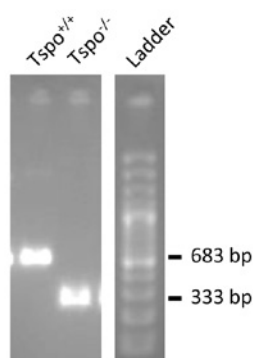


Figure 7. Confirmation of genotype. By deletion of exons 2 and 3, only exons 1 and 4 remain. Therefore $Tspo$ knockout produces a cDNA of 333bp, shorter than the wildtype genotype (683 bp).

Since we did not find any differences in epileptogenesis, we decided not to pursue the pharmacological intervention studies on post-SE epileptogenesis. However, as mentioned in our previous report, we aimed to further identify the role of neuroinflammation in epileptic seizure pathology. We used a pharmacological blocker (JNJ-42253432) of P2X7 receptors, a key receptor involved in the synthesis and release of a pro-inflammatory cytokine IL-1 β . In SD rats 3 months after KASE, one-week of vehicle treatment (20% HP- β -cyclodextrin) was followed by one week of JNJ-42253432 treatment subcutaneously under continuous vEEG monitoring ($n = 17$). We observed a significant decrease of the proportion of type 4 and 5 severe SRS ($p < 0.05$), whereas an increase of type 1-3 seizures was demonstrated ($p < 0.05$) while comparing the treatment to the vehicle period (Figure 7). There was no effect of the P2X7R antagonist on the number of SRS/day, the glial marker or TSPO expression (Figure 7).

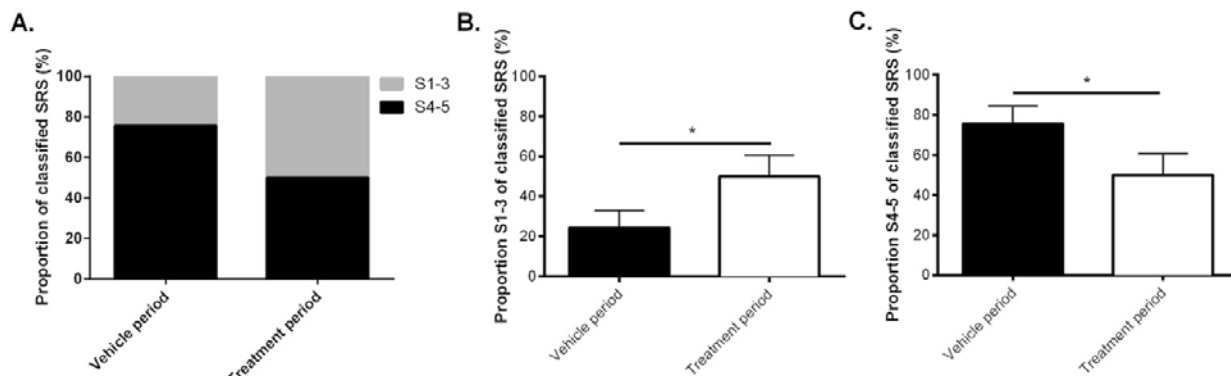


Fig. 7. A. Shift in seizure severity from severe classes (S4-5) to milder classes (S1-3). SRS were categorised into different seizure severity classes from S1-3 and S4-5. Their proportion of the total number of classified SRS is expressed on the Y-axis for the two treatment periods. B.-C. The P2X7R antagonist had a beneficial effect on the severity of the SRS. When comparing the vehicle period with the treatment period, a significant decrease was found for the proportion of the severe convulsive SRS S4-5. In contrast, a significant increase of the milder seizures, including S1-3, was demonstrated. $n = 11$ (only animals that had SRS during both periods were included). Data are represented as mean \pm SEM; * $p < 0.05$; Wilcoxon-signed rank test. Abbreviation: SRS = spontaneous recurrent seizures.

Overall, the P2X7R antagonist gave rise to a less severe profile of chronic seizures, without suppressing the SRS frequency and the levels of microglia or astrocyte activation. This finding is consistent with the expression levels of TSPO, which did not change between the vehicle and treatment period (Figure 8). More studies are needed to evaluate whether TSPO expression can represent changes in the level of neuroinflammation following an anti-epileptic treatment.

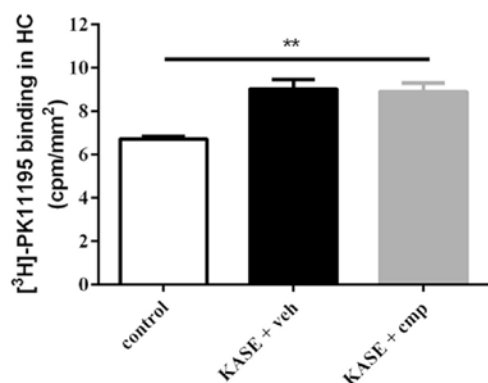


Fig. 8. The P2X7R antagonist had no effect on TSPO levels. A significant increase of the TSPO expression was shown for the hippocampus when comparing the treated KASE group to the naive control group. However, no significant differences could be demonstrated when comparing the vehicle KASE with the treated KASE group. n naive control group = 6; n vehicle KASE group = 3; n treated KASE group = 16. Data are represented as mean \pm SEM; ** $p < 0.01$; KruskalWallis test with post-hoc Dunn's multiple comparisons test. Abbreviations: HC = hippocampus, KASE = kainic acidinduced status epilepticus, veh = vehicle, emp = compound.

2. Budget

As outlined in the description of the project proposal and last year's report, the 2016 budget received from the GSKE was amended for the salary of the laboratory assistant & postdoc, to support animal purchase and various lab consumables.

3. Scientific activities

3.1. Publications acknowledging G.S.K.E support in chronological order:

2016

PhD Thesis:

1. 'Evaluation of brain inflammation in a rat model for temporal lobe epilepsy' 2016, by Halima Amhaoul.

Peer reviewed publications:

1. **Halima Amhaoul, Idrish Ali, Marco Mola, Annemie Van Eetveldt, Krystyna Szewczyk, Stephan Missault, Kenny Bielen, Samir-Kumar Singh, Jason Rech, Brian Lord, Marc Ceusters, Anindya Bhattacharya, Stefanie Dedeurwaerdere**, 2016, P2X7 receptor antagonism modifies seizure severity in a chronic model of temporal lobe epilepsy, *Neuropharmacology*, 105; 175, **IF: 4.936**
2. **Idrish Ali, Stephanie Boets, Pieter Janssens, Annemie Van Eetveldt, Halima Amhaoul, Xavier Langlois, Stefanie Dedeurwaerdere** 2016, Metabotropic glutamate receptor 2/3 density and its relation to the hippocampal neuropathology in a model of temporal lobe epilepsy, *Epilepsy Research*, 127; 55, **IF: 2.237**
3. Markus Aswendt, Martin Schwarz, Walid M. Abdelmoula, Jouke Dijkstra, **Stefanie Dedeurwaerdere**, 2016, Whole-Brain Microscopy Meets In Vivo Neuroimaging: Techniques, Benefits, and Limitations, *Molecular Imaging & Biology*, DOI: 10.1007/s11307-016-0988-z, **IF: 2.569**
4. **Bertoglio D, Verhaeghe J, Santermans E, Amhaoul H, Jonckers E, Wyffels L, Van Der Linden A, Hens N, Staelens S, Dedeurwaerdere S**, 2016, Non-invasive PET imaging of brain inflammation at disease onset predicts spontaneous recurrent seizures and reflects comorbidities, Article in press. *Brain, Behavior, and Immunity*. DOI: 10.1016/j.bbi.2016.12.015. **IF: 5.874**
5. van Vliet EA, **Dedeurwaerdere S**, Cole AJ, Friedman A, Koeppe MJ, Potschka H, Immonen R, Pitkänen A, 2016, Federico P, Workshop on neurobiology of epilepsy appraisal: Imaging biomarkers in epilepsy. *Epilepsia*, doi: 10.1111/epi.13621, **IF: 4.706**
6. **Amhaoul H, Bertoglio D, Houbrechts R, Van De Vijver S, Van Dam D, De Deyn PP, Ali I, Dedeurwaerdere S**, Kainic acid-induced rat models of temporal lobe epilepsy with high and low prevalence of spontaneous recurrent seizures. **In preparation for Epilepsia.**

2015

1. **Amhaoul H, Hamaide J, Bertoglio D, Reichel SN, Verhaeghe J, Geerts E, Van Dam D, De Deyn PP, Kumar-Singh S, Katsifis A, Van Der Linden A, Staelens S, Dedeurwaerdere S**. Brain inflammation in a chronic epilepsy model: Evolving pattern of the translocator protein during epileptogenesis. *Neurobiol Dis.* 2015 Oct;82:526 **IF: 5.078**

2014

1. Pitkänen A, Nodge-Ekane XE, Lukasiuk K, Wilczynski GM, Dityatev A, Walker MC, Chabrol E, **Dedeurwaerdere S**, Vazquez N, Powell EM. Neural ECM and epilepsy. *Prog Brain Res.* 2014;214:229-62.
2. **Amhaoul H, Staelens S, Dedeurwaerdere S**. Imaging brain inflammation in epilepsy. *Neuroscience.* 2014 Oct 24;279:238-52. **IF: 3.231**

3.2. Presentations at national and international scientific meetings

Invited Lectures

Stefanie Dedeurwaerdere

13/10/2016	IIE2016 meeting Immunity and Inflammation in Epilepsy: Imaging of glia as a biomarker of epileptogenesis	Milan, Italy
11/09/2016	12th ECE, Perinatal inflammation: does it contribute to neurodevelopmental deficits?	Prague, Czech Republic
13/09/2016	12th ECE, PET imaging as a biomarker of epileptogenesis?	Prague, Czech Republic
21/04/2016	9th International Symposium on Neuroprotection&Neurorepair: Imaging brain inflammation following brain trauma: implications for acquired epilepsy	Leipzig, Germany
28/01/2016	SWO Midwinter meeting, Molecular imaging in animals models of epilepsy (invited speaker)	Amsterdam, The Netherlands
10/2/2015	Speakers' series of the German Center for Neurodegenerative Diseases (DZNE): Nuclear imaging of maladaptive repair in acquired epilepsy models: opportunities for translational investigations of neuroinflammation and extracellular matrix alterations	Magdeburg, Germany

2/11/2015	1st ECMED workshop , <i>Animal models of epilepsy</i>	Magdeburg, Germany
30/09/2015	UCB summit I , <i>Imaging of brain inflammation biomarkers in epilepsy</i>	Braine l'Alleud, Belgium
29/06-3/7/2014	11th European Congress on Epileptology: PET imaging in models of epileptogenesis and chronic epilepsy.	Stockholm, Sweden

Oral presentation:

Stefanie Dedeurwaerdere

30/01/2016	SWO Midwinter meeting 2016: 'Neuroimaging in Epilepsy': <i>Modulating neuroinflammation as an approach to target temporal lobe epilepsy'</i>	Amsterdam, The Netherlands
18-20/03/2015	European Molecular Imaging Meeting (EMIM) 2015: <i>Identifying brain network dysfunctions during epileptogenesis in a model of temporal lobe epilepsy</i>	Tubingen, Germany
03/09/2015	WONOE 2015: <i>Identifying brain network dysfunctions during epileptogenesis in a model of temporal lobe epilepsy</i>	Istanbul, Turkey

Idrish Ali

30/01/2016	SWO Midwinter meeting 2016: 'Neuroimaging in Epilepsy': <i>Modulating neuroinflammation as an approach to target temporal lobe epilepsy'</i>	Amsterdam, The Netherlands
------------	---	----------------------------

Daniele Bertoglio

08-10/03/2016	European Molecular Imaging Meeting (EMIM) 2016: <i>TSPO PET imaging as a biomarker to predict behavioural comorbidities in a rat model of temporal lobe epilepsy</i>	Utrecht, The Netherlands
---------------	---	--------------------------

Halima Amhaoul

01-06/02/2015	Hot Topics in Molecular Imaging (TOPIM) 2015: <i>Translocator protein as a neuroimaging biomarker of epileptogenesis in a rodent model of temporal lobe epilepsy.</i>	Les Houches, France
---------------	--	---------------------

Poster presentations (presenting author)

Stefanie Dedeurwaerdere

21-24/05/2014	NRM2014: Follow-up of early brain inflammation in a rodent model of epileptogenesis with post-mortem and in vivo imaging techniques.	Amsterdam, The Netherlands
17-22/08/2014	Gordon Research Conference on Mechanisms of Epilepsy & Neuronal Synchronization: Translocator protein as a neuroimaging biomarker of epileptogenesis in a rodent model of temporal lobe epilepsy	West Dover, USA

Daniele Bertoglio

20-26/08/2016	Gordon Research Conference (GRC) and Seminar (GRS) mechanisms of epilepsy and neuronal synchronization: <i>Data-driven modeling of brain inflammation predicts seizure burden and abnormal behavior in a rat model of temporal lobe epilepsy</i>	Girona, Spain
11/03/2015	Sectie Wetenschappelijk Onderzoek (SWO) Meeting 2015: <i>Identifying brain network dysfunction during epileptogenesis in a model of temporal lobe epilepsy.</i>	Amsterdam, The Netherlands
22/05/2015	11th Meeting of the Belgian Society for Neuroscience: Identifying brain network dysfunction during epileptogenesis in a model of temporal lobe epilepsy.	Mons, Belgium

Halima Amhaoul

18-20/03/2015	European Molecular Imaging Meeting (EMIM) 2015: <i>Characterising the spatiotemporal evolution of the translocator protein using post mortem and in vivo techniques in the KASE model of temporal lobe epilepsy.</i>	Tubingen, Germany
24-25/04/2014	Imaging Neuroinflammation in Neurodegenerative Diseases (INMiND) TSPO Symposium 2014: Brain inflammation and epileptogenesis: a role for TSPO?	Manchester, United Kingdom
4-6/06/2014	European Molecular Imaging Meeting (EMIM) 2014: Brain inflammation in a chronic epilepsy model: determining the spatiotemporal profile of glial activation by in vivo 18F-PBR111 PET and standard immunohistochemistry techniques	Antwerp, Belgium



Geneeskundige Stichting Koningin Elisabeth
Fondation Médicale Reine Elisabeth
Königin-Elisabeth-Stiftung für Medizin
Queen Elisabeth Medical Foundation

Final report
of the research group of

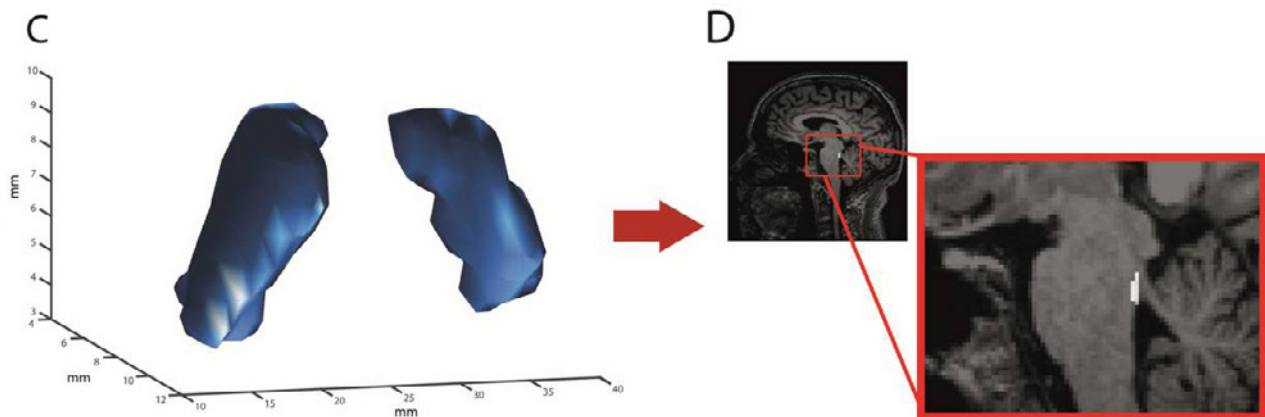
Julie Duque,
Prof. dr. Etienne Olivier, PhD (†) &
dr. Alexandre Zénnon

Université Catholique de Louvain (UCL)

Address for correspondence:

Julie Duque, Prof. dr. Etienne Olivier, PhD & dr. Alexandre Zénon
Institute of Neuroscience
School of Medicine
University of Louvain
Avenue Mounier, 53
COSY- B1.53.04
B-1200 BRUSSELS Belgium
T +32 2 764 54 44
F +32 2 764 54 65
etienne.olivier@UCLouvain.be

Parkinson's disease revisited. A new vision of basal ganglia functions in the context of the Parkinson's disease



1. Introduction

Parkinson's disease (PD) is the second most frequent neurodegenerative disease, caused by a neuronal loss in the pars compacta of Substantia Nigra (SNc), leading to a depletion of dopamine in the striatum. PD is characterized by well-known motor symptoms, namely bradykinesia, rigidity, resting tremor and postural instability, although non-motor symptoms, such as sleep and emotional disorders, are increasingly recognized as an integral part of the clinical picture of PD. However, despite decades of extensive investigation, the precise role of the basal ganglia (BG) to motor and non-motor functions, and their contribution to PD symptoms, are still under heated debates.

Indeed, the exact link between the dopamine depletion in the striatum and motor and non-motor symptoms of PD remains puzzling. Recently, it has been suggested that the loss of dopaminergic neurons in the SNc could affect the reward and decision-making processes and, thus, the main cause of bradykinesia could be the inability to adjust the level of effort invested in movements due to an inappropriate estimate of their cost/benefit ratio. These observations have led to an interesting hypothesis about the role of BG in controlling the movement "vigor" according to motivational factors.

Amongst the motor functions assigned to the BG, a significant one is the storage and recall of overlearned sequential skills. Interestingly, it has been shown recently that the putamen, a part of the striatum, is recruited during chunking, a mechanism which permits to group discrete movements as a single complex action. To determine the neural correlates of chunking, and the contribution of BG to chunking in particular, is the second main question addressed in this project.

Finally, as aforementioned, non-motor symptoms of PD remain largely under-appreciated and under-investigated, although some of them have a significant negative impact on the quality of life of PD patients. Because these non-motor symptoms have a relatively poor response to dopamine replacement therapy, they may involve the serotonergic and noradrenergic systems. One of the most common non-motor symptoms associated with PD is fatigue and interestingly, it has been show that the locus coeruleus – which plays a key role in arousal and is the main source of noradrenaline in the central nervous system – is involved at an earlier (pre-motor) stage of the PD than the SNc (Braak et al., 2003). Investigating these non-motor symptoms may open a possibility to identify individuals at risk in the population.

2. Contribution to the study of effort-based decision making and its link with dopamine

2.1. The Human Subthalamic Nucleus encodes the subjective value of reward and the cost of effort during decision-making

Adaptive behaviour entails the capacity to select actions as a function of their energy cost and expected value and the disruption of this faculty is now viewed as a possible cause of the symptoms of Parkinson's disease. Indirect evidence points to the involvement of the subthalamic nucleus-the most common target for deep brain stimulation in Parkinson's disease-in cost-benefit computation. However, this putative function appears at odds with the current view that the subthalamic nucleus is important for adjusting behaviour to conflict. Here we tested these contrasting hypotheses by recording the neuronal activity of the subthalamic nucleus of patients with Parkinson's disease during an effort-based decision task. Local field potentials were recorded from the subthalamic nucleus of 12 patients with advanced Parkinson's disease (mean age 63.8 years \pm 6.8; mean disease duration 9.4 years \pm 2.5) both OFF and ON levodopa while they had to decide whether to engage in an effort task based on the level of effort required and the value of the reward promised in return. The data were analysed using generalized linear mixed models and cluster-based permutation methods. Behaviourally, the probability of trial acceptance increased with the reward value and decreased with the required effort level. Dopamine replacement therapy increased the rate of acceptance for efforts associated with low rewards. When recording the subthalamic nucleus activity, we found a clear neural response to both reward and effort cues in the 1-10 Hz range. In addition these responses were informative of the subjective value of reward and level of effort rather than their actual quantities, such that they were predictive of the participant's decisions. OFF levodopa, this link with acceptance was weakened. Finally, we found that these responses did not index conflict, as they did not vary as a function of the distance from indifference in the acceptance decision. These findings show that low-frequency neuronal activity in the subthalamic nucleus may encode the information required to make cost-benefit comparisons, rather than signal conflict. The link between these neural responses and behaviour was stronger under dopamine replacement therapy. Our findings are consistent with the view that Parkinson's disease symptoms may be caused by a disruption of the processes involved in balancing the value of actions with their associated effort cost.

Zénon A, Duclos Y, Carron R, Witjas T, Baunez C, Régis J, et al. The human subthalamic nucleus encodes the subjective value of reward and the cost of effort during decision-making. *Brain*. 2016;139(6).

2.2. Dopamine manipulation affects response vigor independently of opportunity cost

Dopamine is known to be involved in regulating effort investment in relation to reward, and the disruption of this mechanism is thought to be central in some pathological situations such as Parkinson's disease, addiction, and depression. According to an influential model, dopamine plays this role by encoding the opportunity cost, i.e., the average value of forfeited actions, which is an important parameter to take into account when making decisions about which action to undertake and how fast to execute it. We tested this hypothesis by asking healthy human participants to perform two effort-based decision-making tasks, following either placebo or levodopa intake in a double blind within-subject protocol. In the effort-constrained task, there was a trade-off between the amount of force exerted and the time spent in executing the task, such that investing more effort decreased the opportunity cost. In the time-constrained task, the effort duration was constant, but exerting more force allowed the subject to earn more substantial reward instead of saving time. Contrary to the model predictions, we found that levodopa caused an increase in the force exerted only in the time-constrained task, in which there was no trade-off between effort and opportunity cost. In addition, a computational model showed that dopamine manipulation left the opportunity cost factor unaffected but altered the ratio between the effort cost and reinforcement value. These findings suggest that dopamine does not represent the opportunity cost but rather modulates how much effort a given reward is worth.

Zénon A, Devesse S, Olivier E. Dopamine manipulation affects response vigor independently of opportunity cost. J Neurosci. 2016;36(37).

2.3. Disrupting the supplementary motor area makes physical effort appear less effortful

The perception of physical effort is relatively unaffected by the suppression of sensory afferences, indicating that this function relies mostly on the processing of the central motor command. Neural signals in the supplementary motor area (SMA) correlate with the intensity of effort, suggesting that the motor signal involved in effort perception could originate from this area, but experimental evidence supporting this view is still lacking. Here, we tested this hypothesis by disrupting neural activity in SMA, in primary motor cortex (M1), or in a control site by means of continuous theta-burst transcranial magnetic stimulation, while measuring effort perception during grip forces of different intensities. After each grip force exertion, participants had the opportunity to either accept or refuse to replicate the same effort for varying amounts of reward. In addition to the subjective rating of perceived exertion, effort perception was estimated on the basis of the acceptance rate, the effort replication accuracy, the influence of the effort exerted in trial t on trial $t+1$, and pupil dilation. We found that disruption of SMA activity, but not of M1, led to a consistent decrease in effort perception, whatever the measure used to assess it. Accordingly, we modeled effort perception in a structural equation model and found that only SMA disruption led to a significant alteration of effort perception. These findings indicate that effort perception relies on the processing of a signal originating from motor-related neural circuits upstream of M1 and that SMA is a key node of this network.

Zénon A, Sidibé M, Olivier E. Disrupting the supplementary motor area makes physical effort appear less effortful. J Neurosci. 2015;35(23).

3. Contribution to the study of chunking

3.1. Chunking improves symbolic sequence processing and relies on working memory gating mechanisms

Chunking, namely the grouping of sequence elements in clusters, is ubiquitous during sequence processing, but its impact on performance remains debated. Here, we found that participants who adopted a consistent chunking strategy during symbolic sequence learning showed a greater improvement of their performance and a larger decrease in cognitive workload over time. Stronger reliance on chunking was also associated with higher scores in a WM updating task, suggesting the contribution of WM gating mechanisms to sequence chunking. Altogether, these results indicate that chunking is a cost-saving strategy that may enhance effectiveness of symbolic sequence learning.

Solopchuk O, Alamia A, Olivier E, Zénon A. Chunking improves symbolic sequence processing and relies on working memory gating mechanisms. Learn Mem. 2016;23(3).

3.2. Non-parametric Algorithm to Isolate Chunks in Response Sequences

Chunking consists in grouping items of a sequence into small clusters, named chunks, with the assumed goal of lessening working memory load. Despite extensive research, the current methods used to detect chunks, and to identify different chunking strategies, remain discordant and difficult to implement. Here, we propose a simple and reliable method to identify chunks in a sequence and to determine their stability across blocks. This algorithm is based on a ranking method and its major novelty is that it provides concomitantly both the features of individual chunk in a given sequence, and an overall index that quantifies the chunking pattern consistency across sequences. The analysis of simulated data confirmed the validity of our method in different conditions of noise, chunk lengths and chunk numbers; moreover, we found that this algorithm was particularly efficient in the noise range observed in real data, provided that at least 4 sequence repetitions were included in each experimental block. Furthermore, we applied this algorithm to actual reaction time series gathered from 3 published experiments and were

able to confirm the findings obtained in the original reports. In conclusion, this novel algorithm is easy to implement, is robust to outliers and provides concurrent and reliable estimation of chunk position and chunking dynamics, making it useful to study both sequence-specific and general chunking effects. The algorithm is available at: <https://github.com/artipago/Non-parametric-algorithm-to-isolate-chunks-in-response-sequences>.

Alamia A, Solopchuk O, Olivier E, Zénon A. Non-parametric algorithm to isolate chunks in response sequences. *Front Behav Neurosci.* 2016;10(SEP).

3.3. Chunking is not a key mechanism of motor sequence learning

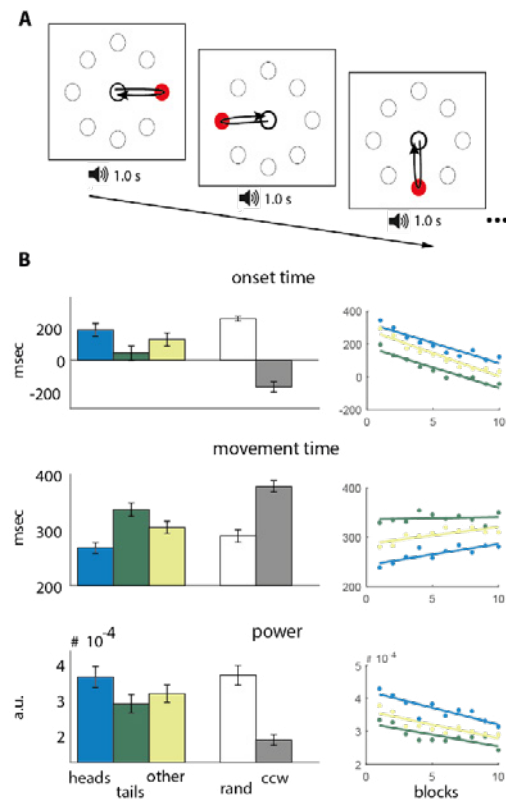


Figure 1. **A.** Subjects were asked to perform sequential movements towards one of eight targets, displayed as circles and located around the central point. **B.** All movement parameters differed significantly between chunk heads, chunk tails and non-chunk sequence items (**left panel**), but evolved similarly overtime (**right panel**).

Chunking, or grouping several sequence items together in an integrated working memory units, has been shown to improve learning rate and to decrease working memory load during symbolic sequence learning (Solopchuk et al. 2016). However, evidence on the role of chunking in motor sequence learning remains sparse and inconclusive. Here, we hypothesized that chunking could affect either only certain parameters of movement kinematics, only certain chunk components, or that it could be unrelated to sequence learning rate.

Nineteen healthy subjects learned a structured motor sequence using KINARM robotic device. We evaluated chunking by means of a novel algorithm and investigated its effect on several parameters of movement kinematics. We found that all of the movement parameters were significantly different between chunk heads, chunk tails and non-chunked sequence items, but all of them improved overtime irrespective of chunking strategies. Our results suggest that chunking may be independent of motor learning, presumably reflecting interactions between working memory limitations, idiosyncratic predispositions, task context, and individual biomechanical constraints.

Solopchuk O, Zénon A., Lefèvre P., Orban de Xivry JJ. Chunking is not a key mechanism of motor sequence learning. In preparation

3.4. Disruption of Broca's Area Alters Higher-order Chunking Processing during Perceptual Sequence Learning

Because Broca's area is known to be involved in many cognitive functions, including language, music, and action processing, several attempts have been made to propose a unifying theory of its role that emphasizes a possible contribution to syntactic processing. Recently, we have postulated that Broca's area might be involved in higher-order chunk processing during implicit learning of a motor sequence. Chunking is an information-processing mechanism that consists of grouping consecutive items in a sequence and is likely to be involved in all of the aforementioned cognitive processes. Demonstrating a contribution of Broca's area to chunking during the learning of a nonmotor sequence that does not involve language could shed new light on its function. To address this issue, we used offline MRI-guided TMS in healthy volunteers to disrupt the activity of either the posterior part of Broca's area (left Brodmann's area [BA] 44) or a control site just before participants learned a perceptual sequence structured in distinct hierarchical levels. We found that disruption of the left BA 44 increased the processing time of stimuli

representing the boundaries of higher-order chunks and modified the chunking strategy. The current results highlight the possible role of the left BA 44 in building up effector-independent representations of higher-order events in structured sequences. This might clarify the contribution of Broca's area in processing hierarchical structures, a key mechanism in many cognitive functions, such as language and composite actions.

Alamia A, Solopchuk O, D'Ausilio A, Van Bever V, Fadiga L, Olivier E, et al. Disruption of broca's area alters higher-order chunking processing during perceptual sequence learning. J Cogn Neurosci. 2016;28(3).

4. Contribution to the study of mental fatigue, including in Parkinson's disease

4.1. Dissociation between mental fatigue and motivational state during prolonged mental activity

Mental fatigue (MF) is commonly observed following prolonged cognitive activity and can have major repercussions on the daily life of patients as well as healthy individuals. Despite its important impact, the cognitive processes involved in MF remain largely unknown. An influential hypothesis states that MF does not arise from a disruption of overused neural processes but, rather, is caused by a progressive decrease in motivation-related task engagement. Here, to test this hypothesis, we measured various neural, autonomic, psychometric and behavioral signatures of MF and motivation (EEG, ECG, pupil size, eye blinks, Skin conductance responses (SCRs), questionnaires and performance in a working memory (WM) task) in healthy volunteers, while MF was induced by Sudoku tasks performed for 120 min. Moreover extrinsic motivation was manipulated by using different levels of monetary reward. We found that, during the course of the experiment, the participants' subjective feeling of fatigue increased and their performance worsened while their blink rate and heart rate variability (HRV) increased. Conversely, reward-induced EEG, pupillometric and skin conductance signal changes, regarded as indicators of task engagement, remained constant during the experiment, and failed to correlate with the indices of MF. In addition, MF did not affect a simple reaction time task, despite the strong influence of extrinsic motivation on this task. Finally, alterations of the motivational state through monetary incentives failed to compensate the effects of MF. These findings indicate that MF in healthy subjects is not caused by an alteration of task engagement but is likely to be the consequence of a decrease in the efficiency, or availability, of cognitive resources.

Gergelyfi M, Jacob B, Olivier E, Zénon A. Dissociation between mental fatigue and motivational state during prolonged mental activity. Front Behav Neurosci. 2015;9(JULY).

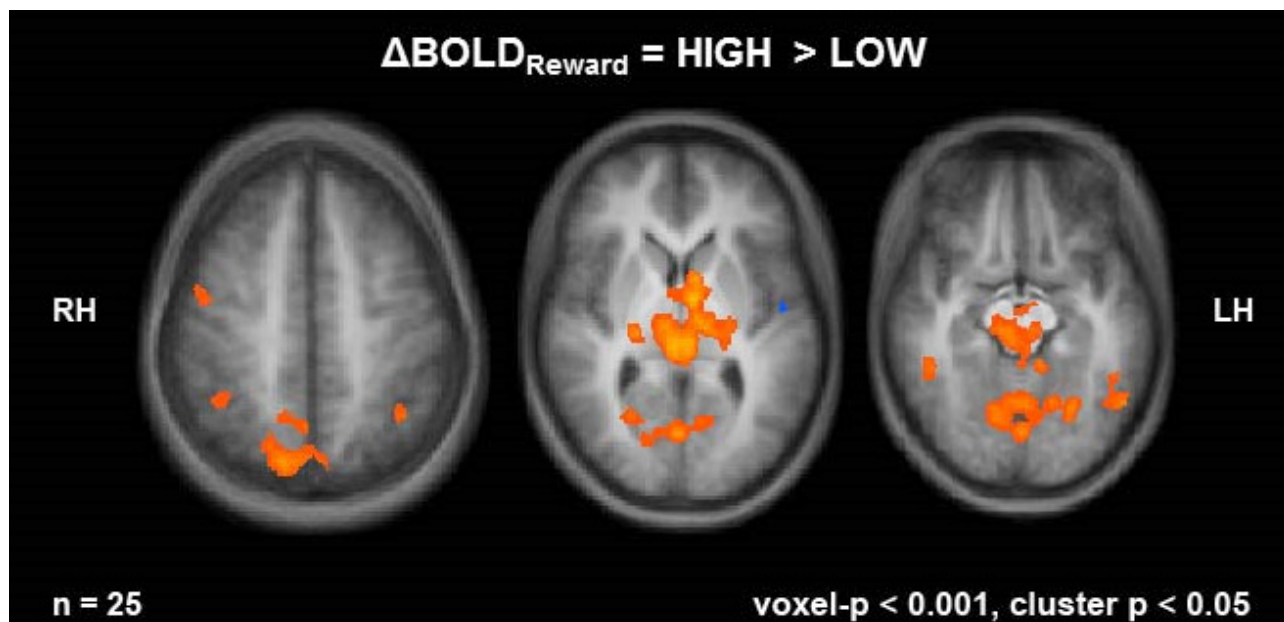
4.2. The brain reward circuitry before and after mental fatigue: an fMRI study

Increased subjective feeling of mental fatigue (MF) and performance decrement often occur following prolonged cognitive activity. This phenomenon is sometimes viewed as a disruption of motivational processes. However, in our previous study we did not find any causal relationship between MF and motivation. The aim of the present study was to further investigate this finding at the neural level. We predicted that, if MF really does consist in a progressive loss of motivation, brain regions involved in reward processing and motivation should be specifically disrupted by MF.

Healthy (25) subjects underwent a fatigue and a control session. In the fatigue session, MF was induced by performing a modified version of the Stroop task (90 minutes), whereas in the control session, the participants were asked to read magazines for 90 minutes prior to the fMRI scan. The neural effects of MF were measured by means of fMRI during a Working memory task with block-wise variations in reward.

The fatigue session was successful in inducing both subjective and objective fatigue. Crucially, we found that subjective MF, but not its behavioural consequences, was associated with the depression of the task-related network whereas reward-related regions were not specifically affected. In addition,

subjective fatigue correlated with a global increase in functional connectivity, especially in the default mode network, consistently with the findings related to the stage of sleep onset. These results indicate that subjective fatigue is associated with depressed task-specific BOLD responses and cannot be reduced to an alteration of motivational processes. The lack of correlation between decreased task-responses and impaired behavioural performance might suggest the existence of compensatory mechanisms, which are not observable with fMRI.

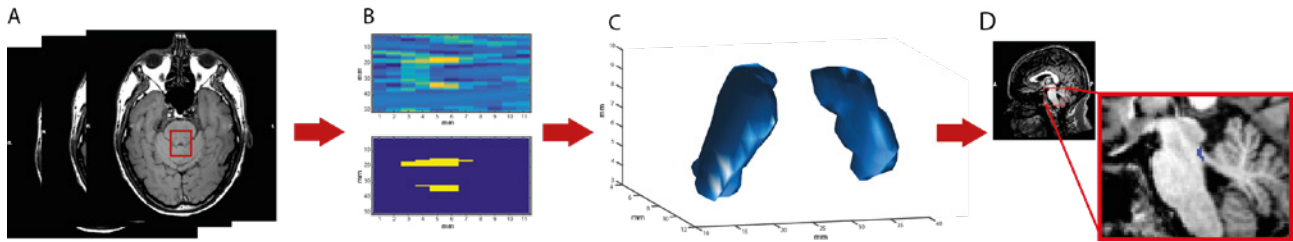


Reward manipulation led to the modulation of BOLD responses. Increased activation was found in high-reward blocs in the precuneus, caudate body, thalamus, ventral tegmental area and substantia nigra. We found that these reward-modulated regions were not more altered by fatigue than other brain regions.

M. Gergelyfi, O. Solopchuk, L. Dricot, A. Zénon, The brain reward circuitry before and after mental fatigue: an fMRI study. In preparation.

4.3. Degeneration of locus coeruleus in Parkinson's disease covaries with fatigue.

Fatigue is one of the most incapacitating symptoms in Parkinson's disease (PD) but bears little relation to the disruption of the dopaminergic system: it evolves independently from the motor symptoms and is poorly treated by dopaminergic replacement therapy. Besides the Substantia Nigra, the Locus Coeruleus (LC), the main source of cortical noradrenaline, is also affected by the disease. We hypothesized that rather than the nigrostriate pathway, LC degeneration and the consequential disruption of the autonomic system would be directly responsible for PD fatigue. PD patients were asked to perform a psychomotor vigilance task (PVT) while different psychophysiological markers were measured (heart rate, respiratory rate, pupil size). Their level of fatigue, the quality of their sleep, and their degree of depression were evaluated through questionnaires (PFS, PDSS-2, BDI). Finally, we evaluated their degree of LC degeneration with a novel, automated method allowing to isolate the LC from neuromelanin MR imaging. Preliminary results (n=20) showed that LC degeneration correlated with the fatigue scores (coeff.=-0.51, p=0.02) but not with the degree of depression or the quality of sleep. Surprisingly, we found that LC degeneration failed to correlate with any of the psychophysiological measures of autonomic responses during the PVT. These findings suggest that LC degeneration may be responsible for fatigue in PD. They also suggest that the increase in heart rate, respiratory rate and changes in pupil size induced by target detection during the PVT may not depend primarily on the LC.



A. A volume of interest (VOI) was extracted from the neuromelanin-sensitive anatomical images, in accordance with our prior knowledge of the theoretical LC location and size (a 12 mm high cube with frenulum as a superior limit, and height/width of 60/50 mm, with the fourth ventricle as a dorsal boundary). **B.** All slices were visually inspected and the slice with the peak signal intensity was selected as a reference slice. In order to identify the voxels belonging to LC, k-means ($k=3$) algorithm was applied to every slice of the VOI. Thus, every voxel was assigned to one of the three classes: zero intensity, noise or LC. **C.** A smoothed 3D model of LC identified in this particular patient, shown for visualization purposes. **D.** LC superimposed in blue on whole brain anatomical images.

Solopchuk O., Sebti M., Bouvy C., Benoît C.E., Jeanjean A., Zénon A. Degeneration of locus coeruleus in Parkinson's disease covaries with fatigue. In preparation.

5. Publications

5.1. Full papers in 2015-2016

1. Zénon A., Time-domain analysis for extracting fast-paced pupil responses. *Scientific Report* (in press)
2. Alamia A, Solopchuk O, D'Ausilio A, Van Bever V, Fadiga L, Olivier E, et al. Disruption of broca's area alters higher-order chunking processing during perceptual sequence learning. *J Cogn Neurosci*. 2016;28(3).
3. Alamia A, Solopchuk O, Olivier E, Zénon A. Non-parametric algorithm to isolate chunks in response sequences. *Front Behav Neurosci*. 2016;10(SEP).
4. Alamia A, Zénon A. Statistical regularities attract attention when task-relevant. *Front Hum Neurosci*. 2016;10(FEB2016).
5. Alamia A, de Xivry J-JO, San Anton E, Olivier E, Cleeremans A, Zenon A. Unconscious associative learning with conscious cues. *Neurosci Conscious*. 2016;2016(1):niw016.
6. Quoilin C, Lambert J, Jacob B, Klein PA, Duque J. Comparison of Motor Inhibition in Variants of the Instructed-Delay Choice Reaction Time Task. *PLoS One*. 2016 Aug 31; 11(8):e0161964.
7. Duque J, Petitjean C, Swinnen SP. Effect of Aging on Motor Inhibition during Action Preparation under Sensory Conflict. *Frontiers in Aging Neuroscience* 8, 322.
8. Derosiere G, Zénon A, Alamia A, Duque J. Primary motor cortex contributes to the implementation of implicit value-based rules during motor decisions. *Neuroimage*. 2016;
9. Solopchuk O, Alamia A, Olivier E, Zénon A. Chunking improves symbolic sequence processing and relies on working memory gating mechanisms. *Learn Mem*. 2016;23(3).
10. Solopchuk O, Alamia A, Zénon A. The role of the dorsal premotor cortex in skilled action sequences. *J Neurosci*. 2016;36(25).
11. Zénon A, Devesse S, Olivier E. Dopamine manipulation affects response vigor independently of opportunity cost. *J Neurosci*. 2016;36(37).
12. Zénon A, Duclos Y, Carron R, Witjas T, Baunez C, Régis J, et al. The human subthalamic nucleus encodes the subjective value of reward and the cost of effort during decision-making. *Brain*. 2016;139(6).
13. Courjon J-H, Zénon A, Clément G, Urquizar C, Olivier E, Péllisson D. Electrical stimulation of the superior colliculus induces non-topographically organized perturbation of reaching movements in cats. *Front Syst Neurosci*. 2015;9(JULY).
14. Davare M, Zénon A, Desmurget M, Olivier E. Dissociable contribution of the parietal and frontal cortex to coding movement direction and amplitude. *Front Hum Neurosci*. 2015;9(MAY).
15. Gergelyfi M, Jacob B, Olivier E, Zénon A. Dissociation between mental fatigue and motivational state during prolonged mental activity. *Front Behav Neurosci*. 2015;9(JULY).
16. Zénon A, Klein P-A, Alamia A, Boursoit F, Wilhelm E, Duque J. Increased reliance on value-based decision processes following motor cortex disruption. *Brain Stimul*. 2015;8(5).
17. Zénon A, Sidibé M, Olivier E. Disrupting the supplementary motor area makes physical effort appear less effortful. *J Neurosci*. 2015;35(23).

5.2. Submitted papers

1. Solopchuk O, Alamia A, Duqué J., Zénon A. cTBS disruption of the Supplementary Motor Area perturbs sequence representation but not performance. Submitted to *eLife*.
2. Duque J, Greenhouse I, Labruna L, Ivry RB. Physiological markers of motor inhibition during human behavior. Submitted to *Trends in Neurosciences*.

5.3. Communications

1. Zénon A., The neurobiology of mental effort. Sixth Biology of Decision Making meeting, Paris, 2016;
2. Zénon A. The neurobiology of mental effort. British Cognitive Neuroscience Society, Budapest, 2016;
3. Zénon A. The neurobiology of mental effort. NeuroCampus, Bordeaux 2016
4. Solopchuk O, Alamia A, Olivier E, Zénon A. cTBS disruption of the Supplementary Motor Area strengthens the involvement of hippocampus in sequence processing. Cognitive Neuroscience Society 2016 Annual Meeting, New York, April 2016
5. Solopchuk O, Alamia A, Duque J, Dricot L, Zénon A. cTBS disruption of the Supplementary Motor Area perturbs sequence representation but not performance. PhD student day, Brussels, November 2016
6. A. Alamia, J.J. Orban de Xivry, A.Cleeremans, E. Olivier, A. Zenon, Implicit Learning: a new design to unveil the unconscious brain, *Neuronus*, Krakow April, 2015
7. A. Alamia, V. Moens, E. Olivier, A. Zenon, Non Bayesian weighting of implicit and explicit information in a motion discrimination task, Cognitive Neuroscience Meeting, New York April, 2016
8. O. Solopchuk, A. Alamia, E. Olivier, A. Zenon, cTBS disruption of the Supplementary Motor Area strengthens the involvement of hippocampus in sequence processing, Cognitive Neuroscience Meeting, New York, April, 2016
9. A. Alamia, A.Cleeremans, E. Olivier, A. Zenon, A novel implicit associative learning framework : validation, role of attention and relation to Bayesian decision making, Society for Neuroscience, Chicago October, 2015

10. Moens V., Zénon A., Habits, action sequences and working memory from a behavioral and a computational perspective, , Society for Neuroscience, Chicago October, 2015
11. Moens V., Zénon A., A Hierarchical Reinforcement Learning / Drift-Diffusion Model reveals key features of habitual decision making, Cognitive Neuroscience Meeting, New York April, 2016
12. E. Pasqualotto, A. Alamia, E. Olivier, A. Zenon, Mental effort induces a shift in the performance-difficulty function, Neuronus, Krakow April, 2015
13. O. Solopchuk, A., Alamia, E. Olivier, JJ. de Xivry, A. Zenon, Kinematics of motor sequence performance in the presence of implicit and explicit structure, Neuronus, Krakow April, 2015
14. Zénon A., Solopchuk O., Sebti M., Bouvy C., Olivier E. Degeneration of locus coeruleus in Parkinson's disease covaries with fatigue. Cognitive Neuroscience Society 2016 Annual Meeting.
15. Alamia A., Solopchuk O., Zénon A., Olivier E. New method to identify chunks finds no evidence for concatenation. Frontiers in Neuroscience. Conference Abstract: 11th National Congress of the Belgian Society for Neuroscience, Mons, Belgium, 2015.
16. Solopchuk O., Alamia A., Olivier E., Orban de Xivry J.-J., Zenon A.. Kinematics of motor sequence performance in the presence of implicit and explicit structure - IBRO&IRUN Neuroscience Forum, Kraków, Poland, 2015.
17. Solopchuk O., Alamia A., Olivier E., Orban De Xivry J.-J., Lefèvre P., Zénon A. Movement kinematics in motor sequence learning task depends on conscious intent. Conference Abstract: 11th National Congress of the Belgian Society for Neuroscience, Mons, Belgium, 2015.
18. Solopchuk O., Alamia A., Olivier E., Zénon A. Chunking mediated improvement in sequence performance depends on working memory gating mechanism. PhD student day, UCL, 2014.
19. Zénon A., Devesse S., Olivier E. Tonic dopamine level modulates response vigor independently of opportunity cost. PhD Student Day, 2014, Brussels, Belgium.
20. Zénon A., Duclos Y., Eusebio A., Reward- and effort-related neuronal activity in the subthalamic nucleus of Parkinson's disease patients. International Symposium on "Biology of Decision Making", Paris, France 2014.
21. Zénon A., Duclos Y., Eusebio A., Reward- and effort-related neuronal activity in the subthalamic nucleus of Parkinson's disease patients. Society for Neuroscience annual meeting, Nov 2014, San Diego, USA.



Geneeskundige Stichting Koningin Elisabeth
Fondation Médicale Reine Elisabeth
Königin-Elisabeth-Stiftung für Medizin
Queen Elisabeth Medical Foundation

Final report
of the research group of

Prof. dr. Jan Gettemans, PhD

Universiteit Gent (UGent)

Prof. dr. Jan Gettemans, PhD

Department of Biochemistry
Faculty of Medicine and Health Sciences
Ghent University
Albert Baertsoenkaai 3, B-9000 Ghent
T +32 9 264 93 40
F +32 9 264 94 90
jan.gettemans@ugent.be
www.ugent.be/ge/biochemie/en/labgettemans

Ongoing collaborations:

- prof. W. Derave (Department of Movement and Sport Sciences, Ghent University)
- prof. J. Van Dorpe (Pathology dept. Ghent University)
- prof. T. Lahoutte (In Vivo Cellular and Molecular Imaging Laboratory, Free University Brussels)
- prof. Marinee Chuah and prof. Thierry Vandendriessche (Department of Gene Therapy & Regenerative Medicine, Free University Brussels)

Offsetting gelsolin degradation in a transgene mouse model by means of chaperone nanobodies.

1. Brief clinical introduction

Gelsolin amyloidosis is an orphan disease but it is a typical amyloid disease with similarities to Alzheimers. Patients with *gelsolin amyloidosis* display diverse clinical symptoms including early aging, peripheral neuropathies affecting the cranial nerves, bilateral progressive facial paralysis, and corneal lattice dystrophy. Recent neuropsychological tests showed abnormalities in visuoconstructional and -spatial performance in patients (Kantanen et al., 2014). There is a minor CNS involvement (impairment of memory, impairment of visuospatial and constructional abilities). Peripheral neuropathies include especially the facial nerves (Figure 1). In the GSKE project, we aimed to study and counter this disease using **nanobody technology**. Our strategy is in principle applicable to other neurological disorders and this project is a proof of principle study to achieve this goal.

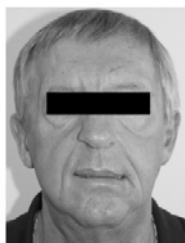


Figure 1. Bilateral upper and lower facial palsy in a FAF patient, caused by amyloid deposition in facial nerves. Reproduced from Luttmann et al., 2010.

2. The molecular basis of the disease

A point mutation (G654A/T) (de la Chapelle et al., 1992) in the **gelsolin** gene results in replacement of an aspartate residue (D187N/Y) that is crucial for calcium binding (Figure 2). As a result, **furin** proteolytically removes the N-terminal segment of gelsolin *en route* through the *trans* Golgi network, leaving a **68 kDa** C-terminal fragment (C68) (Chen *et al.*, 2001). Immediately upon secretion of C68, **MT1-MMP**, a metalloprotease, catalyzes formation of **8 and 5 kDa gelsolin peptides** that associate spontaneously into amyloid fibrils (Page *et al.*, 2005)(Figure 2) and accumulate in cranial nerves. A novel mutation, encoding a N211K protein variant (asparagine to lysine mutation at position 211 in the primary structure) was reported (Efebera et al., 2014) and is associated with proteinurea as the only presenting symptom. **A mouse model** recapitulating the affliction (Page et al., 2009) is available in our lab. In this model, mutant gelsolin is engineered to be secreted from muscle fibers. Hence, we study the pathology by analyzing muscle contractility.

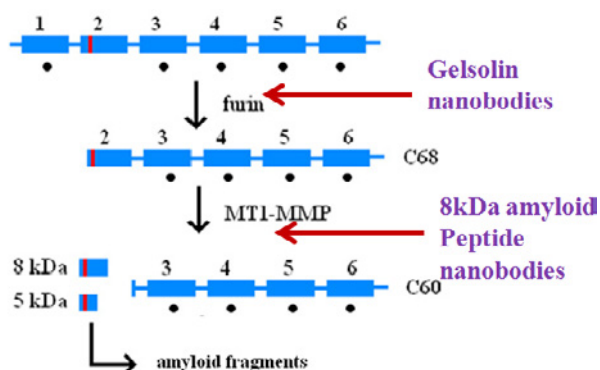


Figure 2. Mutant gelsolin domain 2 (red vertical line) is unable to bind calcium (black circle) and is cleaved twice during secretion, by furin and MT1-MMP, resulting in 8 kDa & 5 kDa peptides.

Nanobodies or VHHs are the smallest intact antigen-binding fragments from heavy chain antibodies present in serum of *Camelidae* species (Muyldermans *et al.*, 2009). Our work has shown that nanobodies act as *bona fide* antagonists of structural and catalytic proteins alike. We have raised nanobodies against a variety of cytoskeletal proteins (De Ganck *et al.*, 2008; Delanote *et al.*, 2010; De Clercq *et al.*, 2013a,b; Van Impe *et al.*, 2008, 2013; Van den Abbeele *et al.*, 2010; Bethuynne *et al.*, 2014; Van Overbeke *et al.*, 2014, 2015; Van Audenhove *et al.*, 2013-2016). Nanobodies not only represent a useful research instrument but they also mimic the activity of drugs by interfering with protein function.

3. Results

This report briefly summarizes the results obtained during the first two years (these findings have been published in the meantime) whereas the findings obtained during the past year are dealt with more extensively.

Over the years we raised three types of gelsolin nanobodies (Figure 3): ^{A)} those that bind to the N-terminal half of gelsolin or the ^{B)} C-terminal half of gelsolin (Van den Abbeele *et al.*, 2010), and another that ^{C)} interacts with the 8 kDa gelsolin amyloidogenic peptide. These nanobodies were used to protect mutant gelsolin from proteolysis by the gelsolinases that degrade gelsolin. We have done this in two different strategies. Finally, both strategies were combined in a single approach.

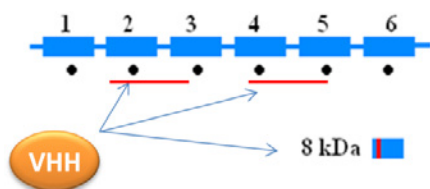


Figure 3. Schematic, showing where in gelsolin the 3 sets of nanobodies bind. The horizontal red lines indicate the epitope determined by pull down assays using GST fusions of gelsolin fragments and nanobodies, by approximation (Van den Abbeele *et al.*, 2010).

3.1. First approach. Curtailing formation of amyloidogenic peptides through indirect blocking of MT1-MMP.

MT1-MMP is a membrane-bound protease and Figure 2 (*supra*) shows that this protease is involved in formation of the 8 kDa gelsolin peptide that aggregates into fibrils. We identified nanobodies (raised against the gelsolin 8 kDa peptide, Figure 3) that protect gelsolin against degradation by MT1-MMP. We termed them FAF nanobodies 1-3 and they act as a molecular chaperone by shielding gelsolin against MT1-MMP.

We next showed that these nanobodies *interact with their target after intraperitoneal injection* in the diseased animals where gelsolin is degraded by furin and MT1-MMP (first paper, **Van Overbeke *et al.*, 2014**).

To assess if these nanobodies trigger a therapeutic response in gelsolin amyloidosis mice, we injected 100 µg of recombinant nanobody weekly. A control group of heterozygous mice was injected with 200 µL PBS at the same time intervals. Typical features of contractile fatigue in 2 different hind leg muscles (extensor digitorum longus (EDL) and soleus), such as the decrease in relaxation rate were attenuated in nanobody-injected mice, compared to PBS. Hence we conclude that nanobodies reduce amyloid deposits around muscle tissue and improve its contractile properties (**Van Overbeke *et al.*, 2014**). The story was picked up by the *Knack* editorial office.

3.2. Second approach. Preventing gelsolin degradation by furin in transgenic mice (**Van Overbeke *et al.*, 2015**)

Using this strategy we aimed to prevent the first cleavage step of gelsolin. The epitope of gelsolin Nb11 resides in gelsolin domain 2 (Vanden Abbeele *et al.*, 2010), encompassing the region where furin proteolyzes mutant plasma gelsolin (¹⁶⁹RVVR¹⁷²↓). We hypothesized that this nanobody might interfere with furin proteolysis, which turned out to be indeed the case.

We reared the first transgenic mice that express a nanobody. These animals were cross bred with the gelsolin amyloidosis mice. We examined muscle contractile properties and found that the decrease in contraction speed was strongly attenuated, across the entire 8-minutes fatigue protocol, in EDL muscles, but not in soleus of the GSN Nb11 mice compared to littermate controls. Hence, as in the previous approach, we can improve physiological muscle performance of these lab animals using nanobody technology, again attesting to the therapeutic potential of gelsolin nanobodies (second paper, [Van Overbeke et al., 2015](#)).

3.3. Visualization of amyloid fibrils in diseased animals using ^{99m}Tc-labeled nanobodies.

A third important goal in this project was to study disease progression in the same animal over time in a non-invasive manner. Following ^{99m}Tc labeling of a gelsolin anti-8kDa peptide nanobody, in combination with *single-photon emission computed tomography/computed tomography* (SPECT/CT) imaging, we succeeded in doing this. We traced gelsolin peptides following peritoneal injection of the nanobody tracer (third paper, [Verhelle et al., 2016](#)).

Using biodistribution analysis and immunohistochemistry we demonstrated the validity of the data acquired via ^{99m}Tc-FAF Nb1 SPECT/CT. Our findings demonstrate the potential of nanobodies as a non-invasive tool to image amyloid deposition (Figure 4).

In this year we were invited to contribute a chapter to a new book on amyloidosis (fourth paper, [Verhelle and Gettemans, 2016](#)).

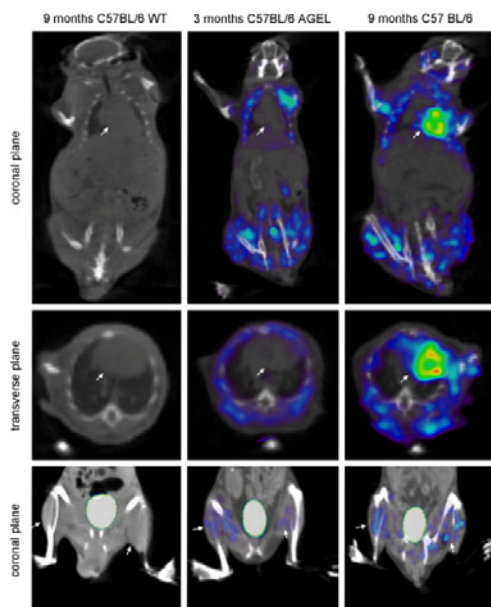


Figure 4. SPECT/CT images obtained with ^{99m}Tc-FAF Nb1. In WT mice (left) no significant background signal can be detected. In AGel mice from 3 months onwards (middle and right), the major muscle groups clearly light up. The heart however, seems unaffected at 3 months (middle) but gives a high signal at 9 months (right). White arrows indicate the heart (upper 2 panels) and major muscle groups of the hind legs (lower panel). Reproduced from Verhelle et al. (2016).

3.4. Simultaneous protection of gelsolin against furin and MT1-MMP.

The possibility to link nanobodies in tandem array format allows us to investigate if we can prevent furin and MT1-MMP mediated hydrolysis using a single construct consisting of two different nanobodies. In collaboration with **prof. Marinee Chuah** and **prof. Thierry Vandendriessche** (Department of Gene Therapy & Regenerative Medicine, Free University Brussels) we generated adeno associated viral particles (AAV) with a tandem nanobody cloned into their genome (Figure 5), because they represent an efficient tool to obtain high level and long term transduction and expression *in vivo*. This study has been submitted to Human Molecular Genetics, underwent peer review and we are currently working on the revision to have this paper published in the first half of 2017 (fifth paper, **Verhelle et al., 2017**).

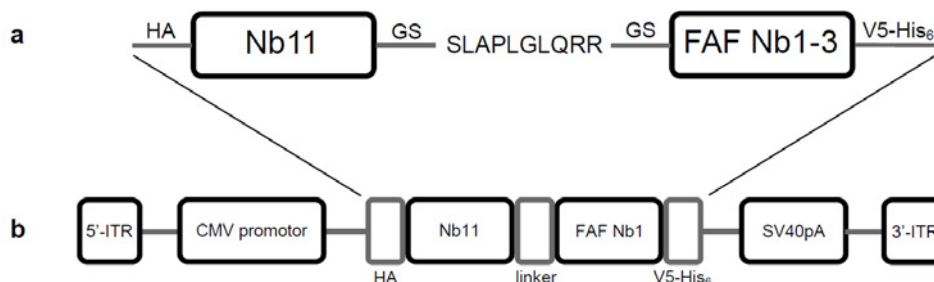


Figure 5. Schematic representation of the bispecific Nb11-FAF format and AAV9-Nb11-FAF1 vector. The two nanobodies, Nb11 and FAF Nb1-3, are linked via the MT1-MMP sensitive sequence SLAPGLQRR, flanked between two GS linkers. An N-terminal HA and C-terminal V5-His₆ tag is present (a). The expression cassette was cloned in a self-complementary (sc) adeno-associated virus backbone that was packaged using AAV serotype 9 capsids (AAV9). Expression of Nb11-FAF1 is driven by the CMV promoter. The 5' and 3' inverted terminal repeats (ITR) and SV40 polyadenylation site (pA) are indicated (b). The final result is a construct where both nanobodies occur in tandem configuration, separated by the MT1-MMP sensitive peptide sequence and GS linker.

The linker between Nb11 and FAF Nb1-3 contains the MT1-MMP sensitive peptide SLAPGLQRR (proteolysis of the GL scissile bond). The purpose of this setup was that, *in vivo*, during secretion, proteolysis of this sequence would release the FAF Nb, enabling it to perform its function without any interference of Nb11. At the same time this mechanism may act as a decoy, luring MT1-MMP away from the C68 being secreted. This was tested *in vitro* using the recombinant catalytic domain of MT1-MMP. The MT1-MMP sensitive peptide proved to be very efficient in all three bivalent Nb11-FAF constructs and they were readily cleaved upon incubation with MT1-MMP (Figure 6).

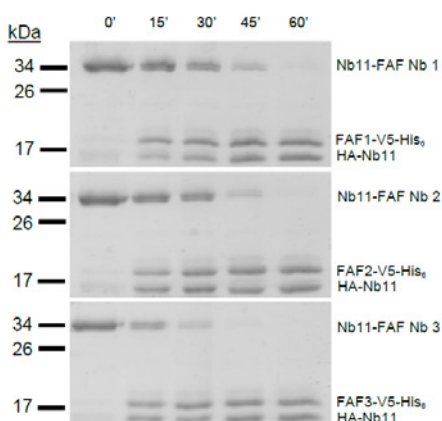


Figure 6. The MT1-MMP linker sequence is cleaved *in vitro*.

The bispecific Nb11-FAF constructs were incubated *in vitro* with MT1-MMP for 1 hour at 37°C. At distinct time points (0, 15, 30, 45 and 60 minutes) samples were taken and the reaction was stopped with Laemmli sample buffer. Visualization was done via Coomassie staining after SDS-PAGE fractionation. MT1-MMP was able to recognize and cleave the SLAPGLQRR sequence, thereby releasing the two individual nanobodies.

Since Nb11 can inhibit furin proteolysis of PG* whereas FAF-3 counteract MT1-MMP proteolysis of C68 by shielding the substrate, we hypothesized that bivalent Nb11-FAF formats might be able to combine both traits, leading to a synergistic inhibitory effect on 8 kDa amyloidogenic peptide production. An *in vitro* assay was set up and we were able to confirm this hypothesis (data not shown for brevity). Quantification of the amyloidogenic 8 kDa fragment showed that all three Nb11-FAF constructs were

able to inhibit formation of the 8 kDa AGel peptide more efficiently than their monovalent counterparts. Hence, the bivalent format is endowed with a double protective activity, and formation of the 8 kDa fragment in particular is strongly reduced in comparison to monospecific Nb11 or FAF nanobodies.

As we wanted to confirm this in a more complex environment, PG (wild type gelsolin), PG* (mutant gelsolin) and the Nb11-FAF constructs were transiently expressed in HEK293T cells. Co-staining of the constructs followed by epifluorescence microscopy confirmed their colocalisation along the secretory pathway. After 24 hours, we analyzed the cell medium via Western blotting. Quantification of the C68 signal revealed a similar pattern as in the *in vitro* setup; the bispecific Nb11-FAF nanobodies show an inhibitory effect towards furin proteolysis. We were unable to assess the effect on MT1-MMP proteolysis as no 8 kDa peptide could be detected within the observed timeframe.

Bispecific Nb11-FAF1 gene therapy in AGel mice via AAV9

An AGel mouse model intervention study was set up. Homozygote neonates (2-3 days old) were injected with 4.7×10^{10} vg/mouse of AAV9-Nb11-FAF1 or PBS (negative control) via the retro-orbital plexus. No adverse effects on the development or behavior of the mice were apparent. Nanobody expression was confirmed at 1, 2 and 3 months of age in the plasma of both WT and AGel mice. At the age of 3 months Nb11-FAF1 gene therapeutic efficacy was determined via SPECT-CT, immunofluorescence and *ex vivo* muscle performance.

In the WT control groups, AAV treatment did not significantly alter the background control signal (Figure 7). In the AGel group however, expression of Nb11-FAF1 resulted in a significantly lower signal (t-test, $p < 0.05$) in the skeletal muscle and a significantly lower signal (t-test, $p < 0.05$) in the heart (Figure 7). This is consistent with a reduction of the characteristic amyloid burden in the AAV9-Nb11-FAF1-treated AGel mice.

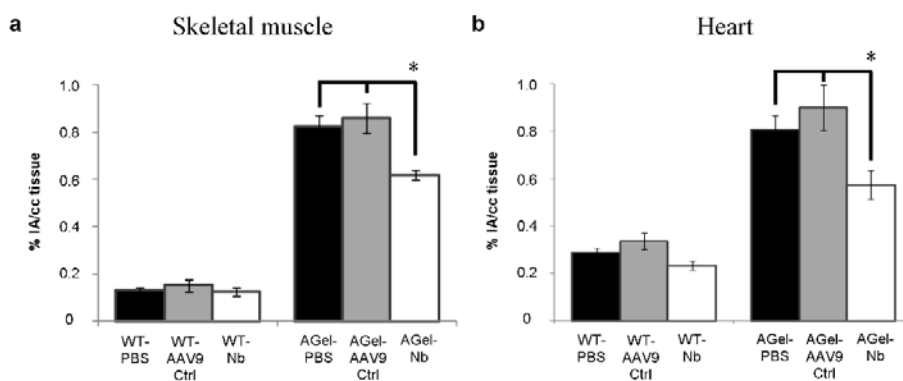


Figure 7. Quantified SPECT-CT data in skeletal muscle and heart. At 3 months of age all mice underwent a SPECT-CT scan with the ^{99m}Tc-FAF Nb1 AGel tracer. Identical regions of interest were drawn around hind leg muscles and heart. Signal quantification showed that Nb expression had no effect on WT background signal, neither in skeletal muscle (a) nor in heart (b). In AGel mice, Nb11-FAF1 expression resulted in a significantly lower signal in skeletal muscle (a) and the heart (b) compared to PBS and AAV9-control groups. Data shown as mean \pm SE. * $P < 0.05$ in a two sided unpaired t-test.

AGel amyloidogenic buildup in skeletal muscle and heart tissue was also stained and quantified. Laminin was used as an internal control. Nb11-FAF1 expression resulted in a significant reduction (t-test, $p < 0.05$) of AGel amyloidogenic buildup in skeletal muscle (39 % vs. PBS and 36% vs. AAV9-ctrl) (Figure 8c) and in the heart (43 % vs. PBS and 55% vs AAV9-ctrl) (Figure 8d) in AGel mice. In contrast, WT control groups expressing Nb11-FAF1 showed no significantly different staining compared to the WT-PBS or WT-AAV9-Ctrl groups (Figure 8a).

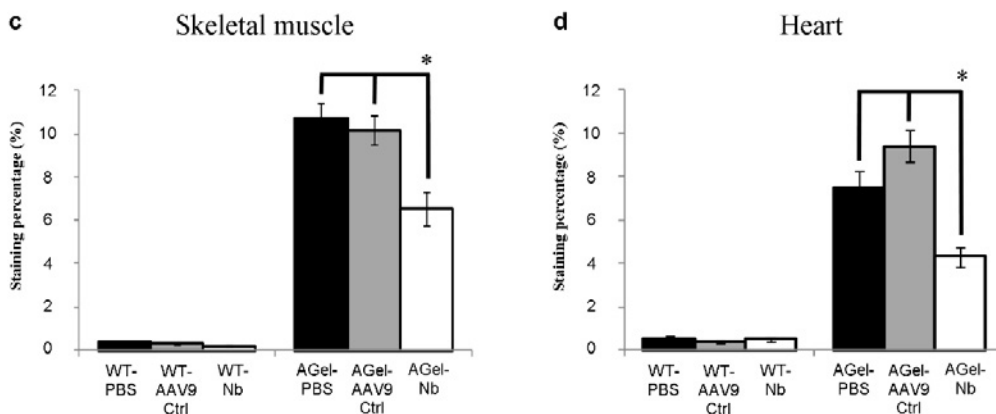
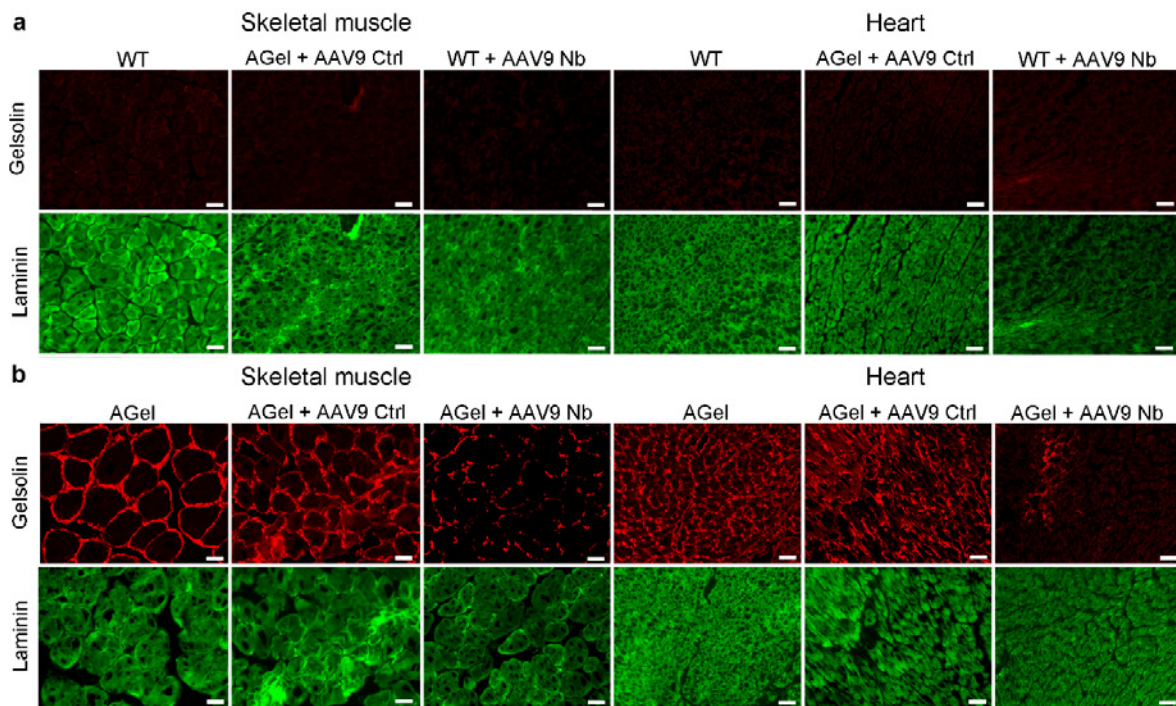


Figure 8. Nb11-FAF1 expressing AGel mice show a decreased immunohistochemistry staining pattern in skeletal muscle and heart tissue. Mice were sacrificed three months post AAV injection. Skeletal muscle and heart tissue was stained for AGel amyloidogenic buildup (a-b, red, scale bar = 50 μm) and laminin (a-b, green, control, scale bar = 50 μm). The staining pattern was reduced in Nb11-FAF1 expressing AGel mice both in skeletal muscle (c) and heart tissue (d) compared to PBS and AAV9-control groups.

At the end of the trial mice were anaesthetized, the extensor digitorum longus (EDL) and soleus were dissected and their contractile properties were measured. The expression of Nb11-FAF1 in AGel mice resulted in a specific twitch force indistinguishable from the WT control groups (t-test, $p < 0.05$) and significantly different compared to the untreated (PBS or AAV9-ctrl) AGel groups in EDL muscle (t-test, $p < 0.05$) but not in the soleus. The amount of force that could be produced for a given frequency (force-frequency) was not affected by the amyloid burden nor by the treatment. Interestingly, fatigue progression was, both in EDL and soleus, significantly more pronounced in the WT versus the (un)treated FAF mice. However, the speed of muscle contraction during fatigue in EDL muscle in the Nb11-FAF1 expressing AGel mice showed, as expected, a similar decline as the WT controls in contrast to the untreated (PBS or AAV9-ctrl) AGel mice. The soleus seemed unaffected (Figure 9).

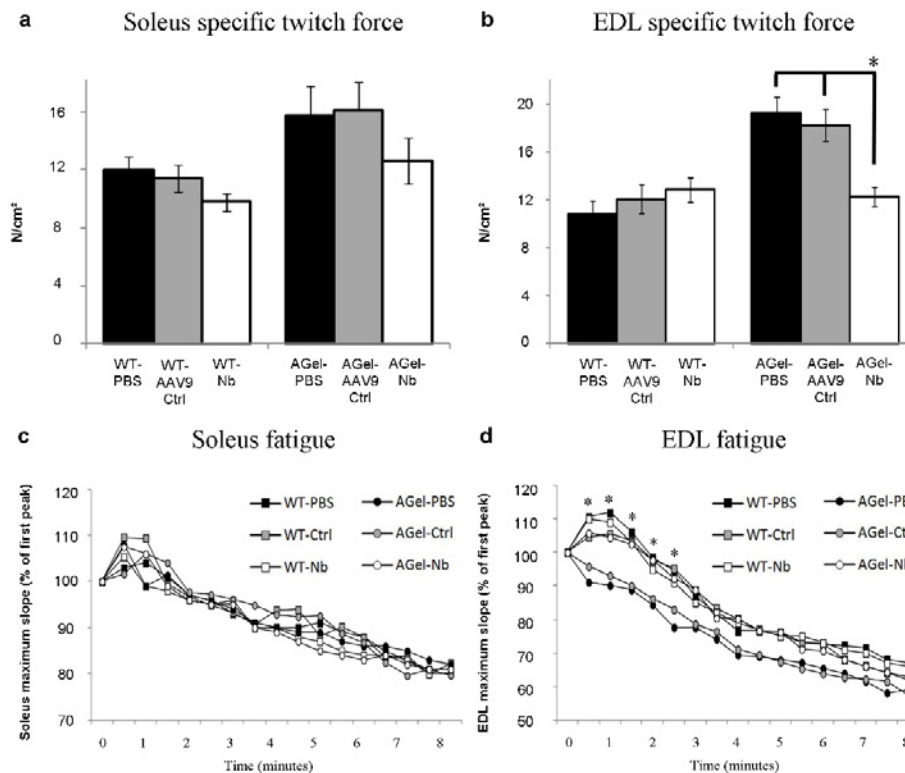


Figure 9. Ex-vivo muscle contractile properties improve after AAV9-Nb11-FAF1 gene therapy. Soleus and EDL muscles were dissected and their ex-vivo contractile properties measured. Expression of Nb11-FAF1 in AGel mice resulted in a specific twitch force significantly different from AGel control mice (both PBS and AAV9-control) and indistinguishable from the WT-control groups in EDL but not soleus (**a-b**, upper panels, data shown as mean \pm SE. * $P < 0.05$ in a two sided unpaired t-test). EDL maximum slope (**d**), during the fatigue protocol, in Nb11-FAF1 expressing AGel mice, displayed the same delay as the WT controls. In contrast, AGel PBS and AAV9-control treated mice displayed a significantly faster fatigue onset. The soleus maximum slope during fatigue protocol (**c**) seemed unaffected. * $P < 0.05$ in a two sided unpaired t-test (**a, b**), one way ANOVA (**c,d**).

Preventing the formation of amyloid precursors, as was attempted here with nanobodies, would be a major step forward in amyloid research. Currently, administration of (R)-1-[6-[(R)-2-carboxy-pyrrolidin-1-yl]-6-oxo-hexanoyl] pyrrolidine-2-carboxylic acid (CPHPC) followed by anti-SAP antibody is the most promising amyloid removing strategy, as has been proven in patients with AL amyloidosis. Obviously, such interventions are only meaningful if, as is the case in AL amyloidosis, one is also able to stop the production of new amyloid precursors. The development of this bispecific, chaperoning, anti-AGel nanobody, may prove to be a fundamental step towards this goal.

The findings described in this last section have been combined into the fifth paper, Verhelle et al., 2017.

We are currently working on the revised version which deals mainly, but not exclusively, with including a control for the AAV virus. We are confident that this study can be published in Human Molecular Genetics.

Other noteworthy events

- On Friday the 16th of January 2015, Drs. Van Overbeke defended his PhD work in public, entitled: **Keeping mutant plasma gelsolin safe from harm: gelsolin nanobodies act as a chaperone against pathological proteolysis.** He is currently employed as a post-doc at the University of Malmö in Sweden.
- Adriaan Verhelle will defend his PhD work in the first half of 2017. He has started writing his PhD dissertation.

In summary:

- 5 papers, published in peer reviewed journals (including one book chapter) will have resulted from this study and **these papers are directly related to this project!**
- In addition, two students will have obtained their PhD degree. Media coverage of the work resulted in broader diffusion of our work, as well as by attending different scientific meetings abroad.
- Both students working on this project, Drs. Wouter Van Overbeke and Drs. Adriaan Verhelle, *received a travel stipend* from the *United States Amyloidosis formation*, valued at 2500 \$ each, to participate at the The XIVth International Symposium on Amyloidosis in Indianapolis, Indiana from 27 April to 1 May, 2014.
- At this meeting, Drs. Van Overbeke was *awarded the Junior Investigation Award* by the International Society of Amyloidosis.

Peer reviewed papers resulting from this study: all papers ensue directly from the project.

1. Van Overbeke W, Verhelle A, Everaert I, Zwaenepoel O, Vandekerckhove J, Cuvelier C, et al. Chaperone nanobodies protect gelsolin against MT1-MMP degradation and alleviate amyloid burden in the gelsolin amyloidosis mouse model. *Mol Ther*. 2014;22:1768-78.
2. Van Overbeke W, Wongsantichon J, Everaert I, Verhelle A, Zwaenepoel O, De Ganck A, Hochepped T, Haigh J, Cuvelier C, Derave W, Robinson R, Jan Gettemans. An ER-directed nanobody targets the first step in amyloid formation in a hereditary gelsolin amyloidosis mouse model by protecting mutant plasma gelsolin from furin proteolysis. 2015. *Human Molecular Genetics*. 24, 2492-507.
3. A nanobody based approach to amyloid diseases. The gelsolin case study, by Verhelle, A. and Gettemans, J. Book chapter, Dr. Ana Maria Fernandez-Escamilla (editor), "Exploring new findings on Amyloidosis". ISBN 978-953-51-2619-5, Print ISBN 978-953-51-2618-8, Published: August 24, 2016. Chapter 13. DOI: 10.5772/63981
4. Verhelle, A., Van Overbeke, W., Peleman, C., De Smet, R., Zwaenepoel, O., Lahoutte, T., Van Dorpe, J., Devoogdt, N., Gettemans, J. Non-invasive imaging of amyloid deposits in a mouse model of AGel using ^{99m}Tc-modified nanobodies and SPECT/CT. *Mol Imaging Biol*. 2016 Dec;18(6):887-897.
5. Adriaan Verhelle¹, Nair Nisha², Inge Everaert⁴, Wouter Van Overbeke¹, Lynn Supply⁵, Olivier Zwaenepoel¹, Cindy Peleman⁶, Jo Van Dorpe⁵, Tony Lahoutte⁶, Nick Devoogdt⁶, Wim Derave⁴, Chuah K. Marinee^{2,3}, Thierry VandenDriessche^{2,3}, Jan Gettemans¹. **AAV9 delivered bispecific nanobody attenuates amyloid burden in the gelsolin amyloidosis mouse model.** *Human Molecular Genetics*, revised version in preparation.

6. Bibliography

- Bethuynne J, De Gieter S, Zwaenepoel O, Garcia-Pino A, Durinck K, Verhelle A, Hassanzadeh-Ghassabeh G, Speleman F, Loris R, Gettemans J (2014) A nanobody modulates the p53 transcriptional program without perturbing its functional architecture. *Nucleic Acids Res* **42**: 12928-12938
- Chen CD, Huff ME, Matteson J, Page L, Phillips R, Kelly JW, Balch WE (2001) Furin initiates gelsolin familial amyloidosis in the Golgi through a defect in Ca(2+) stabilization. *EMBO J* **20**: 6277-6287
- De Clercq S, Boucherie C, Vandekerckhove J, Gettemans J, Guillabert A (2013a) L-plastin nanobodies perturb matrix degradation, podosome formation, stability and lifetime in THP-1 macrophages. *PLoS One* **8**: e78108
- De Clercq S, Zwaenepoel O, Martens E, Vandekerckhove J, Guillabert A, Gettemans J (2013b) Nanobody-induced perturbation of LFA-1/L-plastin phosphorylation impairs MTOC docking, immune synapse formation and T cell activation. *Cell Mol Life Sci* **70**: 909-922
- Efebera YA, Sturm A, Baack EC, Hofmeister CC, Satoskar A, Nadasdy T, Nadasdy G, Benson DM, Gillmore JD, Hawkins PN, Rowczenio D (2014) Novel gelsolin variant as the cause of nephrotic syndrome and renal amyloidosis in a large kindred. *Amyloid* **21**: 110-112
- De Ganck A, De Corte V, Staes A, Gevaert K, Vandekerckhove J, Gettemans J (2008) Multiple isoforms of the tumor suppressor myopodin are simultaneously transcribed in cancer cells. *Biochem Biophys Res Commun* **370**: 269-273
- de la Chapelle A, Tolvanen R, Boysen G, Santavy J, Bleeker-Wagemakers L, Maury CP, Kere J (1992) Gelsolin-derived familial amyloidosis caused by asparagine or tyrosine substitution for aspartic acid at residue 187. *Nat Genet* **2**: 157-160
- Muyldermans S, Baral TN, Retamozzo VC, De Baetselier P, De Genst E, Kinne J, Leonhardt H, Magez S, Nguyen VK, Revets H, Rothbauer U, Stijlemans B, Tillib S, Wernery U, Wyns L, Hassanzadeh-Ghassabeh G, Saerens D (2009) Camelid immunoglobulins and nanobody technology. *Vet Immunol Immunopathol* **128**: 178-183

- Page LJ, Suk JY, Bazhenova L, Fleming SM, Wood M, Jiang Y, Guo LT, Mizisin AP, Kisilevsky R, Shelton GD, Balch WE, Kelly JW (2009) Secretion of amyloidogenic gelsolin progressively compromises protein homeostasis leading to the intracellular aggregation of proteins. *Proc Natl Acad Sci U S A* **106**: 11125-11130
- Page LJ, Suk JY, Huff ME, Lim HJ, Venable J, Yates J, Kelly JW, Balch WE (2005) Metalloendoprotease cleavage triggers gelsolin amyloidogenesis. *EMBO J* **24**: 4124-4132
- Lüttmann RJ, Teismann I, Husstedt IW, Ringelstein EB, Kuhlenbäumer G (2010) Hereditary amyloidosis of the Finnish type in a German Family: clinical and electrophysiological presentation. *Muscle & Nerve* **41**: 679-684
- Kantanen M, Kiuru-Enari S, Salonen O, Kaipainen M, Hokkanen L (2014) Subtle neuropsychiatric and neurocognitive changes in hereditary gelsolin amyloidosis (AGel amyloidosis). *PeerJ* **2**: e493
- Van den Abbeele A, De Clercq S, De Ganck A, De Corte V, Van Loo B, Soror SH, Srinivasan V, Steyaert J, Vandekerckhove J, Gettemans J (2010) A llama-derived gelsolin single-domain antibody blocks gelsolin-G-actin interaction. *Cell Mol Life Sci* **67**: 1519-1535
- Van Impe K, Hubert T, De Corte V, Vanloo B, Boucherie C, Vandekerckhove J, Gettemans J (2008) A new role for nuclear transport factor 2 and Ran: nuclear import of CapG. *Traffic* **9**: 695-707
- Van Audenhove I, Boucherie C, Pieters L, Zwaenepoel O, Vanloo B, Martens E, Verbrugge C, Hassanzadeh-Ghassabeh G, Vandekerckhove J, Cornelissen M, De Ganck A, Gettemans J (2014) Stratifying fascin and cortactin function in invadopodium formation using inhibitory nanobodies and targeted subcellular delocalization. *FASEB J* **28**: 1805-1818
- Van Audenhove I, Debeuf N, Boucherie C, Gettemans J (2015) Fascin actin bundling controls podosome turnover and disassembly while cortactin is involved in podosome assembly by its SH3 domain in THP-1 macrophages and dendritic cells. *Biochim Biophys Acta* **1853**: 940-952
- Van Audenhove I, Gettemans J (2016) Use of Nanobodies to Localize Endogenous Cytoskeletal Proteins and to Determine Their Contribution to Cancer Cell Invasion by Using an ECM Degradation Assay. *Methods Mol Biol* **1365**: 225-241
- Van Audenhove I, Van Impe K, Ruano-Gallego D, De Clercq S, De Mynck K, Vanloo B, Verstraete H, Fernandez LA, Gettemans J (2013) Mapping cytoskeletal protein function in cells by means of nanobodies. *Cytoskeleton (Hoboken)* **70**: 604-622
- Van Impe K, Bethuyne J, Cool S, Impens F, Ruano-Gallego D, De Wever O, Vanloo B, Van Troys M, Lambein K, Boucherie C, Martens E, Zwaenepoel O, Hassanzadeh-Ghassabeh G, Vandekerckhove J, Gevaert K, Fernandez LA, Sanders NN, Gettemans J (2013) A nanobody targeting the F-actin capping protein CapG restrains breast cancer metastasis. *Breast Cancer Res* **15**: R116
- Van Overbeke W, Verhelle A, Everaert I, Zwaenepoel O, Vandekerckhove J, Cuvelier C, et al. Chaperone nanobodies protect gelsolin against MT1-MMP degradation and alleviate amyloid burden in the gelsolin amyloidosis mouse model. *Mol Ther*. 2014;22:1768-78.
- Van Overbeke W, Wongsantichon J, Everaert I, Verhelle A, Zwaenepoel O, De Ganck A, Hochepped T, Haigh J, Cuvelier C, Derave W, Robinson R, Jan Gettemans. An ER-directed nanobody targets the first step in amyloid formation in a hereditary gelsolin amyloidosis mouse model by protecting mutant plasma gelsolin from furin proteolysis. Revision completed. 2015. MS to be resubmitted shortly. *Human Molecular Genetics*.
- Verhelle, A., Van Overbeke, W., Peleman, C., De Smet, R., Zwaenepoel, O., Lahoutte, T., Van Dorpe, J., Devoogdt, N., Gettemans, J. Non-invasive imaging of amyloid deposits in a mouse model of AGel using ^{99m}Tc-modified nanobodies and SPECT/CT. *Mol Imaging Biol*. 2016 Dec;18(6):887-897.
- Adriaan Verhelle¹, Nair Nisha², Inge Everaert⁴, Wouter Van Overbeke¹, Lynn Supply⁵, Olivier Zwaenepoel¹, Cindy Peleman⁶, Jo Van Dorpe⁵, Tony Lahoutte⁶, Nick Devoogdt⁶, Wim Derave⁴, Chuah K. Marinee^{2,3}, Thierry VandenDriessche^{2,3}, Jan Gettemans^{1,*}. **AAV9 delivered bispecific nanobody attenuates amyloid burden in the gelsolin amyloidosis mouse model.** *Human Molecular Genetics*, revised version in preparation.



Geneeskundige Stichting Koningin Elisabeth
Fondation Médicale Reine Elisabeth
Königin-Elisabeth-Stiftung für Medizin
Queen Elisabeth Medical Foundation

Final report
of the research group of

Prof. dr. Pierre Maquet

Université de Liège (ULg)

Prof. dr. Pierre Maquet & dr. Christophe Phillips, ir

Cyclotron Research Centre - B30
University of Liège - Sart Tilman
4000 Liège
Belgium
T + 32 4 366 36 87
F + 32 4 366 29 46
pmaquet@ulg.ac.be

Regulation of waking brain function by sleep debt, circadian and seasonal rhythms

1. Influence of circadian rhythmicity on human brain function

Human performance is modulated by circadian rhythmicity and homeostatic sleep pressure. Whether and how this interaction is represented at the regional brain level has not been established. We quantified changes in brain responses to a sustained-attention task during 13 functional magnetic resonance imaging sessions scheduled across the circadian cycle, during 42 hours of wakefulness and after recovery sleep, in 33 healthy participants. Cortical responses showed significant circadian rhythmicity, the phase of which varied across brain regions. Cortical responses also significantly decreased with accrued sleep debt. Subcortical areas exhibited primarily a circadian modulation that closely followed the melatonin profile. These findings expand our understanding of the mechanisms involved in maintaining cognition during the day and its deterioration during sleep deprivation and circadian misalignment (1).

Prolonged wakefulness alters cortical excitability, which is essential for proper brain function and cognition. However, besides prior wakefulness, brain function and cognition are also affected by circadian rhythmicity. Whether the regulation of cognition involves a circadian impact on cortical excitability is unknown. Here, we assessed cortical excitability from scalp electroencephalography (EEG) responses to transcranial magnetic stimulation in 22 participants during 29 h of wakefulness under constant conditions. Data reveal robust circadian dynamics of cortical excitability that are strongest in those individuals with highest endocrine markers of circadian amplitude. In addition, the time course of cortical excitability correlates with changes in EEG synchronization and cognitive performance. These results demonstrate that the crucial factor for cortical excitability, and basic brain function in general, is the balance between circadian rhythmicity and sleep need, rather than sleep homeostasis alone. These findings have implications for clinical applications such as non-invasive brain stimulation in neurorehabilitation (2).

Several neuropsychiatric and neurological disorders have recently been characterized as dysfunctions arising from a 'final common pathway' of imbalanced excitation to inhibition within cortical networks. How the regulation of a cortical E/I ratio is affected by sleep and the circadian rhythm however, remains to be established. Here we addressed this issue through the analyses of TMS-evoked responses recorded over a 29h sleep deprivation protocol conducted in young and healthy volunteers. Spectral analyses of TMS-evoked responses in frontal cortex revealed non-linear changes in gamma band evoked oscillations, compatible with an influence of circadian timing on inhibitory interneuron activity. In silico inferences of cell-to-cell excitatory and inhibitory connectivity and GABA/Glutamate receptor time constant based on neural mass modeling within the Dynamic causal modeling framework, further suggested excitation/inhibition balance was under a strong circadian influence. These results indicate that circadian changes in EEG spectral properties, in measure of excitatory/inhibitory connectivity and in GABA/glutamate receptor function could support the maintenance of cognitive performance during a normal waking day, but also during overnight wakefulness. More generally, these findings demonstrate a slow daily regulation of cortical excitation/inhibition balance, which depends on circadian-timing and prior sleep-wake history (3).

2. Seasonal rhythmicity in human brain function

Daily variations in the environment have shaped life on Earth, with circadian cycles identified in most living organisms. Likewise, seasons correspond to annual environmental fluctuations to which organisms have adapted. However, little is known about seasonal variations in human brain physiology. We investigated annual rhythms of brain activity in a cross-sectional study of healthy young participants. They were maintained in an environment free of seasonal cues for 4.5 d, after which brain responses were assessed using functional magnetic resonance imaging (fMRI) while they performed two different cognitive tasks. Brain responses to both tasks varied significantly across seasons, but the phase of these annual rhythms was strikingly different, speaking for a complex impact of season on human brain function. For the sustained attention task, the maximum and minimum responses were located around summer and winter solstices, respectively, whereas for the working memory task, maximum and minimum responses were observed around autumn and spring equinoxes. These findings reveal previously unappreciated process-specific seasonality in human cognitive brain function that could contribute to intra- individual cognitive changes at specific times of year and changes in affective control in vulnerable populations (4).

3. Sleep and memory

Motor memory consolidation is characterized, in part, by a sleep-facilitated decrease in susceptibility to subsequent interfering experiences. Surprisingly, the cerebral substrates supporting this phenomenon have never been examined. We used fMRI to investigate the neural correlates of the influence of sleep on interference to motor memory consolidation. Healthy young adults were trained on a sequential motor task, and subsequently practiced a second competing sequence after an interval including diurnal sleep or wakefulness. Participants were then retested on the initial sequence 8 h and 24 h (including nocturnal sleep) after training. Results demonstrated that a post-training nap significantly protected memory against interference at 8 h and modulated the link between cerebral activity and behavior, such that a smaller post-interference decrease in cortico-striatal activity was associated with better performance. Interestingly, the protective effect of a nap was only transitory, as both groups performed similarly at 24 h. Activity in cortico-striatal areas that was disrupted during the day, presumably due to interference and accentuated in the absence of a nap, was restored overnight. Altogether, our findings offer the first evidence that cortico-striatal areas play a critical role in the transient sleep-facilitated reduction in motor memory vulnerability and in the overnight restoration of previously degraded memories (5).

4. Methodology of EEG analysis

Background: In sleep electroencephalographic (EEG) signals, artifacts and arousals marking are usually part of the processing. This visual inspection by a human expert has two main drawbacks: it is very time consuming and subjective. New method: To detect artifacts and arousals in a reliable, systematic and reproducible automatic way, we developed an automatic detection based on time and frequency analysis with adapted thresholds derived from data themselves. Results: The automatic detection performance is assessed using 5 statistic parameters, on 60 whole night sleep recordings coming from 35 healthy volunteers (male and female) aged between 19 and 26. The proposed approach proves its robustness against inter- and intra-, subjects and raters' scorings, variability. The agreement with human raters is rated overall from substantial to excellent and provides a significantly more reliable method than between human raters. Comparison: Existing methods detect only specific artifacts or only arousals, and/or these methods are validated on short episodes of sleep recordings, making it difficult to compare with our whole night results. Conclusion: The method works on a whole night recording

and is fully automatic, reproducible, and reliable. Furthermore the implementation of the method will be made available online as open source code (6).

Sleep spindle is a peculiar oscillatory brain pattern which has been associated with a number of sleep (isolation from exteroceptive stimuli, memory consolidation) and individual characteristics (intellectual quotient). Oddly enough, the definition of a spindle is both incomplete and restrictive. In consequence, there is no consensus about how to detect spindles. Visual scoring is cumbersome and user dependent. To analyze spindle activity in a more robust way, automatic sleep spindle detection methods are essential. Various algorithms were developed, depending on individual research interest, which hampers direct comparisons and meta-analyses. In this review, sleep spindle is first defined physically and topographically. From this general description, we tentatively extract the main characteristics to be detected and analyzed. A nonexhaustive list of automatic spindle detection methods is provided along with a description of their main processing principles. Finally, we propose a technique to assess the detection methods in a robust and comparable way (7).

5. References

1. V. Muto *et al.*, Local modulation of human brain responses by circadian rhythmicity and sleep debt. *Science (80-.)*. **353**, 687–690 (2016).
2. J. Q. M. Ly *et al.*, Circadian regulation of human cortical excitability. *Nat. Commun.* **7**, 11828 (2016).
3. S. L. Chellappa *et al.*, Circadian dynamics in measures of cortical excitation and inhibition balance. *Sci. Rep.* **6**, 33661 (2016).
4. C. Meyer *et al.*, Seasonality in human cognitive brain responses. *Proc. Natl. Acad. Sci. U. S. A.* **113**, 3066–3071 (2016).
5. G. Albouy *et al.*, Cerebral Activity Associated with Transient Sleep-Facilitated Reduction in Motor Memory Vulnerability to Interference. *Sci. Rep.* **6**, 34948 (2016).
6. D. C. 't Wallant *et al.*, Automatic artifacts and arousals detection in whole-night sleep EEG recordings. *J. Neurosci. Methods.* **258**, 124–133 (2016).
7. D. C. 't Wallant *et al.*, Sleep spindles as an electrographic element: description and automatic detection methods. *Neural Plast.* **2016**, 1–34 (2016).



Geneeskundige Stichting Koningin Elisabeth
Fondation Médicale Reine Elisabeth
Königin-Elisabeth-Stiftung für Medizin
Queen Elisabeth Medical Foundation

Final report
of the research group of

Prof. dr. Ann Massie, PhD &
prof. dr. Ilse Smolders

Vrije Universiteit Brussel (VUB)

Prof. dr. Ann Massie, PhD & prof. dr. Ilse Smolders

Vrije Universiteit Brussel - Faculty of Medicine & Pharmacy
Vice-Dean for Student Policy
Center for Neuroscience C4N - Department FASC
Building G - Room G.103
Laarbeeklaan 103, 1090 Brussels, Belgium
T +32 2 477 47 47
amassie@vub.ac.be
www.vub.ac.be/center-for-neurosciences

System x_c^- as a potential target for novel neuroprotective strategies: focus on Parkinson's disease and its psychiatric comorbidities

Introduction on Parkinson's disease and its psychiatric comorbidities: In Parkinson's disease (PD), nigrostriatal degeneration causes a loss of dopamine in the striatum. As a result, the motor loop of the basal ganglia is dysregulated, resulting in hyperactivity of the subthalamic nucleus (STN) and subsequent overactivation of the GABA-ergic output structures (i.e. substantia nigra pars reticulata (SNr), globus pallidus pars interna (GPi)) which in turn inhibits the thalamus. This results in motor impairment (bradykinesia, tremor and rigidity) due to reduced excitatory input from the thalamus to the motor cortex. The hyperactive glutamatergic STN neurons also project to the dopamine containing neurons located in the substantia nigra pars compacta (SNc) and may cause more neurodegeneration due to toxic glutamate levels (excitotoxicity). As such, SNc neuronal loss and STN overactivation sustain each other and may cause progression of the disease^{1,2}. In this respect, the use of NMDA (ionotropic glutamate receptor) antagonists is clearly beneficial as neuroprotective effects can be observed. However, their use is hampered by neurological side effects that are the consequence of impairment of fast excitatory NMDA-mediated synaptic transmission^{3,4}. Moreover, as recently described, the stimulation of extrasynaptic NMDA receptors triggers cell destruction pathways whereas the stimulation of synaptic NMDA receptors is involved in neuroprotection^{5,6}. Antagonists of the postsynaptic group I metabotropic glutamate receptor (mGluR) mGluR5, have also been shown to be neuroprotective in the absence of overt side effects, as they negatively modulate NMDA responses without completely blocking synaptic transmission⁷⁻⁹.

Besides the classical motor symptoms, 65% of PD patients suffer from neuropsychiatric symptoms such as depression and anxiety. The underlying mechanisms of depression and anxiety in PD are still unclear and might be attributed to a combination of medical, neurochemical and psychosocial factors. Interestingly, both depression and anxiety may precede PD onset, indicating they are not merely the result of the difficulties related to PD¹⁰.

Despite therapeutic advances over the last decades, PD can still only be treated symptomatically. Moreover, medication that could treat the neuropsychiatric comorbidities, such as antidepressants or anxiolytic agents, has not been proven to be effective in PD and the risk of deterioration of PD as well as interactions with the PD medication are a major concern¹⁰. In conclusion, new insights into the molecular mechanisms leading to PD and its comorbidities are crucial as they might provide new targets for disease-modifying interventions.

Project background information: System x_c^- or the Na^+ -independent cystine/glutamate antiporter, consisting of xCT as a specific subunit and 4F2hc, is located on glial cells and imports one cystine molecule in exchange for a glutamate molecule in an obligatory 1:1 exchange rate¹¹ (fig. 1). Increased activity can as such contribute to excitotoxic damage. In the context of our research focus, i.e. the role of glutamate transporters in neurological disorders¹²⁻¹⁶, we were the first to propose a possible involvement of system x_c^- in the pathogenesis of PD. This hypothesis is based on the observation that xCT expression levels were increased in the ipsilateral striatum of the unilateral 6-hydroxydopamine (6-OHDA) hemi-Parkinson rat model¹⁷. To understand the functional meaning of this increased xCT expression levels, we used mice with a genetic deletion of xCT ($xCT^{-/-}$)¹⁸ and tested their vulnerability for 6-OHDA-induced neurodegeneration. Although no effect was seen on striatal dopamine loss, the dopaminergic neurons in the SNc of these mice were significantly protected. Apart from the strong decrease in striatal extracellular glutamate levels, we could not observe neurochemical or anatomical changes in the $xCT^{-/-}$ brain under physiological conditions and therefore we concluded that the protective effects of the loss of system x_c^- should probably be linked to the decreased extracellular glutamate levels¹⁹.

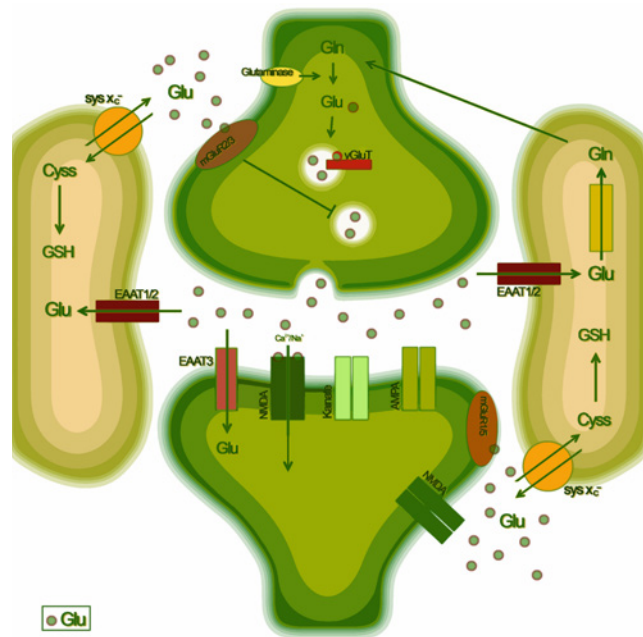


Figure 1: schematic representation of a glutamatergic synapse including glutamate reuptake transporters (EAAT), glutamate receptors (NMDA, AMPA, mGluR) and system x_c^- (sys x_c^-).

The **rationale for studying system x_c^- as a target for treating PD and its comorbidities** is based on the dual role this antiporter can have in neurological disorders that are characterized by increased levels of oxidative stress as well as excitotoxicity. Cystine is intracellularly reduced to cysteine, which is the rate limiting building block in the synthesis of glutathione (GSH), a major brain antioxidant. Consequently, the expression of system x_c^- can be induced by pathways that are activated by oxidative stress or other stress stimuli²⁰. Indeed, we observed increased xCT expression in the ipsilateral striatum of the 6-OHDA hemi-Parkinson rat model¹⁷. However, each time a cystine molecule is imported, glutamate is released into the extracellular space and we demonstrated that under physiological conditions, in certain brain regions 60-70% of extracellular glutamate levels, as measured using *in vivo* microdialysis, originate from system x_c^- ¹⁶⁻¹⁹. This **glutamate**, that is **released extrasynaptically**, can activate extrasynaptic NMDA receptors and mGluRs²¹ and, as such, induce neurodegeneration when present in excess. **Our findings that mice lacking system x_c^- are protected against 6-OHDA-induced neurodegeneration¹⁹ suggest 1/ that mice can perfectly deal with (oxidative) stress situations in the absence of system x_c^- and 2/ that avoiding the upregulation of system x_c^- in response to this cellular stress is protective, probably due to the fact that excessive glutamate release is prevented.** It thus seems that in certain pathological conditions, the brain induces excitotoxic damage in an attempt to protect itself against oxidative stress.

The goal of this project is to strengthen our hypothesis that inhibition of system x_c^- is a novel, neuroprotective strategy for the treatment of PD and its comorbidities. In order to do so, we proposed a validation plan consisting of **four specific aims:** **1/** investigate whether xCT expression levels are affected in PD-related structures of human PD patients, **2/** investigate the susceptibility of mice with a genetic deletion of xCT, and thus lacking functional system x_c^- , for lactacystin (LAC, inhibitor of the proteasome injected into the substantia nigra (SN)) and MPTP (1-methyl-4-phenyl-1,2,3,6-

tetrahydropyridine)-induced parkinsonism. Vice versa, investigate the effect of LAC- and MPTP-induced parkinsonism on the expression of xCT. **3/** unveil whether downregulation or inhibition of system x_c⁻ in the STN at a certain time in life and at a certain stage of the disease, instead of a genetic deletion, can still protect dopamine neurons from the SNc against toxin-induced degeneration. **4/** Ultimately, investigate the link between system x_c⁻ and anxiety/depression in healthy as well as parkinsonian mice. During the time-course of this project, **two additional studies**, related to this project, have been conducted in order to: **5/** characterize antibodies directed against xCT and **6/** investigate neuroprotective effects of zonisamide (ZNS).

Results obtained since the start of the project (2014-2016):

Results that were obtained in 2014-2015 and already reported in our activity report of 2014 or 2015 are in italic. For figures related to these results, we refer to our previous reports.

1. Specific aim 1: Investigate xCT mRNA (real-time PCR) and protein (semi-quantitative Western blotting) levels in tissue samples of PD patients and healthy controls.
-

Up till now, we only collected some preliminary data on human tissue samples. With a limited number of samples, we could observe a trend towards increased xCT protein expression in cortex of PD patients compared to healthy controls and a decreased xCT expression in the SN of PD patients (fig. 2 in report 2014). In the near future, additional samples will be obtained from the Netherlands brain bank.

In this small number of samples we also investigated expression levels of proteins of the phosphoinositide 3-kinase (PI3K)/glycogen synthase kinase 3 β (GSK-3 β)/eukaryotic initiation factor 2 α (eIF2 α)/activating transcription factor (ATF4) pathway (collaboration with P. Maher, Salk Institute, San Diego, US and J. Lewerenz, University Hospital Ulm, Germany). We previously characterized this pathway as being responsible for the increased xCT expression levels in hippocampus of epileptic patients²² as well as a chronic epilepsy mouse model (Leclercq, Van Liefferinge et al., submitted). Yet, in PD samples, there was no correlation between the changes in xCT expression and the proteins of this pathway. Further studies should identify the pathway that modulates xCT expression in PD.

2. For specific aim 2 we investigated whether our observations in the 6-OHDA model can be generalized to other PD models, by studying xCT expression in the LAC/SN model and the chronic, progressive MPTP model. At the same time, we compared the behavioral and neurochemical outcome of xCT^{-/-} and xCT^{+/+} mice in both models.
-

2.1. Characterization of the intranigral lactacystin mouse model

Since we are the first to use a mouse model for PD in which LAC is injected into the SN, we further characterized this model before investigating the involvement of system x_c⁻ in LAC-induced parkinsonism. A very thorough behavioral and neurochemical analysis was performed on three-month-old C57Bl/6 mice, one and three weeks after LAC injection.

In this manuscript that was recently published²³ we report that unilateral administration of LAC to the SN of mice leads to acute and non-progressive dopaminergic neurodegeneration (fig. 3 in report 2014), in the presence of increased levels of Ser129-phosphorylated α -synuclein (fig. 4 in report 2014). These pathological changes induced the development of motor asymmetry and impairment, as assessed in

various motor behavior paradigms (fig. 5 in report 2014). Furthermore, we detected signs of non-motor symptoms resembling early-stage PD, including somatosensory disturbances, akathisia (restlessness), perseverative behaviour (fig. 5 in report 2014), and anxiety-like behaviour (fig. 6 in report 2014). We conclude that the intranigral LAC mouse model can be a relevant model to study the involvement of proteasomal dysfunction and of authentically phosphorylated α -synuclein at Ser129 in the pathogenesis of sporadic Parkinson's disease.

Finally, using electron microscopy (collaboration with C. Meshul; VA Medical Center, Portland, Oregon, USA) we have been studying ultrastructural changes in cortico- and thalamostriatal synapses in the nigral LAC mouse model. In PD, striatal dopamine depletion leads to plastic changes at excitatory corticostriatal and thalamostriatal synapses. The functional consequences of these responses on the expression of behavioral deficits are incompletely understood. In addition, most of the information on striatal synaptic plasticity has been obtained in models with severe striatal dopamine depletion, and less is known regarding changes during early stages of striatal denervation. Using a partial model of nigral cell loss based on intranigral injection of the proteasome inhibitor LAC (fig. 2), we demonstrate that a loss of asymmetric synapses and spines in the dorsolateral striatum (fig. 4) is accompanied by ultrastructural changes at corticostriatal synapses with a 15% increase in the length and 30% increase in the area of the postsynaptic densities at corticostriatal synapses at 1 week following toxin administration (fig. 5, 6 and table 1). This increase was positively correlated with the performance of LAC-lesioned mice on the rotarod task (fig. 3), such that mice with a stronger increase in the size of the postsynaptic density performed better on the rotarod task (fig. 7). We therefore propose that lengthening of the postsynaptic density at corticostriatal synapses acts as a compensatory mechanism to maintain motor function under conditions of partial dopamine depletion. The ultrastructure of thalamostriatal synapses remained unchanged following LAC administration (fig. 8, 9 and table 2). These findings provide novel insights into the mechanisms of synaptic plasticity and behavioral compensation following partial levels of nigral cell loss, such as those occurring during the presymptomatic stage of PD. The results of this study were **submitted for publication to Brain Research Bulletin**.

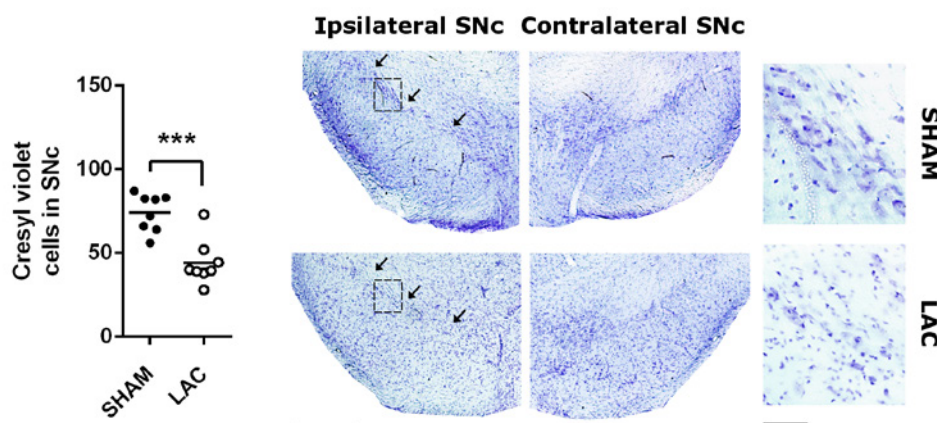


Figure 2: Cresyl violet staining of the SNc following LAC administration. Left: Intranigral injection of LAC caused a significant decrease in the number of cresyl violet stained cells in ipsilateral SNc when compared to sham. Data are presented as scatter dot plot (horizontal line indicates mean) and analyzed using an unpaired t test. *** $p < 0.001$. Right panels: Representative photomicrographs indicating the loss of cresyl violet stained cells in the ipsilateral SNc at 1 week following LAC infusion. Note the loss of stained cells from the ipsilateral SNc of LAC-lesioned mice when compared to the same region of sham-operated animals (arrows). Scale bar 400 μ m. Insets: High-magnification photomicrographs of the delineated regions of sham- and LAC-lesioned mice. Scale bar 50 μ m. LAC lactacystin. SNc substantia nigra pars compacta.

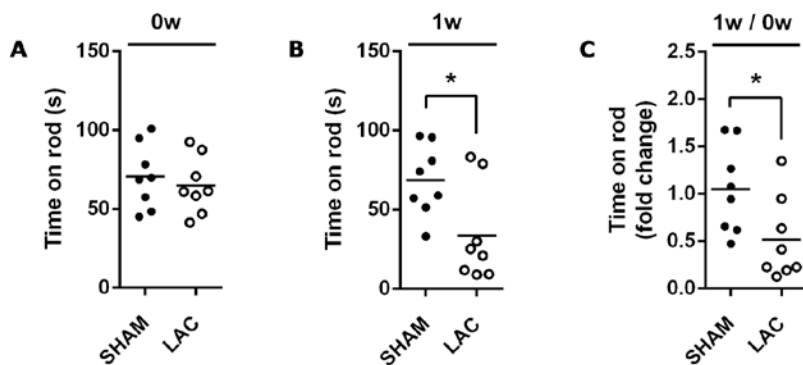


Figure 3. Effect of intranigral infusion of LAC on motor performance in the rotarod test. No difference in rotarod performance was present at baseline between the two groups (A). At 1 week following stereotaxic surgery, LAC-lesioned mice demonstrate a significantly decreased time spent on the rod, both when analyzing absolute values (B) as well as fold change vs. baseline performance (C). Data are presented as scatter dot plot (horizontal line indicates mean) and analyzed using an unpaired t test. * $p < 0.05$. LAC lactacystin.

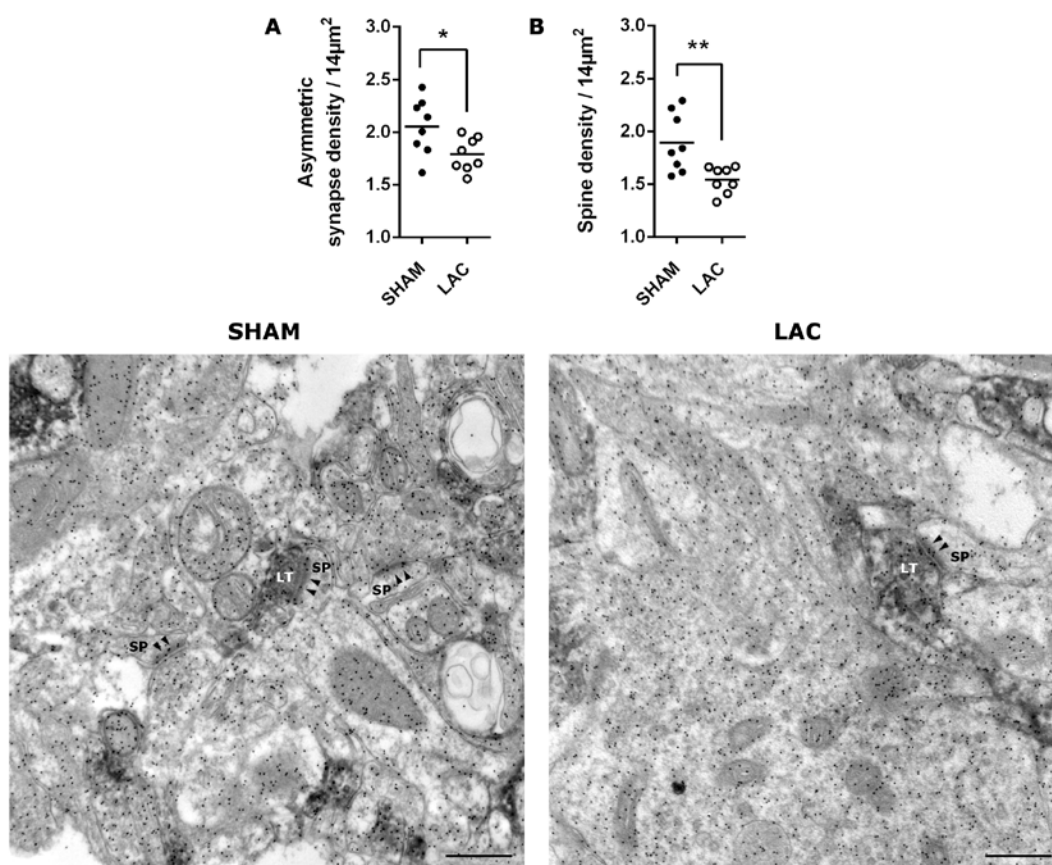


Figure 4. Synapse and spine loss in the dorsolateral striatum following LAC administration. Intranigral injection of LAC led to a significant decrease in both the density of nerve terminals making an asymmetrical synaptic contact (A) and spine density (B) per field of view ($14 \mu\text{m}^2$), compared to sham mice receiving vehicle. Data are presented as scatter dot plot (horizontal line indicates mean) and analyzed using an unpaired t test. * $p < 0.05$, ** $p < 0.01$. Lower panels: Representative electron micrographs of one field of view ($14 \mu\text{m}^2$) showing axospinous asymmetrical synaptic contacts in the dorsolateral striatum of LAC- and sham-lesioned mice (synaptic contacts indicated by arrowheads). Scale bar 500 nm. LAC lactacystin, LT labeled terminal, SP spine.

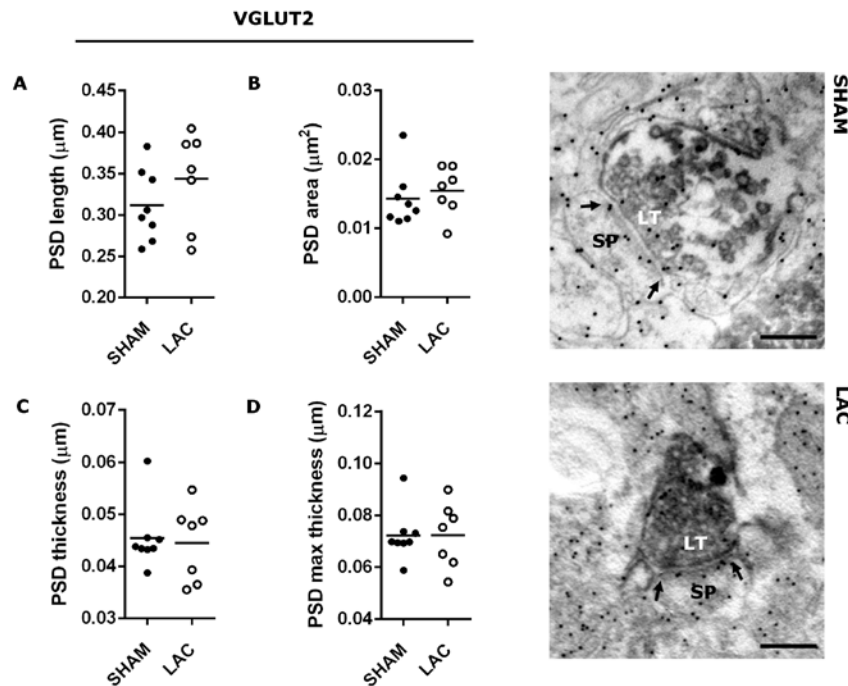


Figure 9. Effect of LAC administration on the size of the PSD at VGLUT2-labeled thalamostriatal synapses. Administration of LAC did not have a significant influence on the length (A), area (B), thickness (C) or maximum thickness (D) of the PSD at thalamostriatal synapses when compared to sham-operated mice. Data are presented as scatter dot plot (horizontal line indicates mean) and analyzed using an unpaired t test. Right panels: Representative electron micrographs of the PSD at VGLUT2-labeled axospinous synapses in the dorsolateral striatum of LAC- and sham-lesioned mice (PSD defined by arrows). Scale bar 250 nm. LAC lactacystin, LT labeled terminal, PSD postsynaptic density, SP spine.

2.2. Involvement of system x_c^- in lactacystin-induced parkinsonism

We next investigated the involvement of system x_c^- in LAC-induced parkinsonism. xCT expression levels were measured in striatum of LAC- and sham-injected mice using semi-quantitative Western blotting (fig. 7 in report 2014). Preliminary data on a limited number of mice show a strong trend towards increased xCT expression levels in parkinsonian striatum. However, groups need to be enlarged and additional brain regions will be investigated in the coming months.

Finally, the behavioral and neurochemical outcome of $xCT^{-/-}$ mice after LAC injection was compared to $xCT^{+/+}$ mice. In adult mice (three months old), we could not observe any differences in susceptibility for LAC-induced nigrostriatal degeneration (fig. 8 in report 2014) or behavioral impairment (fig. 9 in report 2014). On the other hand, in aged mice (i.e. 19-23 month old mice) we could clearly observe neuroprotection as the result of the loss of system x_c^- (fig. 10 in report 2014).

The reason for this age-dependent protection is currently being elucidated.

2.3. Involvement of system x_c^- in MPTP-induced parkinsonism

Next, we studied the involvement of system x_c^- in MPTP-induced parkinsonism, using the progressive, chronic MPTP model. Besides being progressive and chronic, this model has the advantage that no surgery is needed. MPTP is being delivered intraperitoneally instead of intracerebral. These experiments have been performed in collaboration with C. Meshul and are published in **Neuroscience Letters**²⁶. xCT expression levels have been measured in midbrain and striatum of MPTP-treated C57Bl/6 mice and we compared MPTP-induced nigrostriatal degeneration between $xCT^{-/-}$ and $xCT^{+/+}$ mice.

Our results indicate that the expression of xCT undergoes region-specific changes in MPTP-treated mice, with increased expression in the striatum (fig. 11A in report 2014), and decreased expression in the SN (fig. 11B in report 2014). Furthermore, mice lacking xCT were equally sensitive to the neurotoxic

effects of MPTP, as they demonstrate similar decreases in striatal dopamine content, striatal tyrosine hydroxylase (TH) expression, nigral TH immunopositive neurons and forelimb grip strength, five weeks after commencing MPTP treatment (fig. 12 in report 2014). Altogether, our data indicate that progressive lesioning with MPTP induces striatal and nigral dysregulation of system x_c^- . However, loss of system x_c^- does not affect MPTP-induced nigral dopaminergic neurodegeneration and motor impairment in mice.

In the near future, aged $xCT^{+/+}$ and $xCT^{-/-}$ mice will be tested in the MPTP model.

3. For specific aim 3, we will investigate whether a local and timed downregulation (or inhibition) of system x_c^- can have the same protective effects as observed in animals that are born with a total loss of system x_c^- .
-

These experiments are being delayed due to technical reasons.

4. For specific aim 4, we investigated in detail anxiety and depressive-like behavior in non-PD $xCT^{-/-}$ mice compared to $xCT^{+/+}$ littermates. Moreover, xCT expression levels have been investigated in **post-mortem** brain tissue of depressed patients as well as two rodent models for depression. Finally, the effect of loss of system x_c^- on anxiety and depressive-like behavior in a model for depression has been evaluated.
-

We have completed a very thorough phenotyping study of the $xCT^{-/-}$ vs. $xCT^{+/+}$ mice. These results are recently **published in Progress in Neuropsychopharmacology & Biological Psychiatry**²⁷.

We phenotyped adult and aged system x_c^- deficient mice in a battery of tests for anxiety- and depressive-like behavior (open field, light/dark test, elevated plus maze, novelty suppressed feeding, forced swim test, tail suspension test). Concomitantly, we evaluated the sensorimotor function of system x_c^- deficient mice, using motor and sensorimotor based tests (rotarod, adhesive removal test, nest building test). Our results indicate that loss of system x_c^- does not affect motor or sensorimotor function, in either adult or aged mice, in none of the paradigms investigated (fig. 13, 14 in report 2014). On the other hand, in the open field and light/dark tests, and forced swim and tail suspension tests respectively, we could observe significant anxiolytic (fig. 15 in report 2014) and antidepressive-like (fig. 16 in report 2014) effects in system x_c^- deficient mice that in certain cases (light/dark, forced swim) were age-dependent. These findings indicate that, under physiological conditions, nonvesicular glutamate release via system x_c^- mediates aspects of higher brain function related to anxiety and depression, but does not influence sensorimotor function. As such, modulation of system x_c^- might constitute the basis of innovative interventions in mood disorders.

Although recent investigations implicate system x_c^- in the pathology of mood disorders^{27,28}, unambiguous evidence has not yet been established. Therefore we thoroughly evaluated the possible role of system x_c^- in the depressive state. We did not detect any significant changes in expression levels of the specific subunit of system x_c^- in the hippocampus, cingulate cortex, nucleus accumbens and amygdala of the corticosterone mouse model and Flinders Sensitive Line rat model of depression neither in *post-mortem* tissue of depressed patients (table 3), compared to proper controls (fig. 10). We next subjected $xCT^{-/-}$ mice to the corticosterone model and subsequently analyzed their behavior in the forced swim test, mouse tail suspension test, novelty-suppressed feeding test, light/dark paradigm and open field test. Loss of system x_c^- had no effect on chronic stress-induced depression- and anxiety-like behaviour

(fig. 11). After comparing the antidepressant effects of N-acetylcysteine (activator of system x_c^- that has been described to induce anti-depressant-like effects in bulbectomized rats²⁹) in $xCT^{-/-}$ mice and wildtype littermates, we could conclude that the antidepressant effects of N-acetylcysteine that we observed in the mouse tail suspension test, are not mediated via system x_c^- (fig. 12). The results of this study will **soon be submitted for publication**.

Table 3 Overview of *post-mortem* human samples provided by The Netherlands Brain Bank.

	Sample reference	Gender	Age	Structure	Post-mortem delay (hours)	Relative xCT protein expression	
Controls	S01/024	Female	91	cingulate cortex	05:45	91,8	
	S01/245	Female	93	cingulate cortex	05:35	83,5	
	S08/324	Female	89	cingulate cortex	03:52	85,6	
	S09/066	Female	99	cingulate cortex	04:15	117,9	
	S10/023	Female	85	cingulate cortex	05:20	71,1	
	S11/082	Female	84	cingulate cortex	05:55	150,2	
	S08/324	Female	89	hippocampus	03:52	94,3	
	S09/066	Female	99	hippocampus	04:15	71,8	
	S09/301	Male	92	hippocampus	08:25	124,8	
	S11/039	Female	91	hippocampus	04:15	89,6	
	S11/090	Female	85	hippocampus	08:25	131,3	
	S11/114	Female	81	hippocampus	05:30	88,3	
	Depressed patients	S08/090	Female	93	cingulate cortex	04:20	64,9
		S08/242	Female	91	cingulate cortex	05:20	102,3
S09/323		Female	84	cingulate cortex	08:45	90,9	
S11/051		Female	100	cingulate cortex	05:50	101,1	
S11/058		Male	83	cingulate cortex	10:40	49,7	
S07/135		Male	88	hippocampus	06:37	89,8	
S08/090		Female	93	hippocampus	04:20	92,6	
S08/242		Female	91	hippocampus	05:20	117,2	
S09/323		Female	84	hippocampus	08:45	110,6	
S11/051		Female	100	hippocampus	05:50	76,6	
S11/058		Male	83	hippocampus	10:40	70,9	

Both controls and depressed patients are depicted with corresponding sample reference, gender, age at death, dissected brain structure, *post-mortem* delay and relative xCT protein expression per sample. Age and *post-mortem* delay, and gender are not significantly different between test groups, as analyzed by means of respectively the two-sided Mann–Whitney U-test and Fisher’s exact test, P-values indicated.

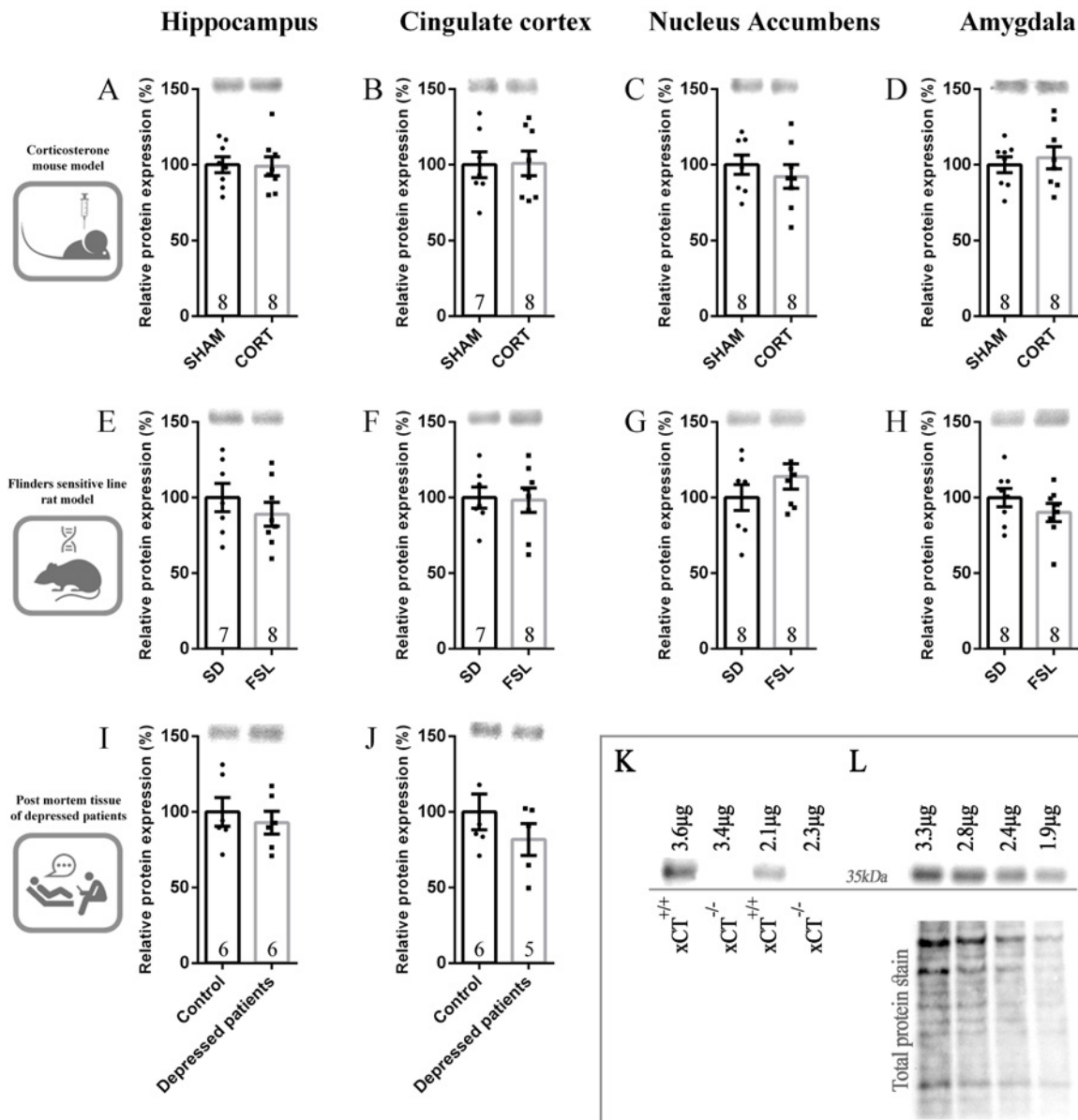


Figure 10. xCT protein expression levels in depression versus appropriate control samples: (A – D) in the corticosterone mouse model, (E – H) in the Flinders Sensitive Line rat model and (I, J) in *post-mortem* tissue of depressed patients. Several depression-related brain areas are depicted: hippocampus, cingulate cortex, nucleus accumbens and amygdala. Each graph is accompanied by a representative example of a Western blot (xCT = 35 kDa). xCT expression levels of the respective control groups were set to 100% and the expression levels of the “depressed” groups were expressed as a percentage of the corresponding controls (similar protein concentrates were loaded). Data are presented as mean ± SEM and were analyzed by means of the two-sided Mann–Whitney U-test, sample size indicated in the graph. Technical controls: hippocampal tissue from xCT^{+/+} and xCT^{-/-} mice depicting the specificity of the xCT antibody (K) and a dilution series of hippocampal mouse tissue (L), total protein loaded is indicated in the graph.

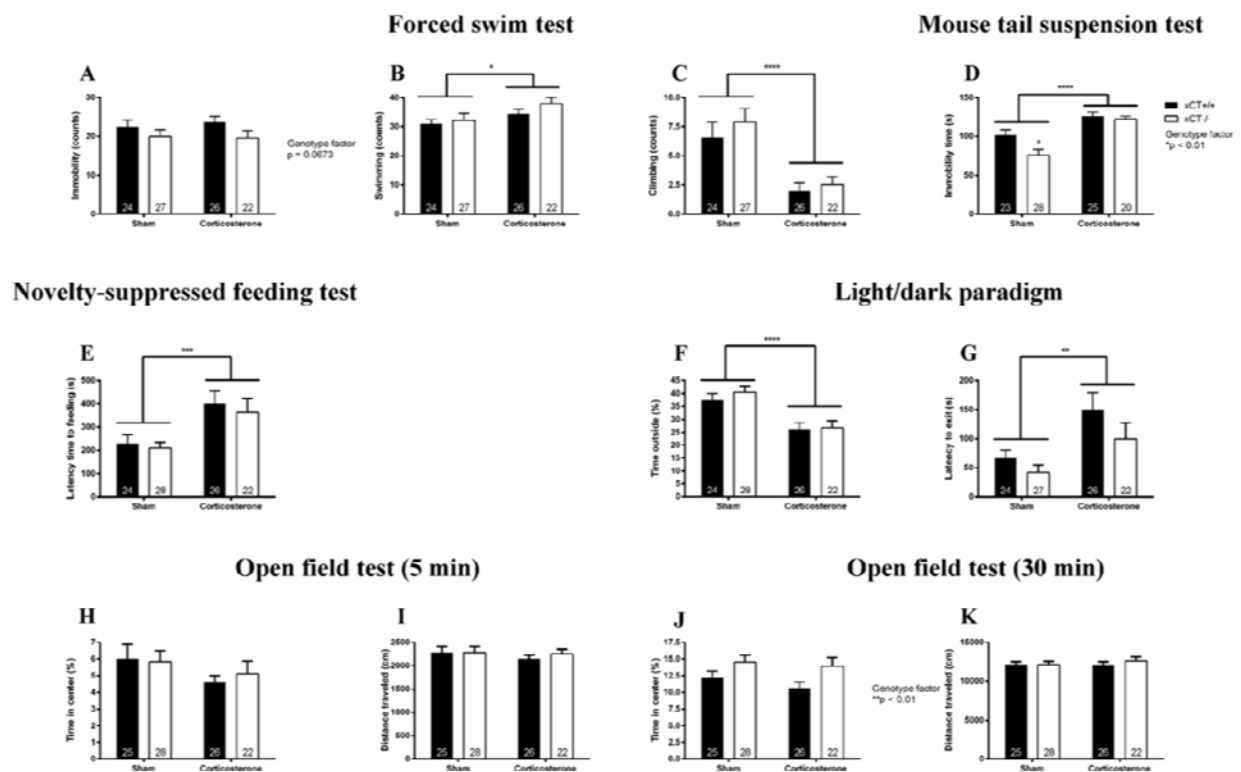


Figure 11. Behavioral analysis of $xCT^{-/-}$ and $xCT^{+/+}$ mice, subjected to the corticosterone mouse model for depression and anxiety. In the forced swim test, a trend towards a genotype effect was seen in the immobility mean counts (A). Furthermore a significant treatment effect was observed in the swimming (B) and climbing counts (C). In the mouse tail suspension test, a significant genotype and treatment effect are observed, but only in the SHAM treated mice the Tukey's post hoc test revealed a significant effect of xCT deletion (D). In the novelty-suppressed feeding test (E) and light/dark paradigm (F, G) only a significant treatment (but no genotype) effect is observed. Finally, in the open field test a significant genotype effect was observed only in the 30 min trial (J) but not in the first 5 min trial (H). No genotype nor treatment effect was furthermore observed in the total distance traveled (I, K). Data are presented as mean + SEM **** $P < 0.0001$, *** $P < 0.001$, ** $P < 0.01$, * $P < 0.05$ (2-way ANOVA and Tukey's post-hoc test for comparison of $xCT^{-/-}$ versus $xCT^{+/+}$ mice), sample size indicated in the figure.

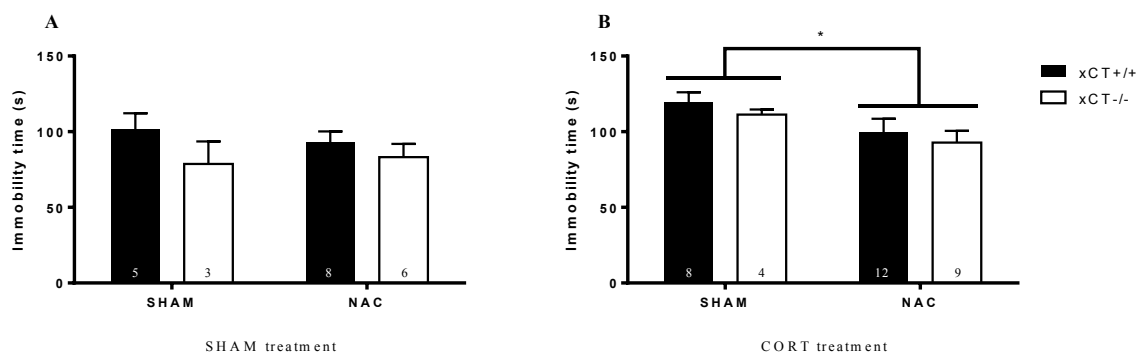


Figure 12. Behavioral analysis in the mouse-tail suspension test of $xCT^{-/-}$ and $xCT^{+/+}$ mice, subjected to the corticosterone (CORT) mouse model and treated with N-Acetylcysteine (NAC). NAC significantly reduces immobility time in the CORT (B) (but not in SHAM (A)) treated animals, independent of genotype. Data are presented as mean + SEM * $P < 0.05$ (2-way ANOVA), sample size indicated in the figure.

5. Specificity of antibodies raised against xCT

Many studies aiming to unveil the distribution or the role of system x_c^- , rely on antibody recognition of its specific subunit, xCT. It is generally accepted however that antibody specificity is a major problem. Until 2004, the only possibility to detect system x_c^- was the use of an antibody against a selective substrate, aminoadipic acid³⁰. After that, distinct antibodies raised against xCT appeared without consensus about the molecular weight of the antiporter. Based on literature, the xCT protein band would be expected around 55.5 kDa³¹. However, it has been reported that our own antibody¹⁷ as well as the antibodies raised by Burdo *et al.* (2006)³², Shih *et al.* (2006)³³ and La Bella *et al.* (2007)³⁴ recognize a fuzzy protein band at about 35 kDa. Antibody specificity of our own polyclonal antibody was confirmed on brain tissue of xCT^{-/-} mice¹⁸, using Western blotting¹⁷. The presence of nonspecific protein bands (present in both xCT^{-/-} and xCT^{+/+} tissue) shows that this antibody also recognizes unrelated proteins and as such cannot be used for immunohistochemistry¹⁷. Many researchers are still identifying the 55.5 kDa sharp immunoreactive band, observed when using most commercial antibodies in Western blot experiments and claimed to be xCT on the datasheets accompanying these antibodies, as xCT. Since often these antibodies are even used for immunohistochemistry, wrong conclusions can easily be drawn. Moreover, inappropriate negative controls are frequently being used to control for antibody specificity, such as pre-adsorption of the antiserum against the peptide or omission of the secondary antibody^{35,36}.

*We therefore verified the specificity of the most commonly used commercial as well as some in-house-developed anti-xCT antibodies (table 1, 2 in report 2015), by comparing their immunoreactivity in mouse brain tissue of xCT^{+/+} and xCT^{-/-} littermates using Western blotting (fig. 3 in report 2015) and immunohistochemistry (fig. 4, 5 in report 2015). A specific signal should be observed exclusively in xCT^{+/+} tissue and be absent in xCT^{-/-} tissue. The Western blot screening results demonstrate that antibody specificity not only differs between batches produced by immunizing different rabbits with the same antigen, but also between bleedings of the same rabbit (table 1 in report 2015). A number of immunohistochemical protocols has been tested for all the anti-xCT antibodies that were specific on Western blots (in table 1 and 2 in report 2015) in order to obtain a specific immunolabeling (fig. 4 in report 2015). Only one of our in-house-developed antibodies could reveal specific xCT labeling and exclusively on acetone-postfixed cryo-sections (fig. 5 in report 2015). Using this approach, we observed xCT protein expression throughout the mouse forebrain, including cortex, striatum, hippocampus, midbrain, thalamus and amygdala, with highest expression in regions facing the cerebrospinal fluid and meninges (fig. 5 in report 2015). **The results of this study were published in the Journal of Comparative Neurology**³⁷.*

6. Neuroprotective effects of zonisamide against lactacystin-induced neurodegeneration are independent of system x_c^-

Zonisamide (ZNS), used in symptomatic treatment of PD³⁸⁻⁴⁰, was recently reported to exert neuroprotection in rodent models⁴¹⁻⁴⁴. One of the proposed neuroprotective mechanisms involves elevated xCT protein expression, inducing GSH synthesis⁴². This is however in contrast with our hypothesis that inhibition of system x_c^- might be a neuroprotective strategy for the treatment of PD¹⁹. Therefore, we investigated the outcome of ZNS treatment in a mouse model of PD based on intranigral proteasome inhibition, and whether the observed effects would be mediated by system x_c^- . The proteasome inhibitor LAC (or vehicle, Sham) was administered intranigally to mice receiving repeated i.p. injections of either ZNS 30mg/kg or vehicle (placebo). Drug administration was initiated three days prior to stereotaxic LAC injection and was maintained until six days post surgery. One week after lesion, mice were behaviorally assessed and investigated in terms of nigrostriatal neurodegeneration and molecular changes at the level of the basal ganglia, including expression levels of xCT. In a separate set of experiments, the

impact of ZNS treatment on system x_c^- was investigated in naive, control conditions in vivo as well as in vitro. ZNS reduced the loss of nigral dopaminergic neurons following LAC infusion (fig. 6 in report 2015) and the degree of sensorimotor impairment (fig. 7 in report 2015). ZNS failed, however, to modulate xCT expression in basal ganglia of lesioned mice (fig. 8 in report 2015). Similarly, ZNS did not influence xCT or GSH levels in naive mice (fig. 9 in report 2015), nor did it alter system x_c^- activity or GSH content in vitro (fig. 10 in report 2015). Taken together, these results demonstrate that ZNS treatment provides neuroprotection and behavioral improvement in a PD mouse model based on proteasome inhibition, via system x_c^- independent mechanisms. These results are **published in Experimental Neurology** (Bentea et al., 2017)⁴⁵.

7. Summary of the main achievements/findings of this project:

1. In-depth analysis of the specificity problem of anti-xCT antibodies
2. Development and characterization of a new intranigral LAC mouse model for PD, showing neurodegeneration, α -synuclein accumulation, motor and non-motor impairment as well as ultrastructural changes in cortico-striatal synapses.
3. Behavioral phenotyping of the xCT^{-/-} mice, with clear anxiolytic and anti-depressive like effects.
4. No changes in xCT expression in tissue of depressed patients or rodent models for depression and no effect of loss of system x_c^- on depressive-like behavior in a validated mouse model for depression.
5. Further evidence for inhibition of system x_c^- as potential neuroprotective strategy for the treatment of PD, without negative effects in the elder and possibly beneficial for neuro-psychiatric co-morbidities
6. Confirmation of system x_c^- - independent, neuroprotective effects of ZNS in the LAC model

8. Publications obtained (or under revision/submitted) in the frame (or with the support) of the current GSKE project (2014-2016)

(*equally contributing authors)

- Demuyser T, Deneyer L, Bentea E, Albertini G, Femenia T, Walrave L, Sato H, Danbolt NC, De Bundel D, Massie A, Smolders I. Slc7a11 (xCT) protein expression is not altered in the depressed brain and system xc⁻ deficiency does not affect depression-associated behavior in the corticosterone mouse model. *In preparation to be submitted*.
- Bentea E, Moore C, Deneyer L, Verbruggen L, Churchill MJ, Hood RL, Meshul CK, Massie A. Plastic changes at corticostriatal synapses predict improved motor function in a partial model of Parkinson's disease. *Brain Research Bulletin*, *submitted*.
- Bentea E, Van Liefferinge J, Martens K, Kobayashi S, Deneyer L, Verbruggen L, Demuyser T, Albertini G, Maes K, Sato H, Smolders I, Lewerenz J, Massie A (2017) Zonisamide reduces lactacystin-induced nigral dopaminergic neurodegeneration and sensorimotor impairment in mice via system xc⁻ independent mechanisms. *Experimental Neurology* 290: 15-28.
- Bentea E, Verbruggen L, Massie A (2016) The proteasome inhibition model of Parkinson's disease. *Journal of Parkinson's disease*, in press.
- Demuyser T, Bentea E, Deneyer L, Albertini G, Massie A, Smolders I (2016) Disruption of the HPA-axis through corticosterone-release pellets induces robust depressive-like behavior and reduced BDNF levels in mice. *Neuroscience Letters* 626: 119-25.
- Demuyser T, Deneyer L, Bentea E, Albertini G, Van Liefferinge J, Merckx E, De Prins A, De Bundel D, Massie A, Smolders I (2016) In-depth behavioral characterization of the corticosterone mouse model and the critical involvement of housing conditions. *Physiology & Behavior* 156: 199-207.
- Massie A, Boillée S, Hewett S, Knackstedt L, Lewerenz J (2015) Main path and byways : non-vesicular glutamate release via system xc⁻ as an important modifier of glutamatergic neurotransmission. *Journal of Neurochemistry* 135: 1062-79.
- Van Liefferinge J, Bentea E, Demuyser T, Albertini G, Follin-Arbelet V, Holmseth S, Merckx E, Sato H, Aerts J, Smolders I, Arckens L, Danbolt NC, Massie A (2016) Comparative analysis of antibodies to xCT (Slc7a11) : forewarned is forearmed. *Journal of Comparative Neurology* 524: 1015-32.
- El Arfani A, Albertini G, Bentea E, Demuyser T, Van Eeckhaut A, Smolders I, Massie A (2015) Alterations in the motor cortical and striatal glutamatergic and D-serinergeric system in the bilateral 6-hydroxydopamine rat model for Parkinson's disease. *Neurochemistry International* 88: 88-96.
- Bentea E, Demuyser T, Van Liefferinge J, Albertini G, Deneyer L, Nys J, Merckx E, Michotte Y, Sato H, Arckens L, Massie A, Smolders I (2015) Absence of system xc⁻ in mice decreases anxiety and depressive-like behavior without affecting sensorimotor function or spatial vision. *Progress in Neuro-Psychopharmacology & Biological Psychiatry* 59: 49-58.
- Bentea E, Van Liefferinge J, Van der Perren A, El Arfani A, Albertini G, Demuyser T, Merckx E, Michotte Y, Smolders I, Baekelandt V, Massie A (2015) Nigral proteasome inhibition in mice leads to parkinsonism including non-motor impairment and alpha-synuclein phosphorylation at Ser129. *Frontiers in Behavioral Neuroscience* 9: 68.
- Bentea E, Sconce MD, Churchill MJ, Van Liefferinge J, Sato H, Meshul CK, Massie A (2015) MPTP-induced parkinsonism in mice alters striatal and nigral xCT expression but is unaffected by the genetic loss of xCT. *Neuroscience Letters*, *Neuroscience Letters* 593: 1-6.
- El Arfani A, Bentea E, Aourz N, Ampe B, De Deurwaerdère P, Van Eeckhaut A, Massie A, Sarre S, Smolders I, Michotte Y (2014) NMDA receptor antagonism potentiates the L-DOPA-induced extracellular dopamine release in the subthalamic nucleus of hemi-parkinson rats. *Neuropharmacology* 85:198-205

9. References

1. Blandini F, Greenamyre JT. Prospects of glutamate antagonists in the therapy of Parkinson's disease. *Fundam Clin Pharmacol.* 1998; 12(1):4-12.
2. Lewis SJ, Caldwell MA, Barker RA. Modern therapeutic approaches in Parkinson's disease. *Expert Rev Mol Med.* 2003; 5(10):1-20.
3. Müller T. Drug therapy in patients with Parkinson's disease. *Transl Neurodegen.* 2012;1:10.
4. Lee JM, Zipfel GJ, Choi DW. The changing landscape of ischaemic brain injury mechanisms. *Nature* 1999; 399:A7-14.
5. Hardingham GE, Fukunaga Y, Bading H. Extrasynaptic NMDARs oppose synaptic NMDARs by triggering CREB shut-off and cell death pathways. *Nat Neurosci.* 2002; 5(5):405-14.
6. Vizi ES, Kisfalvi M, Lörincz T. Role of nonsynaptic GluN2B-containing NMDA receptors in excitotoxicity: Evidence that fluoxetine selectively inhibits these receptors and may have neuroprotective effects. *Brain Res Bull.* 2012; [Epub ahead of print].
7. Aguirre JA, Kehr J, Yoshitake T, Liu FL, Rivera A, Fernandez-Espinola S, Andbjør B, Leo G, Medhurst AD, Agnati LF, Fuxe K. Protection but maintained dysfunction of nigral dopaminergic nerve cell bodies and striatal dopaminergic terminals in MPTP-lesioned mice after acute treatment with the mGluR5 antagonist MPEP. *Brain Res.* 2005 ;1033(2):216-20.
8. Breyse N, Amalric M, Salin P. Metabotropic glutamate 5 receptor blockade alleviates akinesia by normalizing activity of selective basal-ganglia structures in parkinsonian rats. *J Neurosci.* 2003; 23(23):8302-9.
9. Armentero MT, Fancellu R, Nappi G, Bramanti P, Blandini F. Prolonged blockade of NMDA or mGluR5 glutamate receptors reduces nigrostriatal degeneration while inducing selective metabolic changes in the basal ganglia circuitry in a rodent model of Parkinson's disease. *Neurobiol Dis.* 2006; 22(1):1-9.
10. Schneider F, Althaus A, Backes V, Dodel R. Psychiatric symptoms in Parkinson's disease. *Eur Arch Psychiatry Clin Neurosci.* 2008; 258(S5):55-59.
11. Bannai S. Exchange of cystine and glutamate across plasma membrane of human fibroblasts. *J Biol Chem.* 1986; 261(5):2256-63.
12. Massie A, Goursaud S, Schallier A, Vermoesen K, Meshul CK, Hermans E, Michotte Y. Time-dependent changes in GLT-1 functioning in striatum of hemi-Parkinson rats. *Neurochem Int.* 2010; 57(5):572-8.
13. Massie A, Schallier A, Vermoesen K, Arckens L, Michotte Y. Biphasic and bilateral changes in striatal VGLUT1 and 2 protein expression in hemi-Parkinson rats. *Neurochem Int.* 2010; 57(2):111-8.
14. Schallier A, Massie A, Loyens E, Moechars D, Drinkenburg W, Michotte Y, Smolders I. vGLUT2 heterozygous mice show more susceptibility to clonic seizures induced by pentylentetrazol. *Neurochem Int.* 2009; 55(1-3):41-4.
15. Schallier A, Smolders I, Van Dam D, Loyens E, De Deyn PP, Michotte A, Michotte Y, Massie A. Region- and age-specific changes in glutamate transport in the A β PP23 mouse model for Alzheimer's disease. *J Alzheimers Dis.* 2011; 24(2):287-300.
16. De Bundel D, Schallier A, Loyens E, Fernando R, Miyashita H, Van Liefferinge J, Vermoesen K, Bannai S, Sato H, Michotte Y, Smolders I, Massie A. Loss of system x(c)- does not induce oxidative stress but decreases extracellular glutamate in hippocampus and influences spatial working memory and limbic seizure susceptibility. *J Neurosci.* 2011; 31(15):5792-803.
17. Massie A, Schallier A, Mertens B, Vermoesen K, Bannai S, Sato H, Smolders I, Michotte Y. Time-dependent changes in striatal xCT protein expression in hemi-Parkinson rats. *Neuroreport.* 2008; 19(16):1589-92.
18. Sato H, Shiiya A, Kimata M, Maebara K, Tamba M, Sakakura Y, Makino N, Sugiyama F, Yagami K, Moriguchi T, Takahashi S, Bannai S. Redox imbalance in cystine/glutamate transporter-deficient mice. *J Biol Chem.* 2005; 280(45):37423-9.
19. Massie A, Schallier A, Kim SW, Fernando R, Kobayashi S, Beck H, De Bundel D, Vermoesen K, Bannai S, Smolders I, Conrad M, Plesnila N, Sato H, Michotte Y. Dopaminergic neurons of system x(c)-deficient mice are highly protected against 6-hydroxydopamine-induced toxicity. *FASEB J.* 2011; 25(4):1359-69.
20. Lewerenz J, Hewett SJ, Huang Y, Lambros M, Gout PW, Kalivas PW, Massie A, Smolders I, Methner A, Pergande M, Smith SB, Ganapathy V, Maher P. The Cystine/Glutamate Antiporter System x(c)- in Health and Disease: From Molecular Mechanisms to Novel Therapeutic Opportunities. *Antioxid Redox Signal.* 2013; 18(5):522-55.
21. Baker DA, Xi ZX, Shen H, Swanson CJ, Kalivas PW. The origin and neuronal function of in vivo nonsynaptic glutamate. *J Neurosci.* 2002; 22(20):9134-41.
22. Lewerenz J, Baxter P, Kassubek R, Albrecht P, Van Liefferinge J, Westhoff MA, Halatsch ME, Karpel-Massler G, Meakin PJ, Hayes JD, Aronica E, Smolders I, Ludolph AC, Methner A, Conrad M, Massie A, Hardingham GE, Maher P. Phosphoinositide 3-kinases upregulate system xc(-) via eukaryotic initiation factor 2 α and activating transcription factor 4 - A pathway active in glioblastomas and epilepsy. *Antioxid Redox Signal.* 2014;20(18):2907-22.
23. Bentea E, Van der Perren A, Van Liefferinge J, El Arfani A, Albertini G, Demuyser T, Merckx E, Michotte Y, Smolders I, Baekelandt V, Massie A. Nigral proteasome inhibition in mice leads to motor and non-motor deficits and increased expression of Ser129 phosphorylated α -synuclein. *Front Behav Neurosci.* 2015;9:68. doi: 10.3389/fnbeh.2015.00068. eCollection 2015.

24. Anglade P, Mouatt-Prigent A, Agid Y, Hirsch E. Synaptic plasticity in the caudate nucleus of patients with Parkinson's disease. *Neurodegeneration* 1996;5(2):121-8.
25. Sheng ZH, Cai Q. Mitochondrial transport in neurons: impact on synaptic homeostasis and neurodegeneration. *Nat Rev Neurosci.* 2012;13(2):77-93.
26. Bentea E, Sconce MD, Churchill MJ, Van Liefveringe J, Sato H, Meshul CK, Massie A. MPTP-induced parkinsonism in mice alters striatal and nigral xCT expression but is unaffected by the genetic loss of xCT. *Neurosci Lett.* 2015;593:1-6.
27. Bentea E, Demuyser T, Van Liefveringe J, Albertini G, Deneyer L, Nys J, Merckx E, Michotte Y, Sato H, Arckens L, Massie A, Smolders I. Absence of system xc- in mice decreases anxiety and depressive-like behavior without affecting sensorimotor function or spatial vision. *Prog Neuropsychopharmacol Biol Psychiatry.* 2015;59:49-58.
28. Lutgen V, Resch J, Qualmann K, Raddatz NJ, Panhans C, Olander EM, Kong L, Choi S, Mantsch JR, Baker DA. Behavioral assessment of acute inhibition of system xc(-) in rats. *Psychopharmacology* 2014;231:4637-47.
29. Smaga I, Pomierny B, Krzyzanowska W, Pomierny-Chamiolo L, Miszkiewski J, Niedzielska E, Ogorka A, Filip M . N-acetylcysteine possesses antidepressant-like activity through reduction of oxidative stress: behavioral and biochemical analyses in rats. *Prog Neuropsychopharmacol Biol Psychiatry* 2012;39: 280-7.
30. Pow DV. Visualising the activity of the cystine-glutamate antiporter in glial cells using antibodies to amino adipic acid, a selectively transported substrate. *Glia.* 2001;34(1):27-38.
31. Sato H, Tamba M, Ishii T, Bannai S. Cloning and expression of a plasma membrane cystine/glutamate exchange transporter composed of two distinct proteins. *J Biol Chem.* 1999;274(17):11455-8.
32. Burdo J, Dargusch R, Schubert D. Distribution of the cystine/glutamate antiporter system xc- in the brain, kidney, and duodenum. *J Histochem Cytochem.* 2006;54(5):549-57.
33. Shih AY, Erb H, Sun X, Toda S, Kalivas PW, Murphy TH. Cystine/glutamate exchange modulates glutathione supply for neuroprotection from oxidative stress and cell proliferation. *J Neurosci.* 2006;26(41):10514-23.
34. La Bella V, Valentino F, Piccoli T, Piccoli F. Expression and developmental regulation of the cystine/glutamate exchanger (xc-) in the rat. *Neurochem Res.* 2007;32(6):1081-90.
35. Saper CB. An open letter to our readers on the use of antibodies. *J Comp Neurol.* 2005;493(4):477-8.
36. Holmseth S, Zhou Y, Follin-Arbelet VV, Lehre KP, Bergles DE, Danbolt NC. Specificity controls for immunocytochemistry: the antigen preadsorption test can lead to inaccurate assessment of antibody specificity. *J Histochem Cytochem.* 2012;60(3):174-87.
37. Van Liefveringe J, Bentea E, Demuyser T, Albertini G, Follin-Arbelet V, Holmseth S, Merckx E, Sato H, Aerts JL, Smolders I, Arckens L, Danbolt NC, Massie A. Comparative analysis of antibodies to xCT (Slc7a11): Forewarned is forearmed. *J Comp Neurol.* 2016; 524: 1015-32.
38. Murata M. Novel therapeutic effects of the anti-convulsant, zonisamide, on Parkinson's disease. *Curr Pharm Des.* 2004;10: 687-693.
39. Murata M, Hasegawa K, Kanazawa I. Zonisamide improves motor function in Parkinson disease: a randomized, double-blind study. *Neurology* 2007; 68: 45-50.
40. Murata M, Horiuchi E, Kanazawa I. Zonisamide has beneficial effects on Parkinson's disease patients. *Neurosci Res.* 2001; 41: 397-399.
41. Arawaka S, Fukushima S, Sato H, Sasaki A, Koga K, Koyama S, Kato T. Zonisamide attenuates alpha-synuclein neurotoxicity by an aggregation-independent mechanism in a rat model of familial Parkinson's disease. *PLoS One* 2014; 9: e89076.
42. Asanuma M, Miyazaki I, Diaz-Corrales FJ, Kimoto N, Kikkawa Y, Takeshima M, Miyoshi K, Murata M. Neuroprotective effects of zonisamide target astrocyte. *Ann Neurol.* 2010; 67: 239-249.
43. Sano H, Murata M, Nambu A. Zonisamide reduces nigrostriatal dopaminergic neurodegeneration in a mouse genetic model of Parkinson's disease. *J Neurochem.* 2015; 134(2):371-81.
44. Sonsalla PK, Wong LY, Winnik B, Buckley B. The antiepileptic drug zonisamide inhibits MAO-B and attenuates MPTP toxicity in mice: clinical relevance. *Exp Neurol.* 2010; 221: 329-334.
45. Bentea E, Van Liefveringe J, Martens K, Kobayashi S, Deneyer L, Verbruggen L, Demuyser T, Albertini G, Maes K, Sato H, Smolders I, Lewerenz J, Massie A (2016) Zonisamide reduces lactacystin-induced nigral dopaminergic neurodegeneration and sensorimotor impairment in mice via system x_c⁻ independent mechanisms. *Exp Neurol.* 2017; 15-28.



Geneeskundige Stichting Koningin Elisabeth
Fondation Médicale Reine Elisabeth
Königin-Elisabeth-Stiftung für Medizin
Queen Elisabeth Medical Foundation

Final report
of the research group of

Dr. Laurent Nguyen &
dr. Brigitte Malgrange

Université de Liège (ULg)

Dr. Laurent Nguyen

Unité de Neurobiologie du développement
GIGA-Neurosciences
Université de Liège
4000 Liège
T +32 4 366 59 87
F +32 4 366 59 12
lnguyen@ulg.ac.be
www.giga.ulg.ac.be

Dr. Brigitte Malgrange

Unité de Neurobiologie du développement
GIGA-Neurosciences
Université de Liège
4000 Liège
T +32 4 366 59 87
F +32 4 366 59 12
bmalgrange@ulg.ac.be
www.giga.ulg.ac.be

Deciphering the role of protein acetylation in primary ciliogenesis

1. Background and significance

The aim of the present work is to better understand the biology of the primary cilium. Mounting evidence shows that mutations in cilia genes can lead to cortical malformations and deafness. Although primary cilium has been discovered decades ago, little is known about its biology. Cilia are indeed subdivided into two categories: motile cilia (secondary cilia) that enable fluid movement over epithelial surfaces and primary cilia that are localized at the surface of most cell types during G0 and act as a “sensor” to transduce extracellular signaling, thus contributing to a broad array of homeostatic mechanisms [1-4]. The primary cilium is nucleated from and anchored to a basal body (BB), which is composed of an axoneme enriched in microtubules (MT) surrounded by a ciliary membrane connected to the plasma membrane. A transition zone between the BB and the axoneme acts as a molecular barrier and docking station for intraflagellar transport (IFT) and motor proteins [5]. Despite our growing understanding of its biological role, we do not know much about the factors that contribute to its assembly and positioning at the cell membrane during brain development. Accumulating evidence shows that mutations in cilia genes can lead to malformations underlying neurological or psychiatric disorders, as well as deafness and balance disorders [6].

The main goal of the present project is to decipher whether and to what extent lysine acetylation of proteins controls primary ciliogenesis. In vertebrates, lysine acetylation sites are as conserved as those in phosphorylated proteins, suggesting a selective pressure to maintain this protein modification. Recent data indicate that acetylation occurs on thousands of proteins [7]. Although it was, until recently, exclusively associated with transcriptional activation (through neutralization of positive charges of core histone tail lysine residues [8]), there is now growing evidence to support lysine acetylation of a broad range of non-histone proteins [9-11]. This modification is promoted by lysine acetyl-transferases (KATs) and requires acetyl-CoA as acetyl donor. It is believed that lysine acetylation regulates activity, localization, specific interaction as well as stability/degradation of proteins, therefore controlling a variety of cellular processes such as apoptosis, proliferation and differentiation [12]. Recent studies suggest that acetylation of cytoplasmic substrates contributes to brain development [13, 14] and that disruption of this process is associated with various progressive neurological disorders [15, 16]. Elongator deficiency in humans causes Familial Dysautonomia, an autosomal recessive orphan neurodevelopmental and neurodegenerative disease, that mostly targets neurons from the autonomic and sensory system [17, 18]. Elongator comprises six subunits (Elp1-6). Elp1 is a scaffold subunit required for functional assembly of Elongator and Elp3 acts as a DNA demethylase [19] and a KAT. This multiprotein complex promotes N ϵ -acetylation of histone H3 lysines [20], thereby regulating elongation of some RNA messengers. However, the complex is mostly expressed in the cytoplasm where it controls acetylation of targets such as alpha-tubulin [13, 21] and Bruchpilot [22]. In addition, Elongator activity in animals and plants is mostly associated with its role in modifying wobble uridines in selected tRNAs. Our preliminary data support a novel function of Elongator in primary ciliogenesis in the perinatal subventricular zone and at the kinocilium (derived from primary cilium) in hair cell progenitors. Our aim is to uncover the role of acetylation in primary (kino)-ciliogenesis by addressing the role of Elongator as an entry point.

2. Elongator controls primary ciliogenesis in the developing brain

2.1. The cerebral cortex

The cerebral cortex is an evolutionary advanced brain structure made of neuronal layers tangentially organized into areas that serve specialized functions. Cortical layering arises inside-out as progenitors give birth to successive waves of pyramidal projection neurons in the dorsal telencephalon and, GABAergic interneurons in the ventral forebrain. Projection neurons migrate radially to settle in cortical layers and they grow axonal projections towards cortical or sub-cortical targets. Interneurons migrate along multiple tangential paths to integrate local cortical networks. More generally, the development of the cortex implies a continuous rearrangement of a primordial structure that progresses through successive steps including, proliferation, specification, migration, and neuronal differentiation.

Disrupting the completion of one or several of these events often leads to malformations of cortical development (MCDs). MCDs comprise a heterogeneous group of focal or diffuse anatomical brain abnormalities with wide spectrum of clinical presentations, developmental delay or intellectual disabilities.

By coupling analyses with mouse, fly and human stem cells, we discovered a new function for the Elongator complex in stem cell fate specification. While we could not detect major impairment of primary cilia, Elp3cKO newborn mice suffered from microcephaly, a phenotype resulting from depletion of intermediate progenitors (IPs) during embryogenesis thereby leading to reduced number of projection neurons in all cortical layers. Remarkably, we observed a reduction of the neurogenic potential of induced pluripotent stem cells derived from skin fibroblasts of patients suffering from Familial Dysautonomia that show reduced Elongator expression. In mouse, loss of Elp3 activity impaired codon translation speed and triggered endoplasmic reticulum (ER) stress and unfolded protein response (UPR). Moreover, we found that a dynamic regulation of UPR is required for proper cortical neurogenesis and that Elp3 depletion raises the basal level of the UPR via activation of the Perk-eIF2 α -Atf4 signaling. Upregulation of the basal UPR level in apical progenitors (APs) favored direct neurogenesis and further impaired IPs generation and thus indirect cortical neurogenesis. We discovered that: 1/ Elongator safeguards the cellular fate choice of APs to ensure the generation of appropriate number of cortical projection neurons; 2/ a UPR signalling controls cell fate acquisition during mammalian brain development. *These results have recently been published in Developmental Cell, 2015, Laguesse et al.*

2.2. The lateral wall of the subventricular zone of brain newborn mice

The coordinated directional beating of multi-ciliated ependymal cells located at the surface of the postnatal lateral ventricle (LV), creates a unidirectional CSF flow named ependymal flow [23], which is essential for brain homeostasis and olfactory bulb neurogenesis [24]. Disruption of ciliogenesis (e.g. primary ciliopathies such as Joubert's syndrome and Meckel-Gruber syndrome) or ependymal cell polarization often result in hydrocephalus and brain malformations [25-30]. Ependymal cells are polarized along the apico-basal axis as well as also along the epithelial plan through a process called planar cell polarity (PCP). Establishment of PCP during ependymal cell maturation is an essential prerequisite for the coordinated ciliary beating across the lateral wall after birth [26, 28, 29, 31]. PCP was originally identified in *Drosophila* and is characterized by the planar-polarized accumulation of PCP core components (in mammals: atypical seven-pass transmembrane cadherin; Celsr (Celsr1-3), Frizzled3 (Fzd3), Frizzled6 (Fzd6), Van Gogh like1-2 (Vangl1-2), Disheveled1-3 (Dvl1-3), and Prickle like 1-4 (PK1-4)) to distinct regions of the cell. Their mutations impair primary cilium development and function, linking ciliogenesis with planar polarity and hydrocephalus [28, 29, 32-34]. In ependymal cells, motile cilia nucleate from microtubule-based structures/platform called basal bodies (BBs), which are the first determinants of ependymal cell polarity. Planar cell polarity underlies different biological events [26] : (1) rotational polarity, which corresponds to the unidirectional alignment of motile cilia in the cell and the coordination of this process at the tissue level [28, 29]; and (2) translational polarity, which refers to the migration and the positioning of the cluster of BBs (and their corresponding cilia) in ependymal cells

[31]. Moreover, radial glial cells (RGCs), which are the ependymal cell progenitors [35], already show horizontal migration of their primary cilia, suggesting that ependymal cell polarity establishment is a gradual process starting in their progenitors where the primary cilium plays a central role for establishing intrinsic as well as tissular cell polarity [26, 36-39].

By coupling genetic, histological and biochemical approaches, we identified Elp3, the catalytic subunit of the Elongator complex, as a regulator of primary ciliogenesis and PCP establishment in the lateral wall of the postnatal mouse brain. Immunolabelings uncovered Elp1 and Elp3 expression at pericentriolar material (PCM)/basal body and/or transition zone. We crossed FoxG1: Cre mice [40] with Elp3 lox/lox mice to conditionally delete *Elp3* from telencephalon progenitors (Elp3 cKO mouse), including radial glia cells. Our preliminary results showed that the conditional loss of Elp3 in forebrain progenitors leads to postnatal hydrocephalus in mice. ACIII-positive primary cilia were significantly shorter in Elp3 cKO radial glia cells as compared to control, suggesting a role for Elongator in primary ciliogenesis. Ultrastructure analyses performed by electronic microscopy (SEM and TEM) confirmed shortening of the primary cilium upon Elp3 depletion in radial glia cells. Comparable data have recently been obtained in hTERT-RPE1 cells depleted of Elp3 by siRNA transfection.

Functional analyses demonstrated that Elongator is required for proper growth and positioning of the primary cilium of RGCs as well as the establishment of the PCP in maturing ependymal cells of the lateral wall in mouse. This phenotype results from the activation the PERK/Atf4 pathway, which further disturbs Notch signaling via blockade of its intracellular furin-dependant cleavage and thus membrane maturation. This was further supported by western-blot analyses showing a significant reduction of Notch ICD in RGCs from the lateral wall from Elp3cKO postnatal mice as well as in cultured Elp3-depleted hTERT-RPE1 cells. Pharmacological reduction of ER stress induced upon Elp3 depletion rescues primary cilia length in hTERT-RPE1 cells. These results support the existence of a link between Elongator activity and Notch signaling during ciliogenesis and polarity establishment in the lateral wall of the postnatal brain. *A manuscript including these results will be submitted in January 2017.*

3. Deciphering how Elongator is required for the formation of kinocilium and the development of the inner ear

Inner ear hair cells convert mechanical stimuli of sound, gravity and head movements into electrical signals. Each hair cell contains at the apical surface its mechanically sensitive organelle, the hair bundle consisting of actin-filled stereocilia and, at least during development, a tubulin-based primary cilium, known as the kinocilium. In auditory hair cells of mammals and birds, kinocilia regress soon after the onset of mechano-transduction, whereas vestibular hair cells maintain kinocilia throughout maturity. Kinocilia of all the hair cells of the inner ear are polarized in a coordinated manner. The kinocilium is essential in sculpturing the inner ear and the polar hair bundles via the planar cell polarity (PCP) signalling pathway. Indeed, genetic loss or underdevelopment of the kinocilium led to PCP phenotype including misoriented hair bundles and a shorter and wider cochlear duct [36, 41]. Our preliminary results suggest that in the absence of Elp3 the kinocilium is shorter and PCP defects are present in the inner ear. In this project, we will therefore test our hypothesis that genes - such as Elp3 - required for the formation of kinocilia is involved in PCP regulation at multiple steps for normal morphogenesis of the inner ear both in the vestibular and cochlear portions.

Characterization of ciliogenesis in the developing inner ear

Some of the fundamental knowledge about kinocilia is incomplete. For example, it is still unknown if it possesses a motile or non-motile cilium and second. Therefore, in this part of our project we have characterised the auditory and vestibular kinocilia by transmission electron microscopy. We have looked

whether the axoneme of the kinocilium has a 9+0 (classical primary cilium) or 9+2 (classical motile cilium) structure. Looking at the early post-natal mouse cochlea, we have found that the kinocilium of the auditory epithelium possesses a 9+0 structure, but that this structure is modified to a non-canonical 8+1 structure in a base to apex gradient along the axoneme of the cilium. The presence of this non-canonical configuration may reflect the maturity of the kinocilium, as we observed higher frequency of 8+1 structures at the apex of the cochlea, where hair cells are more immature. We were not able to observe the presence of dynein arms - conferring motility - on the peripheral microtubule doublets, and therefore presume the auditory kinocilium to be non-motile.

Assessing PCP and kinocilium phenotype in the inner ear of Elp3 mutant mice

Preliminary results showed that Elp3 invalidation leads to shortening of kinocilium and planar polarity defects - especially misorientation of stereociliary bundles and formation of a mildly truncated cochlear duct. There are two levels of planar polarity within the sensory epithelium of the inner ear – so called tissue planar polarity and cell-intrinsic planar polarity [42, 43]. Disruption to either pathway can result in misoriented stereocilia bundles. Core PCP proteins asymmetrically recruit to the cell membrane in order to orient all sensory epithelial cells along the medio-lateral axis – this is tissue planar polarity and is most obviously defined by the v-shaped stereocilia of hair cells all pointing towards the lateral edge [44]. To investigate the cause of the planar polarity defects we observed, membrane recruitment and asymmetric localization of core PCP proteins have been studied. Surprisingly, we found that Elp3 is not necessary for membrane recruitment and asymmetric position of Frizzled6, Vangl1 and vangl2, three members of the core PCP protein family that controls tissue planar polarity in the inner ear [44]. These results confirm that Elp3 is not necessary for the formation of the PCP protein-mediated tissue planar polarity of the auditory sensory epithelium.

The second level of planar polarity that exists within the sensory epithelium is the formation of cell-intrinsic planar polarity of the auditory hair cells. As the hair cells differentiate and mature, the kinocilium emerges at the centre of the apical surface, and then migrates towards the lateral edge of the hair cell. This migration is coordinated by a lateral membrane-bound belt of Gai3 and LGN, which sequester motor proteins such as dynein, generating pulling forces on microtubules and thus pulling the kinocilium laterally [42, 43]. Furthermore, the medial localisation of aPKC acts to maintain the lateral restriction of the Gai3/LGN complex. We have found that Elp3 has a very important role in establishing the intrinsic polarity of hair cells. The lateral membrane localisation of Gai3 and LGN in hair cells is severely disrupted in the absence of Elp3, and furthermore, the medial localisation of aPKC is also disrupted upon Elp3 deletion. As a result, we have observed that the kinocilium is significantly mispositioned in cochlear hair cells from Elp3 deficient mice – it remains more centrally positioned on the apical surface, failing to migrate correctly towards the lateral edge.

As alpha-tubulin is a target of Elongator mediated acetylation [13, 21], and the kinocilium is a microtubule-based structure, we hypothesized that the phenotypes we have observed are a consequence of reduced acetylation of microtubules. However, analysis of the cochleae of ATAT1 knock-out mice [45] – another mouse model in which alpha-tubulin acetylation is severely diminished in the cochlea– did not reveal a recapitulation of the phenotype observed upon loss of Elp3. In fact, the cochleae of ATAT1 knock-out mice are broadly normal, with the organisation of the sensory epithelium at the level of tissue and intrinsic planar polarity being indistinguishable from that of wild-type littermates. Therefore, we do not believe that the phenotype observed in Elp3 deficient mice is a consequence of diminished acetylation of alpha-tubulin.

GAI3/LGN complexes are commonly used by dividing cells to generate pulling forces on astral microtubules and orient the mitotic spindle to ensure division occurs within the correct plane [46]. Using HEK293T cells, we have been able to show that the loss of Elp3 expression can disrupt LGN localisation during cell division. The asymmetric, membrane-bound localisation of LGN during cell division and kinocilium migration is likely dependent upon correct transport of these proteins to their target regions. Interestingly, protein transport analysis using LysoTracker in HEK293T cells revealed that transport

along microtubules is significantly slowed in the absence of Eip3. We are currently further investigating the hypothesis that impaired transport along microtubules disrupts the delivery/rate of delivery of the intrinsic polarity proteins to their correct location at the apical surface of the hair cell. In doing so, this impairs kinocilium migration and thus creates polarity defects in the developing auditory epithelium. *A manuscript incorporating these results will be submitted in March 2017.*

4. Bibliography

1. Berbari NF, O'Connor AK, Haycraft CJ et al. The primary cilium as a complex signaling center. **Curr Biol.** 2009;19:R526-535.
2. Singla V, Reiter JF. The primary cilium as the cell's antenna: signaling at a sensory organelle. **Science.** 2006;313:629-633.
3. Corbit KC, Aanstad P, Singla V et al. Vertebrate Smoothed functions at the primary cilium. **Nature.** 2005;437:1018-1021.
4. Rohatgi R, Milenkovic L, Scott MP. Patched1 regulates hedgehog signaling at the primary cilium. **Science.** 2007;317:372-376.
5. Pedersen LB, Rosenbaum JL. Intraflagellar transport (IFT) role in ciliary assembly, resorption and signalling. **Curr Top Dev Biol.** 2008;85:23-61.
6. Norris DP, Grimes DT. Mouse models of ciliopathies: the state of the art. **Disease models & mechanisms.** 2012;5:299-312.
7. Choudhary C, Kumar C, Gnad F et al. Lysine acetylation targets protein complexes and co-regulates major cellular functions. **Science.** 2009;325:834-840.
8. Ren Q, Gorovsky MA. Histone H2A.Z acetylation modulates an essential charge patch. **Mol Cell.** 2001;7:1329-1335.
9. Choudhary J, Grant SG. Proteomics in postgenomic neuroscience: the end of the beginning. **Nat Neurosci.** 2004;7:440-445.
10. Close P, Creppe C, Gillard M et al. The emerging role of lysine acetylation of non-nuclear proteins. **Cell Mol Life Sci.** 2010;67:1255-1264.
11. Kim SC, Sprung R, Chen Y et al. Substrate and functional diversity of lysine acetylation revealed by a proteomics survey. **Mol Cell.** 2006;23:607-618.
12. Spange S, Wagner T, Heinzl T et al. Acetylation of non-histone proteins modulates cellular signalling at multiple levels. **Int J Biochem Cell Biol.** 2009;41:185-198.
13. Creppe C, Malinouskaya L, Volvert ML et al. Elongator controls the migration and differentiation of cortical neurons through acetylation of alpha-tubulin. **Cell.** 2009;136:551-564.
14. Reed NA, Cai D, Blasius TL et al. Microtubule acetylation promotes kinesin-1 binding and transport. **Curr Biol.** 2006;16:2166-2172.
15. Dompierre JP, Godin JD, Charrin BC et al. Histone deacetylase 6 inhibition compensates for the transport deficit in Huntington's disease by increasing tubulin acetylation. **J Neurosci.** 2007;27:3571-3583.
16. Hempen B, Brion JP. Reduction of acetylated alpha-tubulin immunoreactivity in neurofibrillary tangle-bearing neurons in Alzheimer's disease. **J Neuropathol Exp Neurol.** 1996;55:964-972.
17. Slaugenhaupt SA, Blumenfeld A, Gill SP et al. Tissue-specific expression of a splicing mutation in the IKBKAP gene causes familial dysautonomia. **Am J Hum Genet.** 2001;68:598-605.
18. Slaugenhaupt SA, Gusella JF. Familial dysautonomia. **Curr Opin Genet Dev.** 2002;12:307-311.
19. Okada Y, Yamagata K, Hong K et al. A role for the elongator complex in zygotic paternal genome demethylation. **Nature.** 2010;463:554-558.
20. Winkler GS, Kristjuhan A, Erdjument-Bromage H et al. Elongator is a histone H3 and H4 acetyltransferase important for normal histone acetylation levels in vivo. **Proc Natl Acad Sci U S A.** 2002;99:3517-3522.
21. Solinger JA, Paolinelli R, Kloss H et al. The *Caenorhabditis elegans* Elongator complex regulates neuronal alpha-tubulin acetylation. **PLoS Genet.** 2010;6:e1000820.
22. Miskiewicz K, Jose LE, Bento-Abreu A et al. ELP3 controls active zone morphology by acetylating the ELKS family member Bruchpilot. **Neuron.** 2011;72:776-788.
23. Miyan JA, Nabiyouni M, Zindah M. Development of the brain: a vital role for cerebrospinal fluid. **Can J Physiol Pharmacol.** 2003;81:317-328.
24. Sawamoto K, Wichterle H, Gonzalez-Perez O et al. New neurons follow the flow of cerebrospinal fluid in the adult brain. **Science.** 2006;311:629-632.
25. Lee L. Riding the wave of ependymal cilia: genetic susceptibility to hydrocephalus in primary ciliary dyskinesia. **J Neurosci Res.** 2013;91:1117-1132.
26. Mirzadeh Z, Han YG, Soriano-Navarro M et al. Cilia organize ependymal planar polarity. **J Neurosci.** 2010;30:2600-2610.
27. Vogel P, Read RW, Hansen GM et al. Congenital hydrocephalus in genetically engineered mice. **Vet Pathol.** 2012;49:166-181.
28. Ohata S, Nakatani J, Herranz-Perez V et al. Loss of Dishevelleds disrupts planar polarity in ependymal motile cilia and results in hydrocephalus. **Neuron.** 2014;83:558-571.
29. Boutin C, Labedan P, Dimidschstein J et al. A dual role for planar cell polarity genes in ciliated cells. **Proc Natl Acad Sci U S A.** 2014;111:E3129-3138.
30. Badano JL, Mitsuma N, Beales PL et al. The ciliopathies: an emerging class of human genetic disorders. **Annu Rev Genomics Hum Genet.** 2006;7:125-148.
31. Guirao B, Meunier A, Mortaud S et al. Coupling between hydrodynamic forces and planar cell polarity orients mammalian motile cilia. **Nat Cell Biol.** 2010;12:341-350.

32. Ohata S, Herranz-Perez V, Nakatani J et al. Mechanosensory Genes Pkd1 and Pkd2 Contribute to the Planar Polarization of Brain Ventricular Epithelium. **J Neurosci**. 2015;35:11153-11168.
33. Sowers LP, Yin T, Mahajan VB et al. Defective motile cilia in Prickle2-deficient mice. **J Neurogenet**. 2014;28:146-152.
34. Tissir F, Qu Y, Montcouquiol M et al. Lack of cadherins Celsr2 and Celsr3 impairs ependymal ciliogenesis, leading to fatal hydrocephalus. **Nat Neurosci**. 2010;13:700-707.
35. Spassky N, Merkle FT, Flames N et al. Adult ependymal cells are postmitotic and are derived from radial glial cells during embryogenesis. **J Neurosci**. 2005;25:10-18.
36. Jones C, Roper VC, Foucher I et al. Ciliary proteins link basal body polarization to planar cell polarity regulation. **Nat Genet**. 2008;40:69-77.
37. Park TJ, Haigo SL, Wallingford JB. Ciliogenesis defects in embryos lacking inturned or fuzzy function are associated with failure of planar cell polarity and Hedgehog signaling. **Nat Genet**. 2006;38:303-311.
38. Ross AJ, May-Simera H, Eichers ER et al. Disruption of Bardet-Biedl syndrome ciliary proteins perturbs planar cell polarity in vertebrates. **Nat Genet**. 2005;37:1135-1140.
39. Wallingford JB. Planar cell polarity, ciliogenesis and neural tube defects. **Hum Mol Genet**. 2006;15 Spec No 2:R227-234.
40. Hebert JM, McConnell SK. Targeting of cre to the Foxg1 (BF-1) locus mediates loxP recombination in the telencephalon and other developing head structures. **Dev Biol**. 2000;222:296-306.
41. Sipe CW, Lu X. Kif3a regulates planar polarization of auditory hair cells through both ciliary and non-ciliary mechanisms. **Development**. 2011;138:3441-3449.
42. Ezan J, Montcouquiol M. Revisiting planar cell polarity in the inner ear. **Semin Cell Dev Biol**. 2013;24:499-506.
43. Tarchini B, Jolicoeur C, Cayouette M. A molecular blueprint at the apical surface establishes planar asymmetry in cochlear hair cells. **Dev Cell**. 2013;27:88-102.
44. Montcouquiol M, Rachel RA, Lanford PJ et al. Identification of Vangl2 and Scrb1 as planar polarity genes in mammals. **Nature**. 2003;423:173-177.
45. Shida T, Cueva JG, Xu Z et al. The major alpha-tubulin K40 acetyltransferase alphaTAT1 promotes rapid ciliogenesis and efficient mechanosensation. **Proc Natl Acad Sci U S A**. 2010;107:21517-21522.
46. Morin X, Jaouen F, Durbec P. Control of planar divisions by the G-protein regulator LGN maintains progenitors in the chick neuroepithelium. **Nat Neurosci**. 2007;10:1440-1448.

5. Publications of the laboratory in 2014 supported by the F.M.R.E.

- Laguesse, S., Peyre, E., and **Nguyen, L.** : Progenitor genealogy in the developing cerebral cortex **Cell Tissue Res** (2014), 32(6): 1398-407 (I.F. 2013= 3.333)
- Volvert, M.-L., Prévot, P.-P., Close, P., Laguesse, S., Pirotte, S., Hemphill, J., Rogister, F., Kruzy, N., Sacheli, R., Moonen, G., Deiters, A., Merckenschlager, M., Chariot, A., **Malgrange, B.**, Godin, J., and **Nguyen, L.**,^{CA}. : MicroRNA targeting of CoREST controls polarization of migrating cortical neurons **Cell Rep** (2014), 7(4): 1168-83 (I.F. 2013=7.207)
- Avila, A., Vidal, P.M., Tielens, S., Morelli, G., Laguesse, S., Harvey, J.H., Rigo, J.-M.*, and **Nguyen, L.***: Glycine receptors control the generation of projection neurons in the developing cerebral cortex. **Cell Death Diff** (2014), 21(11): 1696-708 (I.F. 2013= 8.385)

6. Other publications of the laboratory in 2014

- Genin, E.C., Caron, N., Vandenbosch, R., **Nguyen, L.**, and **Malgrange, B.** : Forkhead pathway in the control of adult neurogenesis **Stem Cells** (2014), 32(6): 1398-407 (I.F. 2013= 7.701)

7. Publications of the laboratory in 2015 supported by the F.M.R.E.

- Laguesse, S., Creppe, C., Nedialkova, D., Prevot, P.-P., Borgs, L., Huysseune, S., Franco, B., Duysens, G., Krusy, N., Lee, G., Thelen, N., Thiry, M., Close, P., Chariot, A., **Malgrange, B.**, Leidel, S., Godin, J., and **Nguyen, L.** : A dynamic unfolded protein response contributes to the control of cortical neurogenesis. **Dev Cell** (2015), 35(5): 553-567 (I.F. 2014= 9.708)

- Peyre, E., Silva, C., and **Nguyen, L.**: Crosstalk between intracellular and extracellular signals regulating interneuron production, migration and integration into the cortex
Front Cell Neurosci (2015), (9, #129): 1-18 (I.F. 2013= 4.175)
- Huyghe, A., Van den Ackerveken, P., Sacheli, R., Prevot, P.-P., Thelen, N., Renault, J., Thiry, M., Delacroix, L., **Nguyen, L.**, and **Malgrange, B.** : MicroRNA-124 dependent modulation of Wnt signaling pathway regulates cell fate specification in the cochlea.
Cell Rep (2015), 13(1): 31-42 (I.F. 2014=8.358)

8. Other publications of the laboratory in 2015

- Ladang, A., Rapino, F., Heukamp, L., Tharun, L., Shostak, K., Hermand, D., Delaunay, S., Klevenic, I., Jiang, Z., Jacques, N., Jamart, D., Migeot, V., Florin, A., Göktuna, S., **Malgrange, B.**, Sansom, O., **Nguyen, L.**, Büttner, R., Close, P., and Chariot, A. : Elp3 drives Wnt-dependent tumor initiation and regeneration in the intestine.
J Exp Med (2015), 212(12): 2057-75 (I.F. 2014=12.515)

9. Publications of the laboratory in 2016 supported by the F.M.R.E.

- Tielens, S.*, Huysseune, S.*, Godin, J.D., Chariot, A., **Malgrange, B.**, and **Nguyen, L.** : Elongator controls cortical migration by regulating actomyosin dynamics.
Cell Research (2016), 26(10): 1131-1148 (I.F. 2015= 14.812)
- Borgs, L.*, Peyre, E.*, Alix, P., Hanon, K., Grobarczyk, B., Godin, J.D., Purnelle, A., Kruzy, N., Maquet, P., Lefebvre, P.P., Seutin, V., **Malgrange, B.***, and **Nguyen, L.*** : Dopaminergic neurons differentiating from LRRK2 G2019S induced pluripotent stem cells show early neuritic branching defects.
Nature Sci Rep (2016) Sep 19;6:33377. doi: 10.1038/srep33377 (I.F. 2015= 5.228)
* equal contributions
- Morelli, g., Avila, A., Ravanidis, S., Aourz, N., Neve, R.L., Rigo, J.-M.*, **Nguyen, L.***, and Brône, B*. : Cerebral cortical circuitry formation requires functional glycine receptors.
Cereb Cortex (2016), doi: 10.1093/cercor/bhw025 (I.F. 2015= 8.285)
* equal contributions
- Godin, J.D., Creppe, C., Laguesse, S., and **Nguyen, L.**: Emerging Roles for the Unfolded Protein Response in the Developing Nervous System.
Trends Neurosci (2016) in press, doi: 10.1016/j.tins.2016.04.002 (I.F. 2015= 13.550)

10. Other publications of the laboratory in 2016

- Delaunay, S., Rapino, F., Tharun, L., Zhou, Z., Heukamp, L., Termathe, M., Shostak, K., Klevernic, I., Florin, A., Desmecht A., Desmet, C., **Nguyen L.**, Leidel, S., Willis, A., Büttner, R., Chariot, A., and Close, P. : Elp3 links tRNA modification to IRES-dependent translation of LEF1 to sustain metastasis in breast cancer.
J Exp Med (2016), 213(11):2503-2523 (I.F. 2015= 11.240)
- Dwyer, N.D., Chen, B., Chou, S.-j., Hippenmeyer, S., **Nguyen, L.**, and Ghahghaei, H.T. : Neural stem cells to cerebral cortex: Emerging mechanisms regulating progenitor behavior and productivity.
J Neurosci (2016), 36(45):11394-11401 (I.F. 2015= 5.924)
- Broix, L., Jagline, H., Ivanova, E., Schmucker, S., Drouot, N., Clayton-Smith, J., Pagnamenta, A. t., Metcalfe, K.A., Isidor, B., Wakther-Louvier, U., Poduri, A., Taylor, J.C., Tilly, P., Poirier, K., Saillour, Y., Lebrin, N., Stemmelen, T., Rudolf, G., Muraca, G., Saintpierre, B., Elmorjani, A., The Deciphering Developmental Disorder study, Bednarek-Weirauch, N., Guerrini, R., Boland, A., Olaso, R., Masson, C., Tripathy, R., Keays, D., Cherif, B., **Nguyen, L.**, Godin, J.D., Kini, U., Nischké, P., Deleuze, J.-F., Bahi Buisson, N., Samara, I., Hinkelmann, M.-V., and Chelly, J. : Mutations in HECT domain of NEDD4L lead to AKT/mTOR pathway deregulation and cause periventricular nodular heterotopia.
Nat Genet (2016), 48(11):1349-1358 (I.F. 2015= 31.616)



Geneeskundige Stichting Koningin Elisabeth
Fondation Médicale Reine Elisabeth
Königin-Elisabeth-Stiftung für Medizin
Queen Elisabeth Medical Foundation

Final report
of the research group of

Prof. dr. Jean-Noël Octave

Université Catholique de Louvain (UCL)

Prof. dr. Jean-Noël Octave, Ilse Dewachter, Pascal Kienlen-Campard

UCL-Secteur des Sciences de la Santé - Institute of Neuroscience - IoNS

Avenue Mounier, 53, bte B1.5302 1200 Bruxelles

jean-noel.octave@uclouvain.be

www.uclouvain.be/ions.html

Alteration of cholesterol turnover in Alzheimer disease: Molecular mechanisms and therapeutic applications.

1. Introduction.

Alzheimer's disease (AD) is a biologically complex dementia characterized by a slow and progressive loss of neurons in the brain. A clear correlation exists between clinical signs of dementia and the presence in the brain of abnormal protein deposits, which are made of intraneuronal hyperphosphorylated protein tau accumulating in neurofibrillary tangles. In AD, extracellular deposits are also found in senile plaques, which contain aggregated amyloid peptide A β , which is produced from the amyloid precursor protein APP. With the discovery that APP mutations can act as fully penetrant AD genes in rare inherited AD cases, the amyloid cascade hypothesis was proposed. In this hypothesis, an imbalance in A β production and clearance leads to gradual accumulation and aggregation of the peptide in the brain, initiating a neurodegenerative cascade that involves amyloid deposition, inflammation, oxidative stress and neuronal loss. Oligomeric A β causes long term potentiation (LTP) impairment and synaptic dysfunction and accelerates the formation of neurofibrillary tangles that cause synaptic failure and neuronal death. In contrast to the rarity of inherited cases, the sporadic form of AD is quite prevalent and there are growing amounts of data, including a number of failed clinical trials, suggesting that the amyloid cascade hypothesis is insufficient to explain the complexity of the dementing illness.

Thanks to the FMRE, we further studied the possible functions of APP, in order to investigate whether APP dysfunctions could contribute to AD pathology. We characterized motifs of APP, which promote the formation of pathogenic A β oligomers. In view of an interesting development in the field with regard to the finding of prion-like propagation of tau-pathology, we have also addressed mechanisms of A β induced tau-pathology, and searched for modifiers of tau-pathology. All the results presented in this final report were published with acknowledgment of the FMRE.

2. Results

2.1. Targretin improves cognitive and biological markers in a patient with Alzheimer's disease.

Polymorphisms in genes encoding proteins involved in cholesterol homeostasis are associated with AD, and abnormal accumulation of cholesterol has been demonstrated in post mortem AD brain, arguing that perturbation of cholesterol homeostasis favors progression of AD. Neuronal cholesterol homeostasis is known to be essential for basic synaptic function, plasticity and behavior and we recently demonstrated that APP controls cholesterol turnover needed for neuronal activity.

The beneficial effects of Retinoic X Receptor (RXR) agonists reported on synaptic and cognitive functions are based on their ability to increase cholesterol efflux, further emphasizing the stimulation of neuronal cholesterol turnover as a possible target for the treatment of dementia. We studied the effects of Targretin® (bexarotene) on cognition and biomarkers in a patient with mild AD. Targretin® is a RXR agonist shown to improve synaptic and cognitive functions in animal models of AD by increasing neuronal cholesterol efflux. After 6 months of treatment with Targretin® 300 mg/day, memory improved by about 40% and the tau protein in the cerebrospinal fluid decreased by about 20%. No significant side effects were noticed. This observation in a single patient indicates that Targretin® may improve memory performance and biological markers at an early stage of AD.

Targretin Improves Cognitive and Biological Markers in a Patient with Alzheimer's Disease.
Pierrot N, Lhommel R, Quenon L, Hanseeuw B, Dricot L, Sindic C, Maloteaux JM, Octave JN, Ivanoiu A.
J Alzheimers Dis. 2016;49(2):271-6.

2.2. APP-dependent glial cell line-derived neurotrophic factor gene expression drives neuromuscular junction formation.

Besides its crucial role in the pathogenesis of AD, the knowledge of APP physiological functions remains surprisingly scarce. We observed that APP regulates the transcription of the Glial cell line-Derived Neurotrophic Factor (GDNF). APP-dependent regulation of GDNF expression affects muscles strength, muscular trophy and both neuronal and muscular differentiation fundamental for neuromuscular junctions (NMJs) maturation *in vivo*. In a nerve-muscle co-culture model set up to modelize NMJs formation *in vitro*, silencing of muscular APP induces a 30% decrease in secreted GDNF levels and a 40% decrease in the total number of NMJs together with a significant reduction in the density of acetylcholine vesicles at the presynaptic site and in neuronal maturation. These defects are rescued by GDNF expression in muscle cells in the conditions where muscular APP has been previously silenced. Expression of GDNF in muscles of APP null mice (APP^{-/-}) corrected the aberrant synaptic morphology of NMJs. Our findings highlight for the first time that APP-dependent GDNF expression drives the process of NMJs formation, providing new insights into the link between APP gene regulatory network and physiological functions.

APP-dependent glial cell line-derived neurotrophic factor gene expression drives neuromuscular junction formation.

Stanga S, Zanou N, Audouard E, Tasiaux B, Contino S, Vandermeulen G, René F, Loeffler JP, Clotman F, Gailly P, Dewachter I, Octave JN, Kienlen-Campard P.
FASEB J. 2016 May;30(5):1696-711.

2.3. Activation of phagocytic activity in astrocytes by reduced expression of the inflammasome component ASC and its implication in a mouse model of Alzheimer disease.

The proinflammatory cytokine interleukin-1 β (IL-1 β) is overexpressed in AD as a key regulator of neuroinflammation. A β peptide triggers activation of inflammasomes, protein complexes responsible for IL-1 β maturation in microglial cells. Downregulation of NALP3 inflammasome has been shown to decrease amyloid load and rescue cognitive deficits in a mouse model of AD. Whereas activation of inflammasome in microglial cells has been described in AD, no data are currently available concerning activation of inflammasome in astrocytes, although they are involved in inflammatory response and phagocytosis. By targeting the inflammasome adaptor protein ASC, we investigated the influence of activation of the inflammasome on the phagocytic activity of astrocytes. We used an ASC knockout mouse model, as ASC is a central protein in the inflammasome, acting as an adaptor and stabilizer of the complex and thus critical for its activation. Lipopolysaccharide-primed primary cultures of astrocytes from newborn mice were utilized to evaluate A β -induced inflammasome activation by measuring IL-1 β release by ECLIA (Electro-chemiluminescence immunoassay). Phagocytosis efficiency was measured by incorporation of bioparticles, and the release of the chemokine CCL3 was measured by ECLIA. ASC mice were crossbred with 5xFAD mice, a well characterized model of AD, and tested for spatial reference memory using the Morris water maze at 7-8 month of age. Amyloid load and CCL3 were quantified by thioflavine S staining and qRT-PCR, respectively. Cultured astrocytes primed with LPS and treated with A β showed an ASC dependent production of IL-1 β resulting from inflammasome activation mediated by A β phagocytosis and cathepsin B enzymatic activity. ASC^{+/-} astrocytes displayed a higher phagocytic activity as compared to ASC^{+/+} and ASC^{-/-} cells, resulting from a higher release of the chemokine CCL3. A significant decrease in amyloid load was measured in brain of 7-8 month-old 5xFAD mice carrying the ASC ^{+/-} genotype, correlated with an increase in CCL3 gene expression. In addition, the ASC ^{+/-} genotype rescued spatial reference memory deficits observed in 5xFAD mice.

These results demonstrate that A β is able to activate astrocytic inflammasome. Downregulation of inflammasome activity increases phagocytosis in astrocytes due to release of CCL3. This could explain why downregulation of inflammasome activity decreases amyloid load and rescues memory deficits in a mouse model of AD.

Activation of phagocytic activity in astrocytes by reduced expression of the inflammasome component ASC and its implication in a mouse model of Alzheimer disease.

Couturier J, Stancu IC, Schakman O, Pierrot N, Huaux F, Kienlen-Campard P, Dewachter I, Octave JN. J Neuroinflammation. 2016 Jan 27;13:20.

2.4. Glycines from the APP GXXXG/GXXXA transmembrane motifs promote formation of pathogenic A β oligomers in cells

Alzheimer's disease (AD) is the most common neurodegenerative disorder characterized by progressive cognitive decline leading to dementia. The amyloid precursor protein (APP) is a ubiquitous type I transmembrane (TM) protein sequentially processed to generate the β -amyloid peptide (A β), the major constituent of senile plaques that are typical AD lesions. There is a growing body of evidence that soluble A β oligomers correlate with clinical symptoms associated with the disease. The A β sequence begins in the extracellular juxtamembrane region of APP and includes roughly half of the TM domain. This region contains GXXXG and GXXXA motifs, which are critical for both TM protein interactions and fibrillogenic properties of peptides derived from TM α -helices. Glycine-to-leucine mutations of these motifs were previously shown to affect APP processing and A β production in cells. However, the detailed contribution of these motifs to APP dimerization, their relation to processing, and the conformational changes they can induce within A β species remains undefined. Here, we describe highly resistant A β 42 oligomers that are produced in cellular membrane compartments. They are formed in cells by processing of the APP amyloidogenic C-terminal fragment (C99), or by direct expression of a peptide corresponding to A β 42, but not to A β 40. By a point-mutation approach, we demonstrate that glycine-to-leucine mutations in the G29XXXG33 and G38XXXA42 motifs dramatically affect the A β oligomerization process. G33 and G38 in these motifs are specifically involved in A β oligomerization; the G33L mutation strongly promotes oligomerization, while G38L blocks it with a dominant effect on G33 residue modification. Finally, we report that the secreted A β 42 oligomers display pathological properties consistent with their suggested role in AD, but do not induce toxicity in survival assays with neuronal cells. Exposure of neurons to these A β 42 oligomers dramatically affects neuronal differentiation and, consequently, neuronal network maturation.

Glycines from the APP GXXXG/GXXXA Transmembrane Motifs Promote Formation of Pathogenic A β Oligomers in Cells.

Decock M, Stanga S, Octave JN, Dewachter I, Smith SO, Constantinescu SN, Kienlen-Campard P. Front Aging Neurosci. 2016 May 10;8:107.

2.5. Heterotypic seeding of Tau fibrillization by pre-aggregated Abeta provides potent seeds for prion-like seeding and propagation of Tau-pathology in vivo.

Genetic, clinical, histopathological and biomarker data strongly support Beta-amyloid (A β) induced spreading of Tau-pathology beyond entorhinal cortex (EC), as a crucial process in conversion from preclinical cognitively normal to Alzheimer's Disease (AD), while the underlying mechanism remains unclear. In vivo preclinical models have reproducibly recapitulated A β -induced Tau-pathology. Tau pathology was thereby also induced by aggregated A β , in functionally connected brain areas, reminiscent of a prion-like seeding process. In this work we demonstrate, that pre-aggregated A β can directly induce Tau fibrillization by cross-seeding, in a cell-free assay, comparable to that demonstrated before for alpha-synuclein and Tau. We furthermore demonstrate, in a well-characterized cellular Tau-aggregation assay that A β -seeds cross-seeded Tau-pathology and strongly catalyzed pre-existing Tau-aggregation,

reminiscent of the pathogenetic process in AD. Finally, we demonstrate that heterotypic seeded Tau by pre-aggregated A β provides efficient seeds for induction and propagation of Tau-pathology in vivo. Prion-like, heterotypic seeding of Tau fibrillization by A β , providing potent seeds for propagating Tau pathology in vivo, as demonstrated here, provides a compelling molecular mechanism for A β -induced propagation of Tau-pathology, beyond regions with pre-existing Tau-pathology (entorhinal cortex/locus coeruleus). Cross-seeding along functional connections could thereby resolve the initial spatial dissociation between amyloid- and Tau-pathology, and preferential propagation of Tau-pathology in regions with pre-existing 'silent' Tau-pathology, by conversion of a 'silent' Tau pathology to a 'spreading' Tau-pathology, observed in AD.

Heterotypic seeding of Tau fibrillization by pre-aggregated Abeta provides potent seeds for prion-like seeding and propagation of Tau-pathology in vivo.

Vasconcelos B, Stancu IC, Buist A, Bird M, Wang P, Vanoosthuyse A, Van Kolen K, Verheyen A, Kienlen-Campard P, Octave JN, Baatsen P, Moechars D, Dewachter I. Acta Neuropathol. 2016 Apr;131(4):549-69.

2.6. Tau-interactome mapping based identification of Otub1 as Tau-deubiquitinase, involved in accumulation of pathological Tau forms in vitro and in vivo.

Dysregulated proteostasis is a key-feature in a variety of neurodegenerative disorders. In Alzheimer's disease (AD), symptoms progression closely correlates with spatio-temporal progression of Tau aggregation, with 'early' oligomeric Tau forms rather than mature NFTs considered as pathogenetic culprits. The ubiquitin-proteasome system (UPS) controls degradation of soluble normal and abnormally folded cytosolic proteins. UPS is affected in AD and is identified by Genome-wide association study (GWAS) as a risk pathway for AD. UPS is determined by the balanced regulation of ubiquitination and deubiquitination. In this work, we performed an iTRAQ (isobaric tags for relative and absolute quantitation) based Tau-interactome mapping, to gain unbiased insight in Tau pathophysiology and to identify novel Tau-directed therapeutic targets. Focusing on Tau-deubiquitination, we here identify Otub1 as a Tau-deubiquitinating enzyme. Otub1 directly affected Lys48-linked Tau-deubiquitination, impairing Tau degradation, dependent on its catalytically active Cysteine, but independent of its non-canonical pathway modulated by its N-terminal domain in primary neurons. Otub1 strongly increased AT8 positive Tau and oligomeric Tau forms and increased Tau-seeded Tau aggregation in primary neurons. Finally, we demonstrate that Otub1 expression but not its catalytically inactive form induced pathological Tau forms already after 2 months in Tau transgenic mice in vivo, including AT8 positive Tau and oligomeric Tau forms. Taken together, we here identified Otub1 as a Tau-deubiquitinase *in vitro* and *in vivo*, which is involved in the formation of pathological Tau forms, including small soluble oligomeric forms. Otub1 and particularly Otub1 inhibitors, currently under development for cancer therapies, may thereby yield interesting novel therapeutic venues for Tauopathies and AD.

Tau-interactome mapping based identification of Otub1 as Tau-deubiquitinase, involved in accumulation of pathological Tau forms in vitro and in vivo.

Wang P, Joberty G, Buyst A, Vanoosthuyse A, Stancu IC, Vasconcelos B, Kienlen-Campard P, Octave JN, Bantscheff M, Drewes G, Moechars D, Dewachter I. Acta Neuropathol. In press.

3. Publications of the team (2014-2016)

3.1. 2014

- Increased misfolding and truncation of tau in APP/PS1/tau transgenic mice compared to mutant tau mice.
Héraud C, Goufak D, Ando K, Leroy K, Suain V, Yilmaz Z, De Decker R, Authélet M, Laporte V, Octave JN, Brion JP.
Neurobiol Dis. 2014 Feb;62:100-12.
- Cholesterol, neuronal activity and Alzheimer disease.
Pierrot N, Octave JN.
Med Sci (Paris). 2014 Mar;30(3):244-6.
- Conformational changes induced by the A21G Flemish mutation in the amyloid precursor protein lead to increased A β production.
Tang TC, Hu Y, Kienlen-Campard P, El Haylani L, Decock M, Van Hees J, Fu Z, Octave JN, Constantinescu SN, Smith SO.
Structure. 2014 Mar 4;22(3):387-96.
- Critical role of aquaporins in interleukin 1 β (IL-1 β)-induced inflammation.
Rabolli V, Wallemme L, Lo Re S, Uwambayinema F, Palmal-Pallag M, Thomassen L, Tyteca D, Octave JN, Marbaix E, Lison D, Devuyst O, Huaux F.
J Biol Chem. 2014 May 16;289(20):13937-47.
- Epigenetic regulations of immediate early genes expression involved in memory formation by the amyloid precursor protein of Alzheimer disease.
Hendrickx A, Pierrot N, Tasiaux B, Schakman O, Kienlen-Campard P, De Smet C, Octave JN.
PLoS One. 2014 Jun 11;9(6):e99467.
- Tauopathy contributes to synaptic and cognitive deficits in a murine model for Alzheimer's disease.
Stancu IC, Ris L, Vasconcelos B, Marinangeli C, Goeminne L, Laporte V, Haylani LE, Couturier J, Schakman O, Gailly P, Pierrot N, Kienlen-Campard P, Octave JN, Dewachter I.
FASEB J. 2014 Jun;28(6):2620-31.
- Increasing membrane cholesterol of neurons in culture recapitulates Alzheimer's disease early phenotypes.
Marquer C, Laine J, Dauphinot L, Hanbouch L, Lemercier-Neuillet C, Pierrot N, Bossers K, Le M, Corlier F, Benstaali C, Saudou F, Thinakaran G, Cartier N, Octave JN, Duyckaerts C, Potier MC.
Mol Neurodegener. 2014 Dec 18;9:60.
- Gamma-secretase inhibitor activity of a *Pterocarpus erinaceus* extract.
Hage S, Marinangeli C, Stanga S, Octave JN, Quetin-Leclercq J, Kienlen-Campard P.
Neurodegener Dis. 2014;14(1):39-51.

3.2. 2015

- Presenilin transmembrane domain 8 conserved AXXXAXXXG motifs are required for the activity of the γ -secretase complex.
Marinangeli C, Tasiaux B, Opsomer R, Hage S, Sodero AO, Dewachter I, Octave JN, Smith SO, Constantinescu SN, Kienlen-Campard P.
J Biol Chem. 2015 Mar 13;290(11):7169-84.
- Characterization of *Pterocarpus erinaceus* kino extract and its gamma-secretase inhibitory properties.
Hage S, Stanga S, Marinangeli C, Octave JN, Dewachter I, Quetin-Leclercq J, Kienlen-Campard P.
J Ethnopharmacol. 2015 Apr 2;163:192-202.
- Templated misfolding of Tau by prion-like seeding along neuronal connections impairs neuronal network function and associated behavioral outcomes in Tau transgenic mice.
Stancu IC, Vasconcelos B, Ris L, Wang P, Villers A, Peeraer E, Buist A, Terwel D, Baatsen P, Oyelami T, Pierrot N, Casteels C, Bormans G, Kienlen-Campard P, Octave JN, Moechars D, Dewachter I.
Acta Neuropathol. 2015 Jun;129(6):875-94.
- Analysis by a highly sensitive split luciferase assay of the regions involved in APP dimerization and its impact on processing.
Decock M, El Haylani L, Stanga S, Dewachter I, Octave JN, Smith SO, Constantinescu SN, Kienlen-Campard P.
FEBS Open Bio. 2015 Sep 6;5:763-73.

3.3. 2016

- Targretin Improves Cognitive and Biological Markers in a Patient with Alzheimer's Disease.
Pierrot N, Lhommel R, Quenon L, Hanseeuw B, Dricot L, Sindic C, Maloteaux JM, Octave JN, Ivanoiu A.
J Alzheimers Dis. 2016;49(2):271-6.
- Activation of phagocytic activity in astrocytes by reduced expression of the inflammasome component ASC and its implication in a mouse model of Alzheimer disease.
Couturier J, Stancu IC, Schakman O, Pierrot N, Huaux F, Kienlen-Campard P, Dewachter I, Octave JN.
J Neuroinflammation. 2016 Jan 27;13:20.
- Heterotypic seeding of Tau fibrillization by pre-aggregated Abeta provides potent seeds for prion-like seeding and propagation of Tau-pathology in vivo.
Vasconcelos B, Stancu IC, Buist A, Bird M, Wang P, Vanoosthuyse A, Van Kolen K, Verheyen A, Kienlen-Campard P, Octave JN, Baatsen P, Moechars D, Dewachter I.
Acta Neuropathol. 2016 Apr;131(4):549-69.
- Glycines from the APP GXXXG/GXXXA Transmembrane Motifs Promote Formation of Pathogenic A β Oligomers in Cells.
Decock M, Stanga S, Octave JN, Dewachter I, Smith SO, Constantinescu SN, Kienlen-Campard P.
Front Aging Neurosci. 2016 May 10;8:107.
- APP-dependent glial cell line-derived neurotrophic factor gene expression drives neuromuscular junction formation.
Stanga S, Zanou N, Audouard E, Tasiaux B, Contino S, Vandermeulen G, René F, Loeffler JP, Clotman F, Gailly P, Dewachter I, Octave JN, Kienlen-Campard P.
FASEB J. 2016 May;30(5):1696-711.
- Tau-interactome mapping based identification of Otub1 as Tau-deubiquitinase, involved in accumulation of pathological Tau forms *in vitro* and *in vivo*.
Wang P, Joberty G, Buyst A, Vanoosthuyse A, Stancu IC, Vasconcelos B, Kienlen-Campard P, Octave JN, Bantscheff M, Drewes G, Moechars D, Dewachter I.
Acta Neuropathol. In press.



Geneeskundige Stichting Koningin Elisabeth
Fondation Médicale Reine Elisabeth
Königin-Elisabeth-Stiftung für Medizin
Queen Elisabeth Medical Foundation

Final report
of the research group of

Prof. dr. Wim Robberecht

Katholieke Universiteit Leuven (KU Leuven)

Prof. dr. Wim Robberecht

Campus Gasthuisberg
Dept of Neurology
Herestraat 49, O&N4 Box 912
3000 Leuven
wim.robberrecht@med.kuleuven.be

The ephrin axon repellent system in amyotrophic lateral sclerosis

1. State of the art and summary of the research project

Amyotrophic lateral sclerosis (ALS) is a neurodegenerative disorder of motor neurons in adults, resulting in muscle atrophy and weakness. Its course is relentlessly progressive; the disease is fatal within three to five years after onset. There currently is no cure for ALS. Mutations in more than 10 different genes are known to cause the hereditary form of ALS: SOD1 and C9ORF72 mutations are the most prevalent ones, while mutations in TDP-43 and FUS are less frequent [1]. Mutant SOD1 transgenic mouse models faithfully reproduce the human disease and have been studied extensively over the last two decades [2]. Phenotypic variability of ALS is considerable, even in patients in whom the disease is caused by the same molecular abnormality. This indicates that factors, environmental or genetic in nature, modify the phenotypic expression of these diseases. It is important to identify such modifying factors, as they may represent targets for therapeutic intervention, in particular for the sporadic forms of neurodegenerative diseases, of which we do not know the cause.

In previous research, we identified one such factor, the ephrin receptor EphA4, as a modifying factor for ALS [3]. Genetic and pharmacological inhibition of EphA4 rescued the phenotype in a zebrafish model of ALS and increased survival in ALS rodent models. In ALS patients an inverse correlation was found between EphA4 expression and disease onset [3].

In order to facilitate a drug development strategy targeting the EphA4 pathway, this project intends to investigate the mechanism through which EphA4 affects motor neuron degeneration in ALS. This is being done by dissecting the EphA4 pathway and exploring the contribution of different biological aspects of the pathway in the motor neuron degeneration that occurs in ALS. This project also contemplates to target EphA4 pharmacologically.

2. Results

WP1. Mechanism of involvement of EphA4 in motor neuron degeneration

WP1.1. Identification of cell type mediating the effect of EphA4 on motor neuron degeneration

Although EphA4 has been shown previously to play a role in reactive astrocytes in spinal cord injury [4, 5], results from our lab show that EphA4 is mainly expressed in motor neurons in the spinal cord of ALS mice [3]. In order to know whether EphA4 in motor neurons is mediating the effect previously observed on motor neuron degeneration, we used the Thy1-CreER mouse (JAX laboratories) that expresses CreER (Cre recombinase-estrogen receptor fusion protein) in a subset of neurons among which the motor neurons. After treatment with tamoxifen the gene flanked with loxP sites is excised by the Cre in the cells that express it. As a control, the CAGG-CreER mouse (JAX laboratories), in which the gene of interest is deleted ubiquitously after tamoxifen treatment, was used. To be able to excise EphA4 ubiquitously or in neurons, we crossed these mice to the SOD1^{G93A} mice and to an EphA4^{lox/lox} mouse (JAX laboratories). To determine EphA4 excision efficiency Thy1-CreER::EphA4^{lox/lox} and CAGG-CreER::EphA4^{lox/lox} were administered with 4 mg tamoxifen at 3 months of age during 4 consecutive days, and were sacrificed 14 days after the last tamoxifen administration. CAGG-CreER::EphA4^{lox/lox} mice presented a reduction of 85% of EphA4 mRNA and protein levels, whereas Thy1-CreER::EphA4^{lox/lox} mice showed a reduction of about 30% of EphA4 mRNA and protein levels as compared to EphA4^{lox/lox} mice, consistent with the fact that in the later mouse EphA4 is only excised in neurons (Figure 1).

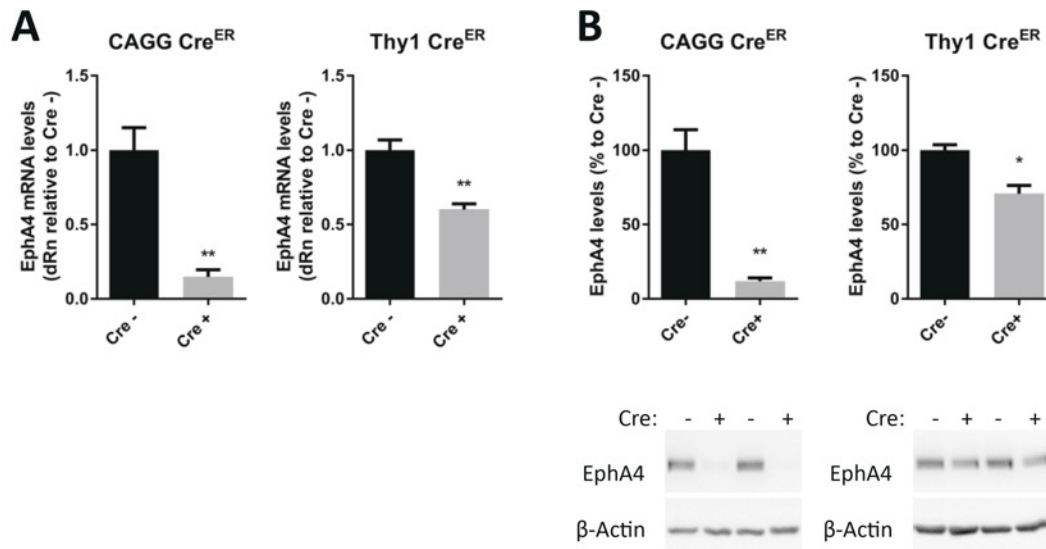


Figure 1 - CAGG-CreER::EphA4^{lox/lox} and Thy1-CreER::EphA4^{lox/lox} mice have reduced levels of EphA4 mRNA and protein after tamoxifen administration. EphA4 mRNA (A) and protein (B) levels were quantified in the spinal cord of 3-months-old mice treated with tamoxifen by qPCR and western-blot respectively. Data represents mean ± SEM, and different conditions were compared with two-tailed t-test (* p<0.05 and ** p<0.01).

Tamoxifen was administered to Thy1-CreER::EphA4^{lox/lox}::SOD1^{G93A} and CAGG-CreER::EphA4^{lox/lox}::SOD1^{G93A} mice at the age of 60 days, a pre-symptomatic age for this model, and were followed to study disease parameters, disease onset and survival. Disease onset was assessed by the hanging wire test and rotarod. For the hanging wire test mice were placed on an elevated inverted grid and onset was defined from the moment mice could no longer perform this test for 60 seconds. Mice also walked for 5 minutes on a rotarod at a fix speed of 15 rpm, and onset was determined when a mouse performed less than 50% of its maximum performance. Mice were followed until they failed the righting reflex test. We then considered the mice end-stage according to ethical end-points. This end-stage point was recorded for survival data. We observed that onset, both based on hanging wire test and the rotarod test, was not altered in Thy1-CreER::EphA4^{lox/lox}::SOD1^{G93A} or CAGG-CreER::EphA4^{lox/lox}::SOD1^{G93A} when compared to EphA4^{lox/lox}::SOD1^{G93A} mice (Figure 2A, 2B and 2D, 2E)[3]. Survival was surprisingly not altered in CAGG-CreER::EphA4^{lox/lox}::SOD1^{G93A} nor in Thy1-CreER::EphA4^{lox/lox}::SOD1^{G93A} mice (Figure 2C and 2F). Excision efficiency in the spinal cord of end-stage mice was confirmed by qPCR and western-blot (Figure 2G and 2H).

These findings need to be confirmed by increasing the number of animals in each group. If confirmed we will consider the possibility to administer tamoxifen at earlier time points before denervation of neuromuscular synapses. Thinning of terminal axonal branches has been detected in the SOD1^{G93A} mice between postnatal days 30 and 40, and denervation starts from postnatal day 45 onwards [6]. In addition, we will perform other experiments with a reduction of EphA4 with only 50% (Thy1-CreER::EphA4^{lox/+}::SOD1^{G93A} and CAGG-CreER::EphA4^{lox/+}::SOD1^{G93A}).

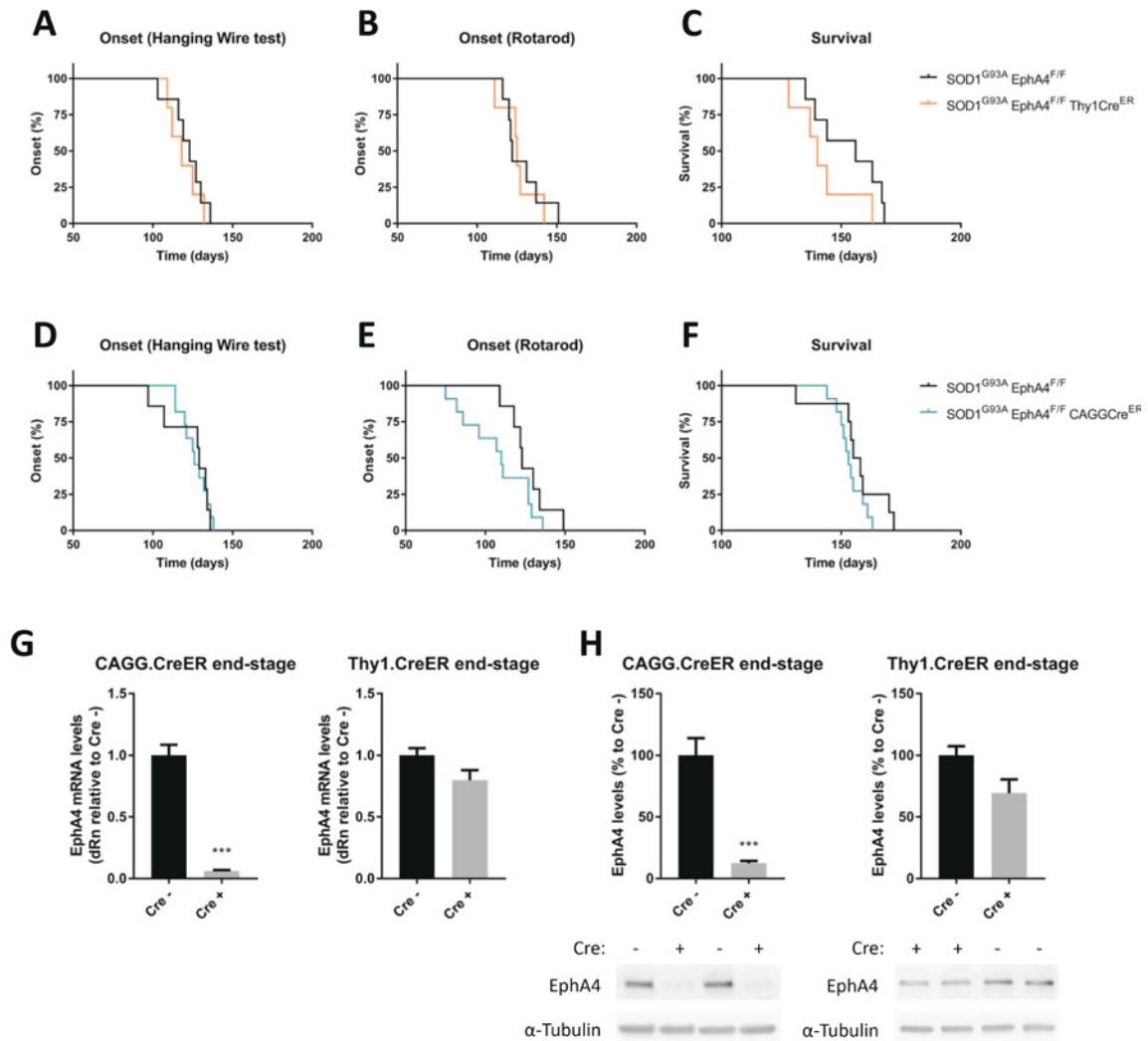


Figure 2 - Ubiquitous or neuron-specific reduction of EphA4 levels does not improve ALS disease parameters. (A-C) Onset and survival were determined in Thy1-CreER::EphA4^{lox/lox}::SOD1^{G93A} mice compared to EphA4^{lox/lox}::SOD1^{G93A} mice (N=7-5). No significant difference was observed in onset (based on hanging wire test, 118 days in Thy1-CreER::EphA4^{lox/lox}::SOD1^{G93A} versus 123 days in EphA4^{lox/lox}::SOD1^{G93A} mice; based on Rotarod, 125 days in Thy1-CreER::EphA4^{lox/lox}::SOD1^{G93A} versus 122 days in EphA4^{lox/lox}::SOD1^{G93A} mice) and neither in survival (140 days in Thy1-CreER::EphA4^{lox/lox}::SOD1^{G93A} versus 156 days in EphA4^{lox/lox}::SOD1^{G93A} mice). (D-F) Onset based on rotarod and hanging wire test, and survival were determined in CAGG-CreER::EphA4^{lox/lox}::SOD1^{G93A} mice compared to EphA4^{lox/lox}::SOD1^{G93A} mice (N=7-11). No significant difference was observed in onset (based on hanging wire test, 126 days in CAGG-CreER::EphA4^{lox/lox}::SOD1^{G93A} versus 129 days in EphA4^{lox/lox}::SOD1^{G93A} mice; based on Rotarod, 110 days in CAGG-CreER::EphA4^{lox/lox}::SOD1^{G93A} versus 123 days in EphA4^{lox/lox}::SOD1^{G93A} mice) and neither in survival (153 days in CAGG-CreER::EphA4^{lox/lox}::SOD1^{G93A} versus 156 days in EphA4^{lox/lox}::SOD1^{G93A} mice). (G) EphA4 mRNA and (H) protein levels were quantified in the spinal cord of end-stage mice treated with tamoxifen by qPCR and western-blot respectively. Data represents mean \pm SEM, and different conditions were compared with two-tailed t-test (***) $p < 0.001$.

WP1.2. Signalling direction of the modifying effect of EphA4 in ALS

EphA4 and its ligands are transmembrane and membrane bound proteins. When the receptor and its ligands interact bidirectional signalling occurs, the so-called forward signalling occurs in the cell that bears the receptor and reverse signalling occurs in the cell that bears the ligand [7]. To be able to determine whether forward signalling plays a role in ALS, we obtained the EphA4-eGFP and the EphA4-KD mice (kindly provided by Prof. Rudiger Klein, Max Planck Institute Martinsried, Germany). These mice have already proved to be a good strategy to discern between these two signalling directions [8-10]. Whereas the EphA4-eGFP has a knock-in replacement of the whole intracellular domain of EphA4 by eGFP and cannot trigger forward signalling (Figure 3A), the EphA4-KD a single point mutation at the kinase domain of EphA4 (K653M) generating a non-functional kinase EphA4 receptor (Figure 3B).

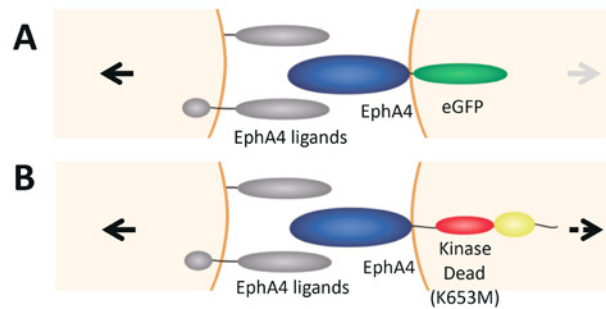


Figure 3 – Schematic representation of the mutant EphA4 protein that EphA4-eGFP and EphA4-KD mice carry. (A) EphA4-eGFP mice have a substitution of the whole intracellular domain of EphA4 by eGFP and cannot trigger forward signalling. (B) EphA4-KD mice have a single point mutation (K653M) in the kinase domain of EphA4, and cannot trigger kinase domain-dependent forward signalling.

We first characterized the mice and determined EphA4 protein levels by western-blot using an EphA4 N-terminal antibody, so that EphA4 wild-type and mutant (EphA4-KD and EphA4-eGFP) isoforms could be detected (Figure 4A and 5A). EphA4-eGFP isoform has a lower molecular weight than wild-type EphA4 [8], and could be detected on western-blot. The levels of EphA4 wild-type isoform dose-dependently decreased as expected in EphA4-eGFP^{+/-} or EphA4-eGFP^{+/+} mice compared to EphA4-eGFP^{-/-} (Figure 4A). However, we observed a dose-dependent significant increase of the EphA4-eGFP mutant isoform, suggesting the possibility of an impaired clearance of this mutant protein although this needs further study (Figure 4A). EphA4-KD isoform has the same molecular weight as EphA4 wild-type and it is not possible to discriminate between the two isoforms on western-blot. As expected, total EphA4 levels were not altered in EphA4-KD^{+/-} or EphA4-KD^{+/+} mice compared to EphA4-KD^{-/-} (Figure 5A).

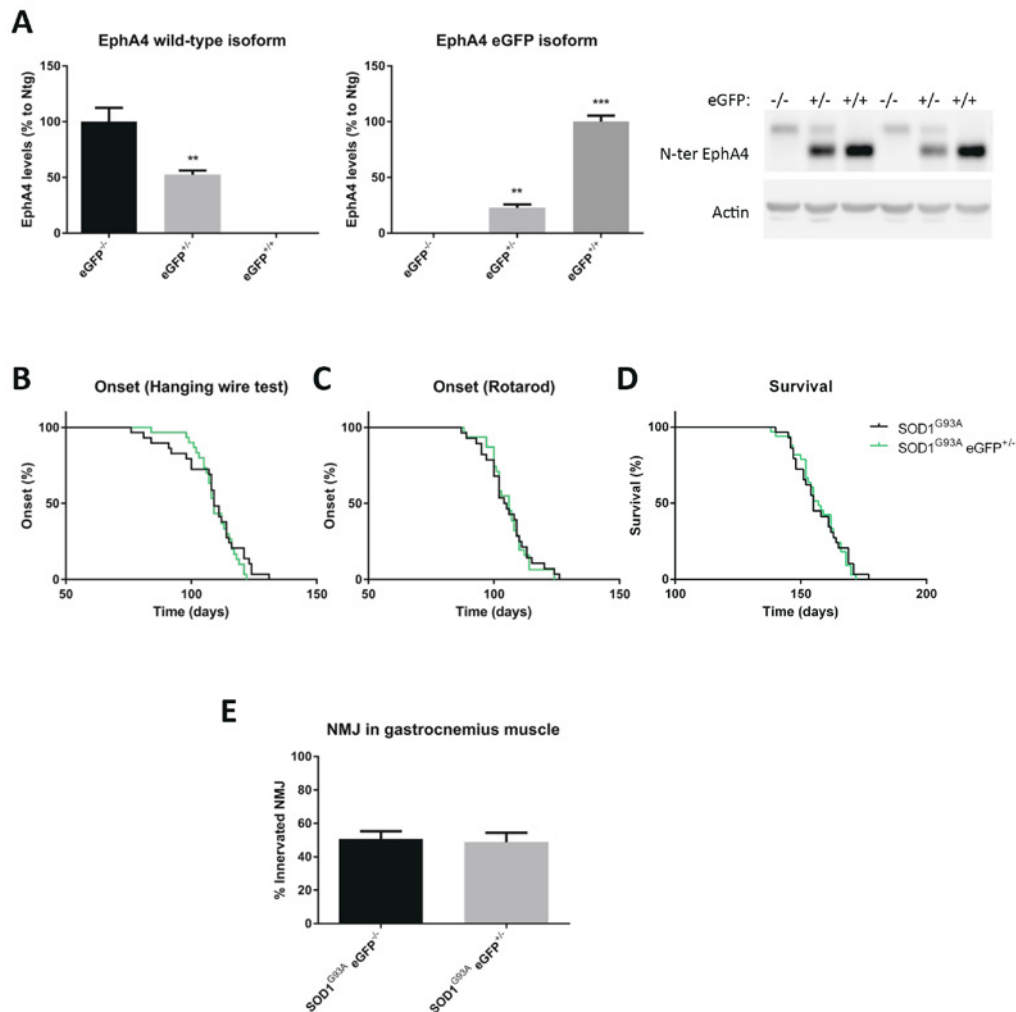


Figure 4 - Substitution of the whole intracellular domain of EphA4 by eGFP protein does not alter disease progression and survival. (A) EphA4 wild-type and mutant isoform levels were determined by western-blot with an EphA4 N-terminal antibody, having the mutant isoform a lower molecular weight than the wild-type. Data represents mean \pm SEM, and different conditions were compared with One-way ANOVA. ** $p < 0.001$ and *** $p < 0.0001$ as compared with eGFP^{-/-}. (B-D) Onset, which was determined by lack of performance on the hanging wire test and on the rotarod, and survival were determined in EphA4-eGFP^{+/-}::SOD1^{G93A} and compared to SOD1^{G93A} mice (N=27-30). No difference was observed in onset (based on hanging wire test, 109 days in EphA4-eGFP^{+/-}::SOD1^{G93A} versus 109 days in SOD1^{G93A}; based on based on Rotarod, 106 days in EphA4-eGFP^{+/-}::SOD1^{G93A} versus 104 days in SOD1^{G93A}) and neither in survival (157 days in EphA4-eGFP^{+/-}::SOD1^{G93A} versus 155 days in SOD1^{G93A}). (E) Percentage of innervated neuromuscular junctions were assessed in the gastrocnemius muscle of both SOD1^{G93A} and EphA4-eGFP^{+/-}::SOD1^{G93A} mice, but no differences were found (49% innervated NMJ in EphA4-eGFP^{+/-}::SOD1^{G93A} compared to 51% innervated NMJ in SOD1^{G93A}). Data represents mean \pm SEM and conditions were compared with a two-tailed t-test.

We next crossed these mice with the SOD1^{G93A} mouse to determine the impact of these mutations on ALS disease progression. If forward signalling is playing a role in the modifying effect of EphA4 in ALS we expect similar effects in the EphA4-eGFP^{+/-}::SOD1^{G93A} and EphA4-KD^{+/-}::SOD1^{G93A} mouse compared to previous results, when EphA4 levels were lowered in the SOD1^{G93A} mouse (EphA4^{+/-}::SOD1^{G93A}) [3]. On the contrary, if the beneficial effect of deleting EphA4 is mediated through a reduction in reverse signalling we expected no difference in the clinical presentation in any of these mice (EphA4-eGFP^{+/-}::SOD1^{G93A} and EphA4-KD^{+/-}::SOD1^{G93A}) compared to the control (SOD1^{G93A}). Disease parameters were measured in the same way as previously reported. Neither disease onset, as determined with the hanging wire test or the rotarod, nor disease survival was altered in EphA4-eGFP^{+/-}::SOD1^{G93A} mice compared to SOD1^{G93A} mice (Figure 4B-D). The percentage of innervated neuromuscular junctions (NMJs) were similar in EphA4-eGFP^{+/-}::SOD1^{G93A} compared to SOD1^{G93A} symptomatic mice (Figure 4E). Onset was unaltered in EphA4-KD^{+/-}::SOD1^{G93A} compared to SOD1^{G93A} mice (Figure 5B and 5C). Survival of EphA4-KD^{+/-}::SOD1^{G93A} mice was not different from SOD1^{G93A} as was the percentage of innervated NMJs in the gastrocnemius muscle of symptomatic mice between EphA4-KD^{+/-}::SOD1^{G93A} and SOD1^{G93A} mice (Figure 5D and E).

These results indicate that EphA4 kinase domain-dependent forward signalling might not be involved in ALS, and suggest the importance of reverse signalling in the disease, by interaction with the EphA4 ligands: the ephrins.

In order to have a positive control for these set of experiments, we obtained the EphA4-PLAP-LacZ mouse (kindly provided by Prof. Rudiger Klein, Max Planck Institute Martinsried, Germany). This mouse has an insertion in the EphA4 endogenous gene, consisting of a secretory trap vector that encodes for β -galactosidase and placental alkaline phosphatase (PLAP) proteins under the EphA4 promoter [11]. Heterozygous (EphA4-LacZ^{+/-}) mice have 50% reduction of EphA4 levels in the cortex and spinal cord, as detected by western-blot (Figure 6A). β -galactosidase fusion protein could also be detected in these mice (Figure 6A). We crossed the SOD1^{G93A} mouse with the EphA4-LacZ^{+/-} mouse, and we analysed the survival of the experimental mice. We indeed observed that survival in EphA4-LacZ^{+/-}::SOD1^{G93A} mice was prolonged by 9 days compared to SOD1^{G93A} mice (Figure 6B), confirming previous published data [3].

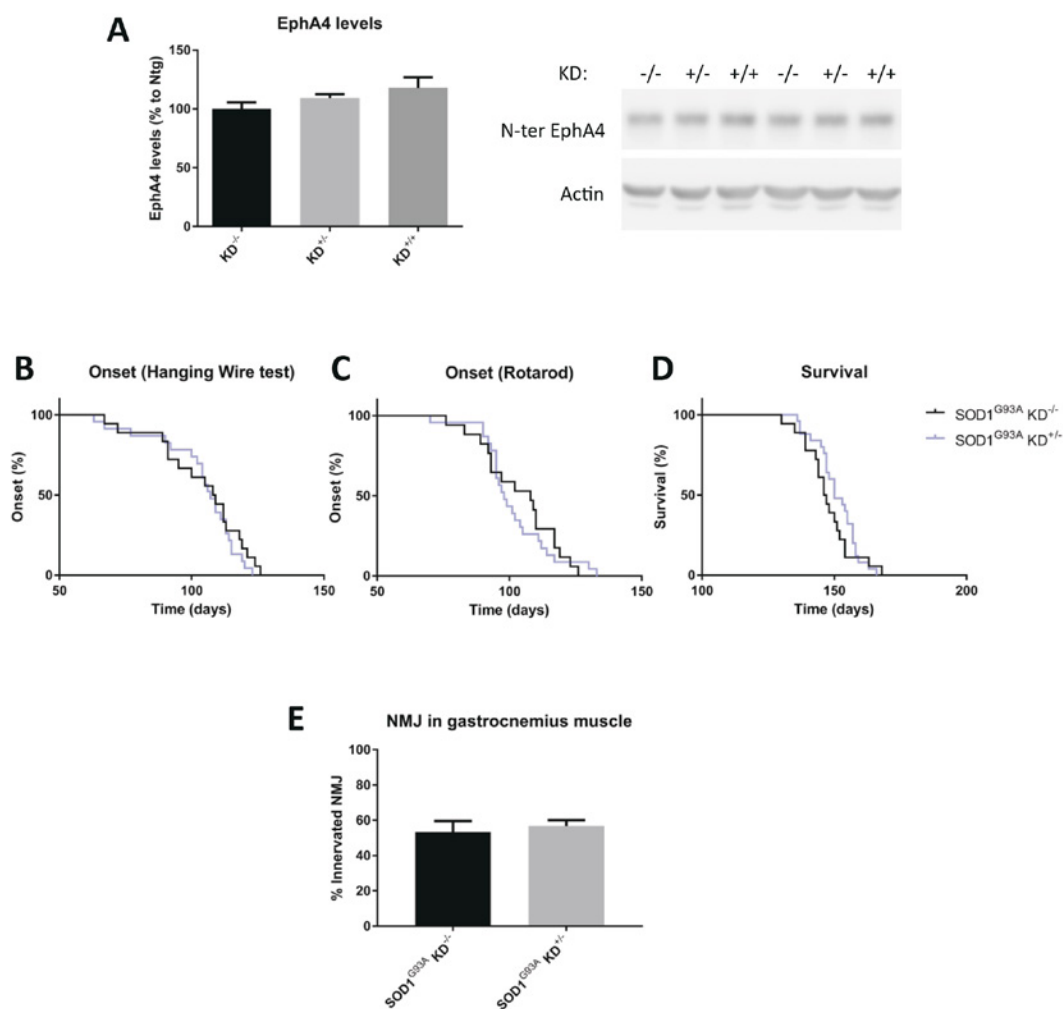


Figure 5 - Kinase domain-dependent forward signalling does not significantly play a role in ALS as determined with the EphA4-KD mouse. (A) EphA4 levels were determined by western-blot with an EphA4 N-terminal antibody. Data represents mean \pm SEM, and different conditions were compared with One-way ANOVA. ** $p < 0.001$ and *** $p < 0.0001$ as compared with KD^{-/-}. (B-D) Onset, which was determined by lack of performance on the hanging wire test and on the rotarod, and survival were determined in EphA4-KD^{+/-}::SOD1^{G93A} and compared to SOD1^{G93A} mice (N=17-25). No difference was observed in onset (based on hanging wire test, 107 days in EphA4-KD^{+/-}::SOD1^{G93A} versus 108 days in SOD1^{G93A}; based on based on Rotarod, 98 days in EphA4-KD^{+/-}::SOD1^{G93A} versus 108 days in SOD1^{G93A}) and neither in survival (150 days in EphA4-KD^{+/-}::SOD1^{G93A} versus 146 days in SOD1^{G93A}). (E) Percentage of innervated neuromuscular junctions were assessed in the gastrocnemius muscle of both SOD1^{G93A} and EphA4-KD^{+/-}::SOD1^{G93A} mice, but no differences were found (53% innervated NMJ in EphA4-KD^{+/-}::SOD1^{G93A} compared to 56% innervated NMJ in SOD1^{G93A}). Data represents mean \pm SEM and conditions were compared with a two-tailed t-test.

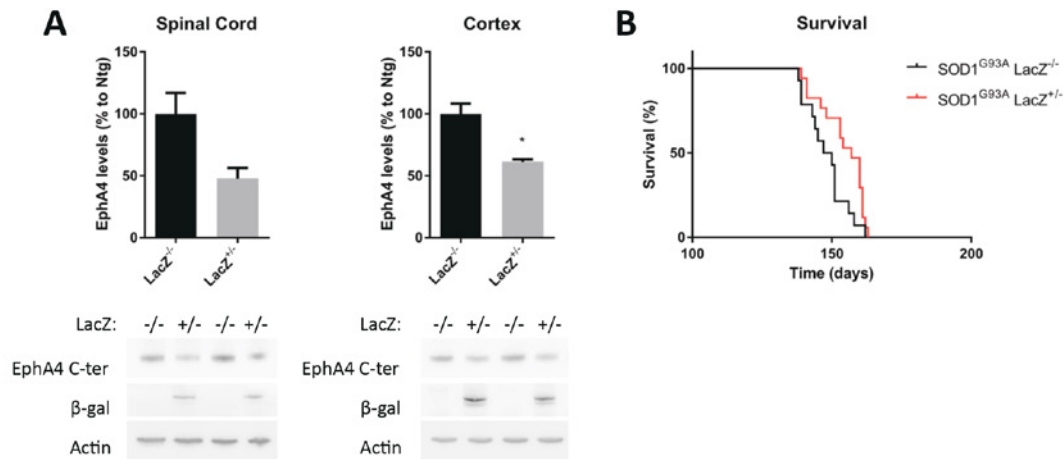


Figure 6 - Reduction in the levels of EphA4 significantly extends survival in the SOD1^{G93A} mouse model of ALS. (A) EphA4 protein levels were determined in heterozygous EphA4-LacZ mice spinal cord and cortex. A β -galactosidase fusion protein could also be detected (β -gal) in EphA4-LacZ^{+/-} mice. Data represents mean \pm SEM, and different conditions were compared with two-tailed t-test. * $p < 0.05$. (B) Survival was determined in EphA4-LacZ^{+/-}::SOD1^{G93A} and compared to SOD1^{G93A} mice (N=14-17). Significant difference was observed in survival (157 days in EphA4-LacZ^{+/-}::SOD1^{G93A} versus 148 days in SOD1^{G93A}). Log rank $p = 0.03$.

WP1.3. Ligands for EphA4 in motor neuron degeneration

There are two major classes of ephrins and ephrin receptors, called A and B. In mammals there are 5 types of ephrin-A (ephrin A1 to A5) and 3 types of ephrin-B (B1 to B3). Ephrin-As are GPI-anchored proteins while ephrin-Bs have a transmembrane domain. EphA4 is a promiscuous receptor that is able to bind most of ephrin-A and B [7]. Therefore, EphA4 could be an ALS disease modifier by interacting with almost any ephrin. Therefore, we have determined the expression levels of ephrins genes by digital droplet PCR (ddPCR) in the spinal cord of non-transgenic (Ntg), and wild-type and mutant SOD1 overexpressing mice (SOD1^{WT} and SOD1^{G93A}) along the disease progression, at 60, 90, 120 and 140 days of age. Expression levels of ephrin-A2, A3, A5, and ephrin-B2 and B3 decreased with disease progression from 120 days onwards (Figure 7B, 7C, 7E, 7G and 7H). Ephrin-A1 and ephrin-B1 gene expression levels did not change over the course of the disease (Figure 7A and 7F). In contrast, ephrin-A4 levels increased from 90 days until the last time point analysed (Figure 7D).

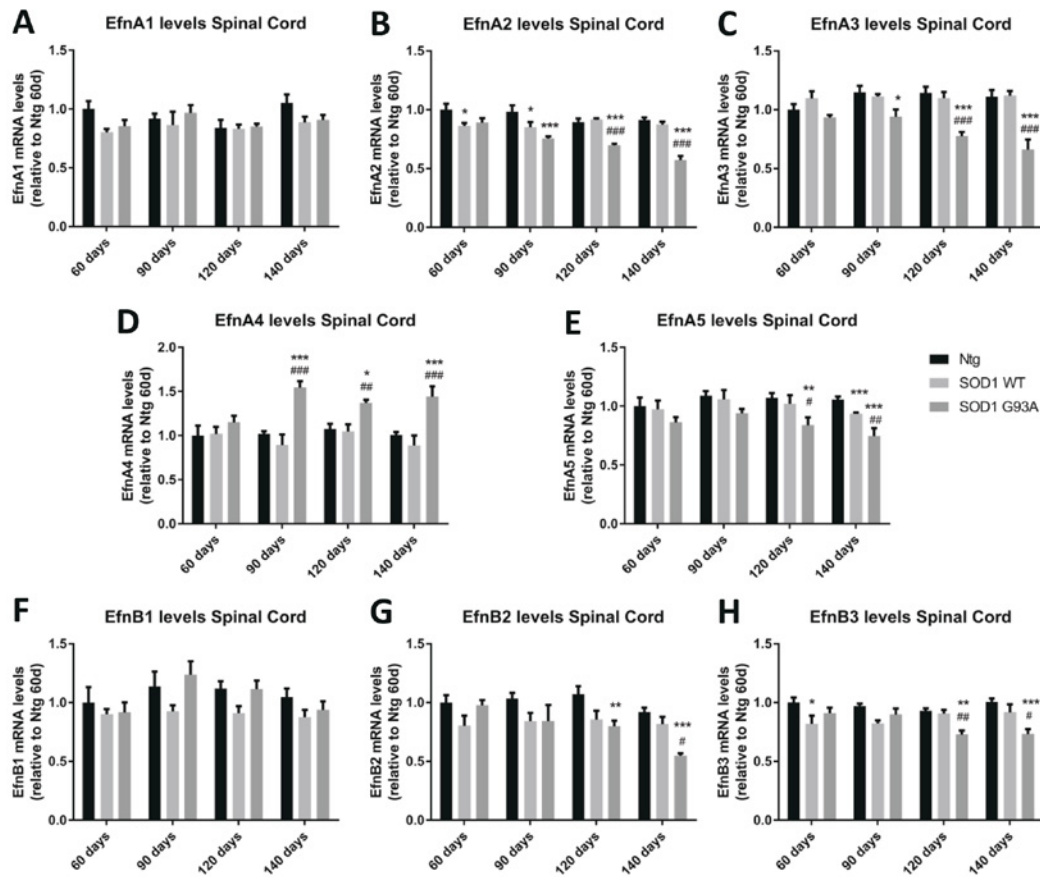


Figure 7 – Ephrin gene expression is dysregulated along disease progression in the SOD1^{G93A} mouse. (A-H) Expression levels of both ephrin-A and ephrin-B ligands were analysed by ddPCR and normalized to the housekeeping gene Polr2a (N = 4-9). Data represents mean ± SEM, and different conditions were compared with Two-way ANOVA followed by Tukey's multiple comparisons test to determine differences at each timepoint analysed. * p<0.05, ** p<0.01 and *** p<0.001 as compared with Ntg; # p<0.05, ## p<0.01 and ### p<0.001 as compared with SOD1 WT.

In previous experiments, we identified one ligand, ephrin-B2, to be abundantly upregulated in reactive astrocytes in ALS. To determine if an upregulation of ephrin-B2 in reactive astrocytes could be implicated in the pathophysiology of ALS, we were kindly provided with a transgenic mouse, which expresses Cre driven by the connexin-30 (Cx-30) promoter, the Cx30-CreER mouse (Dr. J. Frisen, Karolinska Institute, Stockholm, Sweden) and generated a triple transgenic mouse to specifically excise ephrin-B2 from astrocytes in SOD1^{G93A} mice, the Cx30-CreER::ephrin-B2^{fllox/fllox}::SOD1^{G93A}. Disease parameters have been studied in these mice after tamoxifen treatment at 60 days of age, and have been compared to ephrin-B2^{fllox/fllox}::SOD1^{G93A} mice also administered with tamoxifen. No difference was observed in onset, but survival was significantly worsened by 9 days and disease duration was reduced by 11 days (Figure 8A-C).

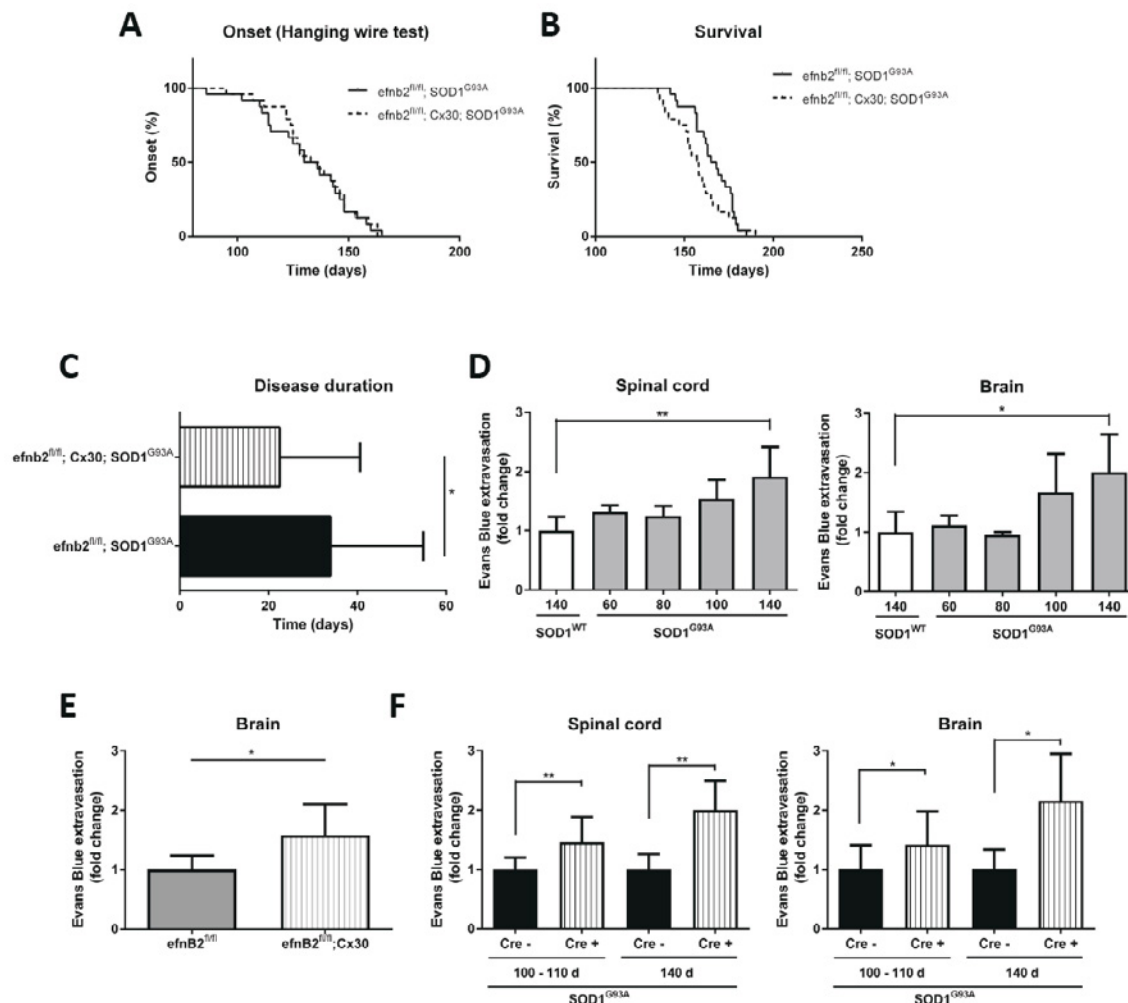


Figure 8 - Excision of ephrin-B2 from astrocytes from the age of 60 days on does not alter disease onset and worsens survival. (A) Onset analysis, as measured with the hanging wire test, did not show any significant delay (135 days, Cx30-CreER::ephrin-B2^{fllox/fllox}::SOD1^{G93A}, n = 24; versus 133 days, ephrin-B2^{fllox/fllox}::SOD1^{G93A}, n = 24). (B) Survival was decreased in these mice (157 days, Cx30-CreER::ephrin-B2^{fllox/fllox}::SOD1^{G93A}, n = 24; versus 166 days, ephrin-B2^{fllox/fllox}::SOD1^{G93A}, n = 24; p = 0.0297) and (C) disease duration was also shorter in mice lacking ephrin-B2 (23 days, Cx30-CreER::ephrin-B2^{fllox/fllox}::SOD1^{G93A}, n = 24; versus 34 days, ephrin-B2^{fllox/fllox}::SOD1^{G93A}, n = 24; p = 0.0482). Data represents mean ± SD (* p<0.05 as compared with ephrin-B2^{fllox/fllox}::SOD1^{G93A}). (D-F) Blood-brain barrier/Blood-spinal cord barrier (BBB/BSCB) leakage was determined by Evans blue fluorescent dye perfusion in (D) in SOD1^{G93A} mice at different time-points, (E) in Cx30-CreER::ephrin-B2^{fllox/fllox} and ephrin-B2^{fllox/fllox} and (F) in Cx30-CreER::ephrin-B2^{fllox/fllox}::SOD1^{G93A} and ephrin-B2^{fllox/fllox}::SOD1^{G93A} mice. Data represents mean ± SD, and different conditions were compared with two-tailed t-test or one-way ANOVA and Tukey's multiple comparison posthoc test (* p<0.05 and ** p<0.01).

Based on our current findings deletion of ephrin-B2 from the astrocytes worsens the disease course in a mouse model of ALS. To explain how impairing astrocyte function through astrocyte-specific deletion of ephrin-B2 worsens ALS, we considered the role that ephrin-B2 plays in the sprouting of endothelial cells [12, 13]. Ephrin-B2 might have a similar effect in astrocytes on the motility and morphology of its processes. As one function of the astrocytes is the establishment and maintenance of the blood brain barrier (BBB) and blood spinal cord barrier (BSCB) with their so-called endfeet, we hypothesized that loss of ephrin-B2 from astrocytes may impair the integrity of the BBB/BSCB, which then may contribute to worsening of the disease. Swollen astrocyte endfeet and leakage of the BBB and BSCB have already been reported for the SOD1^{G93A} mouse model [14-18]. We confirmed this by perfusing SOD1^{G93A} mice at different timepoints of the disease with Evans blue fluorescent dye and using the leakage of the dye into the parenchyma as readout for BBB/BSCB leakiness. We could confirm that at a later disease stage BBB/BSCB leakage occurs in these mice both in the spinal cord and in the brain, while no leakage was detected in age-matched SOD1^{WT} (Figure 8D). Interestingly, in a non-ALS context, perfusion of mice that lacked ephrin-B2 in astrocytes (Cx30-CreER::ephrin-B2^{fllox/fllox}) with Evans blue fluorescent dye, led to extravasation in the brain, indicating a role for ephrin-B2 in astrocytes in maintaining the integrity of the

BBB (Figure 8E). We hypothesized next that loss of ephrin-B2 from astrocytes might contribute to impair the integrity of the BBB/BSCB, leading to the worsening of ALS disease. We again assessed BBB/BSCB integrity by perfusing with Evans blue fluorescent dye Cx30-CreER::ephrin-B2^{flox/flox}::SOD1^{G93A} and ephrin-B2^{flox/flox}::SOD1^{G93A} mice. We could observe then that extravasation of the dye in the brain and spinal cord was enhanced in Cx30-CreER::ephrin-B2^{flox/flox}::SOD1^{G93A} mice compared to ephrin-B2^{flox/flox}::SOD1^{G93A} mice (Figure 8F), suggesting that deletion of ephrin-B2 from the astrocytes worsens the integrity of the BBB/BSCB in ALS. BBB/BSCB is formed by cerebrovascular endothelial cells that are in close contact with astrocyte endfeet. Between adjacent endothelial cells there are intercellular junctional multimolecular complexes named tight junctions that as a barrier and signalling platforms. Astrocyte endfeet can modulate the properties of the barrier leading to tighter tight junctions [19]. A marker for astrocyte endfeet and important protein in the BBB/BSCB is the water channel aquaporin-4 (AQP4), whose levels are upregulated in swollen endfeet and barrier breakdown [19]. In order to determine whether a lack of ephrin-B2 might influence the properties of these astrocyte endfeet, we have first analysed the gene expression and protein levels of AQP4 in non-ALS Cx30-CreER::ephrin-B2^{flox/flox} and ephrin-B2^{flox/flox} mice 2-3 months after tamoxifen administration. No differences were detected in the levels of AQP4 in the brain cortex or spinal cord of these mice (Figure 9A-D). Additionally we have also determined in the same mice the expression levels of three important proteins that among other proteins compose the tight junction complex: claudin-5, occludin and tight junction-1. Similarly to AQP4, no differences were detected in the expression levels of claudin-5, occludin and tight junction-1 in the brain cortex or in the spinal cord of Cx30-CreER::ephrin-B2^{flox/flox} and ephrin-B2^{flox/flox} mice (Figure 9A and 9B).

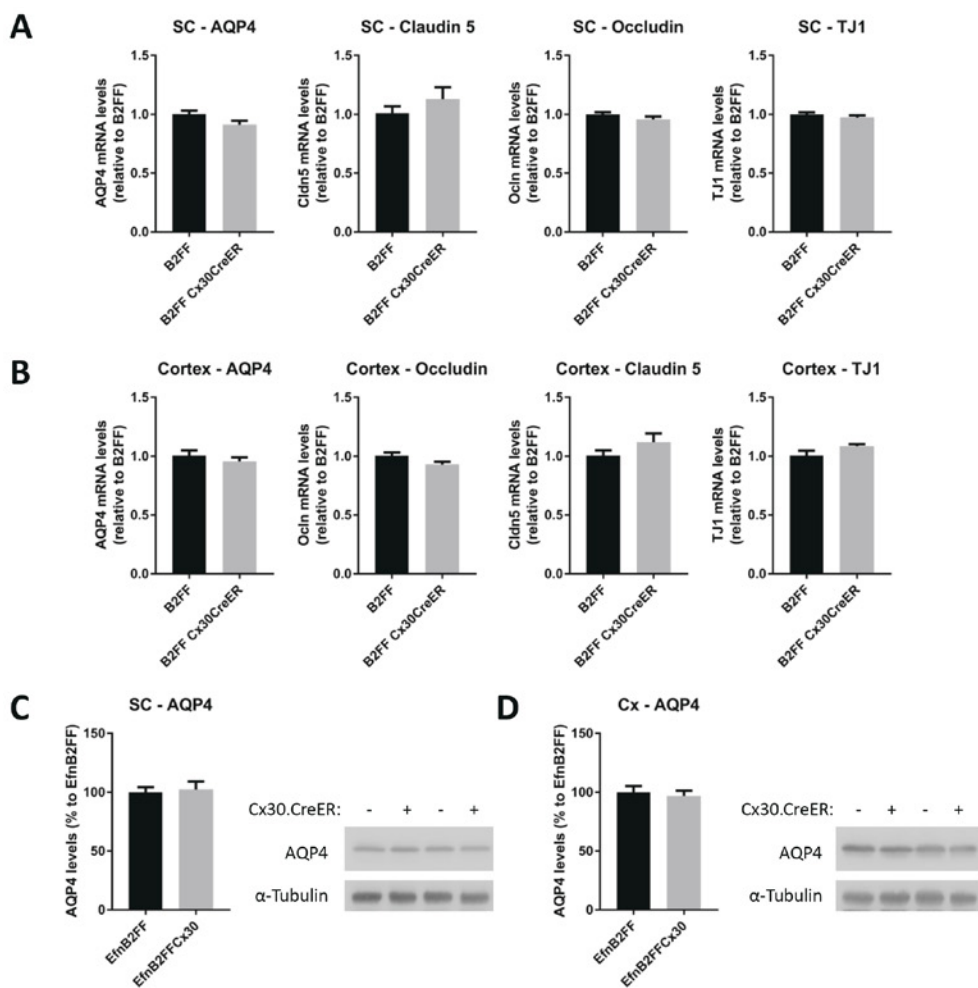


Figure 9 - Protein and expression levels of several BBB/BSCB components are not altered by a lack of astrocytic ephrin-B2. Expression levels of water channel aquaporin-4 (AQP4) and of tight junction proteins claudin-5, occludin and tight junction-1 (TJ1), were analysed in the (A) spinal cord (SC) and in the (B) brain cortex (Cx) of Cx30-CreER::ephrin-B2^{flx/flx} and ephrin-B2^{flx/flx} mice. Protein levels of AQP4 in the (C) spinal cord (SC) and in the (D) brain cortex (Cx) of Cx30-CreER::ephrin-B2^{flx/flx} and ephrin-B2^{flx/flx} mice were also determined by western-blot. Data represents mean \pm SEM, and different conditions were compared with two-tailed t-test.

In summary, ephrin-B2 deletion specifically in astrocytes does not improve ALS pathology; on the contrary it worsens it. And although further experiments need to be performed, we hypothesize that one of the mechanisms for that could be a larger impairment of the BBB and BSCB in the ALS mouse model.

WP2. Therapeutic significance of the involvement of EphA4 in motor neuron degeneration

WP2.1. Use of KYL, an EphA4 antagonist

KYL peptide, a specific EphA4 antagonist, was administered at a concentration to 3 mM and 1.5 mM intracerebroventricularly to cohorts of 60 days-old SOD1^{G93A} mice, corresponding to a presymptomatic stage of the disease, until they were end-stage using Alzet miniosmotic pumps. As controls we injected not only vehicle (ACSF) but also the peptide with a tyrosine-alanine substitution that completely abolishes the inhibitory function (KAL peptide). We evaluated the 4 groups with the previously mentioned clinical parameters, but onset was not altered (determined with the hanging wire test) nor could extended survival be observed (Figure 10).

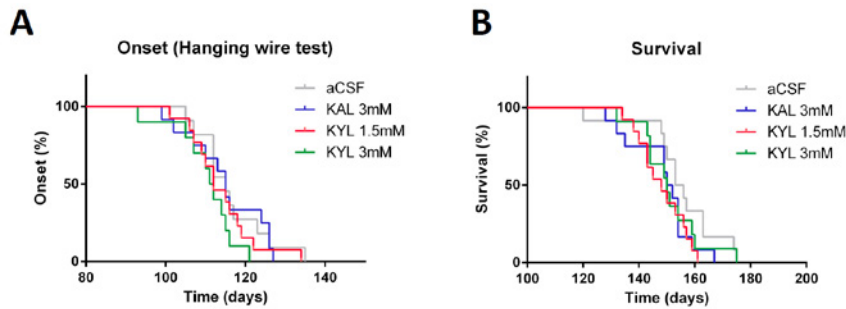


Figure 10 - Treatment with KYL peptide does not improve disease parameters in the SOD1^{G93A} mouse model of ALS. Different concentrations of KYL peptide were infused intracerebroventricularly in SOD1^{G93A} mice with Alzet miniosmotic pumps. ACSF and KAL were infused as controls. No significance difference was observed on onset (median onset was: ACSF, 115 days; KAL 3mM, 115 days; KYL 3 mM, 112 days and KYL 1.5 mM, 112 days) and neither on survival (median survival was: ACSF, 155 days; KAL 3mM, 151 days; KYL 3 mM, 150 days and KYL 1.5 mM, 148 days) N=10-13.

WP2.2. Use of anti-EphA4 nanobodies

EphA4 inhibitors identified so far still have poor physicochemical properties and low pharmacodynamic and pharmacokinetic properties. They have very low stability, affinity or specificity for EphA4 [20]. Nanobodies (Nb) are naturally occurring; heavy-chain only antibodies produced in *Camelidae*, with unique physicochemical and pharmacokinetic properties that make them match the requirements of many biomedical applications. Like conventional antibodies used in biomedicine they have a high specificity and affinity for their target as well as low inherent toxicity. In addition to that, they are very stable and small in size, which gives the opportunity to inhibit enzymes and readily access receptor clefts.

In collaboration with Dr. G. Hassan Zadeh Ghassabeh (Dept of Structural Biology, University of Brussels), we developed 15 Nb, single-chain antibodies produced in *Camelidae*, directed against the extracellular domain of EphA4 (ligand binding domain, LBD), using previously described methods [21]. From the generated Nb, 5 Nb resulted in low expression levels in a bacterial system and presented tendency to aggregate. Therefore these 5 Nb were excluded from the screen. As mentioned in a previous report, affinity for EphA4 was thereafter determined for the 10 Nb left by using surface plasmon resonance (SPR, Biacore), where the EphA4 LBD was immobilized on a chip and Nbs with concentrations from 1 nM to 300 nM were used as analyte. SPR analysis revealed that whereas Nb 34, Nb 47 and Nb 19 only showed none or low binding affinity, the other seven Nbs showed affinity in the low nanomolar range. For those nanobodies with the best K_d , the specificity for EphA4 binding was determined by analyzing their affinity for other Eph receptors with alpha screen technology (Figure 11). Nbs 22, 39, 31 and 53 were the most selective for EphA4, although they could still bind some other Eph receptors such as EphA7 (Figure 11).

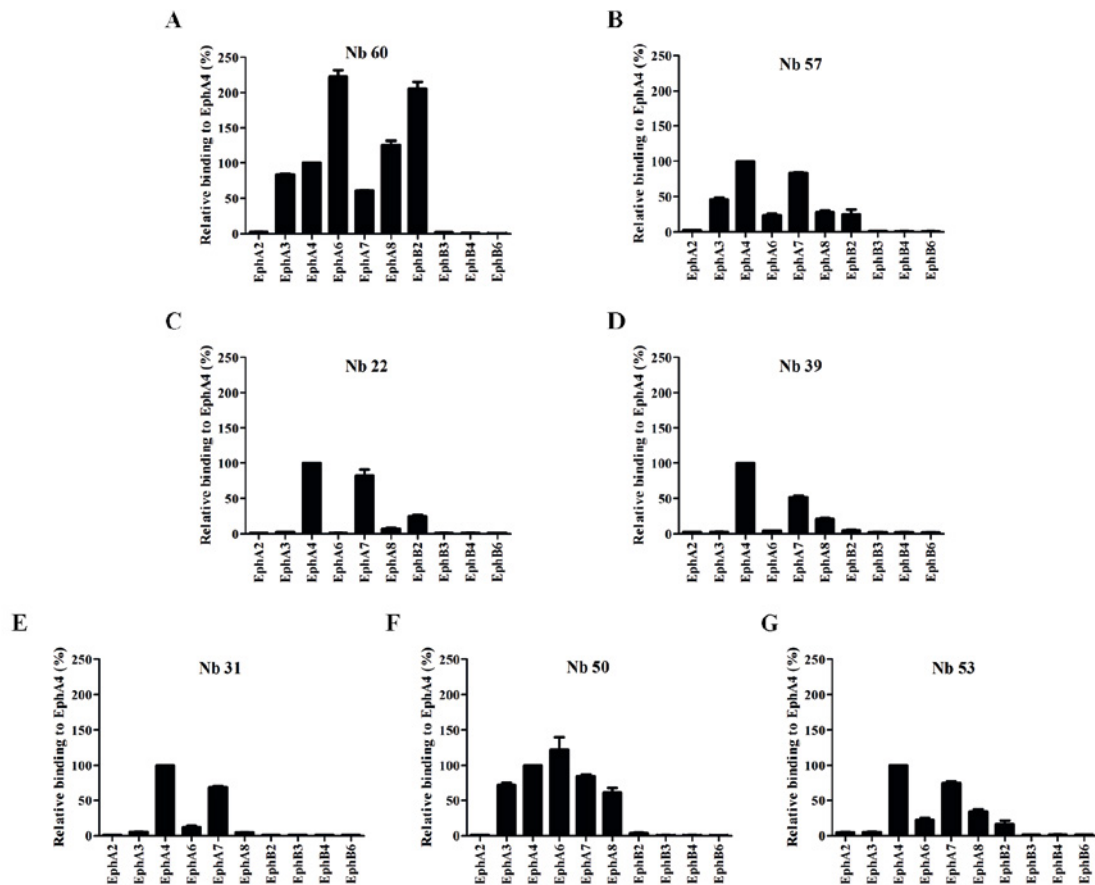


Figure 11 - Nb selectivity for EphA4 and cross-reactivity with other Eph receptors. Using AlphaScreen technology we determined the selectivity of the Nbs for EphA4 receptor and the cross-reactivity with other Eph receptors. (A) Next to EphA4, Nb 60 also interacted with many other different Eph receptors. (B-F) Nb 57, 22, 39, 31 and 53 presented the highest selectivity to the EphA4 receptor. (F) Nb 50 had the lowest selectivity for EphA4 as it also interacted with EphA3, EphA6, EphA7 and EphA8. Data is represented as mean \pm SD.

In order to define the binding properties of the Nbs to the EphA4 such as their specific binding site in the LBD domain and the biological significance of such binding, we next tested the Nbs on binding competition assays with EphA4 ligands as well as activity assays of the EphA4 receptor. In all experiments we used the KYL peptide as a positive control, and also to determine if our aim in obtaining Nbs that would work better than the KYL peptide would be accomplished. Nb 22 could almost completely inhibit the binding of ephrin-A3 and ephrin-B ligands, but not others, to EphA4. Nb 31 completely inhibited the binding of ephrin-A1, A3, B1, B2 at equal or even at lower concentrations than the KYL-peptide. Nb 39 and Nb 53 reached complete inhibition of ligand binding for all ephrin ligands in a concentration range lower than the KYL-peptide. Thus, these two Nbs seemed to be the most interesting outcome of our study (Figure 12).

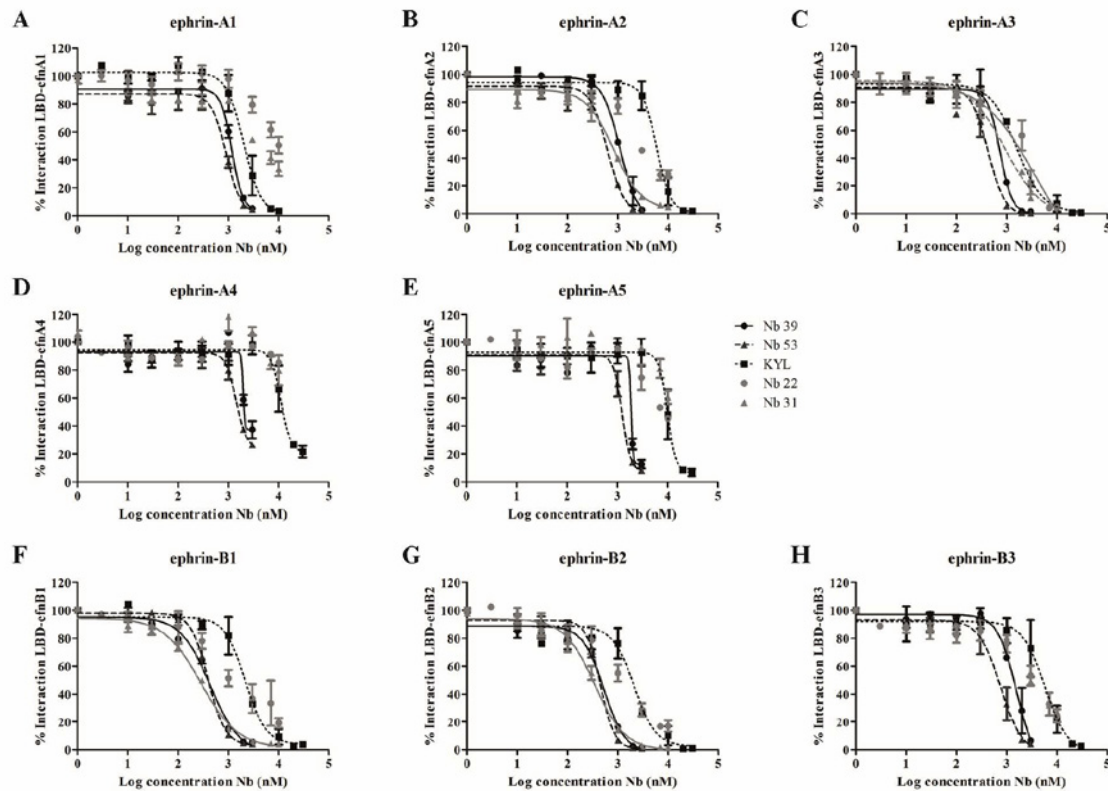


Figure 12 - Nb 39 and 53 bind EphA4 and strongly compete with the binding of all EphA4 ligands. Increasing concentrations of Nb were assessed to determine the capability of these molecules to inhibit the binding of ephrin ligands to the EphA4 receptor. The KYL peptide is always used as a positive control. Values represented indicate mean with SD.

To assess the antagonistic properties of the Nbs we used the DiscoverX PathHunter U2OS EphA4 cell line (DiscoverX), in which ephrin-induced activation of EphA4 in genetically modified cells causes activation and dimerization of the receptor leading to crossphosphorylation and yielding to an active β -galactosidase enzyme, which can be visualized with a chemiluminescent substrate. Cells were stimulated with ephrin-A1 with or without the presence of an EphA4 antagonist (KYL peptide or Nbs), and the resulting EphA4 phosphorylation was measured. The KYL-peptide achieved complete inhibition of ephrin-A1-induced phosphorylation with an IC₅₀ value of 53 μ M (Figure 13). Nbs 39 and 53 completely inhibited ephrin-A1-induced phosphorylation, at lower concentrations than the KYL-peptide, with an IC₅₀ of 170 nM and 261 nM respectively (Figure 13). These data indicate that Nbs 39 and 53 are 200 to 300 times more potent than the KYL-peptide in inhibiting ephrin-A1-induced EphA4 phosphorylation.

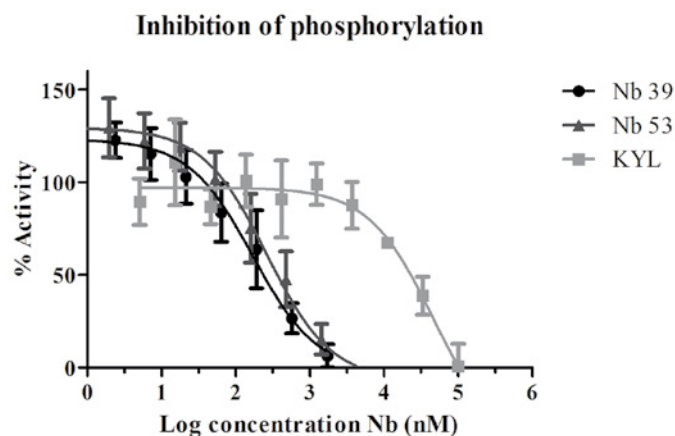


Figure 13 - Nb39 and 53 antagonize the phosphorylation of EphA4 upon ligand stimulation at a higher efficiency than the KYL peptide. Increasing concentrations of Nb were assessed to determine the capability of these molecules to inhibit the phosphorylation and activation of the EphA4 receptor after stimulation with ephrin-A1 ligand. The KYL peptide was used as a positive control. Values represented indicate mean with SD.

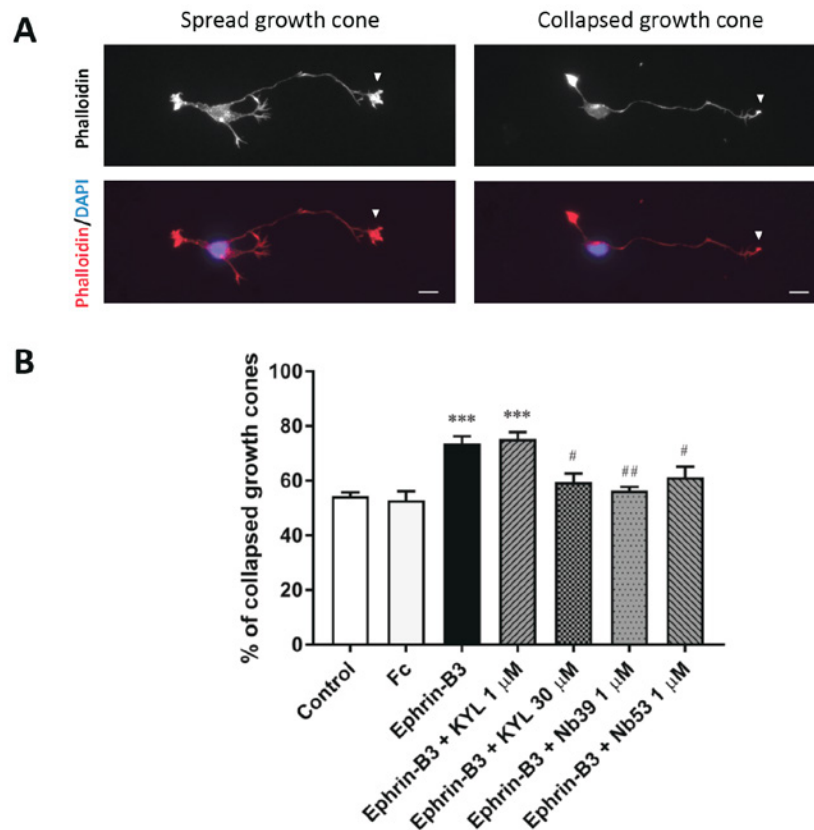


Figure 14 - Nb 53 and Nb 39 (1 μ M) reversed ephrin-B3-mediated growth cone collapse. (A) E17.5 cortical neurons were first treated at 24h after culture with 1 μ M or 30 μ M KYL peptide or 1 μ M Nb for 30 min, and then stimulated with 1 μ g/ml preclustured ephrin-B3-Fc or Fc as a control for 30 min in the presence of the Nb. A control condition without any kind of treatment was also scored (Control). Cells were stained with Alexa Fluor 555-conjugated phalloidin and DAPI. Growth cone collapse was determined for every neuron by analysing the tip of only the longest neurite (white arrowheads). Scale bar, 10 μ m. (B) Percentage of growth cone collapse was determined in every experimental condition by assessing 40-160 neurons under a Zeiss fluorescence microscope. Percentage of collapse is expressed as the mean of collapse of 6 independent experiments \pm SEM, and was compared between different conditions by one-way ANOVA followed by Tukey's multiple comparisons posthoc test (** $p < 0.01$ and *** $p < 0.0001$, as compared with control and Fc conditions; # $p < 0.05$, as compared with the ephrin-B3 condition).

A common cellular response downstream of Eph receptor activation is actin cytoskeleton reorganization, leading to cell morphology changes [22, 23]. Ephrin-B3 treatment of cortical neurons *in vitro* induces collapse of growth cones at the tip of the neurites, by reorganization of actin filaments [24, 25]. Cortical neurons lacking functional EphA4 show insensitivity to the ephrin-B3-mediated growth cone collapse, suggesting that this effect is EphA4-mediated [8]. Therefore, we next determined whether the Nbs were also able to antagonize a cellular response such as growth cone collapse induced by an EphA4 receptor agonist. To this end, we investigated their effect on the ephrin-B3 induced inhibition of neurite elongation in E17.5 embryonic cortical neurons. Stimulation with preclustured recombinant ephrin-B3-Fc resulted in growth cone collapse as compared to an unstimulated condition and a condition stimulated with Fc only (Figure 14). As expected, KYL peptide antagonized this effect on growth cone collapse, but only at a concentration of 30 μ M. Nb 53 as well as Nb 39 also inhibited the growth cone collapse effect mediated by ephrin-B3-Fc, but at the concentration of 1 μ M, a concentration at which the KYL peptide was ineffective (Figure 14).

In summary, we were able to generate Nbs against the LBD of the EphA4 receptor. Two of these Nbs specifically bind the EphA4 receptor with nanomolar affinities and block ephrin-induced EphA4 phosphorylation and EphA4-mediated actin remodelling in a growth cone collapse assay. These Nbs may be useful as a therapeutic strategy in disorders in which EphA4 plays a pathogenic role. These set of results has been finished and a manuscript has been submitted for publication.

WP2.3. Inhibition of the EphA4 signalling cascade: ROCK inhibitors

EphA4 stimulation results in growth cone collapse through activation of GTP-bound RhoA activity, which phosphorylates ROCK. ROCK phosphorylates LIMK, which in turn phosphorylates and thus inhibits cofilin, resulting in reorganization of the actin filamentous network. Fasudil, which is an effective ROCK inhibitor, stabilizes the cytoskeleton and it is in clinical use for vasospasm such as seen after subarachnoid haemorrhage, for stroke and for pulmonary hypertension [26, 27]. Moreover, a study in a mouse model for SMA has shown this compound to have an effect in this disease [28]. Therefore, we aimed to determine whether interference with the downstream signalling cascade of EphA4 may be a therapeutic strategy for motor neuron degenerative disorders. To this end, we have been studying the effect of ROCK inhibition on the motor neuron degeneration in the SOD1^{G93A} mouse.

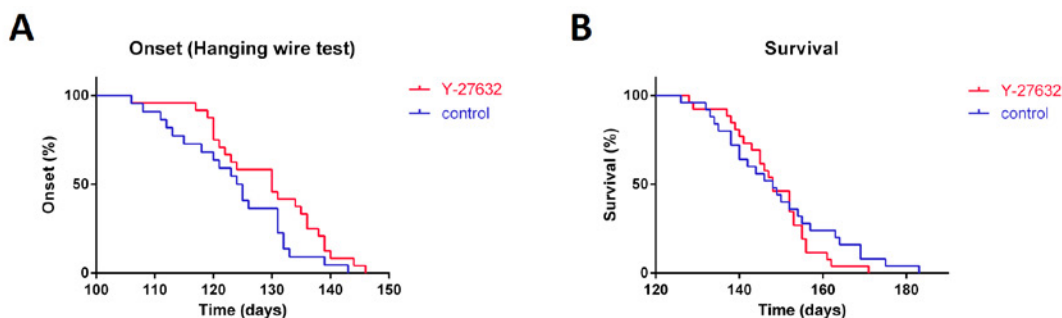


Figure 15 - Treatment of SOD1^{G93A} mice with Y-27362 did not improve onset or survival. Onset analysis of control (124.5 days, N = 22) and Y-27362 (130 days, N = 24) treatment. Survival analysis of control (148 days, N = 25) and Y-27362 (148 days, N = 26) treatment.

To do so, we treated mice with two different ROCK inhibitors, Y-27362 and fasudil. These compounds inhibit both ROCK1 and ROCK2 isoforms, of which Y-27362 is the most specific one. However, fasudil is an FDA-approved drug, facilitating its potential translation to humans. We treated SOD1^{G93A} mice with 30 mg/kg/day Y-27362 by oral gavage starting from P100. We found a small but non-significant delay in onset and no effect on survival (Figure 15).

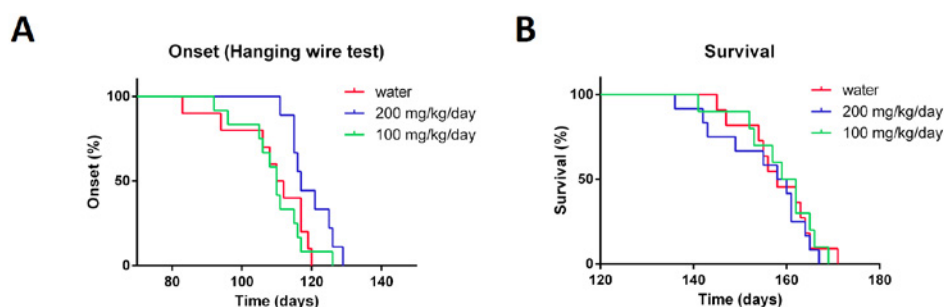


Figure 16 - Treatment of SOD1^{G93A} mice with fasudil delayed onset, but did not affect survival. Onset analysis of control (111 days, N = 11), 100 mg/kg/day (110 days, N = 12) and 200 mg/kg/day (117 days, N = 9) fasudil. Survival analysis of control (158 days, N = 11), 100 mg/kg/day (160.5 days, N = 12) and 200 mg/kg/day (159 days, N = 9) treatment.

Administering 100 mg/kg/day fasudil in drinking water has been shown to result in a therapeutic effect in mice models of various diseases. We administered 100 and 200 mg/kg/day fasudil in drinking water starting from P60. We found a significant effect of 200 mg/kg/day fasudil on onset ($p < 0.05$), which was not present when using a lower doses of 100 mg/kg/day. Treatment with fasudil at any concentration had no effect on survival (Figure 10).

3. References

1. Robberecht, W. and T. Philips, *The changing scene of amyotrophic lateral sclerosis*. Nat Rev Neurosci, 2013. **14**(4): p. 248-64.
2. Joyce, P.I., et al., *SOD1 and TDP-43 animal models of amyotrophic lateral sclerosis: recent advances in understanding disease toward the development of clinical treatments*. Mamm Genome, 2011. **22**(7-8): p. 420-48.
3. Van Hoecke, A., et al., *EPHA4 is a disease modifier of amyotrophic lateral sclerosis in animal models and in humans*. Nat Med, 2012. **18**(9): p. 1418-22.
4. Fabes, J., et al., *Regeneration-enhancing effects of EphA4 blocking peptide following corticospinal tract injury in adult rat spinal cord*. Eur J Neurosci, 2007. **26**(9): p. 2496-505.
5. Goldshmit, Y., et al., *Axonal regeneration and lack of astrocytic gliosis in EphA4-deficient mice*. J Neurosci, 2004. **24**(45): p. 10064-73.
6. Frey, D., et al., *Early and selective loss of neuromuscular synapse subtypes with low sprouting competence in motoneuron diseases*. J Neurosci, 2000. **20**(7): p. 2534-42.
7. Egea, J. and R. Klein, *Bidirectional Eph-ephrin signaling during axon guidance*. Trends Cell Biol, 2007. **17**(5): p. 230-8.
8. Egea, J., et al., *Regulation of EphA 4 kinase activity is required for a subset of axon guidance decisions suggesting a key role for receptor clustering in Eph function*. Neuron, 2005. **47**(4): p. 515-28.
9. Grunwald, I.C., et al., *Hippocampal plasticity requires postsynaptic ephrinBs*. Nat Neurosci, 2004. **7**(1): p. 33-40.
10. Kullander, K., et al., *Kinase-dependent and kinase-independent functions of EphA4 receptors in major axon tract formation in vivo*. Neuron, 2001. **29**(1): p. 73-84.
11. Leighton, P.A., et al., *Defining brain wiring patterns and mechanisms through gene trapping in mice*. Nature, 2001. **410**(6825): p. 174-9.
12. Sawamiphak, S., et al., *Ephrin-B2 regulates VEGFR2 function in developmental and tumour angiogenesis*. Nature, 2010. **465**(7297): p. 487-91.
13. Wang, Y., et al., *Ephrin-B2 controls VEGF-induced angiogenesis and lymphangiogenesis*. Nature, 2010. **465**(7297): p. 483-6.
14. Garbuzova-Davis, S., et al., *Ultrastructure of blood-brain barrier and blood-spinal cord barrier in SOD1 mice modeling ALS*. Brain Res, 2007. **1157**: p. 126-37.
15. Garbuzova-Davis, S., et al., *Evidence of compromised blood-spinal cord barrier in early and late symptomatic SOD1 mice modeling ALS*. PLoS One, 2007. **2**(11): p. e1205.
16. Winkler, E.A., et al., *Blood-spinal cord barrier disruption contributes to early motor-neuron degeneration in ALS-model mice*. Proc Natl Acad Sci U S A, 2014. **111**(11): p. E1035-42.
17. Zhong, Z., et al., *ALS-causing SOD1 mutants generate vascular changes prior to motor neuron degeneration*. Nat Neurosci, 2008. **11**(4): p. 420-2.
18. Lewandowski, S.A., et al., *Presymptomatic activation of the PDGF-CC pathway accelerates onset of ALS neurodegeneration*. Acta Neuropathol, 2016. **131**(3): p. 453-64.
19. Abbott, N.J., L. Ronnback, and E. Hansson, *Astrocyte-endothelial interactions at the blood-brain barrier*. Nat Rev Neurosci, 2006. **7**(1): p. 41-53.
20. Tognolini, M., M. Incerti, and A. Lodola, *Are We Using the Right Pharmacological Tools to Target EphA4?* ACS Chem Neurosci, 2014. **5**(12): p. 1146-7.
21. Vincke, C., et al., *Generation of single domain antibody fragments derived from camelids and generation of manifold constructs*. Methods Mol Biol, 2012. **907**: p. 145-76.
22. Kania, A. and R. Klein, *Mechanisms of ephrin-Eph signalling in development, physiology and disease*. Nat Rev Mol Cell Biol, 2016. **17**(4): p. 240-56.
23. Pitulescu, M.E. and R.H. Adams, *Eph/ephrin molecules--a hub for signaling and endocytosis*. Genes Dev, 2010. **24**(22): p. 2480-92.
24. Dent, E.W., S.L. Gupton, and F.B. Gertler, *The growth cone cytoskeleton in axon outgrowth and guidance*. Cold Spring Harb Perspect Biol, 2011. **3**(3).
25. Kullander, K., et al., *Ephrin-B3 is the midline barrier that prevents corticospinal tract axons from recrossing, allowing for unilateral motor control*. Genes Dev, 2001. **15**(7): p. 877-88.
26. Olson, M.F., *Applications for ROCK kinase inhibition*. Curr Opin Cell Biol, 2008. **20**(2): p. 242-8.
27. Satoh, K., Y. Fukumoto, and H. Shimokawa, *Rho-kinase: important new therapeutic target in cardiovascular diseases*. Am J Physiol Heart Circ Physiol, 2011. **301**(2): p. H287-96.
28. Bowerman, M., et al., *Rho-kinase inactivation prolongs survival of an intermediate SMA mouse model*. Hum Mol Genet, 2010. **19**(8): p. 1468-78.



Geneeskundige Stichting Koningin Elisabeth
Fondation Médicale Reine Elisabeth
Königin-Elisabeth-Stiftung für Medizin
Queen Elisabeth Medical Foundation

Final report
of the research group of

Prof. dr. Serge N. Schiffmann

Université Libre de Bruxelles (ULB)

Principal Investigator

Prof. dr. Serge N. Schiffmann
Laboratory of Neurophysiology
ULB Neuroscience Institute (UNI)
Université Libre de Bruxelles, ULB
808 route de Lennik, CP601
B-1070 Brussels
T +32 2 555 42 30 – +32 2 555 64 07
F +32 2 555 41 20
sschiffm@ulb.ac.be
neurophy.ulb.ac.be/

Co-Investigators

- Alban de Kerchove d'Exaerde
adekerch@ulb.ac.be
- Patricia Bonnavion
pbonnavi@ulb.ac.be
- Jean-Marie Vanderwinden
jmvdwin@ulb.ac.be

Basal Ganglia's Functions and Disorders: from Specific Genes and Signalling Pathways to Neuronal Subpopulations

Parkinson's disease (PD) and drug addiction are two major pathological conditions that rely on profound dysfunctions of the basal ganglia (BG) system. Dysfunctions of BG also occur in other conditions such as Huntington's disease, dystonia, schizophrenia or attention deficit/hyperactivity disorder (ADHD).

The BG system is composed of several interconnected subcortical nuclei including the striatum, subthalamic nucleus, globus pallidus (GP), substantia nigra (SN) and ventral tegmental area (VTA) that is involved in adaptive control of movement, motivational processes and cognitive functions. The major input to BG comes from the cerebral cortex mainly targeting the striatum, which is also under a robust regulatory influence from dopaminergic neurons of SNc and VTA and which works as the major site of integration of cortical, thalamic and midbrain afferents. BG are subdivided into a dorsal part participating in control of movement and procedural memory or skill learning and a ventral part involved in motivation and reward. The striatum, the major input structure of this system is made up several neuronal populations including two efferent medium-size spiny neurons (MSN) sub-populations characterized by their outputs, either SNr or GP; as well as four classes of interneurons. The two populations of MSN, striatonigral and striatopallidal neurons, expressing dopamine D₁ (D₁R) or D₂ (D₂R) receptors, respectively, give rise to the direct and indirect pathways of the BG circuitry, respectively.

The major aims of our project are to dissect out the distinct properties and to identify the precise role of striatal neuronal populations in motor control and movement disorders, procedural memory, instrumental learning and drug addiction by sub-regional optogenetic or pharmacogenetic control of specific striatal sub-populations as well as to cell-specifically and functionally characterize genes expressed in D2R-MSN and/or D1R-MSN.

The main achievements obtained on the 2014-2016 period thanks to the support from QEMF are summarized below.

1. Identification of roles of D1R-MSN and D2R-MSN of striatal subregions in motor control, procedural and instrumental learning by specific optogenetic and pharmacogenetic approaches

We have previously reported the roles of D2R- and D1R-MSN in motor activity, motor learning and reward processes by using a regional and subregional cell-specific ablation models (Durieux et al., 2009, 2011, 2012). These models allowed a functional cell-type dissection of different striatal regions with a reasonable spatial resolution, but are not reversible and could lead to compensation that could preclude adequate interpretation of the data. To circumvent these issues we developed two strategies called optogenetics and pharmacogenetics using light or engineered G-protein coupled receptors, respectively, to reversibly control, in vivo or ex vivo, the activity of genetically targeted neuronal populations.

During the frame of this program, we set up optogenetics both by using activating, the light-sensitive cation channel Channelrhodopsin-2 (ChR2), and silencing, the proton pump Archaeorhodopsin-3 (ArCh), opsins to either activate or silence neurons, respectively. Ex vivo, we tested the functional expression of optogenetic transgenes in D1R and D2R neurons using whole-cell patch clamp recording technique. As shown in our previous report, in voltage-clamp mode, photostimulation of ChR2-transduced D1R- and

D2R-neurons with blue light caused inward current. In current-clamp experiments, neurons that had been transduced with ChR2, 5ms pulses of blue-light, caused action potentials with 100% efficiency at 20 Hz. By contrast, we now showed that neurons transduced with ArCh showed rapid outward photocurrents in voltage clamp recording. In current clamp experiments, ArCh-transduced neurons were hyperpolarized by green light, which completely blocked endogenous action potentials. These *in vitro* results show that AAV-mediated expression of ChR2 or ArCh can stimulate or inhibit action potentials with a millisecond timescale precision, respectively, in the D1R- and D2R-striatal neurons. To develop the technique *in vivo* in the lab, we acquired and installed specific laser systems coupled to implanted optical fibers that allow to deliver optical stimulation deep into the brain area of interest in freely moving animals. After having previously assessed the efficiency of ChR2 activation in a circling behavior as a validation assay, we tested the behavioral outcomes of light-induced neuronal activity from the different striatal subpopulations in different learning tasks and these *in vivo* functional experiments validated the approach and the selectivity of expression in D1R- and D2R-neurons.

The chemogenetic approach called Designer Receptors Exclusively Activated by Designer Drugs (DREADD) is another alternative to cell-specific ablation and was developed in the lab. This technique consists in the Cre-dependent expression of a mutated muscarinic G(α)protein-coupled receptor (hM4Di) in striatal neurons. This approach allows a direct, non-invasive remote control of neuronal activity with high cell-specificity through G-protein coupled receptor (GPCR) signalling pathway. hM4Di receptors are exclusively activated by an inert synthetic ligand clozapine-N-oxide (CNO), which penetrates the blood-brain barrier and results in striatal neurons hyperpolarization for several hours. We applied this technique in Adora2a-Cre and D1r-Cre mice to selectively target the indirect pathway through Adora2a/D2R-expressing striatopallidal neurons, and the direct pathway through D1R-expressing striatonigral neurons, respectively. We validated the specific expression of the hM4Di transgene in striatopallidal neurons exhibiting almost a full-striatum diffusion. We quantified that $98.9 \pm 0.6\%$ of hM4Di-mCherry-expressing neurons are Adora2a positive, and that we transfected $56.8 \pm 4.6\%$ of Adora2a neurons with the hM4Di-mCherry transgene in coronal sections of the central striatum. We then tested the effect of CNO injection on mice locomotor behaviour. The chemogenetic inactivation of Adora2a/D2R neurons induces a progressive increase in locomotion measured as the distance travelled and enhanced velocity in a new open field exploration test, behaviors that are in line with the expected functions of striatopallidal neurons.

2. Properties of striatal fast-spiking interneurons deficient in parvalbumin and their synaptic connections to MSN and roles of FSI of striatal subregions in motor control, procedural and instrumental learning.

Striatal neurons (MSN) excitability and corticostriatal synaptic transmission are tightly regulated both by a large series of neurotransmitters and by striatal interneurons.

Striatal fast spiking interneurons (FSI) modulate the output of the striatum by providing a powerful feedforward inhibition on striatal principal neurons (MSN) and synchronizing their activity. Several studies have broadened our understanding of FSI, showing that they are implicated in severe disorders as Parkinsonism, dystonia, autism spectrum disorders (ASD) and Tourette syndrome. FSI are the only striatal neurons to express the Ca²⁺-binding protein parvalbumin (PV). We have previously demonstrated, by using PV-EGFP::PV^{-/-} mice and double patch recording as well as computer simulation, that in FSI, PV tightly regulates the calcium dynamics and is crucial for the fine-tuning of the temporal responses of the FSI network and for the orchestration of MSN populations (Bischof et al., 2012; Orduz et al., 2013).

Since the network of PV-expressing interneurons has gained particular attention in ASD but little is known on PV's putative role with respect to ASD, we pursued our study by analyzing both the behavior of PV-depleted mice in terms of ASD symptomatology, their cortico-striatal synaptic transmission and the morphology of striatal FSI (Wöhr et al., 2015). We showed that three core symptoms present in ASD patients were detected in these mice: impaired social interactions, reduced communication and repetitive and stereotyped behavior. We showed that both inhibitory and excitatory synaptic transmissions were altered. Indeed, we observed altered short-term synaptic plasticity of the excitatory cortical input to the striatal FSI. Our results suggested that short-term plasticity at this cortical neuron-FSI synapse might have a presynaptic adaptation in the cortical neuron caused by the absence of PV in the postsynaptic FSI, besides PV's more direct role at the presynaptic side in FSI and other PV⁺ interneurons. Finally after filling the recorded striatal FSI, 3D reconstruction was performed by using confocal microscopy. We showed that the number of branches was clearly increased in striatal PV^{-/-} FSI and Sholl analysis revealed a higher number of dendrites in a region between 40 to 150 μm from the soma and also more branches from the 3rd to 5th order. In view of these results and knowing that changes in PV expression pattern have been reported in numerous mouse ASD models, we propose a convergent pathway in ASD, where mutations in ASD-linked genes may lead to a down-regulation of PV resulting in the ASD phenotype (Wöhr et al., 2015).

Our next questions were to identify the roles of these neurons and their PV-regulated Ca²⁺ dynamic in the cortico-striatal circuit and to evaluate *in vivo* the role of these neurons and their coupling by using optogenetics. For this, we developed and validated optogenetics for FSI in the striatum. We genetically targeted expression of ChR2 to PV⁺ cells in order to selectively activate FSIs with 470 nm light pulses. We injected PV-Cre mice with AAV conditionally expressing the fluo-tagged ChR2-tdTomato, thereby achieving specific ChR2 expression in PV⁺/FSIs. Those AAV contain a double-floxed inverted open reading frame encoding the ChR2-eYFP protein. Striatal neurons expressing ChR2-tdTomato are only present in Cre⁺ mice and they account for a sparse neuronal population. These neurons are aspiny and PV-positive; hence confirming the genetic restriction of ChR2 to FSI. Whole-cell recording was performed on tdTomato-expressing neurons in cortico-striatal slices from these mice. We characterized the activation of these neurons by delivering continuous or pulsed illumination. Fluorescent neurons which depolarized upon optical stimulation were shown to be FSI as determined by their electrophysiological properties such as non-accommodating discharge pattern, high discharge rate, narrow action potentials, and fast and deep afterhyperpolarization. FSI depolarised strongly, leading in all cases to action potential discharges. Light pulses of 2 ms duration were usually sufficient to induce these action potentials and this was observed for a broad range of frequencies. Inhibitory post-synaptic current (IPSC) were recorded in MSN. FSI contacting neighboring MSN provided inhibition since light presentation paused firing evoked by current steps. Light-induced synaptic responses are GABA_A-R dependent. We have therefore validated the model *in vitro* and we are now analyzing the network properties of these FSI *in vitro* in terms of their control of MSNs - the striatal principal neurons - activity and have implemented the strategy to correlate these data to the involvement of these neurons on striatal-dependent behavior by using bilateral striatal FSI excitation to assess the role of the FSI microcircuits on the behaviour of awake animals.

3. Specific inactivation of NR1 in D2R-striatopallidal neurons

Neuroadaptation and more specifically synaptic plasticity involve several important neurotransmitter receptors and intracellular signaling cascades. Among the involved receptors, the Ca²⁺ permeable glutamate NMDA receptor is a central and initial player. This has been firmly demonstrated at different excitatory synapses such as in the hippocampus. The NMDA receptor seems to have key influence in the mechanisms of reward and addiction as well as in motor skill learning. Synaptic plasticity

events could be very different in striatopallidal and striatonigral neuronal subpopulations and must have diverse functional and behavioral consequences. In particular, the role of the NMDA-R-initiated signaling pathways in long-term synaptic plasticity in the striatopallidal neurons and their involvement in normal motor learning and striatal neuroadaptation to dopamine depletion, or drug addiction were mostly undetermined. We have generated $A_{2A}R\text{-Cre}::Grin1^{fl/fl}$ mice to specifically inactivate the essential NR1 subunit of the NMDA receptor in striatopallidal neurons.

These mice have been used at 2 months of age for testing their behaviour in relationship to locomotor activity, motor learning and attentional behaviour. The results showed that these mice exhibit motor dysfunctions with spontaneous hyperlocomotion. Indeed, in an *open field* test, $A_{2A}R\text{-Cre}^{+/-} Grin1^{fl/fl}$ mice exhibit a higher locomotor activity as compared to their control $A_{2A}R\text{-Cre}^{-/-} Grin1^{fl/fl}$ littermates. Moreover, when tested on three successive days, unlike control mice, which have a significantly decremental exploratory activity across sessions, the activity of $A_{2A}R\text{-Cre}^{+/-} Grin1^{fl/fl}$ mice remains stable. The motor skill learning was then compared by the rotarod and runway tests. In the accelerant rotarod test, mice learn a new sequence of movements to maintain balance on a rotating rod with constant acceleration. When testing on the runway, mice must run along an elevated line dotted with small obstacles intended to impede their progress. The number of shifts of the hind paw on the visible side of the experimenter is recorded. The analysis of mice showed no significant difference between $A_{2A}R\text{-Cre}^{+/-} Grin1^{fl/fl}$ mice and their controls in motor learning performance during the rotarod and runway tests. However during the accelerating rotarod task, $A_{2A}R\text{-Cre}^{+/-} Grin1^{fl/fl}$ mice deficient in NMDA receptor were turning on themselves in the horizontal plane simultaneously with executing their task. Quantification of this behaviour showed a high significance as compared to control mice. Interestingly, these locomotor deficits are similar to those observed following the selective ablation of D_2R striatopallidal MSN (Durieux et al., 2009, 2012), suggesting that NMDA receptor is required for both learning and spontaneous motor behaviour. This result indicates that iMSN NMDA-R deletion may change the process of action selection within the BG. To further characterize this behavioural alteration we performed a more sophisticated motor-skill learning paradigm: the single-pellet reaching task. This paradigm requires precise and coordinated motor movements of the forelimb, as mice reach for and retrieve objects through a narrow slit. The speed and accuracy of the successful movements were quantified across daily sessions. The average speed as well as the average success rate over time during the training period of the single-pellet reaching task were significantly higher for the control mice compared to cKO mice and the cKO mice were unable to learn the task. In view of putative attentional deficits, a novel object recognition test and instrumental learning task in boxes were performed. The novel object recognition test showed an increase in exploration of both novel and old objects but failure to discriminate between these two objects in the $A_{2A}R\text{-Cre}^{+/-} Grin1^{fl/fl}$ mice. Again this attentional deficit is similar to what was observed following the selective ablation of D_2R striatopallidal MSN (Durieux et al., 2011) and suggests that NMDA receptor in this neuron population is required for selective attention processing. The instrumental learning (or operant conditioning) was performed in a behavioral paradigm of positive reinforcement where the animals must learn to associate an action (placing the nose in a hole, Nose Pokes NP) to its specific result (distribution of granules sweet) and then gradually increase their rate of NP until a stable plateau value. The average NP obtained by the $A_{2A}R\text{-Cre}^{+/-} Grin1^{fl/fl}$ and control mice during appetitive operant conditioning did not differ significantly. Then, a protocol of devaluation was tested to highlight the transition from appetitive character to a goal-directed behavioral habituation. This resulted in a decrease of the instrumental response in the two groups but there was a significantly lower devaluation in $A_{2A}R\text{-Cre}^{+/-} Grin1^{fl/fl}$ than in control mice. In addition, the number of visits to the feeder during the conditioning period was significantly more important for $A_{2A}R\text{-Cre}^{+/-} Grin1^{fl/fl}$ than in control mice supporting again their increased exploratory behavior.

Locomotor sensitization to psychostimulants is widely used in the evaluation of drug reinforcement and drug addiction mechanisms. Drug sensitization is best characterized for the locomotion activation

induced by psychostimulants as cocaine or amphetamine in rodents and consists in an increase in locomotor activity in response to a fixed dose of drug given intermittently (for example daily). We evaluated involvement of NMDA receptor in striatopallidal neurons in these motor responses to psychostimulant by quantifying the presence and intensity of amphetamine-induced locomotor sensitization in $A_{2A}R\text{-Cre}^{+/-} Grin1^{f/f}$ as compared to control mice. Both groups exhibited a similar acute increase in locomotor activity following the first amphetamine injection and demonstrated a locomotor sensitization following repeated amphetamine administration. However, the amplitude of this locomotor sensitization was significantly lower in $A_{2A}R\text{-Cre}^{+/-} Grin1^{f/f}$ than in control mice.

Therefore altogether, these results showed that NMDA receptors in striatopallidal neurons are required for the regulation of motor and attentional behaviour (spontaneous locomotion, reactivity to novelty) and for motivational and reward processes (instrumental learning and conditioning to psychostimulants) (Lambot et al., 2016).

To establish correlation between these behavioural alterations and putative neuroadaptative changes in the striatal microcircuit we have performed an electrophysiological characterization of these neurons. In order to allow the identification of neurons deficient in NR1 in brain slices for patch clamp recordings, $A_{2A}R\text{-Cre}^{+/-} Grin1^{f/f}$ and $A_{2A}R\text{-Cre}^{-/-} Grin1^{f/f}$ mice were further crossed with reporter mice (LoxP-Stop-LoxP-YFP) leading to the expression of *Yellow Fluorescent Protein* (YFP) in recombined neurons.

NMDA currents have been identified in whole-cell configuration in corticostriatal brain slices. A stimulation electrode is placed in the white matter (corpus callosum) separating the striatum from the cortex and permits stimulation of corticostriatal axons and recording of EPSC in targeted striatal neurons. A protocol allowing the extraction NMDA-R of the EPSC has been developed based on the differential kinetics of the NMDA-R- and AMPA-R-mediated components. Recordings in both groups of mice showed that there was a total absence of the NMDA receptor-mediated component of the EPSC in most YFP-positive neurons in $A_{2A}R\text{-Cre}^{+/-} Grin1^{f/f}$ mice with a strong and significant decrease of the averaged NMDA-R component in $A_{2A}R\text{-Cre}^{+/-} Grin1^{f/f}$ as compared to control mice. 3D reconstruction of the recorded neurons of the recorded neurons showed that NR1-deficient striatopallidal neurons displayed a decreased dendritic arborisation and a reduction in spine density. Consistent with these morphological alterations, spontaneous excitatory postsynaptic currents (sEPSCs) amplitudes were decreased demonstrating the dimming of the corticostriatal synaptic transmission. Since the chronic absence of excitatory drive may alter excitability of neurons, we evaluated the intrinsic excitability of these NR1-deficient striatopallidal neurons. These recordings showed that the resting membrane potential is increased, the rheobase is decreased and the excitability is increased as demonstrated in the current/frequency plot as compared to the control cells. Moreover, these neurons are also more prone to accommodation. Altogether, these results showed that the NR1-deficient striatopallidal neurons are hyperexcitable, probably through a mechanism of homeostatic plasticity (Lambot et al., 2016)

4. Gene profiling of striatonigral and striatopallidal neurons and characterization of striatopallidal neuron-specific genes

To gain a more complete picture of the functional diversity of MSN (Ena et al., 2011), we have previously set up protocols to purify MSN subpopulations by FACS-sorting of samples prepared from GFP-striatopallidal ($A_{2A}R\text{-Cre}::Z/EG$) mice retrogradely labelled for striatonigral MSN. We succeed in isolating green (striatopallidal) and red (striatonigral) neurons from individual mice with a very good rate of enrichment and have established gene profiles of these neurons by micro-arrays showing more than 200 striatopallidal neuron specific genes and more than 400 striatonigral neuron specific genes (> 2 fold differential expression) (Ena et al., 2013). This differential gene expression has been validated by using

different techniques for a series of genes. We have previously functionally characterized one of these genes, the ecto-nucleotidase NTe5 selectively expressed in striatopallidal neurons (Ena et al., 2013). We have selected a series of additional genes that are selectively expressed in one MSN subpopulation, that we are characterizing in terms of their functional involvement in the basal ganglia system and its pathologies by using conditional gene inactivation.

One of these genes encodes the β receptor isoform of platelet-derived growth factor, PDGFR β . PDGF is a growth factor whose action is mediated by two receptors with tyrosine kinase activity. In neurons, PDGFR β is the predominant receptor level, and, when activated by PDGF-BB, is responsible for the activation of various intracellular signaling pathways. PDGFR β can also be activated in the absence of its ligand by a transactivation mechanism, resulting from the activation of G protein-coupled receptor such as 5HT1a or D2 receptors. The previous results obtained by microarray have been validated by qPCR and also now by immunofluorescence and showed a preferential expression of PDGFR β in striatopallidal MSN. Given the specific expression of D2R in these neurons, the interaction between PDGFR β and D2-R could therefore also take place.

In order to characterize the functions of this receptor in these neurons, we have used protocols of specific invalidation of PDGFR β in striatopallidal neurons. We are crossing mice bearing a floxed allele of PDGFR β gene (PDGFR $\beta^{f/f}$ mice) and A_{2A}R-Cre mice (Durieux et al., 2009, 2012) or D2R-Cre mice. In parallel, as an alternative, stereotaxic injections of AAV expressing Cre recombinase in the PDGFR $\beta^{f/f}$ mice striatum were also performed. In this latter model, immunofluorescence showed a reduction in the striatal PDGFR β expression, confirming its validity. Behavioral analysis of the resulting mice devoted in PDGFR β in striatopallidal neurons has been carried out to investigate its role locomotor activity, motor learning and procedural learning as well as in motivational processes and drug addiction by using devices and tests available (Durieux et al., 2009, 2012; Ena et al., 2013).

In order to characterize cell signaling pathways initiated by PDGFR β in striatopallidal neurons, we performed primary cultures of wild mice striatal neurons. The PDGFR β activation state (as detected by the phosphorylation T1021 residue) and the activation of a downstream signaling MAP kinase pathway (as detected by p-ERK 1/2) is examined by Western blotting. We have shown that phosphorylation of ERK1/2 induced by PDGF-BB in striatal neurons is dependent on PDGFR β because this effect is suppressed in the presence of TAG1296, an inhibitor of PDGFR β . The effect of the activation of D2R on the activation of PDGFR β and downstream signaling pathways has also been studied by using quinpirole, a specific D2R agonist. We have partially identified the cellular factors involved in the signaling pathway, among which the kinase Src seems to play an important role..

It has been showed in the hippocampus that PDGFR β activation results in inhibition of NMDA receptor-dependent currents. In view of the importance of these receptors in striatopallidal neurons functions (see above), we therefore started to examine the regulatory role of PDGFR β in striatopallidal neurons by using the patch clamp technique. We showed that application of PDGF-BB on striatal slices induced a decrease in NMDA current in striatopallidal neurons in a similar proportion to that observed in the hippocampus and that this effect is specific to striatopallidal neurons.

5. Additional projects and collaborations based on expertise developed under the frame of this program.

- Phosphodiesterase 10A (PDE10A) is located mainly to the striatal medium spiny neurons (MSN) and hydrolyses cAMP and cGMP, key determinants of MSN signaling. We showed that genetic depletion of PDE10A critically mediates attribution of salience to reward-predicting cues, evident in impaired

performance in PDE10A knockout mice in an instrumentally conditioned reinforcement task. We furthermore reported modest impairment of latent inhibition in PDE10A knockout mice, and unaltered prepulse inhibition. We suggested that the lack of effect on PPI is due to the pre-attentional nature of this task. Finally, we performed whole-cell patch clamp recordings and showed changes in intrinsic membrane excitability. A decrease in spontaneous firing in striatal medium spiny neurons was found. These data show that PDE10A plays a pivotal role in striatal signaling and striatum-mediated salience attribution (Piccart et al., 2014).

- Ciliary transport is required for ciliogenesis, signal transduction and trafficking of receptors to the primary cilium. Mutations in inositol polyphosphate 5-phosphatase E (INPP5E) have been associated with ciliary dysfunction, however, its role in regulating ciliary PIPs is unknown. By using conditional inactivation and high resolution confocal microscopy, we have reported that in neural stem cells (NSC), phosphatidylinositol 4-phosphate (PI4P) is found in high levels in cilia while phosphatidylinositol (4,5)-bisphosphate [PI(4,5)P₂] is not detectable. On INPP5E inactivation, PI(4,5)P₂ accumulates at the ciliary tip while PI4P is depleted. This is accompanied by recruitment of the PI(4,5)P₂-interacting protein TULP3 to the ciliary membrane along with Gpr161. This results in an increased production of cAMP and a repression of Shh transcription gene Gli1. Our results have revealed for the first time, the link between ciliary regulation of PIPs by INPP5E and Shh regulation via ciliary trafficking of TULP3/Gpr161, and have provided a mechanistic insight into ciliary alterations found in Joubert and Morn syndromes resulting from INPP5E mutations (Chavez et al., 2015).
- A2AR-D2R heteromers are key modulators of striatal neuronal function. It has been suggested that the psychostimulant effects of caffeine depend on its ability to block an allosteric modulation within the A2AR-D2R heteromer, by which adenosine decreases the affinity and intrinsic efficacy of dopamine at the D2R. We described novel unsuspected allosteric mechanisms within the heteromer, by which not only A2AR agonists but also A2AR antagonists decrease the affinity and intrinsic efficacy of D2R agonists and the affinity of D2R antagonists. Strikingly, these allosteric modulations disappear upon agonist and antagonist co-administration. This can be explained by a model that considers A2AR-D2R heteromers as heterotetramers, constituted by A2AR and D2R homodimers, demonstrated by experiments with bioluminescence resonance energy transfer and bimolecular fluorescence and bioluminescence complementation. As predicted by the model, high concentrations of A2AR antagonists behaved as A2AR agonists and decreased D2R function in the brain (Bonaventura et al., 2015).
- Calcium binding proteins regulate intraneuronal Ca²⁺ homeostasis and hence, supposedly, if present in presynaptic terminals, neurotransmitter release. As expected, absence of the fast Ca²⁺ buffer calbindin (CB) leads to increase in presynaptic action potential-evoked [Ca²⁺]_i transients at the Purkinje cell (PC) recurrent synapses whereas, unexpectedly, IPSC mean amplitudes remained unaltered in connected CB^{-/-} PC. To explain these paradoxical observations, we hypothesized that morphological compensation/adaptation mechanisms might be induced in CB^{-/-} PC axon collaterals including boutons. By using biocytin-filled PC 3D-reconstructions and electron microscopy, we showed larger bouton volume, increased active zone length and a higher number of docked vesicles, in combination with an increase in synaptic cleft width. We propose that these morphological changes likely modify the GABA release properties at this synapse in CB^{-/-} mice and suggested that these changes act as adaptation/homeostatic mechanisms to likely preserve characteristics of synaptic transmission in the absence of the fast Ca²⁺ buffer CB (Orduz et al., 2014).
- The cerebellar pathologies in peroxisomal diseases underscore that these organelles are required for the development and maintenance of the cerebellum, but the mechanisms have not been resolved. We have investigated the origins of the early-onset coordination impairment in a mouse model with

neural selective deficiency of MFP2, the central enzyme of peroxisomal β -oxidation. Although the gross morphology of the cerebellum was normal at the age of 4 weeks, the mice underperformed on the accelerating rotarod and balance beam test. Electrophysiology revealed a reduced Purkinje cell firing rate, a decreased excitability and an increased membrane capacitance. The distribution of climbing and parallel fiber synapses on Purkinje cells was immature and accompanied by increased spine length. Despite normal myelination, Purkinje cell axons degenerated as revealed by numerous swellings. Altogether, these results showed that the electrical activity, axonal integrity and wiring of Purkinje cells are exquisitely dependent on intact peroxisomal β -oxidation in neural cells.

6. Publications

- Bonaventura J, G Navarro, V Casadó-Anguera, K Azdad, W Rea, M Brugarolas, J Mallol, I. Canela, C Lluís, A Cortés, N D. Volkow, S N. Schiffmann, S Ferré and V Casadó. Allosteric mechanisms of caffeine within the adenosine A2A receptor-dopamine D2 receptor heteromer. *Proc Natl Acad Sci U S A*. E3609-E3618, 2015.
- Chavez M, Ena S., Van Sande J., de Kerchove d'Exaerde A., Schurmans S., Schiffmann S.N. Modulation of ciliary phosphoinositide content regulates trafficking and Sonic Hedgehog signaling output. *Dev. Cell*, 34, 338-350, 2015.
- De Munter S, Verheijden S, Vanderstuyft E, Malheiro Ar, Brites P, Gall D, Schiffmann S.N. and Baes M. Early-onset Purkinje cell dysfunction underlies cerebellar ataxia in peroxisomal multifunctional protein-2 deficiency. *Neurobiology of Disease*, 94: 157-168. 2016.
- Lambot L, Chaves Rodriguez E, Houtteman D, Li Y, Schiffmann SN, Gall D and de Kerchove d'Exaerde A. Striatopallidal neuron NMDA-receptors control synaptic connectivity, locomotor and goal-directed behaviours. *36(18):4976–4992*, 2016.
- Piccart E., De Backer J.-F., Gall D., Lambot L., Raes A., Vanhoof G., Schiffmann S.N. and D'hooge R. Genetic deletion of PDE10A selectively impairs incentive salience attribution and decreases medium spiny neuron excitability. *Behavioral Brain Res.*, 268C, 48-54, 2014.
- Orduz D., Booma., Gall D., Brion J.-P., Schiffmann S.N. and Schwaller B., Subcellular structural plasticity caused by the absence of the fast Ca^{2+} buffer calbindin D-28k in recurrent collaterals of cerebellar Purkinje neurons, *Frontiers in Cellular Neuroscience*, Vol. 8, Art 364, 1-14, 2014.
- Wöhr M, D Orduz, P Gregory, H Moreno, U Khan, K J. Vörckel, D P. Wolfer, H Welzl, D Gall, S N Schiffmann and B Schwaller. Lack of parvalbumin in mice leads to behavioral deficits relevant to all human autism core symptoms and related neural morpho-functional abnormalities. *Transl. Psychiatry*, 2015, 5:e525.

7. Additional References

- Bishop D.P., Orduz D., Lambot L., Schiffmann S. N. and Gall D. Control of neuronal excitability by calcium binding proteins: a new mathematical model for striatal fast-spiking interneurons. *Frontiers in Molecular Neuroscience* 5, 78, 1-9, 2012.
- Durieux P.F., Bearzatto B, Guiducci S., Buch T, Waisman A, Zoli, M., Schiffmann S.N. and de Kerchove d'Exaerde A: Striatopallidal neurons inhibit both locomotor and drug reward processes. *Nature Neuroscience*, 12: 393-395, 2009 (Note: S.N. Schiffmann and A. de Kerchove d'Exaerde contributed equally to this study).
- Durieux P.F., S.N. Schiffmann and A. de Kerchove d'Exaerde, Targeting neuronal populations of the striatum, *Frontiers in Neuroanatomy* 5, 40, 1-9, 2011.
- Durieux P.F., S.N. Schiffmann and A. de Kerchove d'Exaerde, Differential regulation of motor control and response to dopaminergic drugs by D1R and D2R neurons in distinct dorsal striatum subregions. *EMBO Journal*, 31, 640–653, 2012
- Ena S., A. de Kerchove d'Exaerde and S.N. Schiffmann, Unravelling the differential functions and regulation of striatal neuron sub-populations in motor control, reward and motivational processes. *Frontiers in Behavioral Neuroscience*, 5, 47, 1-10, 2011.
- Ena S., J.-F. De Backer, S.N. Schiffmann and A. de Kerchove d'Exaerde. FACS-array profiling identifies Ecto-5' nucleotidase as a striatopallidal neuron-specific gene involved in striatal-dependent learning. *Journal of Neuroscience*, 33(20), 8794–8809, 2013.
- Orduz D, Bishop D.P., Schwaller B., Schiffmann S.N., Gall D. Parvalbumin tunes spike-timing and efferent short-term plasticity in striatal fast spiking interneurons. *Journal of Physiology. (Lond.)*, 591, 3215-3232, 2013.



Geneeskundige Stichting Koningin Elisabeth
Fondation Médicale Reine Elisabeth
Königin-Elisabeth-Stiftung für Medizin
Queen Elisabeth Medical Foundation

Final report
of the research group of

Prof. Fadel Tissir, PhD

Université Catholique de Louvain (UCL)

Principal investigator

Prof. Fadel Tissir, PhD, Maître de Recherches FNRS
Institute of Neuroscience, Developmental Neurobiology group
Université Catholique de Louvain
Avenue E. Mounier 73, Box B1.73.16
B1200 Bruxelles
T +32 2 764 73 84
F +32 2 764 74 85
Fadel.Tissir@uclouvain.be

Shaping the nervous system: Role of the planar cell polarity genes

Summary (1 page):

Celsr (Cadherin, EGF-like, Laminin G-like, Seven-pass, G-type Receptor) are developmentally regulated proteins with the ability to signal by homophilic and/or heterophilic interactions. Functional studies have demonstrated a key role for Celsrs in the planar cell polarity (PCP) pathway. PCP is complementary to the intrinsic polarization of single cells and refers to the global coordination of cell behaviour in the plane of a tissue. Most evident in cell sheets and confined to studies in *Drosophila* for years, PCP has emerged during the last decade as an important pathway in vertebrates, where it regulates various developmental processes and is associated with multiple disorders. When we started our studies on Celsr genes in early 2000s, two members (*Celsr1* and *Celsr2*) were listed in databases, but little if any was known about their functions. We identified the third member (*Celsr3*), explored the expression patterns of the three genes and inactivated them in mice. Our analyses show that they are widely expressed in the nervous system where they act as sorting factors for assembly of PCP protein complexes and play crucial roles in neural tube closure, neuronal migration, ependymal polarity, and axon guidance (reviewed in (Tissir and Goffinet, 2010; Boutin et al., 2012; Tissir and Goffinet, 2013)).

During the last 3 years, we have progressed on our understanding of the mechanisms of action of PCP genes in the wiring of the nervous system (paragraph 1), and in cilia polarity (paragraph 2). On the other hand, we have identified novel functions for PCP genes in cortical histogenesis (paragraph 3; points 3.1–3.4). 13 peer-reviewed articles have been published in the framework of the project (Annex 1).

1. Wiring of the nervous system

Since our initial report (Tissir et al., 2005), we and others have accumulated evidence that PCP proteins Celsr3 and Fzd3 are major players in the directional growth of axons and wiring of the central nervous system (Price et al., 2006; Zhou et al., 2007; Zhou et al., 2008b; Zhou et al., 2008a; Zhou et al., 2009a; Zhou et al., 2009b; Fenstermaker et al., 2010; Zhou et al., 2010; Lewis et al., 2011; Feng et al., 2012; Onishi et al., 2013). However, whether these proteins act in collaboration with, or in parallel to, other axon guidance systems such as Eph/ephrins, Slit/Robo, Semaphorins/Plexins was not known; and whether it is involved in the wiring of the peripheral and enteric nervous systems was not investigated.

During the last 3 years, we analyzed the contribution of Celsr2, Celsr3, Fzd3, and Vangl1, Vangl2 to axonal development in the forebrain, by focusing on the anterior commissure (AC), the corticospinal tract (CST), and the internal capsule (IC). The AC contains commissural axons from the anterior olfactory nuclei and from the temporal cortex, which cross the midline at embryonic day (E)13.5. The IC contains three main axonal components. Thalamocortical axons (TCA) emerge from the thalamus, formerly called “dorsal” thalamus at E12.5. They run through the prethalamus (former “ventral” thalamus), turn and cross the diencephalon-telencephalon junction, progress through a corridor-like structure in the ventral telencephalon, and cross the pallial-subpallial boundary to reach the cortical anlage from E14.5. Corticothalamic axons (CTA) emerge initially from neurons in the subplate and future cortical layer 6, around E13.5. They cross the pallial-subpallial boundary and progress in the ventral telencephalon, in opposite direction to TCA. They cross the diencephalon-telencephalon boundary and enter the thalamus at E14.5. Subcerebral (cortico-subcortical) projections such as the CST begin to leave the cortical plate at E14.5-E15.5 to enter the IC, and diverge from CTA to form the cerebral peduncle, en route to their subcortical targets such as the spinal cord. We showed that Celsr3 is required for the development of the AC, IC, and CST, and Cre-mediated regional inactivation indicated that Celsr3 is required in guidepost cells along the pathway. The Celsr3 axonal phenotype is similar to that of Fzd3 mutant mice, hinting that a PCP-like mechanism may regulate axon progression via interactions between growth cones and guidepost cells. To understand further the role of membrane-associated core PCP proteins in axon guidance, we used a panel of mutant mice and show genetically that Celsr2 and 3 regulate the formation of forebrain axon bundles in a redundant manner, and are required in the same cell populations as Fzd3. Unlike epithelial PCP, however, the action of Celsr2-3 and Fzd3 on forebrain axonal fascicles is Vangl1,2-independent. Inactivation of Celsr2-3 or Fzd3 in thalamus generates no evident phenotype, showing that the derailed TCA phenotype in constitutive mutants is non-cell autonomous. Furthermore, we showed that the joint inactivation of Celsr2-3 or Fzd3 in thalamus and cortex perturbs the development of cortical sensory maps. This work was published in *Proc Natl Acad Sci U S A* (Qu et al., 2014).

We also explored the function of PCP in striatal connectivity and found that, PCP genes are required *in vivo* for extension of medium spiny neurons. PCP proteins non-cell-autonomously regulate the entry of MSN axons into an important intermediate target, the globus pallidus (GP), and the positioning of “corridor” cells. These cells are guidepost cells for thalamocortical axons located in between the pallidum and the medial ganglionic eminence. We showed that corridor cells repel MSN axons and that their mislocalization in the GP of PCP mutant mice render the GP non-permissive for MSN axon growth. Conclusively, these data reveal previously uncharacterized aspects of striatal pathway development and identify cell autonomous and non-cell-autonomous roles for PCP in MSN axon guidance. This work was published in *The Journal of Neuroscience* (Morello et al., 2015).

To appreciate the role of PCP genes in the peripheral nervous system, we investigated the impact of their loss-of-function on hindlimb innervation. We found that mice with conditional inactivation of Celsr3 in motor neurons (Isl1 and or Olig2 positive cells) exhibit uni- or bilateral paralysis of the hindlimb.

Muscles of the anterior compartment, particularly the tibialis anterior, are atrophic, pointing to a defect of peripheral motor innervation that was confirmed by electrophysiology. Further studies showed that *Celsr3* mutants have a selective deficit of innervation of extensor muscles innervated by the dorsal, peroneal nerve, whereas axons of tibial nerve (that innervate ventral muscles) are unaffected. *Fzd3* mutants have an identical phenotype. *EphA4* mutant mice as well as mice with inactivation of the GDNF receptor components *Ret* and *GFRa1* have a similar phenotype, namely absence of dorsal peroneal nerve, with rerouting of axons ventrally, hinting at possible interactions between *Celsr3/Fzd3* and those two important signals. Detailed phenotype analysis showed that, in *Celsr3* mutant mice, axons of the peroneal nerve segregate from those of the tibial nerve, but fail to extend dorsally and stall near the superficial versus deep peroneal nerve branching point. Those axons are not rerouted ventrally; thus, the phenotype is not identical to that in *EphA4* and *GDNF* mutant animals. *Celsr3* mutant axons respond to the repulsive signal generated by ephrinsA5 expressed in the ventral limb mesenchyme acting on *EphA4* in motor neurons. They are also able to elicit the attractive signal of GDNF. By contrast, *Celsr3* and *Fzd3* mutant motor neurons, contrary to wild-type axons, are not attracted by *EphA-Fc* in the Dunn chamber assay. This clearly shows that *Celsr3* and *Fzd3*-deficient axons are no longer able to respond to the reverse ephrin signaling triggered by *EphA* expressed in dorsal limb mesenchyme acting on ephrin A receptors in growth cones. Using *EphA4* mutant mice, we showed that *Celsr3* interacts genetically with *EphA4*. We also demonstrated that *Celsr3* associates physically with ephrinA2 and A5 in transfected cells, and co-immunoprecipitates with *Fzd3* (as predicted from phenotypic analyses), as well as with *Ret* and *GFRa1*. Intriguingly, the peripheral axonal phenotype was not seen in mice with inactivation of the core planar polarity gene *Vangl2*, and no physical interaction between *vangl2* and *Celsr3* was detected, indicating that *Celsr3* and *Fzd3* regulate axon guidance in a *Vangl2* independent manner. Our results provide strong evidence that *Celsr3/Fzd3* interact with *EphA:ephrinA* reverse signaling to guide motor axons in the hindlimb. This work was published in *Nature Neuroscience* and in the *The International Journal of Biochemistry & Cell Biology* (Chai et al., 2014; Chai et al., 2015).

2. Polarity of ciliated cells

A fascinating peculiarity of ependymal (multiciliated) cells is their capability to coordinate ciliary beats within and between cells. At the cellular level, all cilia from a given cell need to beat in the same direction. Therefore, their basal feet (lateral extensions of basal bodies (BB) that point in the direction of the effective stroke of cilia beat) rotate during development and adopt a homogeneous orientation (rotational polarity). At the tissue level: all ependymal cells display a shift of BB to the anterior side of the cell (translational polarity). This specific organization of the lateral wall is essential for cerebrospinal fluid (CSF) circulation and its modification is thought to affect stem cell maintenance and adult neurogenesis. We were the first to show/propose that mutation in *Celsr* proteins, and PCP signaling as whole, impairs ciliogenesis and leads to defective CSF flow and lethal hydrocephalus. PCP-deficient ependymal cilia never develop in normal numbers and display abnormalities in morphology, position, and planar organization. Ciliary basal feet are mis-oriented, and basal bodies were seen ectopically deep in the cytoplasm. The conventional method to analyze rotational polarity is to investigate the orientation of the basal foot by transmission electron microscopy. This method is time consuming. To speed up studies of LW in our mutants, we developed an alternative approach wherein we combined immunostaining and confocal microscopy. Gamma tubulin and phospho-beta-catenin localize at opposite sides of the BB and define a vector which nicely delineates rotational polarity of cilia. Using this method, we expanded on our initial finding and show that *Celsr2* and *Celsr3*, together with *Fzd3* and *Vangl2*, control not only the orientation of motile cilia but also their spacing and their lattice organization in individual cells. To investigate the potential role of *Celsrs* in translational polarity, we performed immunostaining on LW whole-mounts. We used antibodies against ZO1 and gamma tubulin which label tight junctions and basal bodies respectively. We analyzed the position of BB patch relative to the center of the cell. In WT

and PCP mutants, ependymal cells showed a displacement of cilia. However, while in WT animals, all ciliary tufts are systematically shifted toward the anterior pole, *Celsr1* mutant mice display abnormal translational polarity with cilia dispersed in any pole of ependymal cells. It has been suggested that the primary cilium of radial glial (RG) cells control the translational polarity of multicilia. We analyzed the presence of primary cilium in our mutants. Immunostaining against either gamma tubulin or acetylated tubulin demonstrated that virtually all RG cells bear a primary cilium at birth suggesting that the translational polarity defects observed in *Celsr1* are not due to lack of the primary cilium. We then carried-out a time course analysis and found that the primary cilium is progressively polarized to the anterior side of the cell in normal animals, anticipating ependymal cell translational polarity. In *Celsr1* mutant mice, the primary (mono) cilium migrates away of the center of the RG cells but not systematically toward the anterior side. The same phenotype is observed in mice mutant for *Fzd3*, and *Vangl2*. Interestingly RG polarity is not affected in *Celsr2* or *Celsr3* mutants. Our results show that *Celsr1*, *Fzd3* and *Vangl2* position the primary cilium in radial progenitors. In ependymal cells, whereas *Celsr2&3*, *Fzd3* and *Vangl2* work together to organize cilia tufts in a given cell; *Celsr1*, *Fzd3* and *Vangl2* coordinate polarity between cells. These signals are relayed by distinct cytoskeletal changes. These data reveal unreported functions of Celsr genes and PCP signaling and provide an integrated view as how polarity is set in radial progenitors and passed on to ependymal. This work was published in *Proc Natl Acad Sci USA* (Boutin et al., 2014). Interestingly enough, a recent, multicenter, study on a large patient cohort of 371 affected individuals from 265 families with the ciliopathy spectrum, identifies causal mutation in CELSR2 thus supporting our data and reinforcing their relevance for human disorders such as Bardet-Biedl, Joubert, and Meckel-Gruber syndromes (Shaheen et al., 2016).

Lastly, with two Japanese groups, we analyzed the roles of *Celsr1* in the development of the mouse oviduct ciliated cells. We found that as in the ependyma, *Celsr1* is essential to the homogenous cilia beating, proper cellular shape and arrangement, and the orderly patterned alignment of epithelial folds along the longitudinal axis of the oviduct. This work published in *Development* (Shi et al., 2014).

3. Novel functions for PCP genes in cortical histogenesis

During cortical development, apical progenitor cells (AP) undergo divisions that are initially symmetrical and increase the pool of progenitors. At the onset of neurogenesis (neurogenic switch), some divisions become asymmetric and generate, in addition to AP, either neurons or intermediate/basal progenitors (BP) which have limited self-renewal capacity and are committed to an excitatory glutamatergic neuron fate. In dorsal telencephalon, neural progenitor cells (NPC, including AP and BP) generate sequentially deep layer (DL, mostly layers 5 and 6) and upper layer (UL, mostly layers 2, 3 and 4) neurons, followed by glial cells (gliogenic switch). Given the huge expansion of the cerebral cortex during evolution and the close link between cortical development and neurological disorders, a hot topic in the field is how those processes (i.e. type of division of progenitors, neurogenic switch, and gliogenic switch) are orchestrated at the molecular and cellular level.

3.1. Role of *Celsr1* in the neurogenic switch

Celsr1 is exclusively expressed by NPC but its function in these cells is unknown. We examined the distribution of *Celsr1* protein in the mouse neocortex and found that it was confined to the apical side of AP until embryonic day (e) 10.5. At the onset of neurogenesis (from e12.5 onwards), *Celsr1* accumulated progressively in basal processes and endfeet of AP. *Celsr1* being an adhesion protein, we investigated the attachment of AP processes to the pia in *Celsr1*^{-/-} mice. AP were radially oriented and their endfeet were in close proximity with the basal lamina. We did not observe any breakdown in the latter or neuronal heterotopia that would suggest an abnormal contact between endfeet and the pial surface. We examined the morphology of APs upon *Gfp* electroporation and found that the number

of basal processes was dramatically reduced in *Celsr1*^{-/-} mice. Given the morphological change of AP in *Celsr1*^{-/-} mice, we asked to what extent this modification could modify neurogenesis. We used a tamoxifen inducible system to label AP and trace their progeny. Compared to controls, mutant AP generated more cells in the ventricular zone (VZ) and less in the SVZ or intermediate zone, suggesting a defect of neurogenesis in *Celsr1*^{-/-} mice. To assess the effect of *Celsr1* loss-of-function on fate decision, we injected mice carrying a floxed allele (*Celsr1*^f) with low concentration of Tamoxifen at e10.5, with the aim to inactivate *Celsr1* in isolated AP and enable a clonal analysis at e14.5. *Enface* view scrutiny of VZ detected larger clones in *Celsr1* conditional mutant embryos, confirming that *Celsr1*^{-/-} AP are more prone to symmetric, proliferative division. We measured the length of the VZ and found that it was increased from e12.5 onwards in mutant versus control samples. At e16.5, the higher expansion of mutant AP led to local bending of the VZ with an increased number of Pax6-positive AP. The number of Tbr2-positive BP was concomitantly reduced, first in the lateral pallium at e12.5, and later in the dorsal pallium at e14.5. This bias in BP and thus in neuron production led to microcephaly with a reduction of cortical upper layers at postnatal stages.

We then inactivated *Celsr1* in all neocortical areas and analyzed the impact loss-of-function of *Celsr1* on behavior. Cortex-specific conditional mice (*Celsr1*^{fl/fl}; *Emx1-Cre*) were all hyperactive and spent more time than controls (*Celsr1*^{+/+}; *Emx1-Cre*) in open areas in elevated plus maze and open field. In addition, females had a social interaction defect in the “three chamber test”. Similar defects are found in rodent models of Autism Spectrum Disorder (ASD). Surprisingly, further to the abnormal behavior observed in the open field and the elevated plus maze, conditional knockout males had learning deficit in the water maze test. This phenotypic defects correlate with Attention-Deficit Hyperactivity Disorder (ADHD) in rodents; a trait with documented comorbidity with ASD. These results suggest that the loss of *Celsr1* and subsequent reduction in the number of endfeet promote proliferative division of AP at the expense of neurogenic divisions in the developing neocortex, decreases the number of upper layer neurons, and ultimately perturb cognitive abilities functions.

Endfeet of APs abut meninges which regulate brain development through secreted molecules. For instance, retinoic acid (RA) derived from meninges triggers the switch from proliferative to neurogenic divisions at the onset of neurogenesis. Of note, meningeal cells that produce RA appear progressively around the telencephalon in a lateral to dorsal gradient between e12.5 and e14.5, which correlates with the defect in BP production seen in *Celsr1*^{-/-} cortex. In addition, Crabp2, a cytosol-to-nuclear shuttling protein facilitating the binding of RA to its cognate nuclear receptors, accumulates in AP endfeet and could improve RA uptake and its relocation to the nucleus. To test whether RA is indeed involved in the defective neurogenesis observed in mutant mice, we exposed *Celsr1*^{-/-} embryos to RA supplementation *in utero* between e11.5 and e14.5. This treatment restored the number of Tbr2-positive BP and the length of the VZ at e14.5, confirming the causal link between RA and *Celsr1* mutant phenotype. To identify partners of *Celsr1* in cell fate determination, we used a gene candidate approach. As *Celsr1* mutants display some ASD features, we used the Simons Foundation Autism Research Initiative (SFARI) database together with the gene expression database genepaint (www.genepaint.org). Of 648 genes listed in SFARI, 63 were involved in both ASD and ADHD. 33 of them were expressed in the frontal cortex at e14.5, and 11 were detected in the VZ. Among those genes, *Ankrd11*, *Auts2*, *Mecp2*, and *Zbtb20* were regulated by RA in AP cultures *in vitro*. We selected *Auts2* for further investigations because this gene has been invariably associated with microcephaly in humans, whereas mutations in *Ankrd11*, *Mecp2* and *Zbtb20* can also lead to macrocephaly. Real time qRT-PCR experiments indicated that *Auts2* was downregulated in *Celsr1*-deficient mice and rescued by *in utero* supplementation of RA. Immunofluorescence analysis confirmed that, in addition to its documented expression in the cortical plate, *Auts2* was expressed by neurogenic AP. Finally, *in utero* electroporation of *Auts2* in *Celsr1*^{-/-} embryos at e14.5, when neurogenesis defect is detectable in the entire telencephalon, was sufficient to counteract the lack of *Celsr1* and to restore neurogenesis to normal levels. To investigate further

the function of *Auts2* in AP fate decision and cortical development, we overexpressed it in cultures of AP isolated from e14.5 cortex. Increasing *Auts2* levels *in vitro* increased the differentiation of AP in proliferative conditions as indicated by the lower number of Sox2-positive cells in *Auts2-Gfp* transfected AP compared to *Gfp* transfected AP. It also accelerated the appearance of Tuj1-positive neurons in differentiation conditions. Given that *in vitro*, *Auts2* increases differentiation of AP, we investigated its effect when overexpressed in the developing neocortex. To this end, we electroporated *Auts2* cDNA *in utero* at e14.5. This increased the delamination of AP from the VZ at e15.5, confirming the role of *Auts2* in AP differentiation. The number of basal mitoses (in the SVZ) was increased suggesting that *Auts2* promotes the differentiation and proliferation of BPs. In line with this, the number of Tbr2-positive cells deriving from electroporated AP increased, whereas that of Pax6-positive cells in and above the SVZ (i.e. basal radial glia) was not affected. As a consequence, the SVZ was enlarged. Considering that increased number of BP could be involved in expansion and gyrification of the brain, we overexpressed *Auts2* in e14.5 cortices and analyzed them at e17.5 and P1. The higher production of BP and the sustained enlargement of the SVZ improved the production of neurons and led to a marked thickening of upper layers and folding of the neocortex at P1.

Collectively, our results show that *Celsr1* sculpts the basal processes of AP and mediate their communication with meninges. *Celsr1*-depleted AP have fewer basal processes and endfeet, reduced expression of *Aust2*, a transcriptional activator involved in neurological diseases such as ASD (autism spectrum disorder), and produce less BP and neurons. Finally, the forced expression of *Auts2* in the cerebral cortex of wild type embryos enlarges dramatically the SVZ, enhances the production of neurons, and induces the folding of the murine cortex. A part of this work has been drafted in a manuscript which is currently under revision in *Molecular Psychiatry*

3.2. Role of *Celsr3*/*Fzd3* in the gliogenic switch

Previous *in situ* hybridization studies showed that *Celsr3* is specifically expressed in postmitotic neurons and BP but not in NPC, whereas *Fzd3* is widely expressed in both NPC and neurons. We have examined PCP mutant brains at a late embryonic stage (e18.5), using layer-specific markers Tbr1 (layer 6), Ctip2 (layers 5–6) and Satb2 and Cux1 (layers 2–4). Compared with control samples, the number of Ctip2⁺ and Satb2⁺ cells was increased in *Celsr3* and *Fzd3* mutant cortices, with increased thickness of the cortical plate. This was confirmed in Tbr1 and Cux1-stained preparations. Of note, despite increased cortical neuron numbers, the border between Satb2 and Ctip2-positive layers was sharply defined in mutant cortex, indicating that radial migration and lamination were unaffected. The similar cortical defects in *Celsr3* and *Fzd3* mutants are therefore probably due to inactivation of *Fzd3* in immature cortical neurons or basal progenitors (BP), rather than in apical progenitors (AP). To ascertain this, we produced conditional *Fzd3*^{f/f}; *Nex-Cre* mutant animals (*Fzd3*^{Nex-ckO}), in which *Fzd3* is specifically inactivated upon expression of *Nex-Cre* in cortical excitatory neurons. In *Fzd3*^{Nex-ckO} animals, increased production of DL and UL cortical neurons was observed, like in *Celsr3*^{-/-} and *Fzd3*^{-/-} mutant embryos. To estimate the number of AP in mutant and control samples, we used the AP marker Pax6 and found a significant decrease of the number of Pax6⁺ cells in *Celsr3*^{-/-}, *Fzd3*^{-/-}, and *Fzd3*^{Nex-ckO} mutant versus control samples. As cortical neurons derive from both AP and BP, we wondered whether the number of BP, which express *Celsr3* at lower levels than neurons, was also affected. Using IHC with the BP marker Tbr2, we found that the number of BP was moderately decreased in *Celsr3*^{-/-}, *Fzd3*^{-/-} and *Fzd3*^{Nex-ckO} mutants versus control cortex. These observations of an excess of both DL and UL cortical neuron numbers, with depletion of NPC numbers suggest a defective feedback regulation from neurons.

To determine when the phenotype was first observed, we looked at earlier time points and found that the relative increase was first noticed at e15.5 and maintained at later stages. To define further the increased production of DL neurons in mutants, BrdU was injected at e13.5, and cells with strong nuclear BrdU labeling were counted. The proportions of BrdU⁺ cells expressing Tbr1 or Satb2 over the total number

of BrdU⁺ cells was determined. The results showed that in *Celsr3* and *Fzd3* mutant cortex, the ratio of BrdU⁺ Tbr1⁺ to all BrdU⁺ cells was increased, whereas the proportion of BrdU⁺ cells that expressed the UL marker *Satb2* was decreased in both *Celsr3* and *Fzd3* mutant samples. Several mechanisms could account for the observed increase of neuron number. It has been proposed that thalamocortical afferents influence neurogenesis in some context. To test a potential role of thalamic fibers, we examined *Celsr3^{Dlx-cko}* mice in which these fibers do not develop and confirmed that the numbers of DL and UL neurons were similar to controls, arguing against a role of thalamic fibers in the phenotype. Another possibility could be differential cell death in mutant and control brains. To assess whether apoptosis was involved in the cortex of *Celsr3* and *Fzd3* mutants, we used immunohistochemistry (IHC) with activated Caspase-3 (aCas3), and found very few aCas3 positive cells, with no difference between control, *Celsr3* and *Fzd3* mutant samples at e14.5 and e16.5. A third possibility for increased neuron numbers could be premature NPC cycle exit and/or changes in cell cycle length. To estimate NPC cell cycle exit, we used BrdU and Ki67 double IHC to estimate cell cycle exit rates. We found no differences between control and mutant samples injected with BrdU at e12.5 and examined at e13.5. By contrast, in samples injected at e13.5 and studied at e14.5, and in those injected at e14.5 and processed at e15.5, the cell cycle exit rate was significantly increased in *Celsr3* and *Fzd3* mutants as compared to controls. To compare cell cycle length, we injected BrdU followed by EdU after 1.5 hour, and estimated S phase and cell cycle length by BrdU and EdU double staining (30 min after EdU injection). No differences were found between control, *Celsr3* and *Fzd3* mutant cortex.

In the mouse neocortex, at e16.5-E17.5 the generation of neurons declines and that of glial cells begins. We considered the possibility that the observed increase of cortical neurons may coincide with a delayed or decreased generation of glial cells. Cortical astrocytes and oligodendrocytes are derived from Olig2⁺ glial precursor cells. We compared Olig2 expression in control and mutants and found that Olig2⁺ cells were more abundant in control than in *Celsr3* and *Fzd3* mutants at e17.5 and at birth. This indicates that neurons are generated at the expense of glial cells. To confirm this, we used GFAP IHC at postnatal days (P) 0 and P2. The intensity of GFAP staining was strongly decreased in mutant cortices, as was the concentration of GFAP, estimated using western blotting. To assess further the relative production of neurons and glia, we used triple IHC for BrdU, *Satb2* to label late-generated neurons, and Olig2 to label glial precursors. We found that the ratio between glial cells and neurons decreased in *Celsr3*, *Fzd3* and *Fzd3^{Nex-cko}* mutant versus control samples. These data suggest that the neurogenesis may be prolonged or increased, and gliogenesis delayed or defective in mutant animals. To understand the underlying mechanisms, we used western blotting with antibodies to phosphorylated Stat3, a readout of Jak-Stat signaling, phosphorylated Erk1 and 2, and phosphorylated Smads, an index of Bmp signaling. No difference was found between control, *Celsr3* or *Fzd3* mutants, suggesting that those signaling pathways are unaffected by inactivation of *Celsr3* or *Fzd3* in cortical neurons. We next focused on Notch signaling, a master regulator of neurogenesis and gliogenesis. We tested Notch activation at different embryonic stages, from e14.5 to e18.5, by IHC and western blotting with an antibody against the N-terminal epitope of the Notch1 intracellular domain (actN1) generated upon cleavage by the gamma secretase complex. IHC at e14.5 and e16.5 disclosed specific actN1 immunoreactivity in AP but no specific signal in postmitotic neurons. The signal was consistently and strongly decreased in *Celsr3* mutant compared to control cortex. Western blot analysis at E18.5 confirmed the downregulation of actN1 signal in *Celsr3* and *Fzd3* mutant versus control samples. Importantly, *Notch1* mRNA levels, estimated by qRT-PCR, remained unchanged, indicating that the modification of actN1 signals did not reflect decreased *Notch1* gene expression. In addition, transcripts of the Notch downstream effectors *Hes1*, implicated in neurogenesis, and *NFIA*, implicated in gliogenesis, were downregulated in both *Celsr3* and *Fzd3* mutant embryonic cortex, providing another independent evidence that Notch signaling is altered in PCP mutants.

What mechanisms could account for decreased Notch1 activation in *Celsr3* and *Fzd3* mutants? To assess the role of Notch ligands, we used an RNA-Sequencing to compare transcriptional profiles in control, *Celsr3* and *Fzd3* mutant cortical samples at e16.5. Among Notch ligands, *Dll1* mRNA was strongly expressed in all samples, whereas *Dll3*, *Dll4*, *Jag1* and *Jag2* were moderately represented. *Jag1* was the sole mRNA significantly downregulated in both *Fzd3* and *Celsr3* mutant samples. It was therefore a key candidate selected for further studies. *Jag1* mRNA expression was widespread, detected in VZ/SVZ as well as in postmitotic CP neurons, and was sharply downregulated at e14.5, e16.5 and E18.5 in *Celsr3*^{-/-} mutant compared to control cortical samples. Using triple IHC with antibodies to Jag1, the neuronal marker Ctip2 and the BP marker Tbr2, Jag1 protein was clearly detected in immature neurons in the IZ and deep CP, with little colocalization with BP. Importantly, Jag1 immunoreactivity in the IZ and deep CP was specifically downregulated in *Celsr3*^{-/-} mutant samples. Jag1 immunoreactivity in the IZ and deep CP was also reduced in *Fzd3*^{-/-} mutant compared to control tissue. If decreased Jag1 expression is implicated in diminished Notch activation and gliogenesis, its overexpression should rescue the phenotype. To test this, we electroporated a plasmid encoding Jag1 under the Cdk5r promoter that drives expression in neurons but not AP. Electroporation was carried out at e13.5, and samples were collected at e18.5 and stained with anti-Jag1 to verify overexpression, anti actN1 to check Notch activation, and anti-Olig2 and antiSatb2 to assess the gliogenesis switch. When Olig2 and Satb2 expression in the electroporated area were compared with that in the contralateral side, a significant increase in the density of Olig2 positive cells, together with a decreases in the density of Satb2 positive neurons and in the actN1 signal in VZ, were seen. We then asked whether Wnt proteins, which bind to Fzd receptors and are known to modify Jag1 expression, could be involved in Jag1 downregulation in *Celsr3* and *Fzd3* mutants. Our RNA-Seq results showed that Wnt7b and Wnt7a are by far the most abundant Wnt factors in the embryonic cortex, followed by Wnt5a, whereas other Wnt factors are expressed at very low, mostly undetectable levels. We tested the putative role of Wnt7 using primary cultures of cortical neurons from E14.5 control, *Fzd3* and *Celsr3* mutant embryos. After one day *in vitro*, neurons were placed in serum-free medium for 6 hours, exposed to Wnt factors for 5 hours, and expression of selected mRNA was assessed by qRT-PCR. Wnt7a is known to have mixed, non-canonical and canonical activities, depending on context. To differentiate between those two activities, we compared the effect of Wnt7a and Wnt3a, a canonical ligand. We measured expression of *Axin2*, a beta-catenin downstream target, and *Jag1*. As predicted, *Axin2* mRNA expression was upregulated upon addition of Wnt3a in both control and *Fzd3* mutant neurons, and remained unaffected upon addition of Wnt7a, indicating that the latter activated preferentially non canonical signaling in embryonic cortical neurons. Remarkably, upon Wnt7a treatment, *Jag1* expression was increased in control but not in *Fzd3* or *Celsr3* mutant neurons, whereas addition of Wnt3a induced *Jag1* expression similarly in control and *Fzd3* mutant neurons. To confirm that this effect of Wnt7a occurred via non canonical Wnt signaling with JNK as a downstream effector, we used the JNK inhibitor SP600125. Addition of SP600125 to cultured neurons counteracted the effect of Wnt7a, and prevented *Jag1* upregulation.

Altogether, these results identify a novel and previously uncharacterized feedback mechanism that regulates the shift from neurogenic to gliogenic fate of NPCs. Expression of *Celsr3* and *Fzd3* in immature cortical neurons and possibly BP cells allows AP to respond to a JNK-dependent, non-canonical Wnt signaling, presumably generated by Wnt7a and Wnt7b. Wnt7a and Wnt7b are both expressed in the embryonic cortex, with peaks of expression in VZ for Wnt7a, and in intermediate zone and cortical plate for Wnt7b. The Wnt7/*Celsr3*/*Fzd3* signal fosters expression of Jag1 in immature neurons, which activates Notch in AP and orchestrates their sequential production of deep and upper layer cortical neurons, followed by glia. This work was published in *Nature Communications* (Wang et al., 2016).

3.3. Role of the formin Diaphanous 3 in neural stem cells

Using a candidate gene approach and expression profiling, we identified five formins as potential regulators of neural stem cell division downstream of the Wnt/planar polarity signaling. Among these,

Diaphanous (Diaph) 3 is highly and specifically expressed by neural stem cells in telencephalon. To better understand the function of Diaph3 in neural stem cells, we generated and analyzed a mouse line carrying a mutation in the *Diaph3* gene. In the knockout mice, cortical progenitor cells undergo apoptosis as early as E10.5. Using flow cytometry analysis, we found a sevenfold increase in the proportion of aneuploid cells in the mutant telencephalon. These cells die therefore depleting progressively the population of progenitors and leading to cortical hypoplasia, as indicated by the marked reduction in all cortical cell types in *Diaph3* ko embryos. Aneuploidy could eventually give rise to neoplastic transformation. Remarkably, mutations in the human *DIAPH3* gene are frequently found in metastatic cancers, and down regulation of *DIAPH3* increases metastatic invasion in xenotransplanted mice (Hager et al., 2012; Morley et al., 2015). The nuclear asymmetric division we reported could increase chromosomal instability, promoting the emergence of new mutations and facilitating the development of tumors and/or acquisition of metastatic properties.

Investigating the molecular mechanisms of action of Diaph3, we found that Diaph3 co-immunoprecipitates with the mitotic spindle protein BubR1 and its mutation reduces by half the overall level of BubR1. Hence, the lack of Diaph3 weakens the spindle checkpoint and behaves as a BubR1 hypomorphic (h) allele. In support of this, the phenotype of *Diaph3* ko phenocopies that of *BubR1^h* mice in which mitotic slippage, formation of micronuclei, premature chromatid separation, aneuploidy, and decreased number of mitotic cells were described (Baker et al., 2004; Dai et al., 2004). A link between BUBR1 and chromatid separation was also reported in patients with mosaic variegated aneuploidy, a rare disease associated with intrauterine growth retardation, aneuploidy, microcephaly, and hydrocephalus (Matsuura et al., 2006; Miyamoto et al., 2011), further supporting the Diaph3-BubR1-nuclear division axis. In addition to the cortical phenotype, *Diaph3* mutant embryos display growth retardation, twisting neural tube, facial deformities, and increased number and size of brain blood vessels. More than 97% of mutants die before E12.5. The very few animals that survive until young adulthood exhibit smaller brain, hydrocephalus, and growth retardation. These features are common findings in mouse models of microcephaly (Murga et al., 2009; Chen et al., 2014), and in patients with type II Microcephalic Osteodysplastic Primordial Dwarfism (MOPD-II)(Hall et al., 2004), whose life is imperiled by modifications of cerebral blood vessels often resulting in stroke or aneurysm.

These results provide evidence that Diaph3 protects neural stem cells against mitotic error induced apoptosis, by preserving the activity of the spindle checkpoint. Loss of Diaph3 function does not trigger nuclear division errors in the strict sense. Such events occur physiologically, especially in fast dividing cells like mammalian cortical progenitor cells. Rather, the lack of Diaph3 loosens the spindle checkpoint enabling a fraction of aberrantly dividing cells, which normally halt in metaphase until nuclear segregation is properly completed, to “slip” into anaphase, causing aneuploidy and /or mitotic catastrophe. We believe that this work uncovers an unanticipated link between the rate of proliferation of neural stem cells and the risk of aneuploidy and may prove valuable to understand the development cortical tumors such as glioblastoma. It has just been published in *Nature Communications* (Damiani et al., 2016).

3.4. Cajal-Retzius cells and patterning of the neocortex

Cajal-Retzius cells (CRc), the earliest born neurons in the cortex, are the major source of the extracellular matrix protein reelin, which is critically involved in lamination of the cerebral cortex. To understand better their role in the developing and mature brain, and unravel their origin and fate, we used the endogenous promoter of the transcription factor p73, the most specific marker of CRc, to knock-in the recombinase Cre, and showed that CRs originate at least from three distinct sites: The septum, ventral pallium/pallial-subpallial boundary (PSB), and hem (Tissir et al., 2009). This knock-in line proved extremely valuable as it allows cell lineage tracing, fate mapping and genetic manipulation, and live imaging of these. Hence, it has been distributed to colleagues and laboratories worldwide and used during the last three years, in collaborative works, to show that: a) the migration and distribution of CRs controls the size of higher-

order areas in the somatosensory, auditory, and visual cortex, and that subtype-specific differences in the onset, speed, and directionality of CR migration determine their differential invasion of the developing cortical surface (Barber et al., 2015); b) the Lot cells that were believed to originate in the dorsal pallium are specifically generated in the lateral thalamic eminence, and give rise to mitral cells of the accessory olfactory bulb and CR cells that invade the piriform cortex (Ruiz-Reig et al., 2016); c) CRs migrate into the neocortex after they have acted as axonal guidepost cells in the olfactory system, and their density severely affects the architecture of cortical layer 1, a key site of input integration for neocortical networks (de Frutos et al., 2016); and d) CRs subtypes display unique distributions and dynamics of cell death in the postnatal mouse cortex (Ledonne et al., 2016).

4. References

- Baker DJ, Jeganathan KB, Cameron JD, Thompson M, Juneja S, Kopecka A, Kumar R, Jenkins RB, de Groen PC, Roche P, van Deursen JM (2004) BubR1 insufficiency causes early onset of aging-associated phenotypes and infertility in mice. *Nat Genet* 36:744-749.
- Barber M, Arai Y, Morishita Y, Vigier L, Causeret F, Borello U, Ledonne F, Coppola E, Contremoulins V, Pfrieger FW, Tissir F, Govindan S, Jabaudon D, Proux-Gillardeaux V, Galli T, Pierani A (2015) Migration Speed of Cajal-Retzius Cells Modulated by Vesicular Trafficking Controls the Size of Higher-Order Cortical Areas. *Current biology* : CB 25:2466-2478.
- Boutin C, Goffinet AM, Tissir F (2012) Celsr1-3 cadherins in PCP and brain development. *Current topics in developmental biology* 101:161-183.
- Boutin C, Labedan P, Dimidschstein J, Richard F, Cremer H, Andre P, Yang Y, Montcouquiol M, Goffinet AM, Tissir F (2014) A dual role for planar cell polarity genes in ciliated cells. *Proceedings of the National Academy of Sciences of the United States of America* 111:E3129-3138.
- Chai G, Goffinet AM, Tissir F (2015) Celsr3 and Fzd3 in axon guidance. *The international journal of biochemistry & cell biology* 64:11-14.
- Chai G, Zhou L, Manto M, Helmbacher F, Clotman F, Goffinet AM, Tissir F (2014) Celsr3 is required in motor neurons to steer their axons in the hindlimb. *Nature neuroscience* 17:1171-1179.
- Chen CT, Hehnlly H, Yu Q, Farkas D, Zheng G, Redick SD, Hung HF, Samtani R, Jurczyk A, Akbarian S, Wise C, Jackson A, Bober M, Guo Y, Lo C, Doxsey S (2014) A unique set of centrosome proteins requires pericentrin for spindle-pole localization and spindle orientation. *Curr Biol* 24:2327-2334.
- Dai W, Wang Q, Liu T, Swamy M, Fang Y, Xie S, Mahmood R, Yang Y-M, Xu M, Rao CV (2004) Slippage of Mitotic Arrest and Enhanced Tumor Development in Mice with BubR1 Haploinsufficiency. *Cancer Research* 64:440-445.
- Damiani D, Goffinet AM, Alberts A, Tissir F (2016) Lack of Diaph3 relaxes the spindle checkpoint causing the loss of neural progenitors. *Nature communications* 7:13509.
- de Frutos CA, Bouvier G, Arai Y, Thion MS, Lokmane L, Keita M, Garcia-Dominguez M, Charnay P, Hirata T, Riethmacher D, Grove EA, Tissir F, Casado M, Pierani A, Garel S (2016) Reallocation of Olfactory Cajal-Retzius Cells Shapes Neocortex Architecture. *Neuron* 92:435-448.
- Feng J, Xu Y, Wang M, Ruan Y, So KF, Tissir F, Goffinet A, Zhou L (2012) A role for atypical cadherin Celsr3 in hippocampal maturation and connectivity. *The Journal of neuroscience : the official journal of the Society for Neuroscience* 32:13729-13743.
- Fenstermaker AG, Prasad AA, Bechara A, Adolfs Y, Tissir F, Goffinet A, Zou Y, Pasterkamp RJ (2010) Wnt/planar cell polarity signaling controls the anterior-posterior organization of monoaminergic axons in the brainstem. *The Journal of neuroscience : the official journal of the Society for Neuroscience* 30:16053-16064.
- Hager MH, Morley S, Bielenberg DR, Gao S, Morello M, Holcomb IN, Liu W, Mouneimne G, Demichelis F, Kim J, Solomon KR, Adam RM, Isaacs WB, Higgs HN, Vessella RL, Di Vizio D, Freeman MR (2012) DIAPH3 governs the cellular transition to the amoeboid tumour phenotype. *EMBO Mol Med* 4:743-760.
- Hall JG, Flora C, Scott CI, Jr., Pauli RM, Tanaka KI (2004) Majewski osteodysplastic primordial dwarfism type II (MOPD II): natural history and clinical findings. *Am J Med Genet A* 130A:55-72.
- Ledonne F, Orduz D, Mercier J, Vigier L, Grove EA, Tissir F, Angulo MC, Pierani A, Coppola E (2016) Targeted Inactivation of Bax Reveals a Subtype-Specific Mechanism of Cajal-Retzius Neuron Death in the Postnatal Cerebral Cortex. *Cell reports* 17:3133-3141.
- Lewis A, Wilson N, Stearns G, Johnson N, Nelson R, Brockerhoff SE (2011) Celsr3 is required for normal development of GABA circuits in the inner retina. *PLoS Genet* 7:e1002239.
- Matsuura S, Matsumoto Y, Morishima K-i, Izumi H, Matsumoto H, Ito E, Tsutsui K, Kobayashi J, Tauchi H, Kajiwara Y, Hama S, Kurisu K, Tahara H, Oshimura M, Komatsu K, Ikeuchi T, Kajiji T (2006) Monoallelic BUB1B mutations and defective

- mitotic-spindle checkpoint in seven families with premature chromatid separation (PCS) syndrome. *American Journal of Medical Genetics Part A* 140A:358-367.
- Miyamoto T, Porazinski S, Wang H, Borovina A, Ciruna B, Shimizu A, Kajii T, Kikuchi A, Furutani-Seiki M, Matsuura S (2011) Insufficiency of BUBR1, a mitotic spindle checkpoint regulator, causes impaired ciliogenesis in vertebrates. *Hum Mol Genet* 20:2058-2070.
 - Morello F, Prasad AA, Rehberg K, Vieira de Sa R, Anton-Bolanos N, Leyva-Diaz E, Adolfs Y, Tissir F, Lopez-Bendito G, Pasterkamp RJ (2015) Frizzled3 Controls Axonal Polarity and Intermediate Target Entry during Striatal Pathway Development. *The Journal of neuroscience : the official journal of the Society for Neuroscience* 35:14205-14219.
 - Morley S, You S, Pollan S, Choi J, Zhou B, Hager MH, Steadman K, Spinelli C, Rajendran K, Gertych A, Kim J, Adam RM, Yang W, Krishnan R, Knudsen BS, Di Vizio D, Freeman MR (2015) Regulation of microtubule dynamics by DIAPH3 influences amoeboid tumor cell mechanics and sensitivity to taxanes. *Scientific reports* 5:12136.
 - Murga M, Bunting S, Montana MF, Soria R, Mulero F, Canamero M, Lee Y, McKinnon PJ, Nussenzweig A, Fernandez-Capetillo O (2009) A mouse model of ATR-Seckel shows embryonic replicative stress and accelerated aging. *Nat Genet* 41:891-898.
 - Onishi K, Shafer B, Lo C, Tissir F, Goffinet AM, Zou Y (2013) Antagonistic functions of Dishevelleds regulate Frizzled3 endocytosis via filopodia tips in Wnt-mediated growth cone guidance. *The Journal of neuroscience : the official journal of the Society for Neuroscience* 33:19071-19085.
 - Price DJ, Kennedy H, Dehay C, Zhou L, Mercier M, Jossin Y, Goffinet AM, Tissir F, Blakey D, Molnar Z (2006) The development of cortical connections. *The European journal of neuroscience* 23:910-920.
 - Qu Y, Huang Y, Feng J, Alvarez-Bolado G, Grove EA, Yang Y, Tissir F, Zhou L, Goffinet AM (2014) Genetic evidence that Celsr3 and Celsr2, together with Fzd3, regulate forebrain wiring in a Vangl-independent manner. *Proceedings of the National Academy of Sciences of the United States of America* 111:E2996-3004.
 - Ruiz-Reig N, Andres B, Huilgol D, Grove EA, Tissir F, Tole S, Theil T, Herrera E, Fairen A (2016) Lateral Thalamic Eminence: A Novel Origin for mGluR1/Lot Cells. *Cerebral cortex*.
 - Shaheen R et al. (2016) Characterizing the morbid genome of ciliopathies. *Genome biology* 17:242.
 - Shi D, Komatsu K, Hirao M, Toyooka Y, Koyama H, Tissir F, Goffinet AM, Uemura T, Fujimori T (2014) Celsr1 is required for the generation of polarity at multiple levels of the mouse oviduct. *Development* 141:4558-4568.
 - Tissir F, Goffinet AM (2010) Planar cell polarity signaling in neural development. *Current opinion in neurobiology* 20:572-577.
 - Tissir F, Goffinet AM (2013) Shaping the nervous system: role of the core planar cell polarity genes. *Nat Rev Neurosci*.
 - Tissir F, Bar I, Jossin Y, De Backer O, Goffinet AM (2005) Protocadherin Celsr3 is crucial in axonal tract development. *Nature neuroscience* 8:451-457.
 - Tissir F, Ravni A, Achouri Y, Riethmacher D, Meyer G, Goffinet AM (2009) DeltaNp73 regulates neuronal survival in vivo. *Proceedings of the National Academy of Sciences of the United States of America* 106:16871-16876.
 - Wang W, Jossin Y, Chai G, Lien WH, Tissir F, Goffinet AM (2016) Feedback regulation of apical progenitor fate by immature neurons through Wnt7-Celsr3-Fzd3 signalling. *Nature communications* 7:10936.
 - Zhou L, Tissir F, Goffinet AM (2007) The atypical cadherin Celsr3 regulates the development of the axonal blueprint. *Novartis Foundation symposium* 288:130-134; discussion 134-140, 276-181.
 - Zhou L, Goffinet AM, Tissir F (2008a) [Role of the cadherin Celsr3 in the connectivity of the cerebral cortex]. *Medecine sciences : M/S* 24:1025-1027.
 - Zhou L, Qu Y, Tissir F, Goffinet AM (2009a) Role of the atypical cadherin Celsr3 during development of the internal capsule. *Cerebral cortex* 19 Suppl 1:i114-119.
 - Zhou L, Gall D, Qu Y, Prigogine C, Cheron G, Tissir F, Schiffmann SN, Goffinet AM (2010) Maturation of "neocortex isole" in vivo in mice. *The Journal of neuroscience : the official journal of the Society for Neuroscience* 30:7928-7939.
 - Zhou L, Bar I, Achouri Y, Campbell K, De Backer O, Hebert JM, Jones K, Kessar N, de Rouvoit CL, O'Leary D, Richardson WD, Goffinet AM, Tissir F (2008b) Early forebrain wiring: genetic dissection using conditional Celsr3 mutant mice. *Science* 320:946-949.
 - Zhou LB, Qu YB, Tissir F, Goffinet AM (2009b) Role of the Atypical Cadherin Celsr3 during Development of the Internal Capsule. *Cerebral Cortex* 19:i114-i119.

5. Annex 1: list of publications 2014-2016

1. Celsr3 is required in motor neurons to steer their axons in the hindlimb. Chai G, Zhou L, Manto M, Helmbacher F, Clotman F, Goffinet AM, Tissir F.
Nature Neuroscience 17: 1171-1179 (2014).
IF: 15.25
2. Celsr1 is required for multi-scale polarities formation of mouse oviduct. Shi D, Komatsu K, Hirao M, Toyooka Y, Koyama H, Tissir F, Goffinet A, Uemura T, Fujimori T
Development 141: 4558-4568 (2014).
IF: 6.7
3. A Dual role for planar cell polarity genes in ciliated cells. Boutin C, Labedan P, Dimidschstein J, Richard F, Cremer H, André P, Yang Y, Mireille Montcouquiol M, Goffinet AM, Tissir F. A Dual role for planar cell polarity genes in ciliated cells.
Proc Natl Acad Sci 111: E3129-3138 (2014).
IF: 10.58
4. Genetic evidence that Celsr3 and Celsr2, together with Fzd3, regulate forebrain wiring in a Vangl-independent manner. Qu Y, Huang Y, Feng J, Alvarez-Bolado G, Grove EA, Yang Y, Tissir F, Zhou L, Goffinet AM.
Proc Natl Acad Sci 111: E2996-3004 (2014).
IF: 10.58
5. Barber M, Arai Y, Morishita Y, Vigier L, Causeret F, Borello U, Ledonne F, Coppola E, Contremoulins V, Pfrieder FW, Tissir F, Govindan S, Jabaudon D, Proux-Gillardeaux V, Galli T, Pierani A. Migration Speed of Cajal-Retzius Cells Modulated by Vesicular Trafficking Controls the Size of Higher-Order Cortical Areas.
Current biology 25: 2466-2478 (2015).
IF: 9.57
6. Chai, G., Goffinet, A. M. & Tissir, F. Celsr3 and Fzd3 in axon guidance.
The international journal of biochemistry & cell biology 64: 11-14 (2015).
IF: 4.17
7. Morello F, Prasad AA, Rehberg K, Vieira de Sá R, Antón-Bolaños N, Leyva-Díaz E, Adolfs Y, Tissir F, López-Bendito G, Pasterkamp RJ. Frizzled3 Controls Axonal Polarity and Intermediate Target Entry during Striatal Pathway Development
The Journal of neuroscience 35: 14205-14219 (2015).
IF: 7.60
8. Wang W, Jossin Y, Chai G, Lien WH, Tissir F*, Goffinet AM*. Feedback regulation of apical progenitor fate by immature neurons through Wnt7-Celsr3-Fzd3 signalling.
Nature communications 7: 10936 (2016).
IF: 11.47
9. Glasco, D. M. *et al.* The atypical cadherin Celsr1 functions non-cell autonomously to block rostral migration of facial branchiomotor neurons in mice.
Developmental biology 417: 40-49 (2016).
IF: 3.85
10. de Frutos CA, Bouvier G, Arai Y, Thion MS, Lokmane L, Keita M, Garcia-Dominguez M, Charnay P, Hirata T, Riethmacher D, Grove EA, Tissir F, Casado M, Pierani A, Garel S. Reallocation of Olfactory Cajal-Retzius Cells Shapes Neocortex Architecture.
Neuron 92: 435-448 (2016).
IF: 15.05
11. Damiani D, Goffinet AM, Alberts A, Tissir F. Lack of Diaph3 relaxes the spindle checkpoint causing the loss of neural progenitors.
Nature communications 7:13509 (2016)
IF: 11.47
12. Ledonne F, Orduz D, Mercier J, Vigier L, Grove EA, Tissir F, Angulo MC, Pierani A, Coppola E. Targeted Inactivation of Bax Reveals a Subtype-Specific Mechanism of Cajal-Retzius Neuron Death in the Postnatal Cerebral Cortex.
Cell Reports 17: 3133-3141 (2016).
IF: 8.12
13. Ruiz-Reig N, Andrés B, Huilgol D, Grove EA, Tissir F, Tole S, Theil T, Herrera E, Fairén A. Lateral Thalamic Eminence: A Novel Origin for mGluR1/Lot Cells.
Cerebral cortex, in press
IF: 8.28

* Equal contribution, Co-corresponding authors



Geneeskundige Stichting Koningin Elisabeth
Fondation Médicale Reine Elisabeth
Königin-Elisabeth-Stiftung für Medizin
Queen Elisabeth Medical Foundation

Final report
of the research group of

Prof. dr. Geert van Loo, PhD

Universiteit Gent (UGent)

Prof. dr. Geert van Loo, PhD

Inflammation Research Center
VIB – Gent University
Technologiepark 927
9052 Gent-Zwijnaarde
Belgium
T +32 9 331 37 61
F +32 9 221 76 73
geert.vanloo@irc.vib-ugent.be

Endoplasmic Reticulum stress in autoimmune central nervous system inflammation and demyelination

Multiple sclerosis (MS) is the most common chronic inflammatory disease of the central nervous system (CNS). MS is prevalent in Caucasians, where it affects about 0.05%-0.15% of the population. The cause of degeneration in MS remains largely unknown, but is generally considered to be the result of an autoimmune inflammatory reaction leading to demyelination, oligodendrocyte loss and axonal damage in the CNS. The disease is characterized by activated auto-reactive myelin-specific lymphocytes that home to the CNS where they initiate a vicious cycle of inflammation and tissue damage. The major targets in MS pathology are oligodendrocytes, the myelin-producing cells of the CNS, and neurons, and their loss is directly associated with clinical manifestations of the disease, including speech disturbances, sensation deficits and paralysis. Much knowledge concerning MS pathogenesis has resulted from studies on its animal model Experimental Autoimmune Encephalomyelitis (EAE).

Studies using gene-targeted deficient and transgenic mice have established the role of multiple **inflammatory chemokines and cytokines** produced by both infiltrating immune cells and resident CNS glial cells in EAE pathology. These cytokines and chemokines orchestrate a pathogenic cascade leading to demyelination and axonal damage. A crucial factor controlling inflammatory responses in MS is **NF- κ B**. Although NF- κ B activation in peripheral immune cells is absolutely essential for the induction of EAE pathology, little is still known about the involvement of NF- κ B in the inflammatory reactions locally in the CNS (Mc Guire *et al.* (2013) *Trends Mol. Med.* 19:604). Although we could previously establish a brain-specific contribution of IKK-dependent NF- κ B activation in the pathology of EAE (van Loo *et al.* (2006) *Nat. Immunol.* 7:954; van Loo *et al.* (2010) *Mol. Endocrinol.* 24:310; Raasch *et al.* (2011) *Brain* 134:1184), the specific role and contribution of NF- κ B signaling in the different neuronal cell types (neurons, astrocytes, oligodendrocytes and microglia) and immune cells for the pathology of MS is still subject of investigation in our research group (Mc Guire *et al.* (2013) *J. Immunol.* 190:2896; Mc Guire *et al.* (2014) *J. Neuroinflamm.* 11:124; Voet *et al.* Submitted for publication).

Endoplasmic reticulum (ER) stress is likely to be a major pathway in the pathogenesis of MS. ER stress occurs upon the accumulation of unfolded or misfolded proteins in the ER initiating the **unfolded protein response (UPR)**. The UPR has to deal with ER stress by increasing the folding capacity of the ER by reducing protein synthesis and promoting protein degradation through ER-associated degradation. Three different signalling cascades can be activated: the inositol-requiring transmembrane kinase/endonuclease 1 (IRE1) pathway, the pancreatic ER kinase (PERK) pathway and the activating transcription factor 6 (ATF6) pathway. Although all three branches are usually activated by any given ER stress event, the timing of activation can differ. ER stress is part of normal cellular physiology, but can, however, become problematic in conditions of chronic, non-resolved stress, giving rise to inflammation and/or apoptosis. Recent observations suggest that the signalling pathways in the UPR and those controlling inflammation are interconnected and can activate each other through various mechanisms including the activation of NF- κ B (Zhang and Kaufman (2008) *Nature* 454:455), suggesting that ER stress contributes to the pathology of many inflammatory diseases, including MS. Indeed, evidence is emerging that the UPR is involved in the disease pathogenesis of MS and EAE. Oligodendrocytes continuously produce large amounts of myelin to perform their function, making them prone to protein misfolding and ER stress. Expression of ER stress markers has been found to be upregulated in macrophages, microglia, astrocytes, and oligodendrocytes within demyelinated white matter lesions from MS patients. Moreover, elevated levels of phosphorylated-eIF2 α , typical for PERK-dependent UPR signalling, have been observed in oligodendrocytes and infiltrating T-cells in the CNS during the course of EAE (Lin and Popko (2009) *Nat. Neurosci.* 12: 379). Notably, IFN- γ exerts protective

activities through the activation of the PERK-eIF2 α pathway in oligodendrocytes (Lin *et al.* (2007) J. Clin. Invest. 117: 448). On the other hand, IFN- γ has suppressive activity on oligodendrocyte regeneration, inhibiting remyelination in MS and EAE demyelinated lesions (Lin *et al.* (2006) Brain 129: 1306). These data suggest that ER stress induction in fully myelinated mature oligodendrocytes promotes cell survival, but in actively (re)myelinating oligodendrocytes leads to cell death (Lin and Popko (2009) Nat. Neurosci. 12: 379). Together, these observations clearly indicate the involvement of ER stress in MS and EAE pathology, suggesting that manipulation of the UPR may be beneficial in order to prevent disease. Since **inflammation and ER stress may induce autophagy** responses as a compensatory mechanism, also autophagy may be involved in MS (Adolph *et al.* (2013) Nature 503: 272). Indeed, several studies have shown that autophagy directly participates in the progress of MS and EAE (Liang and Le (2015) Neurosci. Bull. 31:435).

With our studies we aim to better understand the contribution of NF- κ B, autophagy and UPR signaling in the development and progression of CNS inflammation and demyelination. The basic approach is to genetically manipulate genes coding for proteins essential for NF- κ B, autophagy and UPR signaling in mice in specific neuronal populations, and to determine the effects of such mutation in neuronal development and MS pathogenesis. These studies allow us to specify the role of NF- κ B, UPR and autophagy signalling locally in the CNS, both in target cells (such as in neurons and oligodendrocytes) and in effector cells (such as in astrocytes and microglia) in the inflammatory and neurodegenerative processes happening during MS/EAE. It is critically important to determine how these various cell types at various stages of activation and disease development react to chronic inflammatory stress in order to better understand the pathogenesis of MS (and other demyelinating diseases) which may have implications for the rational design of new therapeutics for the treatment of these pathologies.

1. Results

1.1. Methodology

Conditional 'floxed' mice targeting NF- κ B signaling (A20^{FL}, IKK2^{FL}), autophagy (Atg16L1^{FL}, OPTN^{FL}) and individual UPR signaling pathways (XBP1^{FL}, IRE1 α ^{FL}, and PERK^{FL}) have been generated or obtained from different sources. These mouse lines have been crossed to different Cre transgenic lines allowing CNS specific gene: Nestin-Cre transgenic mice for pan-CNS targeting, Thy1.2-Cre mice for neuron-specific targeting, MOGi-Cre mice for oligodendrocyte targeting, GFAP-Cre mice for astrocyte targeting, and Cx3Cr1-ERT2Cre mice for microglia targeting.

To study the CNS-specific role of NF- κ B, ER stress and autophagy in the immunopathology of MS, we make use of the experimental MS model EAE, which can be induced in C57BL/6 mice by immunization with myelin oligodendrocyte glycoprotein (MOG). Next to EAE, brain-specific demyelination is also induced by putting mice on a diet containing the neurotoxicant cuprizone. Advantage of this approach is that demyelination can afterwards be reversed by administration of normal food, allowing the study of brain remyelination and the involvement of ER stress signalling and autophagy in this. Finally, *in vivo* studies are complemented by *in vitro* studies on primary cells derived from the different tissue-specific knockout mice that have been established, allowing biochemical studies.

1.2. NF- κ B signalling and its regulation by A20 in EAE

Although we could previously establish a brain-specific role of NF- κ B in the neuroinflammation associated with EAE (van Loo *et al.* (2006) Nat. Immunol. 7:954; van Loo *et al.* (2010) Mol. Endocrinol. 24:310; Raasch *et al.* (2011) Brain 134:1184), the regulation of NF- κ B signaling in the different neuronal cell types (neurons, astrocytes, oligodendrocytes and microglia) in MS/EAE is still largely elusive. One critical brake on NF- κ B activation is A20/TNFAIP3 (TNF α induced protein 3). A20 is induced by NF- κ B

under inflammatory conditions where it acts as a negative regulator dampening further signalling. Additionally, A20 has anti-apoptotic protective activities, at least in specific cells and tissues (Catrysse *et al.* (2014) Trends Immunol. 35:22). Interestingly, the *A20/TNFAIP3* gene has been identified in humans as a susceptibility locus for multiple inflammatory pathologies, including multiple sclerosis (De Jager *et al.* (2009) Nat. Genet. 41 :776). To clarify the role of A20 in CNS inflammation and EAE, we generated mice lacking A20 in the different CNS resident cell types and subjected them to EAE. Although A20 inactivation in astrocytes, oligodendrocytes or neurons did not affect EAE pathology, microglia-specific deletion of A20 strongly sensitized mice to EAE (Figure 1, Voet *et al.* submitted for publication), characterized by severe CNS macrophage and lymphocyte infiltration, severe demyelination, and inflammatory cytokine expression (data not shown). We have strong evidence that this phenotype critically relies on Nlrp3 inflammasome hyperactivation in microglia, in agreement with previous findings of our group identifying A20 as a critical control on inflammasome activation in macrophages (Vande Walle *et al.* (2014) Nature 512:69). The microglia-specific function of A20 is subject of further investigation in the research group through combined *in vivo* and *in vitro* studies.

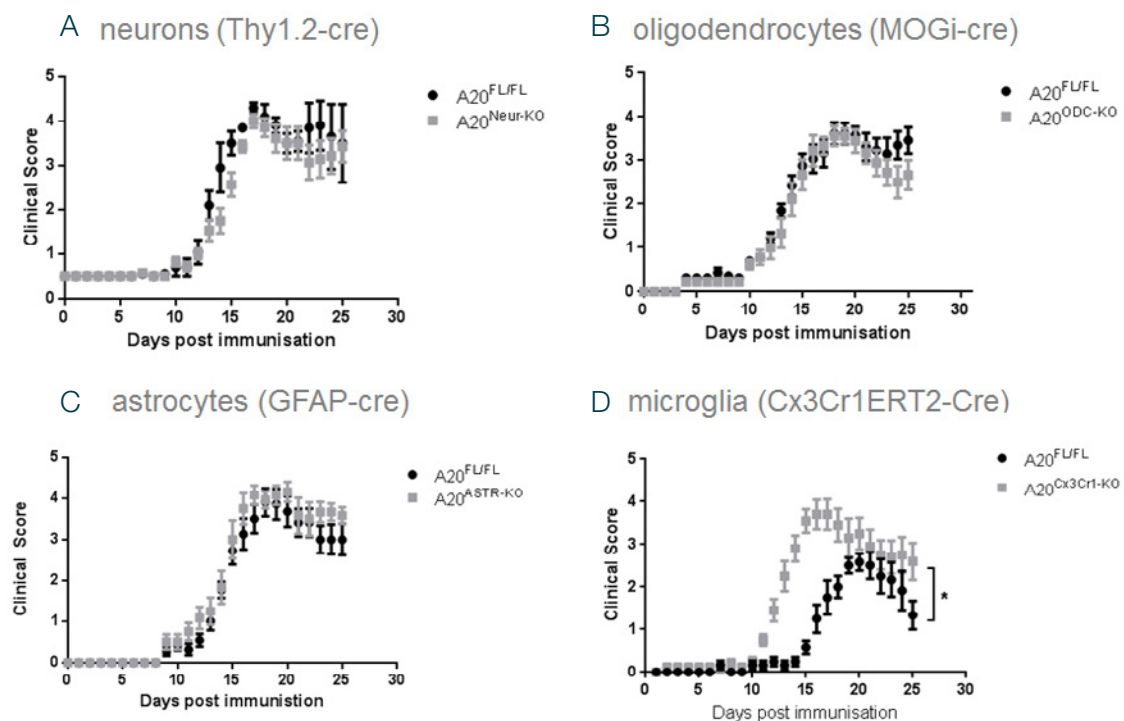


Figure 1. Microglia-specific A20 deletion strongly sensitizes to EAE disease. **A.** Clinical scores of wild-type control (black, n=6) and $A20^{neuron-KO}$ (grey, n=7) mice after immunization with MOG_{35-55} . **B.** Clinical scores of wild-type control (black, n=13) and $A20^{oligodendrocyte-KO}$ (grey, n=9) mice after immunization with MOG_{35-55} . **C.** Clinical scores of wild-type control (black, n=11) and $A20^{astrocyte-KO}$ (grey, n=6) mice after immunization with MOG_{35-55} . **D.** Clinical scores of wild-type control (black, n=6) and $A20^{microglia-KO}$ (grey, n=10) mice after immunization with MOG_{35-55} . Results are expressed as mean values \pm s.e.m. *, $P < 0.05$. (unpublished results)

1.3. UPR signalling and autophagy in cuprizone-induced demyelination

Brain demyelination can be induced through the administration of cuprizone in chow diet. Although little is known of the mechanisms by which cuprizone induces CNS demyelination and inflammation, cuprizone administration clearly induces activation of ER stress response genes (Figure 2) and autophagy genes (Figure 3) in the corpus callosum.

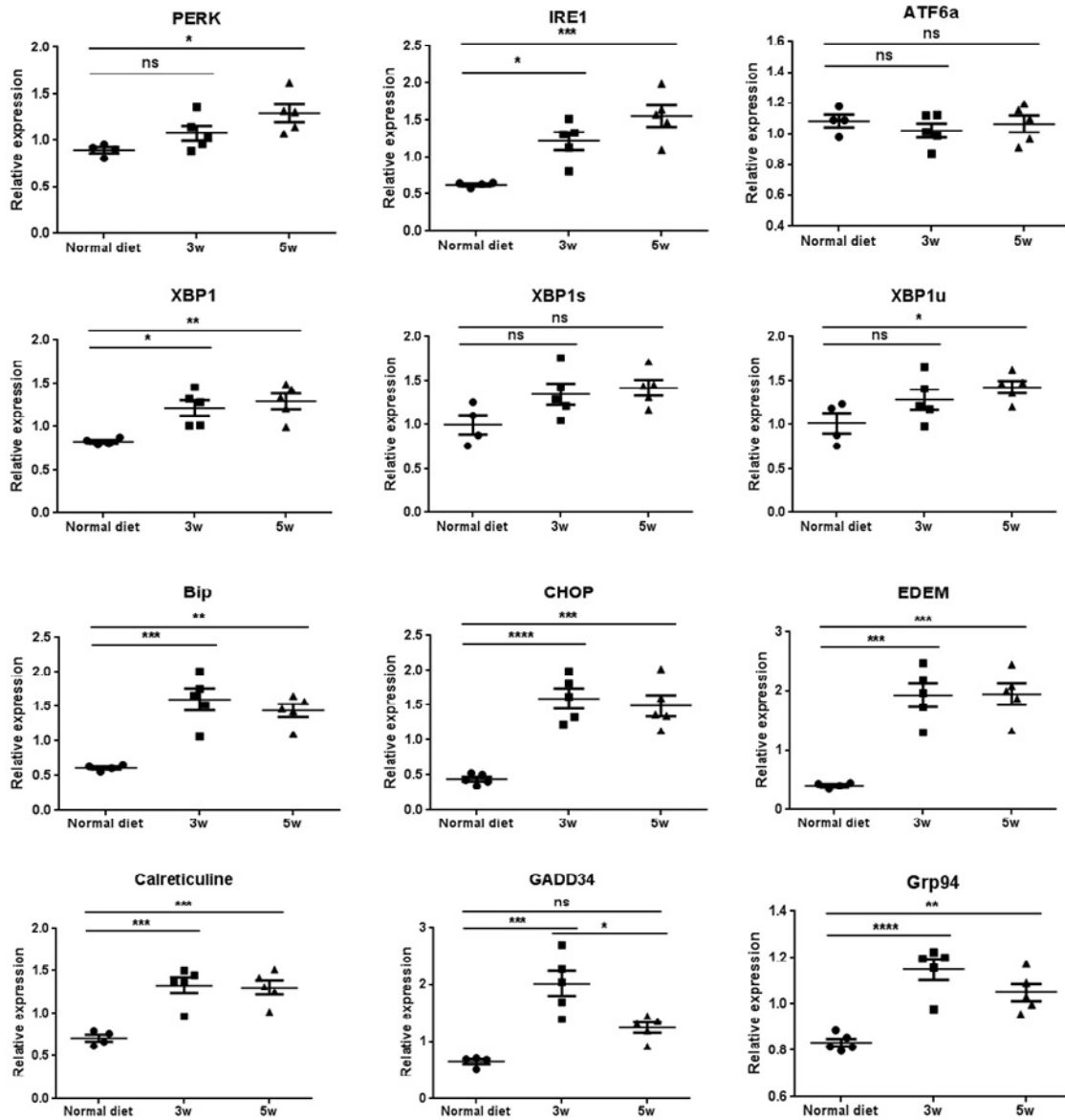


Figure 2. Cuprizone-induced expression of UPR genes. Expression of ER stress markers was assessed through qPCR on corpus callosum lysates isolated from wild-type C57BL/6 mice either or not treated with cuprizone for 3 and 5 weeks. Results are presented as mean values \pm s.d.

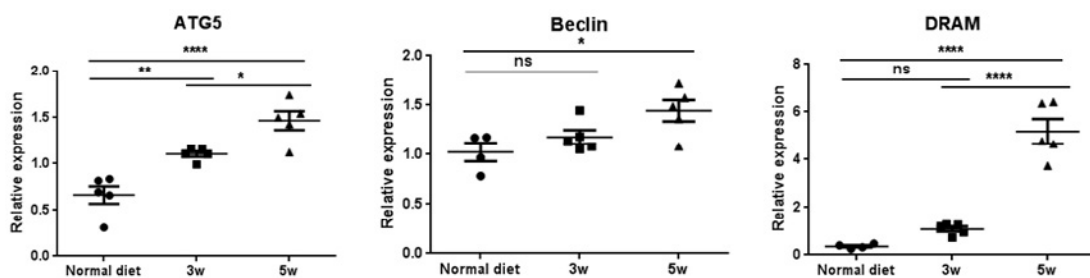


Figure 3. Cuprizone-induced expression of autophagy genes. Expression of autophagy markers was assessed through qPCR on corpus callosum lysates isolated from wild-type C57BL/6 mice either or not treated with cuprizone for 3 and 5 weeks. Results are presented as mean values \pm s.d.

Three different UPR signalling cascades can be activated in response to ER stress: the inositol-requiring transmembrane kinase/endonuclease 1 (IRE1) pathway, the pancreatic ER kinase (PERK) pathway and the activating transcription factor 6 (ATF6) pathway. To investigate the involvement of these signaling cascades in MS-associated neuroinflammation, CNS-specific XBP1, IRE1 α and PERK knockout mice have been generated and analysed in cuprizone-induced demyelinating pathology.

IRE1 α is the most conserved transducer of UPR which acts through unconventional splicing of XBP1 mRNA. XBP1^{CNS-KO} mice and control littermates were given cuprizone for 5 weeks and degree of demyelination and inflammation was assessed in corpus callosum. Wild-type mice show a near complete demyelination of the corpus callosum, as expected, in contrast to XBP1^{CNS-KO} mice which were significantly protected from cuprizone-induced demyelination (Figure 4). On brain histology, XBP1^{CNS-KO} mice also show a significant reduction in microgliosis and astrogliosis, and a higher number of mature oligodendrocytes (Figure 4). Loss of XBP-1 transcriptional activity may result in constitutive IRE-1 α signalling and IRE-1 α dependent degradation (RIDD) of specific mRNAs, as previously shown (Hur *et al.* (2012) *J. Exp. Med.* 209: 307; Osorio *et al.* (2014) *Nat. Immunol.* 15: 248), explaining observed phenotype. Since XBP1 deficiency was shown to be protective in a mouse model of ALS through enhanced clearance of protein aggregates by autophagy (Hetz *et al.* (2009) *Genes Dev.* 23: 2294), the protection of XBP1^{CNS-KO} mice in the model of cuprizone-induced demyelination may also depend on an increased autophagy of dysfunctional mitochondria protecting oligodendrocytes from cell death. These hypotheses are currently under investigation. For this, XBP1^{CNS-KO} mice are being crossed to IRE-1 α ^{CNS-KO} mice and Atg16L1^{CNS-KO} mice, and the response of these CNS-specific double knockout mice to cuprizone is being investigated.

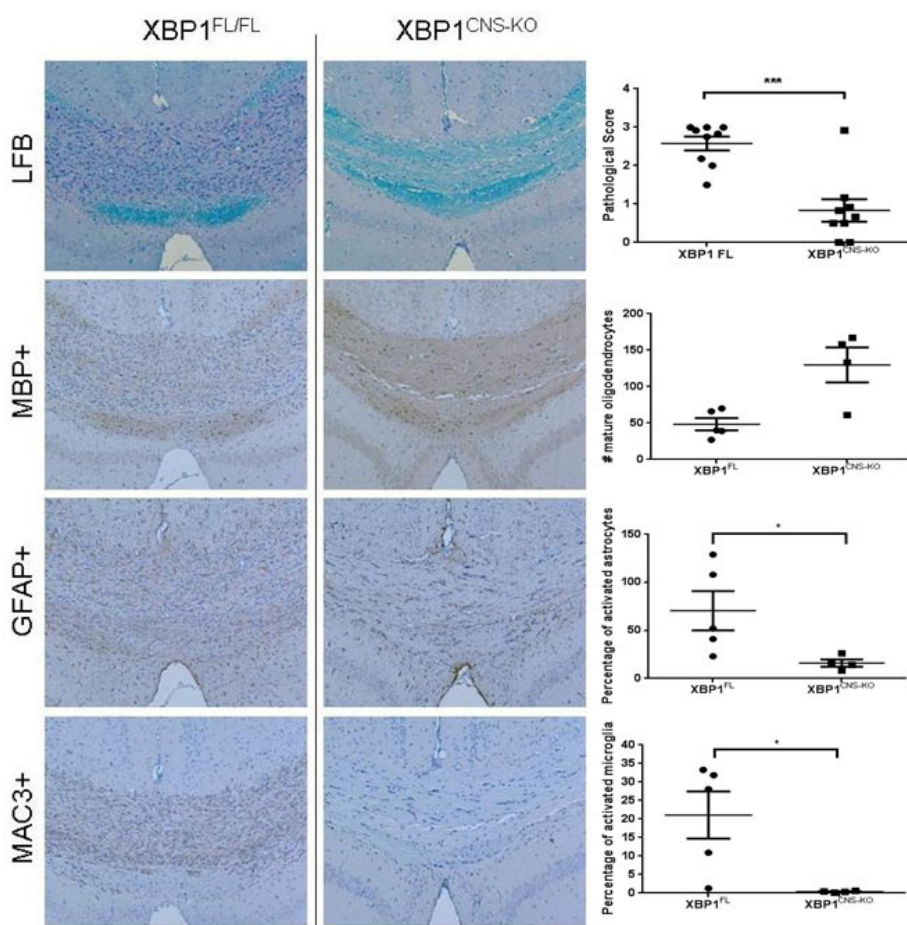


Figure 4. Cuprizone-induced demyelination is reduced in XBP1^{CNS-KO} mice. Representative pictures of coronal sections of the corpus callosum (left) and quantification (right) for degree of demyelination (LFB), oligodendrocyte numbers (MBP), astrogliosis (GFAP) and microgliosis (Mac3) in XBP1^{CNS-KO} mice and XBP1^{FL} littermates after 5 weeks of cuprizone treatment.

1.4. XBP1-, IRE1 α - and PERK-dependent UPR signaling in EAE

Next XBP1^{CNS-KO} mice have been studied in EAE. XBP1^{CNS-KO} mice, however, develop EAE pathology to the same extent as control littermates (Figure 5A). Also, on spinal cord histology or through spinal cord gene expression, no significant differences could be observed (data not shown). Also IRE1 α ^{CNS-KO} mice have been analysed in EAE. However, a lot of variation between different mice within one group was observed, and many mice did not develop a significant degree of disease probably due to the genetic background of the IRE1 α line, excluding conclusions regarding the role of IRE1 α in EAE.

Since elevated levels of phosphorylated-eIF2 α , typical for PERK-dependent UPR signalling, have been observed in oligodendrocytes in the CNS during the course of EAE (Lin and Popko (2009) Nat. Neurosci. 12: 379), oligodendrocyte-specific PERK knockout (PERK^{ODC-KO}) mice have been developed and subjected to EAE. As shown in Figure 5B these mice are protected from clinical disease development. We are currently investigating this further through combined *in vivo* and *in vitro* approaches.

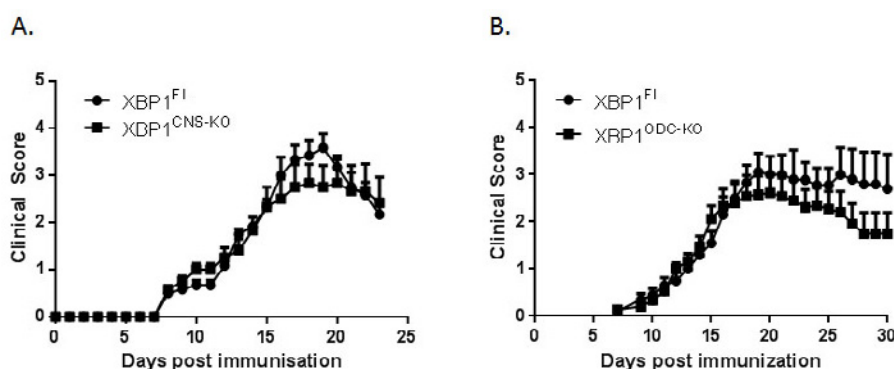


Figure 5. A. Clinical disease score of XBP1^{F1} (n=6) and XBP1^{CNS-KO} (n=6) littermate mice after immunization with MOG peptide. **B.** Clinical disease score of PERK^{F1} (n=14) and PERK^{ODC-KO} (n=13) littermate mice after immunization with MOG peptide. Results are presented as mean values \pm s.e.m.

1.5. Atg16L1 and optineurin (OPTN) dependent autophagy in CNS and EAE

Several studies have shown that autophagy directly participates in the progress of MS and EAE (Liang and Le (2015) Neurosci. Bull. 31:435). Although the primary role of autophagy is the adaptation to starvation, autophagy is also thought to be essential for the normal turnover of cytoplasmic proteins. As such, autophagy is thought to be a protective mechanism. In inflammatory conditions, autophagy is often induced, probably as a compensatory mechanism. Moreover, autophagy not only regulates inflammatory reactions, but selective autophagy of mitochondria, so called 'mitophagy', may also be important in MS. Indeed, dysfunction of mitochondria produces reactive oxygen species (ROS) which may be an important factor in the pathogenesis of MS and EAE. One essential signaling mediator in autophagy signalling is the protein Atg16L1.

Since Atg16L1 knockout mice are not viable, we generated a floxed *Atg16L1* mouse allowing cell type-specific Atg16L1 deletion. For the study of autophagy in brain and EAE pathology, Atg16L1 floxed mice were first crossed with the NestinCre line in order to generate CNS-specific Atg16L1 knockout mice. These mice are viable, however, progressively develop motor and behavioral deficits (Figure 6A). The gross anatomy of the brain of these mice was normal. Histological examination, however, revealed degenerative changes in specific neuronal populations in Atg16L1^{CNS-KO} mice, most evident in the cerebellum demonstrating severe loss of Purkinje cells (Figure 6B). Further studies are ongoing in order to characterize the cause of neurodegeneration in these mice. Because of the spontaneous neurodegenerative phenotype of Atg16L1^{CNS-KO} mice, these mice have not been challenged in EAE. However, Atg16L1-specific signalling and autophagy in microglial cells has been studied in the context of neuroinflammation and EAE. Indeed, microglia play crucial roles in neuroinflammation, and autophagy in glial cells may play important roles in responding to stress in MS. For this, Atg16L1^{microglia-KO} mice

have been generated and have been subjected to EAE, however, no differences between control and $Atg16L1^{microglia-KO}$ mice could be observed (Figure 7).

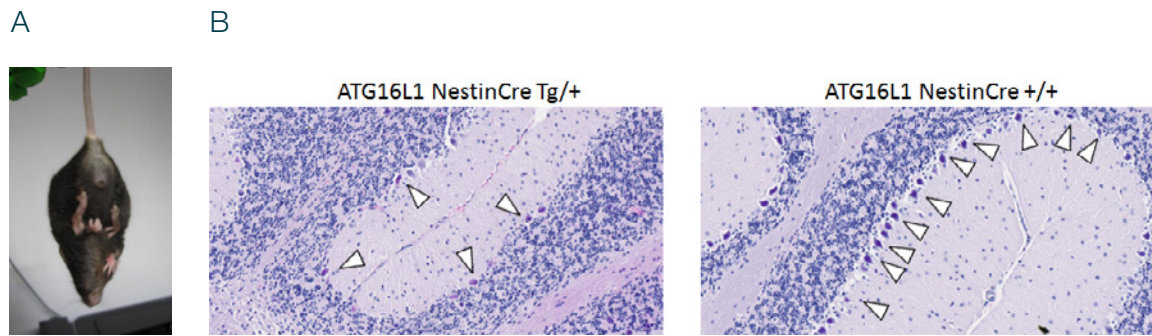


Figure 6. Neuronal degeneration in $Atg16L1^{CNS-KO}$ mice. **A.** Abnormal limb-clasping reflexes, tremor and movement ataxia in $Atg16L1^{CNS-KO}$ mice at 36 weeks of age. **B.** H&E stained sections of cerebellum from control ($Atg16L1^{NestinCre Tg/+}$) and $Atg16L1^{CNS-KO}$ ($Atg16L1^{NestinCre Tg/+}$) mice at three months of age. Purkinje cells are indicated with arrowheads.

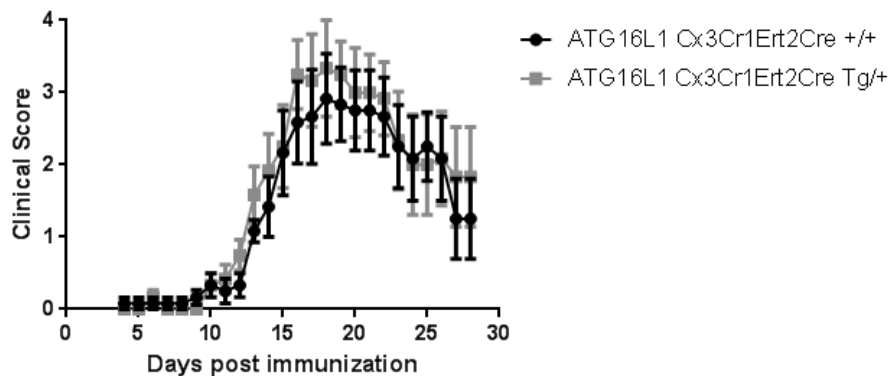


Figure 7. Clinical disease score of $Atg16L1^{FL}(Cx3Cr1Ert2Cre+/+, n=6)$ and $Atg16L1^{microglia-KO}(Cx3Cr1Ert2CreTg/+, n=6)$ littermate mice after immunization with MOG peptide. Results are presented as mean values \pm s.e.m.

Finally, the role of Optineurin (OPTN) in MS/EAE has been investigated. OPTN is a ubiquitously expressed ubiquitin-binding protein that has been implicated, through genetic studies in patients, in amyotrophic lateral sclerosis (ALS) and other neurodegenerative diseases. Importantly, OPTN has recently been identified as an autophagy receptor important not only for the autophagic removal of pathogens and protein aggregates, but also of damaged mitochondria (mitophagy) (Slowicka *et al.* (2016) Trends Immunol. 37:621), a process which may be very important in the context of MS/EAE. We recently generated OPTN deficient mice and identified the *in vivo* importance of OPTN in inflammatory signalling and autophagy. In agreement with previous *in vitro* data, we could show a role for OPTN in the activation of TBK1 and the production of type I IFNs, establishing OPTN as a positive regulator of IRF3 signalling and IFN- production (Slowicka *et al.* (2016) Eur. J. Immunol. 46:971). Interestingly, TBK1 controls T cell activation and migration during neuroinflammation (Yu *et al.* (2015) Nat. Commun. 6: 6074), also suggesting a role for OPTN in this process.

To determine whether OPTN plays a role in neuroinflammation and EAE pathogenesis, we induced EAE in control heterozygous ($OPTN^{+/+}$) and OPTN deficient ($OPTN^{-/-}$) littermate mice. However, no differences in clinical EAE pathology could be observed between both groups of mice (Figure 8), excluding an important role for OPTN in the autoimmune and inflammatory processes associated with EAE.

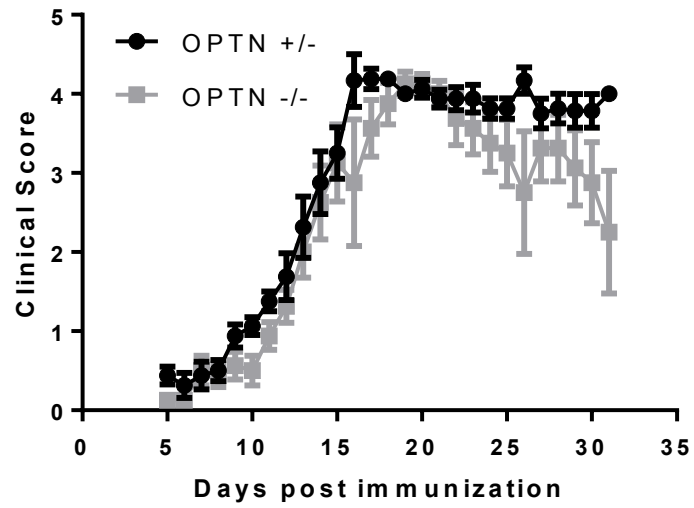


Figure 8. Clinical disease scores of OPTN^{-/-} (n=8) and OPTN^{+/-} (n=8) mice after immunization with MOG peptide. Results are from three independent experiments and presented as mean values ± s.e.m.

2. Publications van Loo group 2013-2016 (acknowledging GSKE support)

- Slowicka, K., Vereecke, L. and van Loo, G. (2016) Optineurin functions in health and disease. *Trends Immunol.* 37(9), 621-633.
- De Wilde, K., Martens, A., Lambrecht, S., Jacques, P., Drennan, M.B., Debusschere, K., Coudenys, J., Verheugen, E., Windels, F., Beyaert, R., van Loo, G. and Elewaut, D. (2016) A20 inhibition of STAT1 signaling in myeloid cells: a novel endogenous regulatory mechanism preventing development of enthesitis. *Annals of the Rheumatic Diseases*, in press.
- Catrysse, L., Farhang Ghahremani, M., Youssef, S.A., Mc Guire, C., Vereecke, L., Sze, M., Weber, A., Heikenwalder, M., De Bruin, A., Beyaert, R. and van Loo, G. (2016) A20 prevents chronic liver inflammation and cancer by protecting hepatocytes from death. *Cell Death Dis.*, 7, e2250.
- Maelfait, J., Roose, K., Vereecke, L., Mc Guire, C., Sze, M., Schuijs, M.J., Willart, M., Ibañez, L.I., Hammad, H., Lambrecht, B.N., Beyaert, R., Saelens, X. and van Loo, G. (2016) A20 Deficiency in Lung Epithelial Cells Protects against Influenza A Virus Infection. *PLoS Pathog.*, 12 (1), e1005410.
- Slowicka, K., Vereecke, L., Mc Guire, C., Sze, M., Maelfait, J., Kolpe, A., Saelens, X., Beyaert, R. and van Loo, G. (2016) Optineurin deficiency in mice is associated with increased sensitivity to Salmonella but does not affect proinflammatory NF- κ B signaling. *Eur. J. Immunol.*, 46(4), 971-980.
- Fukaya, M., Brorsson, C.A., Meyerovich, K., Catrysse, L., Delarochette, D., Vanzela, E.C., Ortis, F., Beyaert, R., Nielsen, L.B., Andersen, M.L., Mortensen, H.B., Pociot, F., van Loo, G., Størling, J., and Cardozo, A.K. (2016) A20 inhibits β cells apoptosis by multiple mechanisms and predicts residual β cell function in Type 1 diabetes. *Mol. Endocrinol.*, 30(1):48-61.
- Catrysse, L., Fukaya, M., Sze, M., Meyerovich, K., Beyaert, R., Cardozo, A.K. and van Loo, G. (2015) A20 deficiency sensitizes pancreatic beta cells to cytokine-induced apoptosis *in vitro* but does not influence type 1 diabetes development *in vivo*. *Cell Death Dis.*, 6, e1918.
- Vereecke, L., Vieira-Silva, S., Billiet, T., van Es, J.H., Mc Guire, C., Slowicka, K., Sze, M., van den Born, M., De Hertogh, G., Clevers, H., Raes, J., Rutgeerts, P., Vermeire, S., Beyaert, R. and van Loo, G. (2014) A20 controls intestinal homeostasis through cell-specific activities. *Nat. Commun.*, 5, 5103.
- Takahashi, N., Vereecke, L., Bertrand, M.J.M., Duprez, L., Berger, S.B., Divert, T., Goncalves, A., Sze, M., Martens, S., Lefebvre, S., Gilbert, B., Gunther, C., Becker, C., Bertin, J., Gough, P.J., Declercq, W., van Loo, G. and Vandenabeele, P. (2014) RIPK1 ensures intestinal homeostasis by protecting the epithelium against apoptosis. *Nature*, 513, 95-99.
- Mc Guire, C., Elton, L., Wieghofer, P., Staal, J., Voet, S., Demeyer, A., Nagel, D., Krappmann, D., Prinz, M., Beyaert, R. and van Loo, G. (2014) Pharmacological inhibition of MALT1 protease activity by mepazine protects mice from experimental autoimmune encephalomyelitis. *J. Neuroinflamm.*, 11, 124-135.
- Verhelst, K., van Loo, G. and Beyaert, R. (2014) A20: attractive without showing cleavage. *EMBO Rep.*, 15 (7), 734-735.
- Vande Walle, L., Vanopdenbosch, N., Jacques, P., Fossoul, A., Verheugen, E., Vogel, P., Beyaert, R., Elewaut, D., Kanneganti, T.V., van Loo, G.* and Lamkanfi, M.* (2014) Negative regulation of the NLRP3 inflammasome by A20 protects against arthritis. *Nature*, in 512, 69-73 (*equally contributed)
- Catrysse, L., Vereecke, L., Beyaert, R. and van Loo, G. (2014) A20 in inflammation and autoimmunity. *Trends Immunol.*, 35 (1), 22-31.
- Mc Guire, C., Prinz, M., Beyaert, R. and van Loo, G. (2013) Nuclear Factor- κ B in multiple sclerosis pathology. *Trends Mol. Med.*, 19 (10), 604-613.
- Mc Guire, C., Rahman, M., Schwaninger, M., Beyaert, R. and van Loo, G. (2013) The ubiquitin editing enzyme A20 (TNFAIP3) is upregulated during permanent middle cerebral artery occlusion but does not influence disease outcome. *Cell Death Dis.*, 4:e531.
- Mc Guire, C., Wieghofer, P., Elton, L., Muylaert, D., Prinz, M., Beyaert, R. and van Loo, G. (2013) Paracaspase MALT1 deficiency protects mice from autoimmune-mediated demyelination. *J. Immunol.*, 190, 2896-2903.



Geneeskundige Stichting Koningin Elisabeth
Fondation Médicale Reine Elisabeth
Königin-Elisabeth-Stiftung für Medizin
Queen Elisabeth Medical Foundation

Final report
of the research group of

Prof. Pierre Vanderhaeghen, PhD &
dr. Anja Hasche

Université Libre de Bruxelles (ULB)

Prof. Pierre Vanderhaeghen, PhD & dr. Anja Hasche

Institute of Interdisciplinary Research (IRIBHN)

ULB, Campus Erasme

808, Route de Lennik

B-1070 Brussels

T +32 2 555 41 86

F +32 2 555 46 55

pvdhaegh@ulb.ac.be

Mechanisms of neurogenesis and cortical development, and implications for brain diseases.

1. State of the art and objectives.

The cerebral cortex is one of the most important structures in our brain: to a large extent it is considered to underlie what we are as a species, and as individuals. In correlation with its elaborate functions, the cerebral cortex displays multiple levels of complexity. Its surface is parcellated into numerous areas characterized by specific patterns of connectivity, and thereby underly selective functional modalities such as motor control, vision, or language for instance (Grove and Fukuchi-Shimogori, 2003; Sur and Rubenstein, 2005). Each cortical area is further divided through its depth into distinct cortical layers, each of which consists of neurons displaying stereotypic patterns of input and output (Molyneaux et al., 2007). Within each layer, several classes of neurons can be further distinguished on the basis of their gene expression, neurotransmission, morphology and/or connectivity. Overall, the cerebral cortex can thus be thought of as a collection of hundreds of different types of neurons, and this diversity is at the core of its powerful computational capacities.

The mechanisms of neurogenesis and cortical development have important implications for our understanding of pathological brain development and in the long run for the rational design of replacement therapies of neurological conditions, many of which strike the cerebral cortex.

We previously uncovered an intrinsic pathway of cortical neurogenesis, whereby pluripotent stem cells (embryonic stem cells (ESC) or induced pluripotent stem cells (iPSC)), whether of mouse or human origin, efficiently generate neurons that share most molecular, cellular and functional landmarks of pyramidal neurons of the cerebral cortex (Anderson and Vanderhaeghen, 2014; Espuny-Camacho et al., 2013; Gaspard et al., 2009; Gaspard et al., 2008; van den Aemele et al., 2014). This model opens new opportunities to study corticogenesis and its disorders (Brennand et al., 2015; Suzuki and Vanderhaeghen, 2015). Here we have followed a multidisciplinary research programme combining developmental neurobiology and pluripotent stem cell technology, centered on the mechanisms of neurogenesis and cortical development, and their application to the design of innovative models and potential treatments of human brain diseases.

The results obtained through the Programme 2014-2016 are detailed below:

- 1. Mechanisms of neurogenesis, and implication in brain cancer.**
- 2. Exploring new ways to repair the diseased cortex.**
- 3. Modelling human neurological diseases.**

2. Obtained results and significance.

2.1. Mechanisms of neurogenesis, and implication in brain cancer.

Using our *in vitro* model of corticogenesis, we recently identified BCL6, a transcriptional repressor and B cell oncogene, as a key factor to promote the generation of pyramidal neurons in the cortex (Tiberi et al., 2012). To follow up on these results, we have now explored additional roles of BCL6 in brain development, focusing on the cerebellar cortex, where we found BCL6 to be expressed prominently during postnatal neurogenesis.

We first found that BCL6 was necessary and sufficient to induce the differentiation of granule neuron precursors (GNP) into cerebellar granule neurons, the most abundant neurons of the brain. Then using a combination of cell and molecular approaches, we discovered that BCL6 promoted GNP differentiation through the repression of Gli1/2 transcription factors, the main effectors of the Sonic Hedgehog (SHH) pathway, which is key for the expansion and self-renewal of GNP (Hatten and Roussel, 2011).

Given that the SHH pathway is frequently mutated and overactivated in specific forms of medulloblastoma (MB) (Olson, 2014), the most frequent pediatric brain tumour, we then explored whether and how BCL6 could be implicated in this form of cancer, using ad how mouse models. We thus found that BCL6 overexpression was sufficient to block the initiation and growth of MB in a mouse model of SHH-dependent MBn which was confirmed in an *in vitro* model of human SHH medulloblastoma cell line. Besides and importantly, we found that mouse defective in BCL6 and p53 function were much more prone to develop MB, thus qualifying BCL6 as a bona fide tumour suppressor.

Our findings identify BCL6 as a potent repressor of the SHH pathway in normal and oncogenic neural development, with direct relevance for human SHH medulloblastoma (Tiberi et al., 2014). These findings thus identify new therapeutic and diagnostic targets for this brain tumour, and illustrate how the same gene can act as an oncogene (in B lymphocytes) and an oncosuppressor (in granule neuron precursors), depending on the cellular context.

In parallel, and in close collaboration with the Hassan lab (KULeuven), we studied further mechanisms of neurogenesis by focusing on the highly conserved basic-Helix-Loop-Helix (bHLH) transcription factors called Proneural Proteins, in particular Neurogenin2 (Quan et al., 2016). Current models ascribe the transient activity of bHLH proteins to dynamic transcriptional regulation, but the Bassem lab identified several posttranslational modifications of proneural factors that are instrumental for correct neural fate specification in the fly visual system. Using *in utero* electroporation targeting the cortex we demonstrated that this novel mechanism is conserved throughout evolution, by identifying the critical role of a specific Threonine phosphorylation site of mouse Neurogenin2, which regulates the rate of neurogenesis and thereby the laminar fate of cortical neurons (Quan et al., 2016).

This part of the project led to the following main publications:

- A BCL6/BCOR/SIRT1 complex Triggers Neurogenesis and Suppresses Medulloblastoma by Repressing Sonic Hedgehog Signalling.

Tiberi L, Bonnefont J, van den Ameele J, Le Bon S, Herpoel A, Bilheu A, Baron BW, and *Vanderhaeghen P*.

Cancer Cell (2014) 26, 797-812.

Preview and Featured Article in *Cancer Cell*.

IF: 23.8

- Post-translational Control of the Temporal Dynamics of Transcription Factor Activity Regulates Neurogenesis.

Quan XJ, Yuan L, Tiberi L, Claeys A, De Geest N, Yan J, van der Kant R, Xie WR, Klisch TJ, Shymkowitz J, Rousseau F, Bollen M, Beullens M, Zoghbi HY, **Vanderhaeghen P**, Hassan BA.

Cell (2016);164(3):460-75. doi: 10.1016/j.cell.2015.12.048.

Preview in Cell.

IF: 32.2

2.2. Exploring new ways to repair the diseased cortex.

While pluripotent stem cell-derived neurons constitute an attractive source for replacement therapies, it remains unclear whether they could be useful for cortical diseases. We have started to explore the relevance of ESC-derived *in vitro* corticogenesis for brain repair, using intracerebral grafting in experimental models of cortical lesions in the adult mouse.

To achieve this, we first implemented a well established experimental setup (Gaillard et al., 2007): focal neuronal lesions of the cerebral cortex were generated following stereotactic injections of ibotenic acid neurotoxin, resulting in a focal loss of neurons in defined cortical domains, in frontal or occipital cortex. Three days after lesioning, mouse ESC-derived cortical progenitors and neurons (generated following (Gaspard et al., 2009), which mostly display an identity of neurons of the visual cortex (Gaspard et al., 2008), were grafted at the same site of the lesion.

Analysis of grafted animals 1-3 month after grafting indicated that most of them (80%) contained a graft, consisting mainly of differentiated pyramidal neurons. Most importantly, inspection of the rest of the brain revealed in 40% of the cases far-reaching graft-derived axonal growth, following specific paths and reaching specific targets of endogenous cortical neurons. Remarkably, we also found that the patterns of axonal growth were area-specific, i.e. ES-derived neurons with visual cortex identity and grafted in

visual cortex send axons to visual and limbic targets, like in neonatal brain (Gaspard et al., 2008), but not following grafting in frontal (motor) cortex. These data indicate that ES-derived cortical neurons can display area-specific patterns of projections even in the adult brain, and that optimal restoration of cortical projections requires a precise match between the areal identity of the lesioned neurons and of the grafted neurons. Finally we assessed the functionality of the grafts using *in vivo* electrophysiology recordings. Specifically, in order to assess the potential of grafted ESC-derived cortical neurons for specific repair of the visual cortex, we tested whether they could be responsive to visual stimuli, using *in vivo* extracellular recordings. These studies revealed that grafted ESC-derived cortical neurons display robust integration and functional properties similar to those of intact visual cortex, including responsiveness to physiological light stimulation. Collectively, these findings demonstrate that transplantation of mouse ESC-derived neurons of appropriate cortical areal identity can contribute to the reconstruction of an adult damaged cortical circuit (Michelsen et al., 2015). We are now following up on these findings by testing whether and how human PSC-derived neurons can integrate and contribute to reconstruction of damaged cortical circuits in the adult mouse, using our recently established protocols of human corticogenesis (Espuny-Camacho et al., 2013), as well as new improved methods of intracortical transplantation (Nagashima et al., 2014).

This set of results is part of the following publications:

- Specific reestablishment of damaged circuits in the adult cerebral cortex by cortical neurons derived from mouse embryonic stem cells.
Michelsen KA, Acosta-Verdugo P, Benoit-Marand M, Espuny-Camacho I, Gaspard N, Saha B, Gaillard A, **Vanderhaeghen P**.
***Neuron* (2015), 85(5):982-97.**
Featured Article in *Neuron*.
IF: 15.9
- Novel and robust transplantation reveals the acquisition of polarized processes by cortical cells derived from mouse and human pluripotent stem cells.
Nagashima F, Suzuki IK, Shitamukai A, Sakaguchi H, Iwashita M, Kobayashi T, Tone S, Toida K, **Vanderhaeghen P**, Kosodo Y.
***Stem Cells Dev.* (2014) 23(18):2129-42.**
IF: 3.9

2.3. Modelling human neurological diseases.

Based on our previous results showing that corticogenesis can be faithfully recapitulated from human ESC and iPSC (Espuny-Camacho et al., 2013), we have started to use this technology to model cortical neurological diseases for which the underlying causes remain poorly known, and where human-specific mechanisms may be implicated.

On the one hand, we applied our novel technology combining pluripotent stem cell cortical differentiation and intracortical transplantation (Espuny-Camacho et al., 2013) to the most common neurodegenerative disease, Alzheimer's disease (AD), in a joint collaborative effort with the De Strooper lab (KULeuven). One major challenge in AD research is that the mouse models alone have so far failed to reveal full-blown neurodegeneration, ie neuronal loss, suggesting that genuine AD may only develop in a *human-specific* context (Crews and Masliah, 2010; Kokjohn and Roher, 2009; Morrissette et al., 2009). On the other hand, although several human PSC-derived models of AD have been described (Israel et al., 2012; Kondo et al., 2013), their *in vitro* nature constitutes a severe limitation to study affected neurons in a physiological and pathological context that fully mimics the human AD brain.

To circumvent these limitations we applied our model of transplantation of human cortical cells in the mouse cortex (Espuny-Camacho et al., 2013) to investigate whether the abundant amyloid- β species generated in an AD mouse model (Radde et al., 2006) are sufficient to induce full AD pathology in non-affected, genetically non-manipulated human neurons.

We first found that this "*humanized* model" presents robust extracellular deposition of amyloid- β including numerous A β plaques and A β -associated neuroinflammation close to, and inside the location

of the transplanted human neuronal cell clusters (Espuny-Camacho et al., 2017). In addition and most importantly, the transplanted human neurons show remarkable signs of neurodegeneration, including aberrant accumulation of pre-synaptic markers, axonal degeneration and myelination defects, tau pathology, as well as major neuronal loss. Importantly, these pathological features are not detected or are far less important in host mouse brain, and in transplanted PSC-derived mouse neurons, revealing that human neurons respond to A β pathology very differently from their murine counterparts *in vivo*. This “humanized model” provides a novel and highly promising way to test the effects of amyloid-associated pathology *in vivo* on human neurons and could become instrumental to analyze the responses of different genetic AD risk profiles in the presence of A β (Espuny-Camacho et al., 2017).

On the other hand, we have applied novel models of corticogenesis from PSC to study a specific class of neurodevelopmental disease that also displays human-specific traits : microcephaly. We have implemented iPSC models of non syndromic primary microcephaly (MCPH) (Bond and Woods, 2006; Kaindl et al., 2010), a rare autosomal recessive condition where patients display mental retardation and a small brain size, in particular of the cerebral cortex. Mutations in a dozen genes have been implicated in MCPH, most of which encode centrosomal proteins, but the mechanisms by which their disruption causes defects in corticogenesis remain unclear. Using standard iPSC reprogramming technology (Takahashi et al., 2007) we have generated pluripotent cell lines from skin fibroblasts of patients affected by 3 microcephaly gene mutations: MCPH2 (WDR62); MCPH4 (CASC5), and MCPH5 (ASPM), as well as from control unaffected subjects (Espuny-Camacho et al., 2013).

We have used these lines to try and decipher the developmental mechanisms underlying primary microcephaly. Cortical-like progenitors derived from microcephaly or control patient iPSC have been examined for various key parameters of neurogenesis, including proliferation and survival of progenitors, patterns of symmetrical or asymmetrical division, as well as neuronal production and specification. Doing so we obtained first exciting results on the mechanisms underlying the pathogenesis of microcephaly caused by mutations in ASPM. We found that ASPM-deficient cortical progenitors undergo precocious neurogenesis, display abnormal orientation of the mitotic spindle pole, and defective acquisition of forebrain/cortical identity. Intriguingly, the defects could be linked to Wnt signalling in ASPM deficient neuroepithelial cells, as the phenotypes of ASPM mutated cells were partially rescued by Wnt inhibition, while Wnt overactivation in control cells could result in ASPM-mutant like phenotypes. These data reveal how ASPM mutations may lead to decreased human brain size, and uncover a surprising link between this pericentrosomal protein and Wnt signalling during human neurogenesis (Hasche et al., in revision). In parallel, we have used our protocols of corticogenesis, in collaboration with the groups of Prof. Van Hesch (KU Leuven) and Muotri (UCSD) to explore the mechanisms of pathogenesis of another class of neurodevelopmental diseases caused by the duplication of MecP2, revealing altered patterns of neuronal differentiation and synaptogenesis (Nageshappa et al., 2016). Finally in collaboration with the group of Prof Verfaillie (KU Leuven), the application of our protocols of corticogenesis to a neurodegenerative condition (fronto-temporal dementia) caused by progranulin mutation, revealed early developmental phenotypes in affected neurons, thus leading to novel insights on this disease (Raitano et al., 2015).

This set of results is part of the following publications:

- Hallmarks of Alzheimer’s disease in stem cell-derived human neurons transplanted into mouse brain.
Espuny-Camacho I, Arranz AM, Fiers M, Snellinx A, Ando K, Munck S, Bonnefont J., Lambot L, Corthout N, Omodho L, Vanden Eynden E, Radaelli E, Tesseur I, Wray S, Ebner A, Hardy J, Leroy K, Brion JP, **Vanderhaeghen P***, De Strooper B*.

***Co-Senior authors.**

***Neuron* (2017) ; in press.**

IF: 15.9

- Altered neuronal network and rescue in a human MECP2 duplication model.
Nageshappa S, Carromeu C, Trujillo CA, Mesci P, Espuny-Camacho I, Pasciuto E, **Vanderhaeghen P**, Verfaillie CM, Raitano S, Kumar A, Carvalho CM, Bagni C, Ramocki MB, Araujo BH, Torres LB, Lupski JR, Van Esch H, Muotri AR.

***Mol Psychiatry* (2016), doi: 10.1038/mp.2015.128.**

IF: 14.4

- Restoration of Progranulin Expression Rescues Cortical Neuron Generation in an Induced Pluripotent Stem Cell Model of Frontotemporal Dementia.
Raitano S, Orдовàs L, De Muyne L, Guo W, Espuny-Camacho I, Geraerts M, Khurana S, Vanuytsel K, Tóth BI, Voets T, Vandenberghe R, Cathomen T, Van Den Bosch L, **Vanderhaeghen P**, Van Damme P, Verfaillie CM.
Stem Cell Reports (2015) 13;4(1):16-24.
IF: 5.6
- Microcephaly-associated mutations in *ASPM* gene lead to defective human corticogenesis through overactivation of Wnt signaling.
Anja Hasche, Matteo Piumatti, Daisuke H. Tanaka, Adèle Herpoel, Angéline Bilheu, Harmen van Benthem, Isabelle Pirson, Gert Matthijs, Kathelijn Keymolen, Julie Désir, Pierre Gressens, Sandrine Passemard, Marc Abramowicz, and **Pierre Vanderhaeghen**.
Neuron, in revision.
IF: 15.9

3. Most significant publications published from the programme 2014-2016

- Hallmarks of Alzheimer's disease in stem cell-derived human neurons transplanted into mouse brain.
Espuny-Camacho I, Arranz AM, Fiers M, Snellinx A, Ando K, Munck S, Bonnefont J, Lambot L, Corthout N, Omodho L, Vanden Eynden E, Radaelli E, Tesseur I, Wray S, Ebneith A, Hardy J, Leroy K, Brion JP, **Vanderhaeghen P***, De Strooper B*.
***Co-Senior and corresponding authors.**
Neuron (2017) ; in press.
IF: 15.9
- Post-translational Control of the Temporal Dynamics of Transcription Factor Activity Regulates Neurogenesis.
Quan XJ, Yuan L, Tiberi L, Claeys A, De Geest N, Yan J, van der Kant R, Xie WR, Klisch TJ, Shymkowitz J, Rousseau F, Bollen M, Beullens M, Zoghbi HY, **Vanderhaeghen P**, Hassan BA.
Cell (2016);164(3):460-75. doi: 10.1016/j.cell.2015.12.048.
Preview in *Cell*.
IF: 32.2
- Altered neuronal network and rescue in a human MECP2 duplication model.
Nageshappa S, Carromeu C, Trujillo CA, Mesci P, Espuny-Camacho I, Pasciuto E, **Vanderhaeghen P**, Verfaillie CM, Raitano S, Kumar A, Carvalho CM, Bagni C, Ramocki MB, Araujo BH, Torres LB, Lupski JR, Van Esch H, Muotri AR.
Mol Psychiatry (2016), doi: 10.1038/mp.2015.128.
IF: 14.4
- Specific reestablishment of damaged circuits in the adult cerebral cortex by cortical neurons derived from mouse embryonic stem cells.
Michelsen KA, Acosta-Verdugo P, Benoit-Marand M, Espuny-Camacho I, Gaspard N, Saha B, Gaillard A, **Vanderhaeghen P**.
Neuron (2015), 85(5):982-97.
Featured Article in *Neuron*.
IF: 15.9
- Restoration of Progranulin Expression Rescues Cortical Neuron Generation in an Induced Pluripotent Stem Cell Model of Frontotemporal Dementia.
Raitano S, Orдовàs L, De Muyne L, Guo W, Espuny-Camacho I, Geraerts M, Khurana S, Vanuytsel K, Tóth BI, Voets T, Vandenberghe R, Cathomen T, Van Den Bosch L, **Vanderhaeghen P**, Van Damme P, Verfaillie CM.
Stem Cell Reports (2015) 13;4(1):16-24.
IF: 5.6
- Is this a brain which I see before me? Modelling human neural development with pluripotent stem cells.
Suzuki I, and **Vanderhaeghen P**.
Development (2015),142(18):3138-50. doi: 10.1242/dev.120568.
IF: 7.8
- Creating Patient-specific Neural Cells for the In Vitro Study of Brain Disorders.
Brennand KJ, Marchetto MC, Benvenisty N, Brüstle O, Ebert A, Izpisua Belmonte JC, Kaykas A, Lancaster MA, Livesey FJ, McConnell MJ, McKay RD, Morrow EM, Muotri AR, Panchision DM, Rubin LL, Sawa A, Soldner F, Song H, Studer L, Temple S, Vaccarino FM, Wu J, **Vanderhaeghen P**, Gage FH, Jaenisch R.
Stem Cell Reports. 2015 Dec 8;5(6):933-45.
IF: 5.6

- A BCL6/BCOR/SIRT1 complex Triggers Neurogenesis and Suppresses Medulloblastoma by Repressing Sonic Hedgehog Signalling.
Tiberi L, Bonnefont J, van den Ameele J, Le Bon S, Herpoel A, Bilheu A, Baron BW, and **Vanderhaeghen P**.
Cancer Cell (2014) 26, 797-812.
Preview and Featured Article in Cancer Cell.
IF: 23.8
- Novel and robust transplantation reveals the acquisition of polarized processes by cortical cells derived from mouse and human pluripotent stem cells.
Nagashima F, Suzuki IK, Shitamukai A, Sakaguchi H, Iwashita M, Kobayashi T, Tone S, Toida K, **Vanderhaeghen P**, Kosodo Y.
Stem Cells Dev. (2014) 23(18):2129-42.
IF: 3.9
- Thinking out of the dish: what to learn about cortical development using pluripotent stem cells.
van den Ameele, J., Tiberi, L., **Vanderhaeghen, P***, and Espuny-Camacho, I.
***Corresponding author.**
Trends Neurosci. (2014), 37, 334-342.
IF:12.9
- Cortical neurogenesis from pluripotent stem cells: complexity emerging from simplicity.
Anderson, S., and Vanderhaeghen, P.
Curr Opin Neurobiol (2014) 27C, 151-157.
IF: 7.9

4. References

- Anderson, S., and Vanderhaeghen, P. (2014). Cortical neurogenesis from pluripotent stem cells: complexity emerging from simplicity. *Curr Opin Neurobiol* 27C, 151-157.
- Bond, J., and Woods, C.G. (2006). Cytoskeletal genes regulating brain size. *Curr Opin Cell Biol* 18, 95-101.
- Brennand, K.J., Marchetto, M.C., Benvenisty, N., Brustle, O., Ebert, A., Izpisua Belmonte, J.C., Kaykas, A., Lancaster, M.A., Livesey, F.J., McConnell, M.J., *et al.* (2015). Creating Patient-Specific Neural Cells for the In Vitro Study of Brain Disorders. *Stem cell reports* 5, 933-945.
- Crews, L., and Masliah, E. (2010). Molecular mechanisms of neurodegeneration in Alzheimer's disease. *Human molecular genetics* 19, R12-20.
- Espuny-Camacho, I., Michelsen, K.A., Gall, D., Linaro, D., Hasche, A., Bonnefont, J., Bali, C., Orduz, D., Bilheu, A., Herpoel, A., *et al.* (2013). Pyramidal neurons derived from human pluripotent stem cells integrate efficiently into mouse brain circuits in vivo. *Neuron* 77, 440-456.
- Gaillard, A., Prestoz, L., Dumartin, B., Cantereau, A., Morel, F., Roger, M., and Jaber, M. (2007). Reestablishment of damaged adult motor pathways by grafted embryonic cortical neurons. *Nat Neurosci* 10, 1294-1299.
- Gaspard, N., Bouschet, T., Herpoel, A., Naeije, G., van den Ameele, J., and Vanderhaeghen, P. (2009). Generation of cortical neurons from mouse embryonic stem cells. *Nat Protoc* 4, 1454-1463.
- Gaspard, N., Bouschet, T., Hourez, R., Dimidschstein, J., Naeije, G., van den Ameele, J., Espuny-Camacho, I., Herpoel, A., Passante, L., Schiffmann, S.N., *et al.* (2008). An intrinsic mechanism of corticogenesis from embryonic stem cells. *Nature* 455, 351-357.
- Grove, E.A., and Fukuchi-Shimogori, T. (2003). Generating the cerebral cortical area map. *Annu Rev Neurosci* 26, 355-380.
- Hatten, M.E., and Roussel, M.F. (2011). Development and cancer of the cerebellum. *Trends Neurosci* 34, 134-142.
- Israel, M.A., Yuan, S.H., Bardy, C., Reyna, S.M., Mu, Y., Herrera, C., Hefferan, M.P., Van Gorp, S., Nazor, K.L., Boscolo, F.S., *et al.* (2012). Probing sporadic and familial Alzheimer's disease using induced pluripotent stem cells. *Nature* 482, 216-220.
- Kaindl, A.M., Passemar, S., Kumar, P., Kraemer, N., Issa, L., Zwirner, A., Gerard, B., Verloes, A., Mani, S., and Gressens, P. (2010). Many roads lead to primary autosomal recessive microcephaly. *Prog Neurobiol* 90, 363-383.
- Kokjohn, T.A., and Roher, A.E. (2009). Amyloid precursor protein transgenic mouse models and Alzheimer's disease: understanding the paradigms, limitations, and contributions. *Alzheimer's & dementia : the journal of the Alzheimer's Association* 5, 340-347.
- Kondo, T., Asai, M., Tsukita, K., Kutoku, Y., Ohsawa, Y., Sunada, Y., Imamura, K., Egawa, N., Yahata, N., Okita, K., *et al.* (2013). Modeling Alzheimer's disease with iPSCs reveals stress phenotypes associated with intracellular Abeta and differential drug responsiveness. *Cell Stem Cell* 12, 487-496.

- Michelsen, K.A., Acosta-Verdugo, S., Benoit-Marand, M., Espuny-Camacho, I., Gaspard, N., Saha, B., Gaillard, A., and Vanderhaeghen, P. (2015). Area-Specific Reestablishment of Damaged Circuits in the Adult Cerebral Cortex by Cortical Neurons Derived from Mouse Embryonic Stem Cells. *Neuron* 85, 982-997.
- Molyneaux, B.J., Arlotta, P., Menezes, J.R., and Macklis, J.D. (2007). Neuronal subtype specification in the cerebral cortex. *Nat Rev Neurosci* 8, 427-437.
- Morrisette, D.A., Parachikova, A., Green, K.N., and LaFerla, F.M. (2009). Relevance of transgenic mouse models to human Alzheimer disease. *The Journal of biological chemistry* 284, 6033-6037.
- Nagashima, F., Suzuki, I.K., Shitamukai, A., Sakaguchi, H., Iwashita, M., Kobayashi, T., Tone, S., Toida, K., Vanderhaeghen, P., and Kosodo, Y. (2014). Novel and robust transplantation reveals the acquisition of polarized processes by cortical cells derived from mouse and human pluripotent stem cells. *Stem Cells Dev.*
- Olson, J.M. (2014). Therapeutic opportunities for medulloblastoma come of age. *Cancer cell* 25, 267-269.
- Quan, X.J., Yuan, L., Tiberi, L., Claeys, A., De Geest, N., Yan, J., van der Kant, R., Xie, W.R., Klisch, T.J., Shymkowitz, J., *et al.* (2016). Post-translational Control of the Temporal Dynamics of Transcription Factor Activity Regulates Neurogenesis. *Cell* 164, 460-475.
- Radde, R., Bolmont, T., Kaeser, S.A., Coomaraswamy, J., Lindau, D., Stoltze, L., Calhoun, M.E., Jaggi, F., Wolburg, H., Gengler, S., *et al.* (2006). Abeta42-driven cerebral amyloidosis in transgenic mice reveals early and robust pathology. *EMBO reports* 7, 940-946.
- Raitano, S., Ordovas, L., De Muyneck, L., Guo, W., Espuny-Camacho, I., Geraerts, M., Khurana, S., Vanuytsel, K., Toth, B.I., Voets, T., *et al.* (2015). Restoration of progranulin expression rescues cortical neuron generation in an induced pluripotent stem cell model of frontotemporal dementia. *Stem cell reports* 4, 16-24.
- Sur, M., and Rubenstein, J.L. (2005). Patterning and plasticity of the cerebral cortex. *Science* 310, 805-810.
- Suzuki, I.K., and Vanderhaeghen, P. (2015). Is this a brain which I see before me? Modeling human neural development with pluripotent stem cells. *Development* 142, 3138-3150.
- Takahashi, K., Tanabe, K., Ohnuki, M., Narita, M., Ichisaka, T., Tomoda, K., and Yamanaka, S. (2007). Induction of pluripotent stem cells from adult human fibroblasts by defined factors. *Cell* 131, 861-872.
- Tiberi, L., Bonnefont, J., van den Aemele, J., Le Bon, S.D., Herpoel, A., Bilheu, A., Baron, B.W., and Vanderhaeghen, P. (2014). A BCL6/BCOR/SIRT1 Complex Triggers Neurogenesis and Suppresses Medulloblastoma by Repressing Sonic Hedgehog Signaling. *Cancer cell* 26, 797-812.
- Tiberi, L., van den Aemele, J., Dimidschstein, J., Piccirilli, J., Gall, D., Herpoel, A., Bilheu, A., Bonnefont, J., Iacovino, M., Kyba, M., *et al.* (2012). BCL6 induces neurogenesis through Sirt1-dependent epigenetic repression of selective Notch transcriptional targets. *Nat Neurosci in revision.*
- van den Aemele, J., Tiberi, L., Vanderhaeghen, P., and Espuny-Camacho, I. (2014). Thinking out of the dish: what to learn about cortical development using pluripotent stem cells. *Trends Neurosci.*



Geneeskundige Stichting Koningin Elisabeth
Fondation Médicale Reine Elisabeth
Königin-Elisabeth-Stiftung für Medizin
Queen Elisabeth Medical Foundation

Geneeskundige Stichting Koningin Elisabeth – G.S.K.E.

Fondation Médicale Reine Elisabeth – F.M.R.E.

Queen Elisabeth Medical Foundation – Q.E.M.F.

Mailing address:

The scientifique director:

Prof. dr. Jean-Marie Maloteaux
3, avenue J.J. Crocq laan
1020 Bruxelles - Brussel
Belgium
Tel.: +32 2 478 35 56
E-mail: jean-marie.maloteaux@uclouvain.be

and

Secretary:

Mr. Erik Dhondt
3, avenue J.J. Crocq laan
1020 Bruxelles - Brussel
Belgium
Tel.: +32 2 478 35 56
E-mail: fmre.gske@skynet.be
E-mail: erik.dhondt@skynet.be, e.l.dhondt@skynet.be
www.fmre-gske.be
www.fmre-gske.eu
www.fmre-gske.com